The Use of Maxillary Sinus Imaging as a Tool in Human Identification

Teresa Margaux Runge

A thesis submitted in partial fulfilment of the requirements of Liverpool John Moores University for the degree of Doctor of Philosophy

May 2023

"(…) Wie eine Ohrfeige schlug uns die Wahrheit ins Gesicht
dass die Welt, die Natur aufblüht ohne uns.
Nach und nach trauten sich wilde Tiere
weltweit auf die sonst bevölkerten Plätze.
In Venedig schwankten Gondeln und Boote
auf kristallklarem Wasser.
Zu Besuch kamen nun Fische, Delfine, Schwäne.
In Japan wagten sich Hirsche tief in die Städte. (...)

Wie eine Ohrfeige schlug uns die Wahrheit ins Gesicht
dass die Welt, die Natur aufblüht ohne uns
einfach nur durch unser Fortbleiben. (...)"

Nach Safiye Can 2021

'(…) Like a clout the truth slapped us in the face
that the world, the nature, flourishes without us.
Little by little wild animals
dared to enter otherwise populated places.
In Venice, gondolas and boats swayed
on crystal clear water.
Fishes, dolphins and swans came to visit.
In Japan, venison ventured deep into the cities. (…)

Like a clout the truth slapped us in the face
that the world, the nature, flourishes without us
simply because we stay away. (…)'

Translation by Teresa Runge

Abstract

The presented research performs evaluations of maxillary sinus morphologies for human identification purpose. Due to the durability of maxillary sinuses, morphological analyses of the structure can prove to be extremely valuable and informative, even when parts of the skull are destroyed and dental records cannot be applied. This research is comprised of 4 studies evaluating maxillary sinus morphologies in order to build a comprehensive outlook on the methodological potentials. In total the used sample is comprised of right and left maxillary sinuses from 988 individuals divided into 12 populations. The morphologies are assessed by extracting the maxillary sinuses from radiographic and CT images and applying elliptic Fourier analyses on the structures. Morphological variability is investigated by converting the maxillary sinus morphology into multiple closed curves, and embedding them into a cartesian system. Principal component analyses on four components further simplifies the processing.

The first two studies of this research are concerned with morphological uniqueness testing both in a simulated and real-life scenario to lay a comprehensive foundation for method applicability. Uniqueness testing is executed as a morphological ante- and postmortem comparison by calculating Euclidean and Mahalanobis distances. Euclidean correlation values from 0.000 in the simulated sample up to 0.002 in the real-life sample indicate maxillary sinus morphological uniqueness for each ante- and postmortem sinus morphology pair. Mahalanobis distances are used for visualisation. The third study is assessing the reproducibility of maxillary sinus morphological extraction by applying Cohen's kappa values. The high kappa values in intra- and inter-observer reliability testing indicate high quality extraction and interpretation of morphologies, increasing the methodological confidence level. Finally, the last study is dedicated to understanding age-related changes in maxillary sinuses by calculating growth rates by population and by sex on Euclidean distances. All evaluations reveal quasi-linear and monotonously rising distances with growth rates varying among left and right sinuses and population.

This research advances the potential of maxillary sinus morphologies for human identification and demonstrates its advantages over other paranasal identification methodologies. Therefore, this research acts as an essential first step toward using the proposed methodological framework in future forensic casework.

Zusammenfassung

Diese Arbeit untersucht die Eignung des *sinus maxillaris* für die Identifikation unbekannter menschlicher Überreste. In vier Teilstudien werden verschiedene Aspekte der Morphologien des *sinus maxillaris* evaluiert, um einen umfassenden Überblick über die methodischen Möglichkeiten zu erhalten. Dazu wird eine Stichprobe der linken und rechten Kieferhöhlen von 988 Individuen, aufgeteilt in 12 Populationen, untersucht. Die Auswertungen aller vier Teilstudien basieren auf der quantitativen Extraktion morphologischer Parameter, ausgehend von Röntgen- und CT Bildern des Schädels, mithilfe der elliptischen Fourier-Analyse. Dabei werden die individuellen Morphologien in Scharen geschlossener Kurven überführt, in ein kartesisches System eingefügt und schließlich einer Hauptkomponentenanalyse unterzogen. Die ersten beiden Teilstudien befassen sich innerhalb eines simulierten bzw. eines realitätsnahen Szenarios mit morphologischen Einzigartigkeits-Tests, um eine gesicherte Grundlage für die Anwendbarkeit der Methode zu legen. Die Einzigartigkeits-Prüfung wird mithilfe des Vergleichs der ante und post mortem-Morphologien der Individuen durchgeführt, indem Euklidische und Mahalanobis-Abstände berechnet werden. Euklidische Korrelationswerte von 0,000 in der simulierten Studie bis zu 0,002 in der realitätsnahen Studie weisen auf die morphologische Einzigartigkeit des *sinus maxillaris* für jedes Morphologiepaar der ante- und postmortalen Nasennebenhöhlen hin. Kalulationen von Mahalanobis Distanzen werden zur Visualisierung verwendet. In der dritten Teilstudie wird die Reproduzierbarkeit des angewendeten Verfahrens der Morphologie-Extraktion bewertet unter Zuhilfenahme von Cohen´s κ-Statistik. Insgesamt weisen die hohen κ-Werte bei Intra- und Inter-Observer-Auswertung auf eine qualitativ hochwertige Extraktion und Interpretation der Morphologien hin, was die methodologische Zuverlässigkeit des Verfahrens untermauert. Teilstudie 4 schließlich widmet sich dem morphologischen Wachstum und den Entwicklungsmustern des *sinus maxillaris*, indem Wachstumsraten nach Bevölkerung und Geschlecht auf euklidischen Distanzen berechnet werden. Diese Berechnungen helfen altersbedingte Veränderungen zu verstehen. Alle Auswertungen zeigen quasi-lineare und monoton ansteigende Distanzen mit Wachstumsraten, die je nach linker und rechter Nebenhöhle und Population variieren. Die Ergebnisse dieser Arbeit zeigen, dass die Untersuchung der Morphologien von *sinus maxillaris* vorteilhaft zur menschlichen Identifizierung herangezogen werden können, und demonstrieren den Fortschritt gegenüber anderen paranasalen Identifizierungsmethoden.

Résumé

La présente recherche évalue la morphologie des sinus maxillaires dans le but de procéder à l'identification humaine. Cette recherche est composée de quatre études afin d'évaluer la morphologie des sinus maxillaires sous différents angles pour unifier les résultats et ainsi obtenir une vision globale des possibilités méthodologiques. L'échantillon total investigué est composé de sinus maxillaires droit et gauche de 988 individus répartis en 12 populations. La forme est évaluée en extrayant les sinus maxillaires des radiographies et des images CT puis en appliquant des analyses de Fourier elliptiques sur les structures. La variabilité morphologique est étudiée en convertissant la morphologie des sinus maxillaires en plusieurs courbes fermées et en les intégrant dans un système cartésien. Les analyses en composantes principales sur quatre variables simplifient encore le traitement.

Les deux premières études portent sur les tests d'unicité morphologique dans deux conditions, l'une simulée et l'autre rélle, afin de décrire la méthode et son application pratique. Le test d'unicité est effectué par comparaison morphologique ante- et post-mortem en calculant les distances euclidiennes et de Mahalanobis. Les valeurs de corrélation euclidienne de 0,000 dans l'échantillon simulé jusqu'à 0,002 dans l'échantillon réel vérifient l'unicité de forme des sinus maxillaires pour chaque paire de sinus ante et post-mortem. Les distances de Mahalanobis sont utilisées pour la visualisation. La troisième étude évalue la reproductibilité de l'extraction morphologique des sinus maxillaires en calculant les taux d'accord grâce au kappa de Cohen. Ses valeurs élevées en intra- et en inter-observateurs indiquent une très bonne reproductibilité de l'extraction et de l'interprétation, augmentant le niveau de confiance méthodologique. Enfin, la dernière étude est consacrée à la compréhension des changements liés à l'âge au niveau des sinus maxillaires en calculant les taux de croissance par population et par sexe sur à l'aide des distances euclidiennes. Toutes les évaluations révèlent des distances quasi linéaires et monotones variant selon les sinus gauche et droit et la population.

Ce travail de recherche fait progresser nos connaissances sur la potentielle utilité de la des morphologies des sinus maxillaires pour l'identification humaine et identifie certains avantages par comparaison avec d'autres méthodologies d'identification paranasale. Ainsi, il constitue une première étape essentielle vers l'application pratique de l'étude des sinus maxillaires pour de futurs dossiers médico-légaux.

Contents

List of Figures

List of Tables

Acknowledgements

Since the start of this research lots has changed both on a personal as well as a global level. Most distinctively, as every member of the world community, I have been affected by Covid-19. Although I have been fortunate enough to evade an infection myself to date, many of my friends and family have been infected. On top of the worrying virologic effects, the pandemic caused university closures for the better part of my research period. Everyone writing a doctoral thesis knows about the strains such a project can cause, even with the active support of a thriving PhD community. Hence, I am sure the added tension of writing a thesis in home office, with only limited connection to a research group, is understandable. I would like to thank my lead supervisor Dr Matteo Borrini and all my family and friends for supporting me through this time.

On the professional side, I had the pleasure of working with many engaged people who encouraged my professional development enormously. My first introduction to anthropology was during my BSc in one of Dr Alicia Ventresca Miller's human osteology courses. Dr Ventresca Miller saw my potential and started my career in anthropology by offering the opportunity to work alongside her on a research project in Kyiv, Ukraine. Since then I have acquired many new skills and had the opportunity of working with a massive dataset of human skeletal remains. Due to a sinusitis six years ago, when I had to determine my research topic for my MSc thesis, I stumbled upon the maxillary sinuses in a forensic context. I am very grateful to have had the opportunity to develop my own research project from that point onwards, and for the trust, Dr Matteo Borrini and my supervisory team laid into me and my independent work process. I appreciate the opportunities this research has given me and am excited to see what the next step will bring.

I would like to thank my supervisor team Dr Matteo Borrini, Prof Joel Irish, and Dr Alicia Ventresca Miller, for their support. Their input and guidance have been invaluable and are a decisive factor in successfully completing this thesis. Furthermore, I would like to thank the staff of the School of Biological and Environmental Sciences of the Liverpool John Moores University (LJMU). Especially Dr James Ohman for his introduction and help with the radiographic equipment and the staff of the forensic anthropology department for making available information on the collection of Poulton Chapel and St. Owen's Church. An additional

thanks to the staff of the LJMU doctoral academy for doing their best to foster a positive and connective work environment during the pandemic.

A very special thanks to Jelena Bekvalac, curator of human osteology at the Museum of London. Jelena has supported my research of maxillary sinuses since the very beginning of my MSc thesis in 2016. I owe it to her help that I was allowed to study the collections of Chelsea Old Church, St. Mary Spital, and St. Bride's Lower Churchyard. Access to Poulton Chapel and St. Owen's Church collections was granted via the Anthropology department of LJMU. Through Dr Matteo Borrini, I was able to use the collections of Florence and Siracusa. I am very grateful for their help in procuring the data. Many thanks to Dr Michael Francken and Prof Katerina Harvati for hosting me at the University of Tübingen and granting me access to the osteological collection. Thanks a lot, to Taylor Otto for helping to access the NESPOS database. Furthermore, I would like to thank Dr Mark Hans (Bolton-Brush Growth Study Center), Steven Duckworth (Oregon Health & Science University), and Dr Sunjay Suri (University of Toronto) for granting access to the longitudinal growth studies. A special thanks to Sean Curry of the AAOF Craniofacial Growth Legacy Collection, who took the time and transferred multiple hundred high-resolution digital radiographs for this research to use.

The largest thanks go to my family and friends. To Dr Frank Runge, who helped me with countless technical discussions of the research and without whose help the thesis would not have been what it is today. To Ele Runge, who encouraged me multiple times and gave me a space to work during the pandemic. To Nicola Runge and Lukas Müller for having my back. To Dr Céleste Rousseau for her French language expertise. Additional thanks to Rebecca Bradshaw, who always had time to listen to my problems and encouraged me to go on, although living on the other side of the world.

Finally, the most heartfelt thanks go to Panini. You have been with me for 16 years, and one of the saddest moments was letting you go. You have always been my best friend, and especially during the pandemic, you helped me to preserve my mental health. You will always be missed!

Chapter 1 Introduction

The human paranasal sinuses are air-filled voids located in the frontal, ethmoidal, and sphenoidal bone as well as the maxilla (see section 1.3 for detailed information on the maxillary sinus). Assessments of human paranasal sinuses date back as early as the beginning of the 20th century, examining the possibility to identify human remains of specific persons from x-ray images of frontal sinuses (Schüller, 1921; Runge, 1928; Law, 1934). Nowadays, it is a common belief in forensic literature that human frontal sinuses are unique, and many studies work on identification methods (Gibelli et al., 2019; Cameriere et al., 2019). However, methods utilising other human sinuses are scarce. Usually, studies approach the testing of sinuses by using linear measurements, descriptive variables and volumetric assessments (Xavier et al., 2015) and very little research involves morphological assessments.

Practitioners often apply visual comparisons of outlines to establish sinuses antemortem and postmortem data matches in medicolegal situations (Smith et al., 2010). Assessments of visual patterns are a commonly employed forensic method, for example, in fingerprinting and tool mark evaluations (Albright, 2021). However, analyses, especially on sinus outlines, only relying on visual assessments are highly subjective to the individual practitioner and should be rendered inadmissible before the court. This is as the Daubert standard requires error rates and standardised measurements of methodological approaches (Holobinko, 2012). Metrology standards are used in forensics, and therefore, methods need to be reliable, repeatable, standardised, and valid (Albright, 2021). To withstand cross-examination in court, however, not only the characteristics of the method have to be outstanding, but the experience and credibility of the expert need to be apparent in the testimony. As early as the 19th century, the standing of the anthropological expert is discussed in court settings, identifying: "… it is for the jury, not the expert, to decide on the identity of the skeleton; it is for the expert to show whether the identity is possible or probable. The opinion he will give will depend not only on his professional acquirements but on his honesty and common sense" (Dwight, 1878).

Since then, much has changed for the expert witness in court. Following the 1993 *Daubert* decision (Lesciotto, 2015), experts testimonies get regularly challenged for admissibility instead of being accepted solely due to their "honesty and common sense" (Dwight, 1878).

Aside from challenges to the experts' qualifications, courts have set standards to question the methods validity, reliability, and relevance (Lesciotto, 2015). All those standards need consideration when testifying in court and when establishing a new method in forensic anthropology.

In the following chapters, this study will investigate if and how maxillary sinus morphologies can be used for human identification. Chapter 1 delivers background information on standard human identification methods, the maxillary sinus in general, a description of forensic radiology, and a description of the research question.

Chapter 2 introduces all 12 populations as well as the methods used for this research. Results of this research can be found in chapters 3 to 6 and are discussed in chapter 7. Concluding statements are found in chapter 8, giving a final overview on this studies topic.

1.1 Human Identification

The recognition of identities is essential for criminal, civil, and social reasons. Firstly, identifying a deceased person is a pivotal step to give closure to family and friends on a psychological level, as the loss of a loved one and the inability to grieve are closely related to significant mental health issues (de Boer et al., 2020). Secondly, identifications will aid, for example, in matters of inheritance and child custody, solve legal issues, and aid in prosecuting homicides (Christensen, 2003). More important, however, is the humanitarian importance of identification. Every human being has the right to be identified with proper methods and endurance of the practitioner, defined through every individual's right to an identity in the Universal Declaration of Human Rights (United Nations, 1948) and the international humanitarian law (IPU and ICRC, 2016).

Setting aside the psychological part of a person's character, the term ‘identity’ describes physical markers set on a scale between normal and pathological, defining the individual (Mutalik et al., 2013). Early on, forensic professionals thought about ways to differentiate between individuals. For example, when a positive identification was impossible due to a lack

of personal identification documents, body marks and tattoos were thought to be possible identification markers (Wilder and Wentworth, 1932).

Then as now, the identification of a deceased body is easier to obtain the fresher it is. However, time not being the only determinant factor, the more identification methods used for cross-examination, the better. When appropriate, well-preserved corpses can be visually identified by family and friends. Once that is impossible, or if no one is available for visual identification, biometric methods are used instead (Ølberg and Goodwin, 2016). Interpol (2018) states in their information material a clear order of identification methods. Friction ridge analysis, forensic odontology, and DNA analysis are defined as primary identification methods as they are most frequently used and provide quick and reliable results. Secondary identification methods are used when primary methods fail to deliver sufficient identification results. Most commonly, analyses of personal data, medical findings and clothing evidence fall in this category (Interpol, 2018).

Other methods to identify unknown remains are radiological examinations on for example paranasal sinuses, osteological methods for facial reconstruction, and the comparison of special bodily marks (Wlodarczyk, 2012; de Boer et al., 2020). Regardless of the method used, when successfully matching the skeletal features of the deceased individual and antemortem data material, a positive identification is established. Therefore, the higher the number of skeletal variables, the higher the possibility to establish an actual identification (Christensen, 2003).

1.1.1 Dactyloscopy

As one of the primary identification methods, analyses of friction ridges are executed using an individual's palms, fingers, soles, and toes, as those ridges are unique in every individual (Kumar et al., 2017). Papillary ridges are developed before birth and build permanent patterns on hands and feet (Pankanti et al., 2002). When injured, the ridges grow back in the original pattern or scar, which are additional identification markers. Especially fingerprinting is used in medicolegal settings and law enforcement all over the world. Easy retrieval and quick digital

comparisons allow for systematic searches on national and international databases (Interpol, 2018). Biometric recordings of fingerprints were first taken by ink only and improved to digital printing over time. It is one of the fastest and inexpensive methods using digital comparison aids (Wlodarczyk, 2012). Recorded features on finger ridges include, firstly, the general pattern of the prints. Secondly, the specific regular or irregular shape of the edges is described, as well as every wrinkle, minutiae, dot and line, and individual ridge. As the prints, once taken, are recorded in the database, they can be saved for future comparisons to confirm identities on borders and during police operations and identify corpses and unknown individuals. Furthermore, saving those biometric data makes it possible to connect and prove the guilt or innocence of a person connected to a crime scene even after many years have passed. Nowadays, fingerprinting is also used as a security feature (Wlodarczyk, 2012).

1.1.2 Forensic Odontology

Another primary identification method is forensic odontology. Dental structures such as teeth are significantly resistant against degradation and external impacts, making forensic dentistry one of the main specialities used for identification (Modesti et al., 2014). The utilisation of dental comparisons in this context is mainly due to the variability of the craniofacial skeleton. Furthermore, the resilience of the teeth makes it possible to utilise their structures even when the bodies' soft tissue is gone due to defleshing or deterioration (Interpol, 2018). Therefore, practitioners use examinations of dentition and pathological changes on the teeth and surrounding skeletal areas primarily to compare antemortem and postmortem data from a specific individual (Malik et al., 2012). Next to pathological changes like for example lesions, caries, abscesses, and missing teeth, medical interference e.g. implants, crowns, fillings, root canal procedures and orthodontic changes can be used as a marker to establish a positive identification. Furthermore, prostheses are especially useful as they are custom made for one person, sometimes delivering unique ID numbers suitable for identification (Dhanapal and Divyanand, 2016).

As the teeth are very durable, dental comparisons can be applied for skeletonised and charred remains as well as heavily putrefied bodies and in mass disaster settings. Antemortem and

postmortem comparisons are usually executed using x-ray images from the patient's dentist (Adams, 2002). Furthermore, when no antemortem records are available, teeth can give other information about the deceased individual to narrow down potential candidates. For example, the development and eruption stages of the teeth give information about the deceased individual's age at death. In addition, wear indicators help identify dietary and oral hygiene habits, and congenital traits might help establish the person's ancestral origin (Interpol, 2018). Usually, dental methods are applied together with fingerprinting, DNA analysis and other secondary identification methods (Modesti et al., 2014). All these factors together help the investigators to narrow down the pool of possible candidates and help to limit the results in databases.

1.1.3 DNA Analysis

Like Fingerprinting and Dental odontology, DNA analysis is a primary identification method. DNA profiling was first applied in the UK around the 1980s and is now a powerful tool for prosecution and policing (Johnson and Williams, 2004). DNA, available in most cells of the body, is left behind everywhere a person goes. It is unique for every individual and simultaneously can reveal family relationships between people. Therefore, DNA is a powerful tool for identifying a suspect or deceased person and connecting them to a crime scene (Sense about Science, 2017; Jobling and Gill, 2004).

DNA evidence is primarily perceived as the gold standard in identification; however, DNA sampling also has its limitations. Traces might not always be detected, and misinterpretation of DNA profiles is possible. After collecting DNA samples, the expert matches the unknown material to a known person's reference DNA profile for identification (Kayser, 2015). An advantage of DNA profiling is the possibility to perform analyses even on severely decomposed remains. Here, rapid testing with excellent quality standards is achieved because of automated DNA analyses (Interpol, 2018). As with dental analyses, the protected location of the teeth from environmental factors makes them a primary resource for harvesting DNA material. However, DNA can also be extracted from bone material, blood, semen, and saliva, depending on the availability (Higgins and Austin, 2013; de Boer et al., 2018). Storage in

databases allows to quickly compare DNA profiles even when only partial profiles or the DNA of relatives are available. Furthermore, this storage makes it possible to solve cases even years after the incident happened (Jobling and Gill, 2004).

DNA profiles can also predict certain biometric features such as hair and eye colour from the sample. Although limitations exist, for example in the prediction of non-blue and non-brown eye colours, (Chaitanya et al., 2017; Dembinski and Picard, 2014) advantages outweigh the shortcomings, as specific features can help get the public involved to find possible matches of the deceased person and help in disaster victim identification cases.

1.1.4 Secondary Identification Methods

The primary identification methods mentioned above are often used simultaneously for cross evidencing, depending on the availability of the examined structures. All of them offer quick and reliable results. However, it would be erroneous to only focus on primary methods for identification as secondary methods have immense capability and advantages. While primary identification methods have the potential to be used individually to establish a positive identification, secondary methods are mostly used when primary methods cannot be applied to secure an identification match. Interpol (2018) states that “secondary identifiers in combination may provide sufficient information to make identification in selected cases, and where access to primary identifiers may be limited or absent, they may be the only means whereby the deceased can be identified”.

1.2 Forensic Radiology

The application of radiographic images is standard practice in medicolegal investigations. Imaging the body is an investigative tool applied by the coroner or anthropologist to, for example, plan autopsies, search for foreign objects, confirm identities, and ensure the health and safety of the practitioner when exposed to highly infectious diseases (Swift and Rutty, 2006). Primarily, “forensic radiology […] comprises the performance, interpretation, and

reportage of […] radiological examinations and procedures that have to do with the courts and/or law" (Brogdon, 2011).

The starting point of forensic Radiology was discovering "eine neue Art der Strahlung"[1] by Wilhelm Conrad Röntgen in 1895 (Brogdon and Lichtenstein, 2011). He already was among the leading scientist of his time and discovered a new ray able to surpass great distances, travel through solid matter, stimulate fluorescent barriers, and expose photographic plates (Brogdon, 1998). When he experimented with electron beams in a Hittorf tube, he observed how a screen coated with barium platinocyanide started to fluoresces. However, the Hittorf tube was covered and sealed with cardboard which should have hindered the radiation (Harris, 2021).

After some testing with various materials, he found that only lead prevents the ray from penetrating. It was in line with those experiments when he revealed the ray's ability to expose fluoroscopic images of bone as described by Glasser (1958): "To test further the ability of lead to stop the rays, he selected a small lead piece, and in bringing it into position observed to his amazement not only that this round shadow of the disk appeared on the screen, but that he suddenly could distinguish the outline of his thumb and finger, within which appeared darker shadows—the bones of his hand".

Using photographic plates instead of the fluorescent screen, he was able to preserve the images permanently and published his findings, including a radiograph of his wife's hand in 'Sitzungsberichte der physikalischen-medizinischen Gesellschaft zu Würzburg'[2] (Röntgen, 1895). Additionally, he sent his findings to other scientists in Germany and Austria, who soon after published his discovery of the 'Röntgenstrahlung' in newspapers all over the world (Brogdon, 1998).

After its discovery in 1895, x-ray imaging was quickly adapted by the forensic community, especially as all tools needed to build the apparatus were frequently available in most western countries (Brogdon and Lichtenstein, 2011; Collins, 1964). Even before Röntgen submitted his

[1] Translation: "a new kind of ray"
[2] Translation: 'meeting reports of the physical-medical society of Würzburg'

research to the ‘Physikalisch-Medizinische Gesellschaft zu Würzburg’, a court in Montreal, Canada, used an x-ray image of a leg with a gunshot wound to convict the shooter. The first murder trial, including radiographic evidence, was brought before the court in 1896 in Lancashire, UK. However, acceptance of x-ray images as evidence varied significantly among countries and individual courts. Moreover, if allowed into evidence, procedures were not standardised (Brogdon and Lichtenstein, 2011). Aside from court applications, radiographic investigation in anthropology was also applied for examinations of archaeological samples as soon as the anthropological community learned of the non-destructive properties of the method. In 1898 the first Egyptian and Peruvian mummies were examined (Petrie, 1898), followed by general analyses of bone growth and pathologies (Garn, 1959; Mollison, 1932; Merbs, 1969).

Since the first recommendation to use radiology for identification by Schüller (1921) (who suggested the first radiological identification method and proposed frontal sinus variability for this task), more direct identification and biological profiling methods were developed quickly. Anthropologists were now using x-ray imaging to distinguish between animal and human bone material (Messmer and Fierro, 1986), to estimate age (Garn, 1959), sex (Iscan and Steyn, 2013; McCormick et al., 1985), dental morphologies (Eckert and Garlant, 1984), and trauma wounds on the body (Eckert and Garlant, 1984; Fatteh and Mann, 1969; Schmidt and Kallieris, 1982).

Each new application solidified the reputation of radiography. Especially the comparison of features on antemortem and postmortem x-ray images is a common and standardised procedure in medicolegal investigations to date. Next to DNA analyses and Fingerprinting, radiographic analyses, for example of the dentition, are a primary identification method (Interpol, 2018). Due to dental and other medical data storage, radiographic comparisons have become one of the most vital methods when working on mass disasters, as the teeth and the whole maxillofacial area are highly durable against environmental disturbances (Bass, 1984). When establishing identities based on antemortem and postmortem comparisons on radiographs, any pathological change and variability from the norm on the skeleton aids in a positive identification (Brogdon, 2011). Provided with antemortem reference material, every bone of the human skeleton can give information about the deceased's identity. Therefore, if antemortem data is unavailable, the anthropologist can

evaluate the x-rayed structures and narrow down the field of potential candidates (Interpol, 2018).

Since the 1970s, computed tomography (CT) and magnet resonance imaging (MRI) complimented and/or reduced conventional radiography for medical and medicolegal purposes. CT and MRI imaging offer the advantage of cross-sectional images with greater detail (Spoor et al., 2001). Similarly, to digital radiography, CT and MRI images can be processed quickly, stored electronically, and manipulated after exposure. However, radiography is still essential in the forensic context despite CT and MRI imaging advancing in the field (Beck, 2011). One of the most significant advantages, for example, is the storage of antemortem dental x-ray images at dental practices. Panoramic images cover both the dental arcade and the surrounding maxillofacial structures, which are then available for comparison methods (Altug and Ozkan, 2011). For more technical details on radiology please see chapter 2.

1.3 The Maxillary Sinus

Craniofacial pneumatic structures are frequently found within the taxa of vertebrates. Those structures can either be grooves on the external craniofacial skeleton, like with archosaurs or, as with mammals, inwardly enclosed bony chambers (paranasal sinuses) (Witmer, 1999). Aside from investigations in the classes Mammalia (Paulli, 1900c; Paulli, 1900b; Paulli, 1900a; Dieulafe and Loeb, 1906; Ingersoll, 1922; Nemours, 1931; Negus, 1958), where an emphasis was laid on primates (Keith, 1902; Cave and Haines, 1940; Du Brul, 1965; Hershkovitz, 1977; Maier, 1986; Schwartz, 1987; Dean and Delson, 1992; Rae, 1997; Koppe and Ohkawa, 1999; Rossie et al., 2002), analyses of paranasal sinuses in the late 19th and early 20th century have also been executed on Aves (Bignon, 1889; Buhler, 1970), Reptilia (Mihalkovics, 1898; Edinger, 1938; Witmer, 1999), extinct humans (Davis, 1865; Vlcek, 1965; Tillier, 1977; Kimbel et al., 1997; Spoor et al., 2000; Spoor et al., 1994; Arsuaga et al., 1997; Seidler et al., 1997; Ponce de León and Zollikofer, 2001; Márquez et al., 2001), and *H. sapiens* (Zuckerkandl, 1882a; Bosworth, 1888; Mouret, 1898; Killian, 1900; Sieur and Jacob, 1901; Onodi, 1903; Grünwald, 1925). Due to their location, maxillary sinuses have especially been interesting for

orthodontists in connection with implantology and sinus augmentations (Amorosa and Latini, 2016; Bahadir et al., 2008; Benjaphalakron et al., 2021; Dandekeri et al., 2020; Iwanaga et al., 2019; Khandelwal and Hajira, 2017; Kiran Kumar Krishanappa et al., 2018; Pelinsari Lana et al., 2012).

Internal craniofacial pneumatisation is a significant factor for skull construction, and especially its function is highly discussed to date. Although questions of terminology and phylogeny are still under deliberation, it is widely accepted to identify the sinuses by the ostium's position, and the sinus is named after the bone they pneumatise into (Rae, 2008). There are four paranasal sinuses within the order of primates: maxillary sinus, frontal sinus, ethmoidal sinus, and sphenoidal sinus (Negus, 1958; Cave and Haines, 1940).

The first mention of the paranasal sinuses can be found in reports by Hippocrates in 400 BC, when he studied the nose as a drainage system. (Blanton and Biggs, 1969; Márquez, 2008). Six hundred years later, although not calling the paranasal sinuses by name, the Greek anatomist Claudius Galen reported about the structures and the porosity of the skull (Blanton and Biggs, 1969; Amorosa and Latini, 2016). The first description of the maxillary and frontal sinus can be found in illustrations of human dissections by Leonardo Da Vinci (1489) (Figure 1), followed by descriptions of the frontal and sphenoid sinuses by Berengario da Carpi (1521) and descriptions by Highmore in 1651 (Passali and Bellussi, 1995).

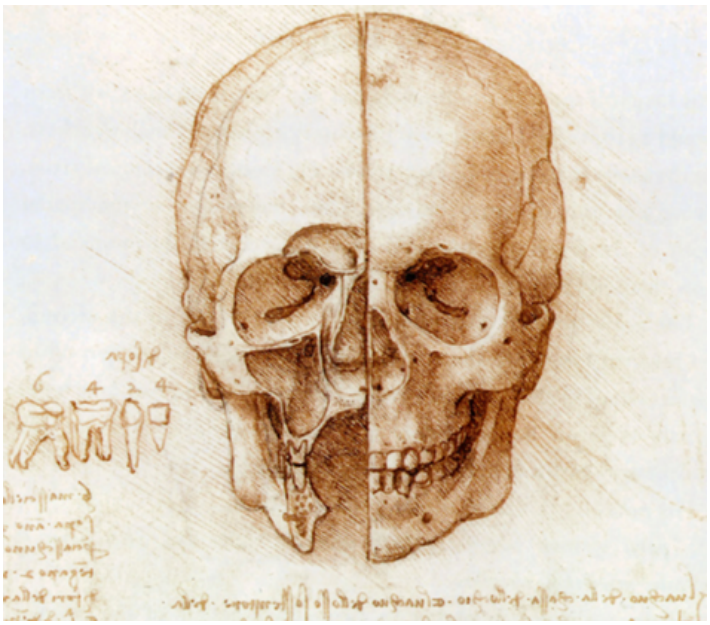

Figure 1: 'The skull sectioned' showing paranasal sinuses by Leonardo da Vinci (1489). The Royal Collection Trust London © Sheila Terry / Science Photo Library

Until the 19th century, medical philosophers and most anatomists focussed on descriptions and theoretical questions rather than addressing why the air-filled voids existed (Márquez et al., 2014). The first functional anatomical description was produced by Zuckerkandl (1882a; Zuckerkandl, 1892b; Zuckerkandl, 1893), who started the modern sinus anatomy.

1.3.1 Anatomy

The maxillary sinus is the largest structure within the group of paranasal sinuses (Figure 2). All paranasal sinuses are air-filled voids lined with mucosa and are centred around the nasal cavity within the maxillofacial region of the skull (Whyte and Boeddinghaus, 2019).

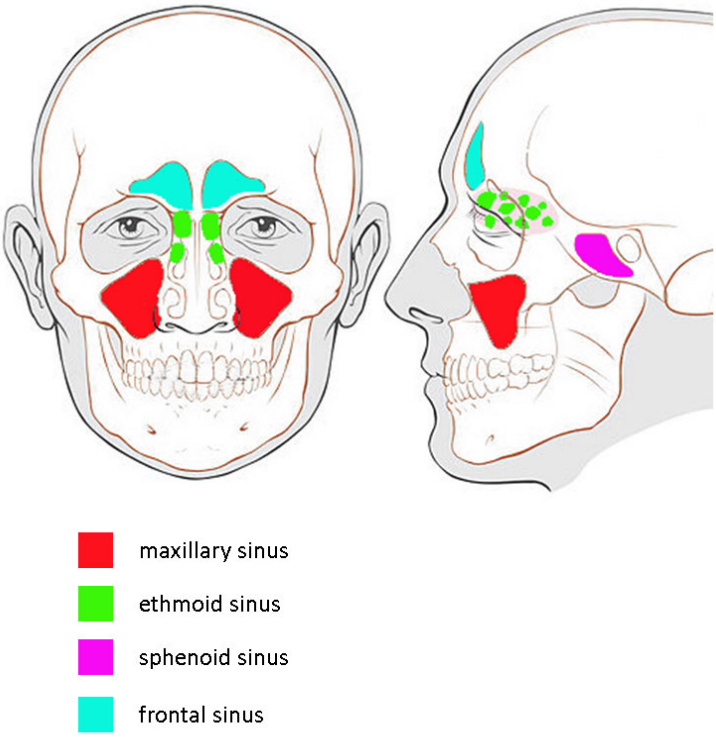

Figure 2: Anatomy of the paranasal cavities in frontal and lateral view (adapted after Lamperti, 2020)

Being the most prominent sinuses, the maxillary sinuses lie within the maxillary bone and form a pyramidal structure when fully developed. Their walls are significantly thin, and size and shape vary considerably between the right and left sinus. Due to their location in the cranium, protected by the dental arcade, their structure is highly durable, which makes them useful for identification, even when main parts of the skull are destructed (Sidhu et al., 2014).

As the development of maxillary sinuses is highly variable, mean volumes of fully grown sinuses vary between 10 ml (Jacob, 2008) and 15 ml per side (Lawson et al., 2008; Hettiarachchi et al., 2021). However, degrees of asymmetry do not favour one side of the two maxillary sinuses within one individual, and so far, there is no agreement about their morphological similarities (Márquez et al., 2014). Average volumes change depending on sex, age, and ancestry and cannot be used as absolute measurements. Furthermore, dimensions vary significantly on the factors mentioned above, including changes due to tooth loss and tooth absence (Hettiarachchi et al., 2021).

Maxillary sinuses consist of six walls. The nasal cavity's inferior part of the lateral wall builds their medial wall (Beitler et al., 2016). The medial wall is very variable in height, and its anterosuperior part presents an hourglass-shaped opening called the natural ostium. The average size of the natural ostium varies between 1 to 17 mm, with an average of 2.4 mm (DeHaven Jr., 2014). In some sinuses, an accessory ostium is present on the medial wall. The location of the natural ostium in an anteromedial position in the superior aspect of the medial wall makes it impossible to conduct sinus drainage by gravity. Therefore, drainage depends on the beating of the *cilia* on the sinus mucous, which is transporting drainage material towards the ostium (Amorosa and Latini, 2016; DeHaven Jr., 2014). The natural ostium opens into the infundibulum, which leads to the middle meatus. The infundibulum holds a fundamental status for the maxillary, frontal, and ethmoidal sinus as the ostium-meatal complex leads their secretions out of the body (Amorosa and Latini, 2016).

The maxillary sinuses superior wall is created by the orbital floor, which is the most fragile part. Here the infraorbital canal, including nerves and vessels, crosses the sinus (Beitler et al., 2016; Amorosa and Latini, 2016; Iwanaga et al., 2019). The most robust wall of the maxillary sinus is the posterior wall, which is located anteriorly of the sphenoid sinus. The wall is formed by the infratemporal fossa of the maxillary and creates the anterior border of the pterygopalatine fossa (Márquez et al., 2014; Amorosa and Latini, 2016; Iwanaga et al., 2019).

The apex of the maxillary sinus frequently extends into the zygomatic bone, and the inferior wall is built by the alveolar process (Amin and Hassan, 2012). Here, the roots of the first and

second molar, as well as the second premolar, come closest to the sinuses (Amorosa and Latini, 2016). The maxillary sinuses inferior wall is created by the palatine and the alveolar process of the maxillary. It is located below the nasal cavity and lined with Schneiderian membrane, which has a high osteogenic potential. When ruptured, for example, during dental procedures or as a result of inflammatory diseases, sinus inflammations can be developed (Dandekeri et al., 2020; Iwanaga et al., 2019).

The anterior wall is formed by the facial surface of the maxilla and faces the infraorbital nerve. Landmarks of this wall are the infraorbital groove, the thin canine fossa, and the infraorbital foramen (Iwanaga et al., 2019). The lateral wall extends into the zygomatic bone and is close to the posterosuperior alveolar nerves. Together the nerves of the anterior and lateral walls are responsible for the innervation of the upper incisors and canines as well as the upper molars and premolar (Amorosa and Latini, 2016).

1.3.2 Auxology

Information about sinus development have been collected since the early 20th century (Killian, 1900; Schaeffer, 1910), presenting development through analysis of plain radiographs, CT and MRI scans, as well as cadaveric specimens (Shah et al., 2003). All sinuses are built through pneumatisation, which describes a physiological process initiating the sinuses to increase their volume (Amine et al., 2020).

The maxillary sinus is the earliest sinus to appear in utero, around the 10th week of gestation (Maspero et al., 2020). During that time, invaginations are visible on the mucosa of the ethmoid infundibulum towards the surrounding mesenchyme. The primordial cavity for the maxillary sinus is formed as soon as the invaginations fuse. Fusion usually happens around the 11th week of gestation. The primordial sac forms the anlage of the maxillary sinus, presenting an oval shape (Iwanaga et al., 2019; Márquez et al., 2014). Starting in the 12th week of foetal development, the primordial maxillary sinus builds a visible three-dimensional structure. Between gestational weeks 17 and 23, caudal and dorsal expansion starts. First ossifications on the lateral wall are visible around the 16th foetal development week, followed by the

anterior sinus wall around the 20th week and the posterior wall around the 21st week of development (Nuñez-Castruita et al., 2012).

In utero, the maxillary sinus is filled with fluid and pneumatises into the alveolar ridge after birth (Lawson et al., 2008; Sidhu et al., 2014). The onset of postnatal development starts parallel in both the sinuses of an individual, as confirmed by Lorkiewicz-Muszyńska et al. (2015). After birth, growth is described as biphasic with two rapid phases between years 1 to 3 and 7 to 12. Between the two progression phases and after the 12th year of age, development slows until early adulthood. Primary dentition does not influence sinus growth; however, the maxillary sinus floor descends as soon as the permanent dentition erupts (Lawson et al., 2008; Iwanaga et al., 2019; Márquez et al., 2014). Sinus growth happens simultaneously with bordering bones, and they reach approximately ¼ of their adult size by year 3 and ½ by year 9 (Lorkiewicz-Muszyńska et al., 2015). During growth, the main restricting factors are the eruption of the dentition, pressure against the orbital wall, and facial muscle traction (Lawson et al., 2008).

While there is a lack of consensus about the growth during later adult life, most studies suggest the maxillary sinuses reach adult size with the eruption of the third molar. This is usually associated with the 18th to 20th year of life of an individual (Iwanaga et al., 2019; Amin and Hassan, 2012; Adibelli et al., 2011). After reaching this threshold, some studies suggest a decrease in volume (Ariji et al., 1996; Ikeda, 1996; Emirzeoglu et al., 2007; Karakas and Kavakli, 2005; Jun et al., 2005), while other studies indicate no voluminal change after reaching adulthood (Schatz and Becker, 1984; Dhanak et al., 2019).

Studies exploring maxillary sinus growth almost exclusively determine sinus development on dimensional and voluminal approaches (Dhanak et al., 2019). However, it is still unclear which dimension alters sinus volumes at which developmental stage (Bhushan et al., 2016). To date, there is only little debate regarding prenatal sinus development, in contrast to postnatal growth and differences between studies are thought to arise due to varying methods used to determine volumes, as well as the variety of age ranges and numbers of individuals (Değermenci et al., 2016). Furthermore, although voluminal approaches are favoured, the

methodological approach to obtaining the volumes is nonhomogeneous, making comparisons difficult (Maspero et al., 2020).

1.3.3 Anatomical Variation

As stated before, maxillary sinus development exhibits significant inter-individual variation as developmental bone expansion occurs during different development stages and with different dimensions and growth speeds for every individual. While development begins before birth, most variable growth happens postnatally (Bhushan et al., 2016; Lorkiewicz-Muszyńska et al., 2015; Hettiarachchi et al., 2021). After understanding normal development, the knowledge of sinus abnormalities enables the further use of the structure for forensic purposes.

There are two main maxillary sinus variants (Table 1). Most variation stems from sinus enlargement (Ata-Ali et al., 2017; Pelinsari Lana et al., 2012). While pneumatisation into the maxillary is highly variable both inter-and intra- populational, hyperpneumatisations like pneumasinus dilitans, pneumocele, and mucocele often call for medical intervention. Both pneumocele and mucocele show exterior symptoms when the enlarged sinus walls pressure the orbital floor (Lawson et al., 2008).

Table 1: Summary of anatomical variations on maxillary sinuses

Sinus Attribute	**Variant**
Enlargement	Pneumatisation Mucocele
Reduction	Septa Hypoplasia Neoplasms / Tumors Sinusitis Antroliths Trauma Operations

There are however, also multiple reasons for maxillary sinus reductions. Usually, the maxillary sinus is built as one coherent cavity; however, internal septation can divide the sinus into multiple sections. Septa either occur as an irregular expansion of the inferior sinus wall after tooth loss (secondary septa) or a congenital anomaly (primary septa). When septa are developed, they divide the maxillary sinus into two or more compartments with thin, sickle-shaped walls. Both primary and secondary septa locations vary and can be found above edentulous ridges with varying heights (Dandekeri et al., 2020; Amine et al., 2020; Iwanaga et al., 2019).

Hypoplasia describes an underdevelopment of the sinus cavity and can be congenital or acquired due to surgery or trauma during development (Bahadir et al., 2008; Resnik and Preece, 2017; Whyte and Boeddinghaus, 2019). Trauma on the facial skeleton alters the maxillary sinus morphology long-lasting by turning bony structures towards the sinus cavity (Lawson et al., 2008). The same occurs due to operations like sinus floor augmentations, especially as damages to the Schneiderian membrane can cause acute or chronic sinusitis, which alters mucosal thickness (Benjaphalakron et al., 2021; Pelinsari Lana et al., 2012). Appearances of septa and in smaller-scale antroliths have a considerable impact on maxillary sinus variability, as they split the sinus in different compartments (Ata-Ali et al., 2017). The most significant impact on maxillary sinus morphology next to pneumatisation and septa have neoplasms. While malignant tumours erode the walls of the maxillary sinuses, benign cysts condense the sinus externally (Bell et al., 2011). However, Márquez (2008) observed that although the morphology of the maxillary sinus can be significantly altered due to neoplasms, its alignment can, in most cases, still be described as pyramidal shaped.

It is demonstrated that maxillary sinus variation occurs both in regular and irregular anatomy. However, as with most studies, sinus variation is mainly determined using dimensions and volumes. Nevertheless, the essential function of morphological variations in human biology is not to be neglected, and while development is primarily advanced through genetic factors, inter- and intra-population variation on facial morphology is also determined by environmental qualities (Lorkiewicz-Muszyńska et al., 2015; Viðarsdóttir et al., 2002).

1.3.4 Purpose and Function

Until today the role of the maxillary sinuses remains unclear (Sieron et al., 2020). A selection of the most prominent hypotheses is summarised in Table 2.

Table 2: Summary of hypotheses of maxillary sinus purpose and function

Hypotheses	**Purpose and Function**
Evolution	Aquatic adaption Evolutionary remains
Structure	Weight reduction Crumple zone' and shock resorption Facial growth assistance and normal skull-pneumatisation Thermal insulation
Physiology	Vocal resonation Enlargement of olfactory area Immune defence Air conditioning Intranasal pressure regulation

When discussing the purpose of the maxillary sinus, it is crucial to consider their temporal context. For example, the medical philosophers of the 16th century believed that breathing into the sinuses invited spirits into the body infusing the person with life (Zimmer, 2004). Nowadays we can exclude this hypothesis from the scientific discussion. However, as the sinuses were considered to be somewhat of an "evolutionary enigma" (Rae and Koppe, 2014) over the years, multiple aquatic adaptation theories were developed to bridge this gap (Bignon, 1889; Proetz, 1953; Wegner, 1958; Rhys Evans, 1992).

Those aquatic theories more or less suggest the sinuses act as flotation devices keeping the head over water. However, nowadays studies show that an evolutionary reversal happens

with mammals that become aquatic, making them lose their sinuses. Therefore, paranasal sinuses in *H. sapiens* indicate no evolutionary aquatic phase breaking the link between sinuses and flotation (Rae and Koppe, 2014). Additionally, multiple evolutionary studies propose the sinuses to be useless air-filled remnants (Ingersoll, 1906; Negus, 1957; Takahashi, 1983).

Structural hypotheses of maxillary sinus function include theories about skull lightening (Blanton and Biggs, 1969; Paulli, 1900c; Nemours, 1931; Shea, 1977; Schummer et al., 1979), the assistance in facial growth (Eckley, 1904; Blaney, 1990) and normal skull pneumatisation (Witmer, 1999). However, the idea of maxillary sinuses promoting facial symmetry was invalidated as Negus (1957) showed that individuals with no maxillary sinuses do not suffer from skull deformations.

Another possible function of the maxillary sinus is as a trauma shock absorption zone. When trauma to the face occurs, the air-filled void of the maxillary sinus absorbs the shock (crumple zone), and predetermined breaking points prevent injury on the orbitals and the brain (Márquez et al., 2014; Kellerman and Schmidt, 2009; Lee et al., 2014). Another popular structural hypothesis promotes the maxillary sinus as a thermal insulation system for the skull and the lungs (Bremer, 1940; Proetz, 1953).

For a long time, an increase of the olfactory surface area through the maxillary sinuses was hypothesised as well (Braune and Clasen, 1877) until it was realised that the sinuses are not lined with this type of mucosa (Sieron et al., 2020). Other physiological hypotheses state that the maxillary sinuses help with air conditioning during inspiration (Gannon et al., 1997) and aid in voice resonance (Bignon, 1889; Underwood, 1910; Wegner, 1958; Leakey and Walker, 1997). However, both theories have been challenged heavily (Negus, 1957; Aust et al., 1994). Recently the most accepted theory is the production of nitric oxide and the function of the maxillary sinus as a gas reservoir to aid immune defence (Lundberg et al., 1994; Naraghi et al., 2007). However, although there are many theories about the maxillary sinuses purpose, their role still remains unclear, and each new theory usually raises more questions than it answers.

1.4 The Paranasal Sinus in Positive Identification

In the past, information about sinuseal pneumatisation have been established by using measurements and radiographic assessments. Furthermore, injections of liquids give data for volumetric calculations. Presently, CT and MRI scans using sectioning on sagittal and coronal levels give more exact information about volume and dimensions (Sanchez Fernandez et al., 2000). However, to be used in human identification, comparative methods using radiographic images instead of CT or MRI scans offer more chances of success, as the probability is higher to get access to radiographic images from dental offices. Furthermore, teeth overview images often cover the maxillary sinus area and can therefore be used as antemortem data to be compared against postmortem data.

Human identification from skeletal structures is a significant forensic procedure (Amin and Hassan, 2012). Visual comparisons of radiographic images taken antemortem and postmortem can be used as a source for identification. Even fragmented sinuses can be helpful for positive identification (Ruder et al., 2012). Often dimensions are taken to assess differences (Uthman et al., 2011). However, assessments show that maxillary sinuses distinctly vary between volumetric and distributional expanses, as two similar-sized structures can show variability in morphology (Butaric and Maddux, 2016). Additionally, examinations using dimensions of the frontal sinuses (Quatrehomme et al., 1996; Ribeiro, 2000; Riepert et al., 2001; Christensen, 2005; Deog et al., 2013; Beaini et al., 2015; Xavier et al., 2015) have been applied more often than of the maxillary sinuses (Musse et al., 2009; Butaric et al., 2010).

The maxillary sinuses can be used for human identification due to their variability in morphology, volume, and dimensions (Xavier et al., 2015). Therefore, it is essential to detect the origin of variation. The shape and volume of these structures vary among sex (Musse et al., 2009; Uthman et al., 2011; Amin and Hassan, 2012; Sidhu et al., 2014; Jehan et al., 2014), as the maxillary sinus is said to be more prominent in males than in females. Furthermore, origin and ancestry are essential in the maxillary sinus dimension variation (Bolzan and Tucunduva, 2012). In general, variation in populations occurs due to genetic diversity within a population and the exchange of these genetic features. Due to this diversity, a population can adapt to new environmental conditions, which permits its survival (Campbell et al., 2015).

Firstly mentioned by Schüller is the research of paranasal sinuses in 1921. Here, the unique quality of frontal sinus morphologies was assessed. This built the foundation for the subsequent paranasal sinus uniqueness testing which is the qualitative and quantitative assessment of sinus variability for human identification purposes (Gibelli, 2019; Patil, 2012). However, within the field of human identification, only little research has been conducted using maxillary sinuses (Musse et al., 2009; Musse et al., 2011; Pinto et al., 2012; Ruder et al., 2012; Sidhu et al., 2014), compared to work performed on the frontal sinuses (Quatrehomme et al., 1996; Ribeiro, 2000; Riepert et al., 2001; Silva et al., 2009; Tang et al., 2009; Patil et al., 2012; Ruder et al., 2012; Deog et al., 2013; Beaini et al., 2015; Rabelo et al., 2016; Cameriere et al., 2019). More often, comparisons of the structural features of the maxillary sinuses have been used for sex determinations.

Musse *et al.* (2011) studied the morphology of maxillary sinuses and compared dental conditions to identify an unknown skeleton by radiographic images. Yet, radiographic images have been applied in multiple other studies, for example, to determine if these images are adequate to identify unknown human individuals (Bolzan and Tucunduva, 2012). Bolzan and Tucunduva (2012) used radiographic images of 29 skulls to compare the sinuses for human identification, stating that the characteristics of maxillary sinuses on radiographic images are not as detailed in comparison to the frontal sinuses. Pinto *et al.* (2012) examined methods for human identification by measuring the maxillary sinuses. These studies examine the reliability of comparison methods. Further research on maxillary sinuses has been executed to detect whether volumes or dimensions of maxillary sinuses can be used for sex identification (Musse et al., 2009; Uthman et al., 2011; Amin and Hassan, 2012; Jasim and Al-Taei, 2013; Masri et al., 2013; Vidya et al., 2013; Sidhu et al., 2014; Ekizoglu et al., 2014; Jehan et al., 2014). Significantly less research regarding the maxillary sinuses has been executed using x-ray scans (36 %) as the majority of the studies used CT scans (64 %) for dimensional and volumetric assessments (Xavier et al., 2015).

1.5 Research Question

Early childhood development and high durability provide support for the use of maxillary sinus morphologies in human identification. However, in the field of forensics the use of frontal sinuses is emphasized. Therefore, benchmark testing has to be performed in order to proof the forensic suitability of maxillary sinus morphologies. Building on this a methodology can be developed that has high potential to jump from theory to practice.

There are two approaches taken when using skeletal material for identifying a person. With known antemortem reference material, the ante- and postmortem datasets are compared against each other to produce either positive or negative identification. With unknown material a biological profile is produced to narrow down potential matches. In order to use maxillary sinus morphologies in human identification, a certain operational framework has to be established. As with all ante- and postmortem identification methods the reputation and usability stands and falls with the structure's exclusivity. In this field of work misinterpretations can lead to wrongful legal persecution as well as grieving relatives. Hence, a simple rareness of the interpreted structure is not sufficient to use a methodological approach in court settings. Instead the uniqueness of skeletal features, which describes features showing statistically significant differences, needs to be considered. When matching ante- and postmortem data, the achieved confidence level must provide the practitioner with a trustworthy result and a match between the datasets must indicate a positive identification.

Transferred to the intentions of this study, maxillary sinus morphologies need to be evaluated to that effect before proposing an application. If even two individuals possess the same morphologies the approach is void and indicates that maxillary sinus morphologies cannot be used in identification. Furthermore, the morphologies properties need to be evaluated. In order to use them for biological profiling the effects of age and sex have to be investigated.

This study marks the starting point of investigating the potential of maxillary sinus morphologies for human identification purposes. Here, the study concentrates on morphological uniqueness and the effects of age-related changes. The identified objectives for this study are fourfold and can be retraced in this exact order in the results chapters of this study:

1. To test for morphological uniqueness between the ante- and postmortem dataset of the sample;
   1.1. To assess differences between the maxillary sinus morphologies of the sample;
   1.2. To determine biological properties of the sample;

2. To determine uniqueness of maxillary sinus morphologies in a real-life application (case study);

3. To assess the reproducibility of the approach;

4. To establish age-related changes in maxillary sinus morphologies of the sample;
   4.1. To develop an age clustering system for the sample;
   4.2. To calculate growth rates for the sample.

1.6 Thesis Structure

This thesis is comprised of 8 chapters. Chapter 1 provides necessary anatomical information, as well as the state of the art in sinus identification. The following chapter 2 includes the materials and methods applied in this research. Here, the sample, the morphometric foundation, and an itemization of the methodological approach used in each study is introduced. Chapter 3 to 6 provide the results of each study. Chapter 3 covers the uniqueness testing and chapter 4 is concerned with the results of the case study. Furthermore, chapter 5 holds information about intra- and inter-observer reliability results, while results of the age study can be found in chapter 6. These chapters are followed by a discussion of the previously presented results in chapter 7 and the conclusion in chapter 8. Included here are potential limitations of the research and future recommendations. In addition, this thesis provides two appendices to present necessary figures and tables.

Chapter 2 Materials and Methods

2.1 The Sample

This research uses a total of 988 individuals deriving from 12 skeletal collections. Sinus morphologies are evaluated on radiographic and CT skull images taken homogenously in the anteroposterior plane. Information on radiological processing can be found in section 2.2.1 Radiography.

For the uniqueness test and case study, only fully-developed sinus morphologies were evaluated. Therefore, only individuals over the age of 20 years are included in those parts of the study. The uniqueness testing study uses a sample of 1,105 left and right maxillary sinuses. The sample of the case study is comprised of 32 left and right sided maxillary sinuses (Table 3). Furthermore, the study evaluating the reproducibility uses a sample of 20 % of the 1,105 sinus images used for the uniqueness testing. The age study is concerned with estimating the individuals' ages through sinus morphologies. Here, radiographic images taken throughout both the childhood and adult life of the individuals are assessed. The sample of the age study comprises 1,818 left and right maxillary sinuses (Table 3). Images were evaluated for suitability before processing, making sure only skulls without changes to the maxillofacial region were admitted to the study. Therefore, the number of sinuses used for all studies is reduced compared to the individuals in total and age gaps between images can vary between individuals. Population-specific information, including the dating of the skeletal collections and specific imaging techniques, can be found in Table 3, while Figure 3 gives an overview of the site locations

Table 3: Summary of all collections and morphologies used for this research

Sample	Imaging	Date	Sample Size				Uniqueness testing		Case study		Age estimation	
			♀	♂	Ind.	Total Individuals	X	Total Sinuses Used	X	Total Sinuses Used	X	Total Sinuses Used
Poulton Chapel (Poulton)	X-ray	1275 - 1640	4	6	2	12	X	14	≠	≠	≠	≠
St. Owen's Church (Gloucester)	X-ray	11th to 15th Century	13	2	≠	15	X	5	≠	≠	≠	≠
Florence	X-ray	Late 19th Century	24	27	≠	51	X	78	≠	≠	≠	≠
Siracusa	X-ray	Late 19th Century	≠	≠	≠	18	X	34	≠	≠	≠	≠
Chelsea Old Church	X-ray	1700 - 1850	11	9	4	24	X	46	≠	≠	≠	≠
St. Mary Spital	X-ray	1100 - 1539	159	206	≠	365	X	442	≠	≠	≠	≠

Sample cont.	Imaging	Date	Sample Size				Uniqueness testing		Case study		Age estimation	
			♀	♂	Ind.	Total Individuals	X	Total Sinuses used	X	Total Sinuses used	X	Total sinuses used
St. Bride's Lower Churchyard	X-ray	1770 - 1849	⊬	⊬	⊬	140	X	219	⊬	⊬	⊬	⊬
Osteological Collection University of Tübingen	CT	19th Century	15	25	1	41	X	80	⊬	⊬	⊬	⊬
Anatomical Collection, University of Leipzig	CT	19th Century	15	25	1	41	X	80	⊬	⊬	⊬	⊬
Bolton Brush Growth	X-ray	20th Century	41	50	⊬	91	X	60	X	24	X	632
Oregon Growth	X-ray	20th Century	52	46	⊬	98	X	52	X	8	X	694
Burlington Growth	X-ray	20th Century	43	49	⊬	92	⊬	⊬	⊬	⊬	X	786
Total						**988**[3]		**1,105**[4]		**32**		**1,818**[5]

[3] A total of 988 individuals was used for this study. However, the number of used individuals does not correlate directly with the sinuses used for the uniqueness testing and the age estimation study. Firstly, individuals from Burlington Growth were excluded from the uniqueness testing. Secondly, certain sinuses had to be discarded due to unsuitable age ranges, maxillofacial pathologies, or image overexposure.
[4] 1,792 sinuses were available for this part of the study (988 Individuals – 92 Individuals from Burlington Growth = 896 images x 2 (right and left side) = 1,792. However, images had to be discarded during extraction due to unsuitable age ranges, maxillofacial pathologies or image overexposure. Leaving 1,792 – 687 (discarded sinuses) = 1,105 sinuses used for the uniqueness study (left = 556; right = 549).
[5] In the age estimation study, each individual possesses multiple images throughout their lifetime. Hence, the higher number of images used than individuals present. Of 2,112 sinuses evaluated for this study, 294 had to be discarded to fit into the applied age cluster system = 1,818 sinuses used for this study.
X indicates which populations are used in each study.
⊬ indicates which populations are not used in each study.

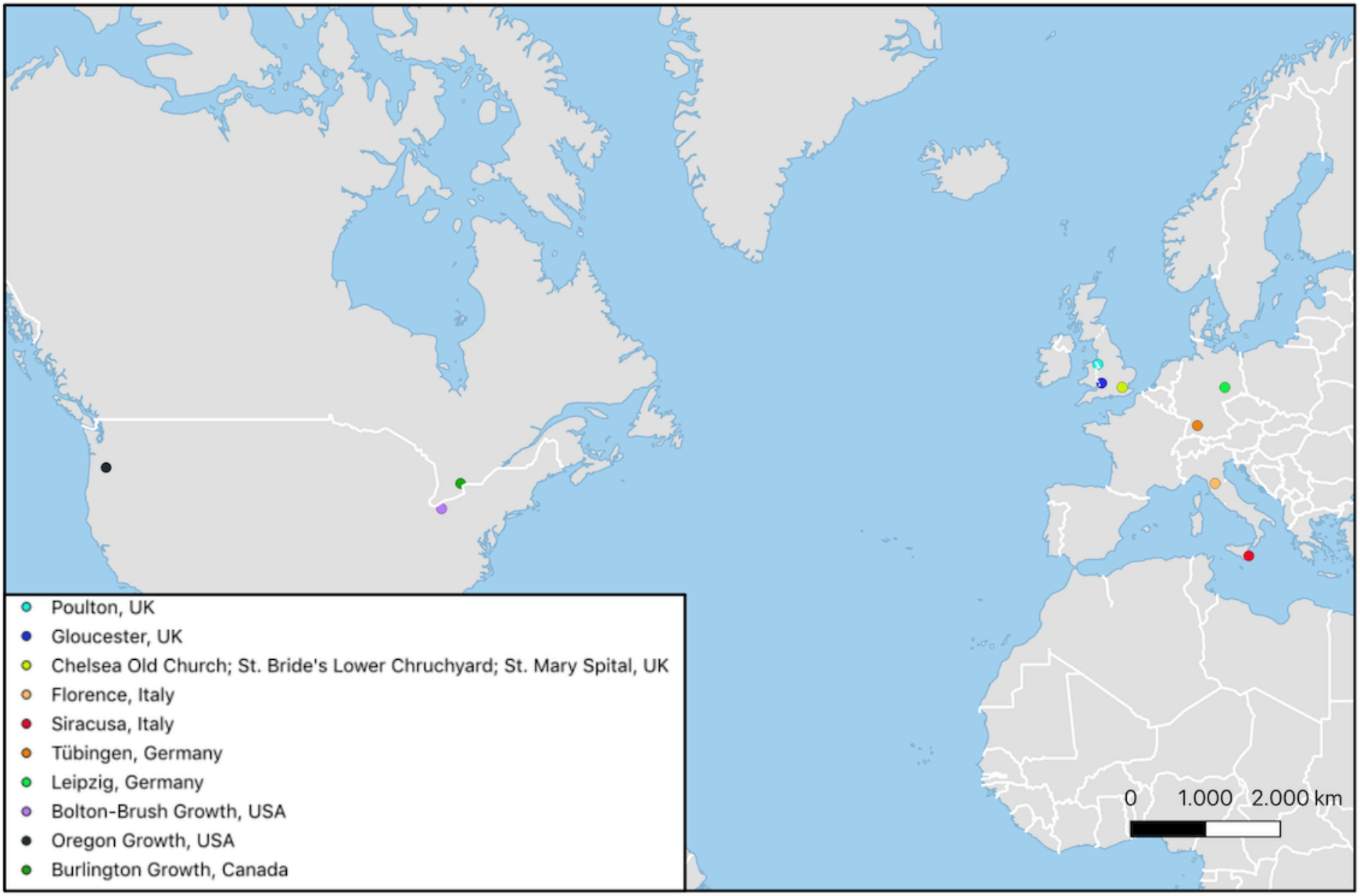

Figure 3: Geographic distribution of all populations used for this research (created with QGIS)

2.1.1 European Sample

2.1.1.1 Poulton and Gloucester

Radiographic images from the two collections of Poulton and Gloucester housed at Liverpool John Moores University were taken explicitly for this study by the author. The archaeological site of Poulton (UK) dates back to 1147 and excavations on the burial ground adjoining the chapel started in 1995 (Emery, 2000). The Poulton Research Project carries out excavations in cooperation with the Liverpool John Moores University, and to date, more than 900 skeletons are discovered (Poulton, 2014). The skeletal material used in this study was buried near the Poulton medieval chapel. Skeletal remains used in this study from the collection of Gloucester (UK) were uncovered during the Southgate Street excavations. The Romans founded the city and the related burial ground. Modern excavations were carried out by the Western Archaeological Trust in 1989 (Atkin, 1990; Atkin and Garrod, 1990).

Of the 27 individuals imaged from the collections of Poulton and Gloucester, only 19 sinuses were suitable for this study due to damage to the maxillofacial area, unsuitable age ranges or unclear exposure of the images. Furthermore, a series of skulls from Gloucester was reconstructed in a previous PhD project (Valoriani, 2019). However, this research only uses skulls without reconstructions to the maxillofacial area to prevent false morphological results.

2.1.1.2 Florence

The 51 skull radiographs used from the collection of Florence (Italy) derive from the 'Cranioteca' of the Florence Museum of Natural History, section Anthropology and Ethnology. This collection contains the skeletal remains of unclaimed corpses, who died at the S. Maria Nuova Hospital in Florence in the 19th century. Due to the hospital's central location the catchment area includes aside from Florence the provinces of Fiesole, Pontassieve, Bagno a Ripoli, and Lastra a Signa (Capaccioli and Mannucci, 2003). Causes of death involve pneumonia, tuberculosis, cancer, and syphilis. While 12 individuals were under the age of 20 and therefore, are disqualified for this research, the rest of the collection belongs to a middle to low socioeconomic population (Capaccioli and Mannucci, 2003).

2.1.1.3 Siracusa

Skull radiographic images used from individuals of the collection of Siracusa (Italy) are also housed at the Anthropology section of the Florence Museum of Natural History, which build the largest human skeletal collection in Italy. In total the collection counts 64 complete adult skeletons, which were buried at the municipal cemetery of Siracusa in Sicily at the end of the 19th and early 20th century (Papini et al., 2015). Subsequent exhumations took place in 1909. (Parenti, 1952). In this research skull x-ray images of 17 individuals are used with unknown biological profiles and causes of death.

2.1.1.4 Chelsea Old Church

Frontal sinus radiographs of the collection of Chelsea Old Church were made available by the Museum of London Archaeology (MOLA). Skeletal remains deriving from the post-medieval cemetery of Chelsea Old Church (London, UK) are also housed and curated at the MOLA. In 2000, over 290 skeletal remains were excavated from the churchyard close to the Chelsea Church. The church itself was destroyed during World War II and rebuilt in 1950 (Bekvalac and Kausmally, 2009). As part of the excavation, a sample of 198 remains was examined for age and sex estimations. Due to coffin plates, family vaults, and inscriptions, some of the individuals could be identified via biographical data (Cowie et al., 2008).

2.1.1.5 St. Bride's Lower Churchyard

The collection of St. Bride's Lower Churchyard (London, UK) curated at MOLA is comprised of the post-medieval populations surrounding the St. Bride's church. Due to the parish's record, the buried individuals are well documented and mainly consist of a population with low socioeconomic status due to the cemetery's close location to the Fleet prison and Bridewell workhouse. 497 individuals were excavated in the open yard with tightly placed burials (Kausmally, 2008). The cemetery of St. Bride is fascinating for comparisons as it is one of the largest accurately documented post-medieval populations in London (Bekvalac, 2018).

2.1.1.6 St. Mary Spital

The third population curated at MOLA is the collection of St. Mary Spital (London, UK). St. Mary Spital has been one of the largest medieval infirmaries in England until 1539, and the individuals excavated and used for this study were found on a large cemetery east of the infirmary wall. Excavations took place between 1991 and 2007 (Harward et al., 2019). The cemetery has been in full use between 1100 and 1539. However, most of the individuals used in this study date between 1200 to 1250, when the priory was established and the final years of the cemeteries between 1400 and 1539 (Bekvalac, 2021).

Radiographic skull images from over 500 individuals deriving from all three London populations were examined for this study.

2.1.1.7 Osteological Collection, University of Tübingen

Material made available from the Osteological Collection, University of Tübingen (Germany) differs from the sample discussed so far, as analyses were executed on CT rather than X-ray images (please refer to chapter 2.2.4 for x-ray and CT image comparability). The material is part of an extensive collection including skeletal material of 10,000 individuals located primarily in Baden-Württemberg dating from Palaeolithic times to the early 20th century (Francken, 2016). The collection was established in 1934 as part of the Faculty of Earth Sciences. The osteological part of the collection was then taken out of the initial collection in 1973 and has been used independently as a research and teaching collection since 1982 (Czarnetzki, 2006). The remains used for this study all derive from excavation sites within Germany, except for two individuals from Toblosk (Russia) and Kalish (Poland). All individuals date into the 19th century and are over 20 years of age (Francken, 2019).

2.1.1.8 Anatomical Collection, University of Leipzig

Skeletal remains deriving from the Anatomical Collection, University of Leipzig (Germany) were analysed, similar to the material from the osteological collection, University of Tübingen, on CT images rather than X-ray images (please refer to chapter 2.2.4 for x-ray and CT image comparability). Images were made available through the NESPOS database. The NESPOS Society e. V. manages the open-source database of the German Neanderthal Museum. The database contains digitized information about Pleistocene and modern archaeology with digital datasets, photographs, 3D objects and publications (Bradtmöller et al., 2010). The sample used for this study includes CT images of individuals from NESPOS' modern reference (dated as 'recent') originating from Europe, Asia, North America, and Africa. Aside from the geo-referencing data, each individual is additionally provided with supporting biological data (Pastoors, 2016).

2.1.2 North American Sample

The three samples used for age estimations in this study were made available on radiographs by the AAOF Craniofacial Growth Legacy Collection through their website (AAOF, 2020). All three collections give extensive data about longitudinal human growth by taking x-ray images of the same individual throughout its lifetime.

2.1.2.1 Bolton - Brush Growth

The Bolton-Brush Growth (BBG) Collection is a coalition of the Brush Inquiry founded in 1926 and the Bolton Study, which started in 1929. Both were initiated to examine average human growth and development of both teeth and face as well as body joints. With 6.000 participants, images were taken on an annual basis throughout the participant's childhood with two follow-ups in early 1980 and 2000 to examine adult changes. The original hard copies of all radiographic images are housed at the Bolton-Brush Growth Study Center at Case Western Reserve University, Ohio, USA (Hans, 2021).

2.1.2.2 Oregon Growth

The Oregon Growth (OG) Study was carried out between the 1950s and 1970s by the Child Study Clinic, and records are currently housed at the Oregon Health and Science University Historical Collections and Archives, Oregon, USA. Throughout the study's duration, radiographic images of the skull and wrist were taken of healthy white American children semi-annual or annual. Within the study, a total of 357 individuals was imaged longitudinally from 3 to 18 years. Furthermore, for some individuals also adult images are available. Additional to the cephalograms, records for each individual include dental moulds, photographs, radiographic wrist imaging, and health evaluations (AAOF, 2020).

2.1.2.3 Burlington Growth

The Burlington Growth (BG) Center in Ontario, Canada was founded in 1952 and started a growth and development study on Caucasian children. Imaging took place annually between the ages of 3 to 20 years. The study had a sample size of 1258 individuals and presents complete orthodontic records combined with wrist images, dental casts, photographs and health evaluations (AAOF, 2020). Radiographic images of all three growth studies have been used for uniqueness testing (only images from individuals over 20 years of age) and age estimation in this research. There are up to seven x-ray images for each individual, with the majority of the images taken during childhood.

2.2 Morphometrics

2.2.1 Radiography

In the context of this work, the term 'radiography' refers to the process of creating projectional images of a specimen's internal structure by transilluminating it with x-rays and recording the not absorbed portion of this radiation on photographic plates, solid-state detectors or any other suitable devices. The term 'x-ray' relates to the radiation itself, whereas a 'radiograph' or 'x-ray image' is the result of the imaging process.

Within the spectrum of electromagnetic radiation, x-rays cover the range between extreme ultraviolet (EUV) and γ radiation, i.e. wavelengths between ca 10^4 and 10^1 pm. Due to the quantum mechanics wave-particle duality of energy, x-rays can also be referred to as particles ('photons'), their energy ranging between ca 10^{-1} and 10^2 keV (Seibert, 2004) .

X-ray emission is either produced by external stimulation of electronic transitions within the electron shell of atoms (element specific-peaks = 'characteristic radiation') and as a consequence of energy losses of accelerated charged particles when deflected or decelerated by interaction with matter (continuous emission = 'bremsstrahlung') (Omar et al., 2020).

X-rays permeate matter to an extent depending on their energy and on the atomic composition of this matter. This makes them a powerful tool for creating projectional radiographs. Standard technical applications use a high-vacuum tube fitted with a resistance-heated cathode, an anode with a cooling system, lead shielding to prevent diffuse radiation, and an exit window to direct the radiation onto the specimen to be examined (Kareem et al., 2017) (Figure 4).

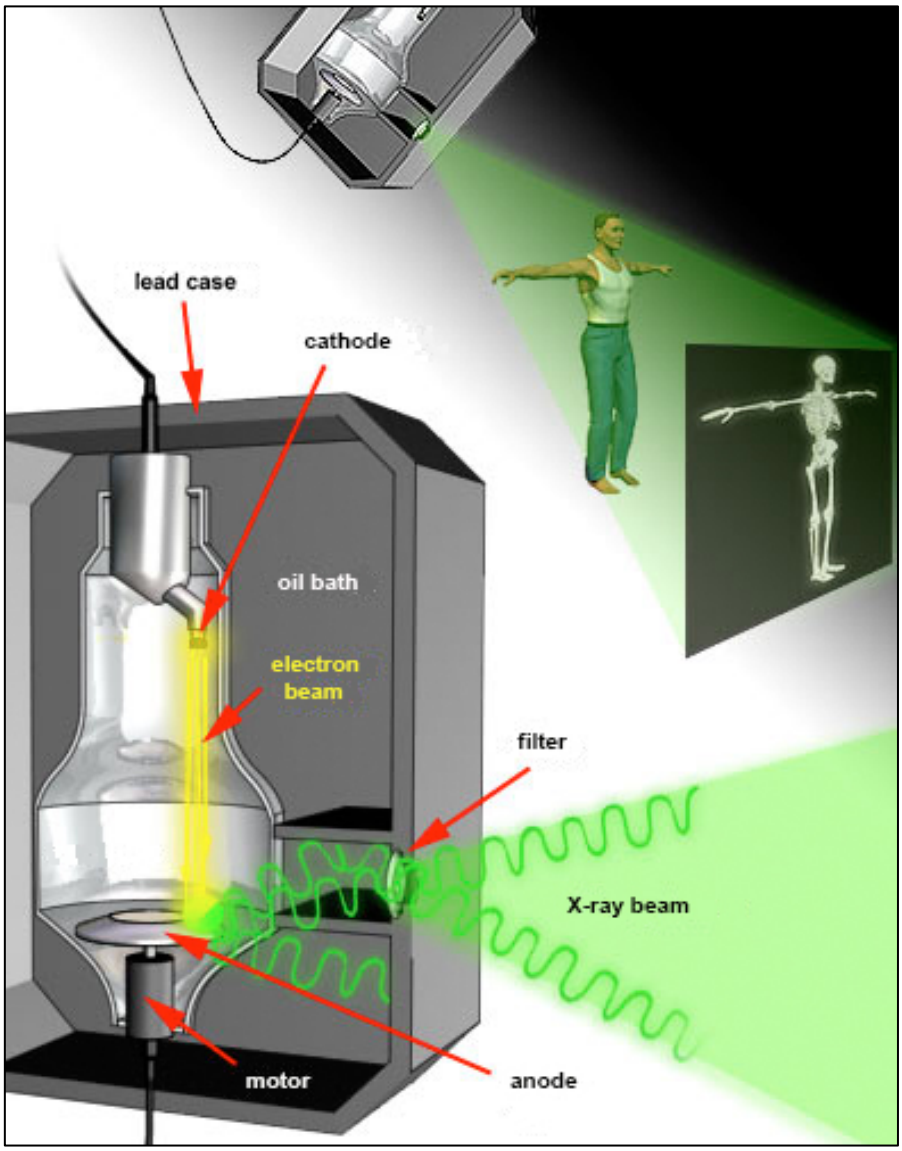

Figure 4: Schematic drawing of an x-ray tube (adapted after Harris, 2021)

The hot cathode is a source of thermal electron emission. By applying a high-voltage electric field, such electrons are accelerated onto the anode. Upon hitting the anode material, said processes (excitation of electronic transitions, electron deflection/deceleration) deliver a typical x-ray spectrum as a superimposition of characteristic and continuous radiation (Seibert, 2004) (Figure 5).

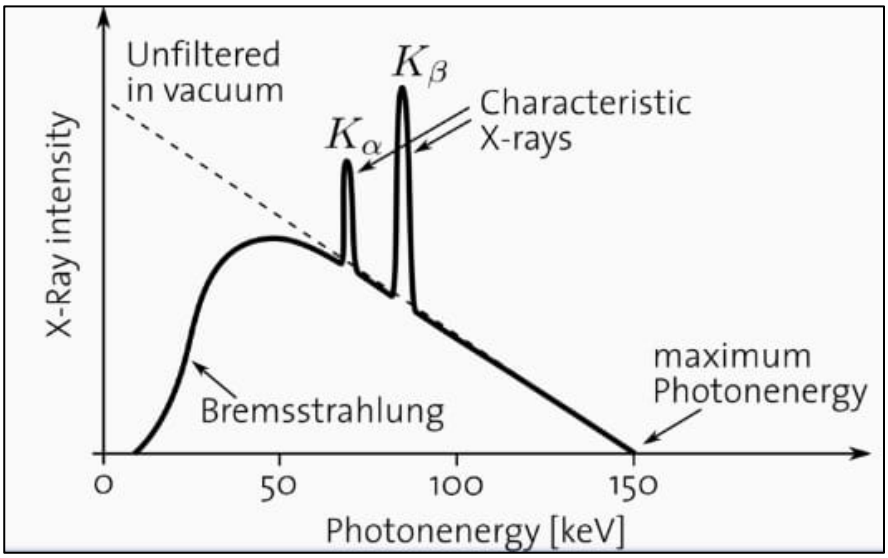

Figure 5: Schematic drawing of the x-ray spectrum (adapted after OncologyMedicalPhysics, 2021)

Only about 1 % of the electron energy is converted to x-rays, dissipating the rest as thermal energy, to be removed by the anode cooling system. The energy distribution of the emitted x-rays depends on the chosen accelerating voltage and the anode material. The shortest available wavelength (= highest energy) is given by:

$$\lambda_{min} = (c \,/\, \nu) = (h \times c)/(q_e \times V)$$

with λ: wavelength, c: velocity of light, ν: frequency, h: Planck constant, q_e: electron charge, V: accelerating voltage. Thus, the continuous ('bremsstrahlung') spectrum cuts off at the photon energy corresponding to the accelerating voltage, whereas the peaks are specific for the chemical elements present in the anode.

Historically x-ray images were recorded on photographic plates or film. More recent equipment makes use of solid-state flat panel detectors with or without intermediate scintillation, offering the advantage of direct input of radiograph raw data into dedicated IT systems for further processing (Seibert and Boone, 2005) (Figure 6).

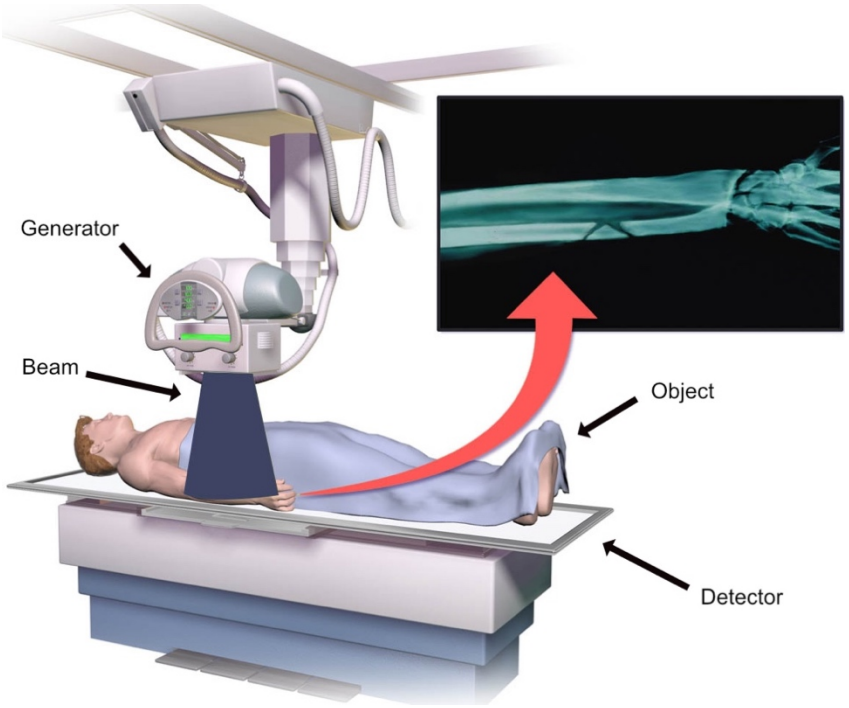

Figure 6: Schematic drawing of an x-ray detector (adapted after Aastha, 2020)

Volumetric mass density and proton number Z are the determinants of a specimen volume increment´s radiodensity. Higher radiodensity means the lower transmission of x-rays and hence less signal received by the detector, and vice versa. Thus the radiograph can be understood as a two-dimensional 'radiodensity map' of the area permeated by x-rays, rendering an image of the specimen´s internal structure.

Radiographs used in this research are all available in a standardized anteroposterior positioning to ensure forensic comparability. Furthermore, images from the collections of Poulton Chapel and St. Owen's Church were taken explicitly for this research by the author.

2.2.2 CT Imaging

Computed tomography (CT) is the advancement of the conventional radiographic two-dimensionality. In CT imaging, an x-ray beam rotates around the imaged body to generate multiple cross-sectional images (also called slices) of the object (NIA 2022). While a conventional x-ray machine sends x-rays directional using a fixed tube, a CT scanner uses a

motorized x-ray source, rotating around the gantry in which the body is located. After travelling through the body, the x-ray beams are absorbed by an equally rotating x-ray detector, which digitally transmits the information to a computer system (NIA 2022). With a sufficient number of consecutive slices, the body's three-dimensionality can be recreated by stacking the images digitally. The resulting high-quality CT images allow for a more detailed view of bones, blood vessels, soft tissues and organs (NIA 2022). As with the two-dimensional radiography, CT images used for this study were available in an standardized anteroposterior alignment.

2.2.3 Morphological Extraction and Evaluation

Maxillary sinus outlines are highly visible on x-ray and CT images. In contrast the lower limits of frontal sinus are often challenging to locate and have to be fabricated by drawing a horizontal line on the planum sphenoidale (Schüller, 1943), at the nasion (Brothwell et al., 1968), or close to the orbitals' upper margin (Libersa and Faber, 1958). The lower border of the maxillary sinuses is sharply defined through the dentition, while the lateral and upper limit is harder to register. An x-ray image is a two-dimensional image of a three-dimensional structure. Acknowledgement of this factor makes it easier to understand the visible structures on the image as different septations of the same sinus and helps to capture the sinuses body as a whole. Visibility of the maxillary sinuses air-filled space on CT images is not problematic because of the images' clearly defined borders between adjoining structures.

In this study, the morphologies get first extracted from the x-ray and CT images, and the geometrical shape approximation properties are then used to calculate differences (Figure 7). All digital radiographs and CT images were loaded into Photoshop (Adobe Inc., 2019) for first examinations. After detecting the maxillary sinus area, the images were prepared by adjusting the brightness, density, contrast, colour grades, gradation, and colour scheme of each digital radiograph. Thus, helping to identify the sinus structures for further processing. Utilizing a pen driven digitiser board (WACOM Intuous 2 DIN A5), the outer borders of each sinus are then traced in a separate layer on top of the digitized sinus in Photoshop. After deleting the layer

with the original radiograph, only the traced outline of the maxillary sinus remains and is coloured in. Images are then saved in .bmp and .psd format.

After extracting the images, morphologies of the maxillary sinus were then calculated using the software SHAPE ver. 1.3 (Iwata and Ukai, 2002). This software package simplifies the evaluation process as it applies elliptic Fourier descriptors to the biological morphology and computes the Fourier coefficients independently. Instead of manually calculating x and y coordinates and the offset of the contour, the program is generating contours from radiographic images, using elliptic Fourier descriptors and Fourier coefficients to apply principal component analyses automatically. This is especially useful as the maxillary sinus morphology does not possess any biological landmarks. All analyses are carried out on 20 harmonics to obtain a sufficient number of Fourier coefficients for each morphology. The decision of using 20 harmonics is influenced by Kuhl and Giardinas (1892) explanations on harmonic representation. Here, they demonstrate, that the number of harmonics is detrimental to the resulting shape description detail. It is shown that the predictable bound error increases with too low harmonic numbers. In turn, too high numbers of harmonics result in data that is overfitted of noise (Kuhl and Giardina, 1982), while the shape description does not improve significantly (Crampton, 1995). The use of 20 harmonics is frequently used as in this research to find a balance between morphological data loss and data overfitting (Christensen, 2004; Radinovic and Kajtez, 2021; Nino-Sandoval et al., 2021; Lestrel et al., 2011).

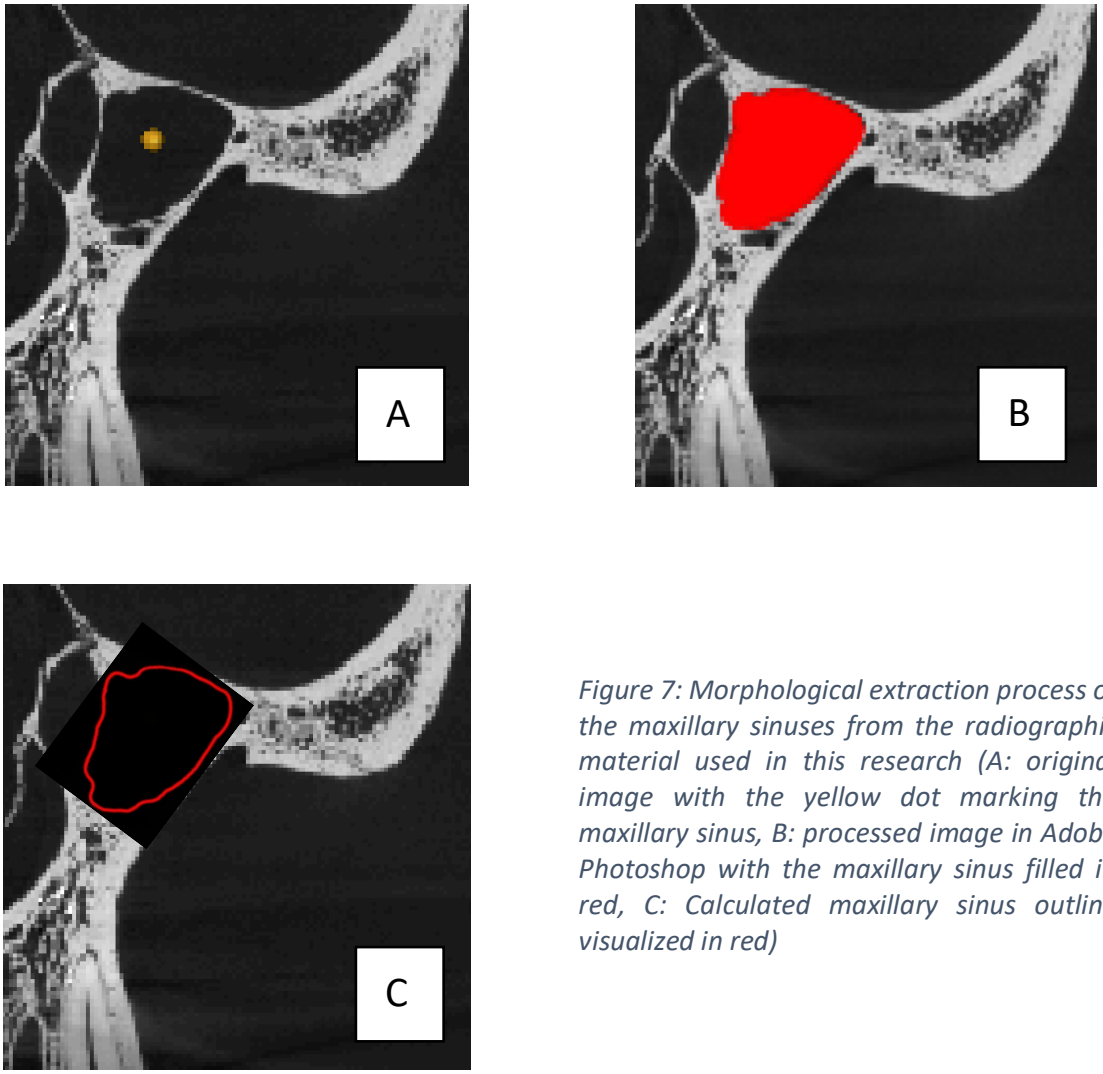

Figure 7: Morphological extraction process of the maxillary sinuses from the radiographic material used in this research (A: original image with the yellow dot marking the maxillary sinus, B: processed image in Adobe Photoshop with the maxillary sinus filled in red, C: Calculated maxillary sinus outline visualized in red)

The software SHAPE ver. 1.3 combines three applications necessary for elliptic Fourier analyses. The Chain Coder application extracts and records the sinuses contours from the .bmp file and describes the geometrical information via a coding system made of pixel (Figure 8). This coding system includes values ranging from zero to seven. In order to translate the morphologies into a chain code, an arbitrary starting point is automatically defined by the software. Using the chain coding scheme, the software converts all pixel of the morphologies outline into a numerical code. Thereby, the length of a chain code is defined by the amount of measuring points in the shape as well as the number of nodes on the coding scheme (Freeman, 1987). Simultaneously to describing the object's contour, the object is converted into a binary image. Then the sinuses' morphological variation is recorded. The Chain Coder application is running autonomously and automatically reduces noise in the images, traces the

morphology's contour, and saves the geometrical information of each morphology in an output file suitable for further analyses within the software package.

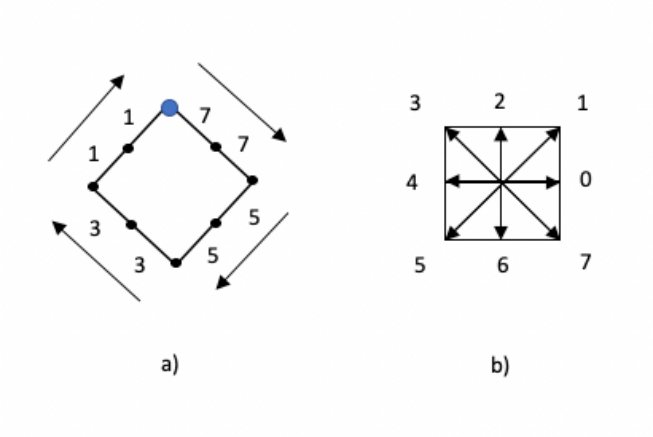

Figure 8: Chain code example after Freeman 1978. a) Chain coded object with the blue dot marking the starting point. Object is measured in clockwise direction resulting in a chain code of 77553311. b) Reference pixels and the corresponding chain code values to measure objects (adapted after Skaudickas et al., 2014)

The second application in the software package is the program Chc2Nef. It is used to further process the resulting chain code file (Figure 9). An elliptic Fourier transformation programme can calculate the normalised elliptic Fourier descriptors with the information delivered by the chain code. This procedure is per the procedure by Kuhl and Giardina stated in 1982. The mathematical normalization is based on the first harmonic ellipse corresponding to the first Fourier approximation on the contour information. For description matters, the outlines are described on 20 harmonic numbers.

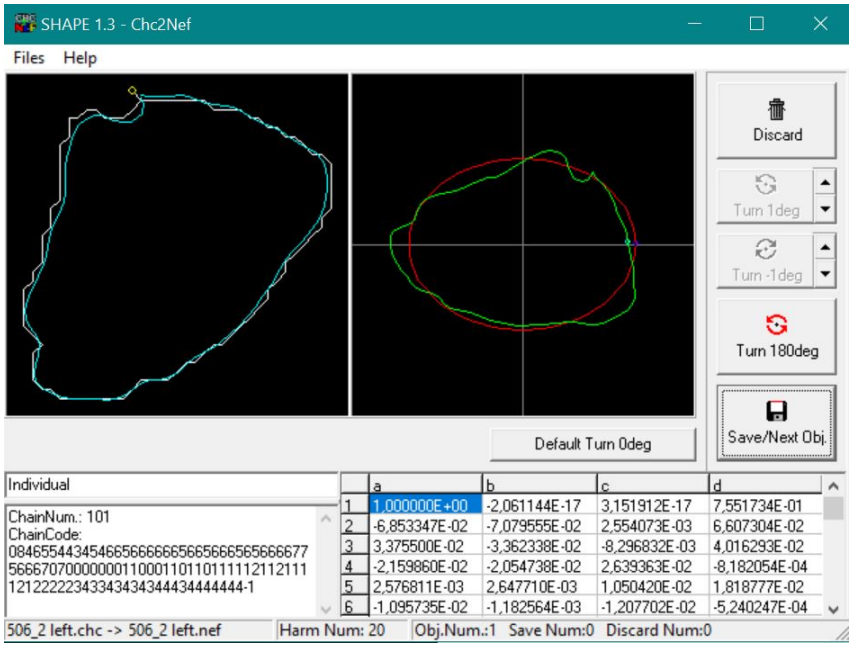

Figure 9: Digitization of the morphology in SHAPE ver. 1.3 (program: Chc2Nef) (Iwata and Ukai, 2002). Blue and green lines visualise the calculated maxillary sinus outline as seen in this software. The numerical chain code value of the object is accessible in the lower left box. Information on the normalised elliptic Fourier descriptors is available in the lower right box

The next automated step in the SHAPE ver. 1.3 software package is the Prin Comp application. This application executes the principal component analysis (PCA) of the normalised coefficients of the elliptic Fourier descriptors as the number of coefficients per morphology is too high to be efficient in effective interpretation (Iwata and Ukai, 2002). The PCA reduces the dimensionality of the data and condenses the high number of correlated variables per morphology by simultaneously preserving sufficient variation among the dataset. The resulting effective principal components can then be used for morphological evaluations and are based on the elliptic Fourier analysis's variance-covariance matrix. The first principal component (PC) possesses the most available variance. Therefore, each following PC holds highest variance under the limitation to be orthogonal to its prior component (Iwata, 2002). Using the software Prin Print, the shape variation accounted for each principal component is visualised (Iwata and Ukai, 2002).

2.2.4 Testing the Comparability of Radiographs and CT Scans

While x-ray images project the imaged structures simultaneously on a two-dimensional plane, CT scans are perceived as a series of x-ray images taken from different angles and assembled as a three-dimensional model. Therefore, in x-ray images, all structures are stacked with softer edges whereas, in CT images, it is possible to scale through individual slices, acknowledge each structure independently with sharp borders, and understand the relationship between them. The display difference makes it difficult to compare and utilize both types of images within the same study.

Next to their easy accessibility and low-cost application, sinus morphologies can be extracted quicker from x-ray images than from the more expensive CT scans. As all structures are projected simultaneously on the same plane, the outmost borders of the morphologies can be traced in a simple layering system in Photoshop as described in 2.2.3 Morphological Extraction and Evaluation.

Extraction of morphologies on CT scans is more time-consuming than on x-ray images. Tomography and the DICOM view make it impossible to simply trace the outmost borders. Before evaluating morphologies anteroposterior, the outline has to be observed from a superior angle. Now, the three-dimensional view allows browsing through each slice starting superiorly. While scanning the slices, every slice is marked that displays the most morphological expansion of the sinus in any direction. Then, when switching to the anteroposterior view, markings are transferred, and slices are scanned in an anteroposterior direction (Figure 10). Following, sinus morphologies on each marked slice have to be traced as described in 2.2.3 Morphological Extraction and Evaluation. The number of markings within one individual depends on the specific morphology and is not standardized.

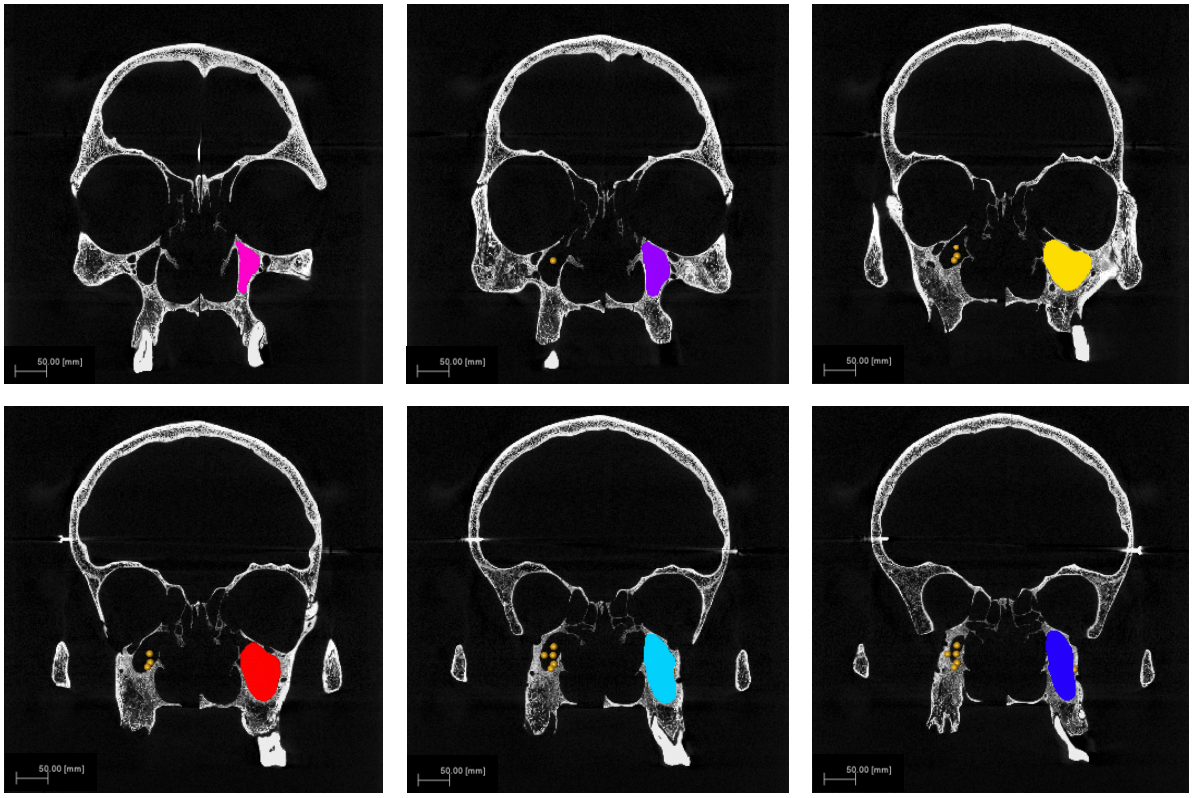

Figure 10: Anteroposterior view of all CT image slices with the most morphological expansion of the maxillary sinus in any direction in the same skull of one individual. Upper left image marks the most anterior CT slice of the individual with the maxillary sinus coloured in pink. The maxillary sinuses coloured in purple, yellow, red, light blue, and dark blue are respectively taken CT slices in posterior direction. The one coloured in dark blue is the sinus of the individual taken the most posteriorly

After extracting the morphologies on each marked slice, sinus outlines are stacked to re-create the original morphology. As the last step, this original morphology, created by all morphology slices layered on top of each other, is traced (Figure 11). This technique makes it possible to project the three-dimensionality of a CT image onto a two-dimensional plane. Thereby, making CT and x-ray images comparable.

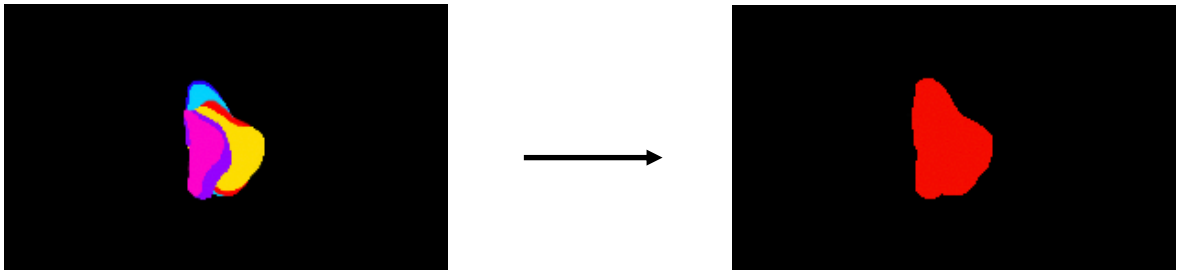

Figure 11: Layering of the in figure 10 extracted maxillary sinus morphologies of one individual on different CT image slices. The layers are then merged in the right image with a red block colour to create the individual's whole maxillary sinus morphology

This morphological extraction method in this research was used for CT images of the Osteological Collection, University of Tübingen and the Anatomical Collection, University of Leipzig.

2.2.5 Elliptic Fourier Analysis

Morphological analyses are essential in taxonomic research. Fourier mathematical applications allow describing any two-dimensional forms without specific biological landmarks as an infinite linear combination of cosines and sines (Haines and Crampton, 2000). Therefore, Fourier analysis is an essential mathematical application for naturally irregular shaped structures as maxillary sinus morphologies.

The most common Fourier shape method is the elliptical Fourier analysis. The method measures contour shape variations and converts the contour of an object into multiple closed curves (harmonics). These harmonics vary in orientation, shape, and size and recreate the objects original shape (Yoshioka et al., 2004). Using elliptic Fourier analysis, the morphologies contour can be normalised and simplified (Kuhl and Giardina, 1982). After reconstructing the shape's contour, a set of points within the coordinates of the analysed contour are applied. This Fourier transform process allows quantifying the object's contour (Hâruta, 2011). Using sequences of sums correlated to ellipses, Fourier coefficients, Fourier constants, or spatial

coordinates can be described. This results in digitised data, recorded as contour coordinates (Hâruta, 2011).

Fourier shape analyses describe contour outlines as a polygon digitised in an *x* - *y* coordinate system. The contour is broken down into harmonic curves within this coordinate system described by Fourier coefficients (Haines and Crampton, 2000). Those Fourier coefficients represent angular offset and amplitude concerning each curve's phase angle (starting position). The *x* and *y* coordinates pass along the morphologies' contour, measuring it clockwise (Iwata et al., 2015). The contour of the shape is then defined by a chain code, which describes the shape's numerical description of the geometrical information (Freeman, 1974). In the methodology following Kuhl and Giardina (1982) the shapes are a series of ordered points which x- and y- coordinates are measured clockwise. Important to note: the starting point of those chain code measurements is arbitrary (Iwata 1998). Using the Fourier transformation of each shapes chain code, the coefficients of elliptic Fourier descriptors are calculated (Iwata 1998). Elliptic Fourier descriptors separate bi-dimensional contours and describe those using periodic functions. Those periodic functions of *t* describe the variance of coordinates and approximate those with Fourier series (Kuhl and Giardina, 1982; Caple 2017):

$$x(t) = A_0 + \sum_{n=1}^{k} (A_n \cos kt_n + B_n \sin kt_{n-1})$$

$$y(t) = C_0 + \sum_{n=1}^{k} (C_n \cos kt_n + D_n \sin kt_{n-1})$$

where A_0 and C_0 are constants as defined by Kuhl and Giardina (1982), characterising *x*- and *y*-coordinates of the forms' centre. Furthermore, *t* is the outline points chord length and A_n, B_n, C_n, as well as B_n are the Fourier coefficients that define the harmonics to the *n*th order.

The coefficients within these Fourier series are standardised after Kuhl and Giradina (1982) based on the ellipse of the first harmonic (Iwata 1998). As an effect of this standardisation, the coefficients become independent of shift, rotation, chain coding starting point, and size. Therefore, they act as transformable variables and can be further processed in principal component (PC) analyses to examine their functional relationships (Yoshioka et al., 2004).

Principal component analyses can be applied to reduce the number of variables available to simplify the processing. Therefore, principal component analyses are similar to exploratory factor analyses (Iwata and Ukai, 2002). Artificial variables are created by reducing variable sets into principal components. These new variables contain the whole variance of the original variables; however, as the data is compressed, it simplifies its processing (Iwata and Ukai, 2002).

Elliptic Fourier analysis and Fourier descriptors evaluate shape variation and classification in multiple research fields but are especially popular in natural sciences. Using these tools of description to track shapes of plants and animals as a whole or in separated parts (Zhan and Wang, 2012; Hâruta, 2011; Eguchi and Ninomiya, 2008; Haines and Crampton, 2000; Iwata et al., 2015; Mori et al., 2005; Palmer et al., 2004; Sayıncı et al., 2015; Yoshioka et al., 2004). For example, to assess clam shapes and determine their origin (Palmer et al., 2004), investigate environmental and genotypic effects on petal shapes (Yoshioka et al., 2004), predict rice shapes in the context of genome polymorphisms (Iwata et al., 2015), and check shape differences in hazelnut cultivars (Sayıncı et al., 2015). Especially irregular shapes can be tracked, with elliptic Fourier descriptors being quantitatively characterised in the analysis. Elliptic Fourier descriptors/coefficients normalise the contour of the analysed biological shape by eliminating variability, dimensional deformations, rotation, and translation (Hâruta, 2011). For example, Fourier analyses have been applied in human identification when assessing the uniqueness of frontal sinuses (Christensen, 2005; Cox et al., 2009).

Data deriving from elliptical Fourier analyses can be interpreted with clustering methods. Various clustering methods use Euclidean geometry in order to describe similarities, differences, and relationships (Liberti et al., 2014). These methods are traditionally applied in biology and other life sciences, as well as for medical purposes. Over time applications of clustering analysis spread into social and behavioural sciences. As a tool for pattern recognition, cluster analyses were applied in engineering and, in addition to that, inspired their application in informative science and with forensics (Anderberg, 2014).

2.3 Uniqueness Testing

To analyse the morphological uniqueness of the maxillary sinuses, an experimental design had to be created that sufficiently simulates real-life applications. As most of the CT and X-ray images are not explicitly taken for this study, except for the collections of Poulton Chapel and St. Owen's Church, only one set of images is available for each individual. However, in real-life scenarios, the medical examiner has two sets of images at their disposal. One set taken antemortem and a second set taken postmortem. As this was impossible to re-create with this studies dataset, an ante-, and postmortem situation was generated by extracting the morphological data twice from the images. The first round of extractions simulates the antemortem dataset with 1,105 sinus morphologies, while the second round of extractions simulates the postmortem dataset with the same amount of sinus morphologies (Figure 12).

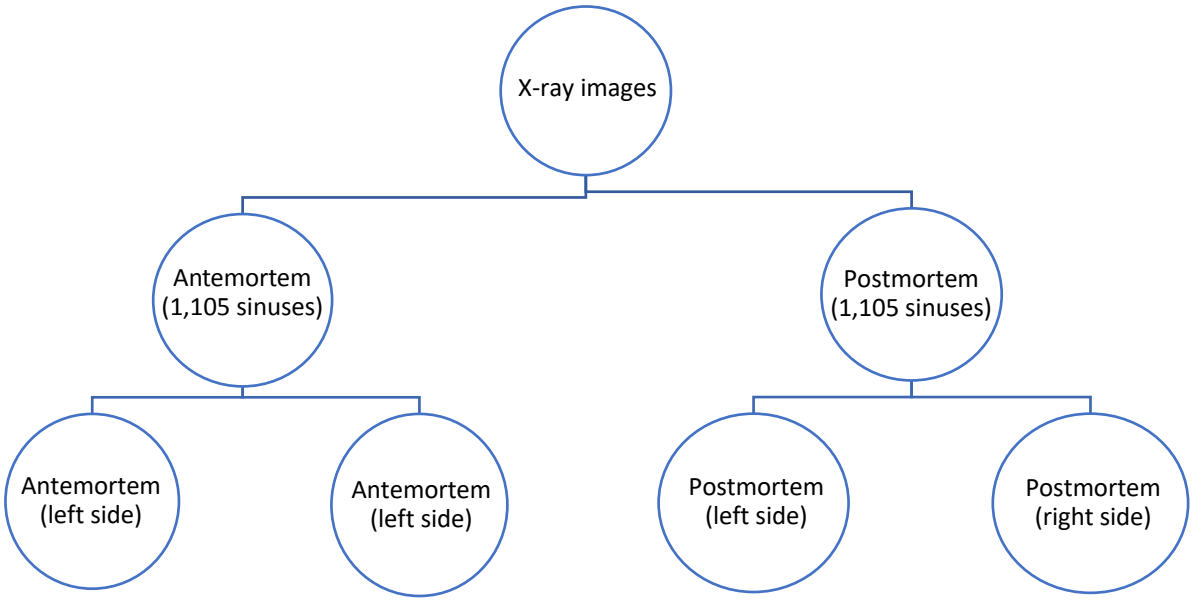

Figure 12: Schematic representation of the distribution and amounts of maxillary sinuses used for the ante- and postmortem dataset on left and right side in the study of uniqueness testing

The premise of sinus comparison identification methods on x-ray images is the standardised imaging of the structure. Ensuring standardisation, practitioners use an anteroposterior alignment when imaging human skulls for identification purposes (Silva et al., 2009). As the skull's standardised orientation is given in the images used, the twofold extraction simulates this scenario.

Of course, this study acknowledges the limitations of the experimental design, as the images used in this study were not taken during different times of the individuals' lives. However, the approach of independently extracting morphological data twice from the radiographic material is a beneficial first step testing the methodological approach.

It is important to note that the antemortem dataset was not simply duplicated to create the postmortem dataset, but each morphology of the postmortem dataset was extracted independently following the guidelines in chapter 2.2.3 Morphological Extraction and Evaluation. To ensure a blind study, each X-ray and CT image was anonymised after the first round of extractions by changing the image name to a numerical code. Furthermore, the order of images was changed randomly between first and second extraction to avoid anticipation of the order of morphologies and, therefore, the shape to extract. With 1,105 sinus morphologies to extract twice (first extraction builds the antemortem dataset; second extraction builds the postmortem dataset), sinus morphologies could not be predicted. Utilizing a code key, file names were changed after extracting the morphologies, thus enabling correct assignment of the same individuals' ante- and postmortem sinus morphologies.

2.3.1 Statistical Analysis

After extracting the morphologies and evaluating the elliptic Fourier coefficients, the uniqueness of maxillary sinus morphologies was assessed using different statistical methods (Table 4). All analyses were executed separated into right-sided morphologies and left-sided morphologies. As a first step for evaluation, the principal component data was tested for normality and corrected using the Johnson transformation (Johnson, 1949). Following, Analyses of Variance (One-way ANOVA) statistics were applied in SPSS v.27, to evaluate morphological differences between populations and age groups. As individuals from the populations of Poulton Chapel and St. Owen's Church are combined as one population due to the sample size, a total of 10 populations is examined. Furthermore, used for this part of the study is an age classification in seven clusters. Ages start above year 20 in cluster one and cluster seven incorporates the indeterminate specimens (Table 5). No individuals aged

younger than 20 years are used for this study. Additional scatterplots help to further get familiar with morphological variability and differences across populations.

After understanding the general structure of the populations, uniqueness was assessed among the ante- and postmortem datasets by measuring and correlating Euclidean distances on principal components between the morphologies in SPSS v.27. With help of the Euclidean distance the shortest distance between two morphologies in the Euclidean space is measured. Applying neighbour joining-clustering, Mahalanobis distances between the morphologies were then visualised in PAST v.405. Mahalanobis distances are frequently used in geometric morphometrics and is used here to measure the distance between maxillary sinus morphologies in a multidimensional vector space. Neighbour-joining clustering allows visual distinguishing between similar and different morphological groups. Here, sinus morphologies are grouped according to shape differentiation based on each morphologies' individual elliptic Fourier descriptors to form a hierarchy of groups (Hartigan 1975, Pietrusewsky, 2007).

Table 4: Statistical analyses used in the uniqueness testing study

Statistical Evaluation Uniqueness Testing
Evaluation of morphological variation on PC scatterplots
ANOVA statistics between all populations
ANOVA statistics between age categories
Correlation of Euclidean distances between the ante- and postmortem dataset
Calculation of Mahalanobis distances between the ante- and postmortem dataset

Table 5: Age classification used in the uniqueness testing study with cluster numbers and responding age categories

Cluster Number	Age in years
1	20 - 30
2	31 – 40
3	41 – 50
4	51 – 60
5	> 60
6	Indeterminate

2.4 Case Study

This research proposes identifying maxillary sinus morphologies on the premises that every individual's maxillary sinus morphology is unique and that the morphologies stay comparable throughout an individual's life.

The experimental design for this research's uniqueness testing is appropriate for the scope of this study however; it is lacking real life applications as the antemortem and postmortem datasets originally derive from the same x-ray or CT image. Therefore, it is crucial to test uniqueness in a more realistic case application. To this effect, eight individuals deriving from the Bolton Brush Growth Collection and Oregon Growth Collection were used to simulate a more applicable ante- and postmortem scenario.

In this case study, two images of every included individual, taken during different stages of their lives, are used for examinations. Individuals are chosen for this study with their antemortem radiograph taken around their 20th year of age and the subsequently available adult radiograph simulating the postmortem counterpart. The second image is not an original postmortem image but part of the collection's growth study (Table 6). Although the individuals were still alive at the time of the second radiograph, the pass of time during the images makes the images suitable for this case study.

Table 6: Sample of the case study including ages within the ante- and postmortem dataset as well as sex per individual

Collection	Individual	Antemortem (age in years)	Postmortem (age in years)	Sex
Bolton-Brush Growth	CS001	21	49	Male
Bolton-Brush Growth	CS002	20	27	Male
Bolton-Brush Growth	CS003	20	22	Male
Bolton-Brush Growth	CS004	20	24	Female
Bolton-Brush Growth	CS005	20	22	Female
Bolton-Brush Growth	CS006	20	25	Male
Oregon Growth	CS007	25	28	Male
Oregon Growth	CS008	25	29	Female

2.4.1 Statistical Analysis

As with the previous studies, the data was tested for normality and corrected with help of the Johnson transformation in SPSS v.27. Following, Euclidean distances are measured and correlated between morphologies from both datasets in SPSS v.27. This gives an insight into which ante- and postmortem maxillary sinus morphologies from which individuals 'match'. As a next step, a neighbour-joining clustering visualises the Mahalanobis distances between the ante- and postmortem morphologies. Lastly, morphological variability is visualised (Table 7).

Table 7: Statistical analyses used in the case study

Statistical Analysis: Case Study
Correlation of Euclidean distances between the ante- and postmortem dataset within populations
Calculation of Mahalanobis distances between ante- and postmortem datase
Evaluation of morphological variability

2.5 Intra- and Inter-Observer Reliability

As this project proposes maxillary sinus morphological evaluations as a means for identification, reproducibility is of the utmost importance. In the context of forensic investigations, methods need to be accurate and precise to resist cross examination in court.

The confidence into a method rises proportional to the introduced error however; absolute agreement between the observers is almost never achieved (McHugh, 2012) and does not automatically stand for an extraordinary methodology. As multiple observers, by matter of human variability and interpretation, will determine the outlines of the maxillary sinus morphologies slightly different, the degree of agreement between the observers needs to be measured.

When assessing skeletal material, the margin of error is sizable. Different observers can make mistakes by evaluating skeletal landmarks, handling the tools, or interpreting radiographic images. Especially when untrained, the evaluation of radiographic and CT images can be an obstacle. As radiographic images display three-dimensional objects on a two-dimensional plane, it is often difficult to differentiate between structures. However, in context of this study it is important to ensure reproducibility of the method. To address the topic of reproducibility, 20 % of the morphologies used for this study have been reassessed by the author as well as independent observers. Observer 1 (OB1) and observer 2 (OB2) both studied towards a MSc at Liverpool John Moores University in Forensic Anthropology at the time the research was conducted.

Before collecting data, the observers were trained in interpretation and capturing of the maxillary sinus morphologies on exercise images. Naturally, those images were excluded from the reproducibility study. All observers had no particular experience in interpreting x-ray images. During the course of the training multiple potential sources of error were identified: inadequate drawing software, inexact capturing and drawing of the morphology, insecurity when inspecting and identifying the morphology. However, the observer's quick improvement of capturing and interpreting maxillary sinus morphologies on radiographic images suggests a steep learning curve. The assessment of a quantity of images improves interpretation skills extremely.

2.5.1 Statistical Analysis

In this part of the research, the collection of morphologies was compared to the authors second evaluation (intra-observer reliability) as well as to the assessments of the independent observers (inter-observer reliability). Before applying Cohen's Kappa statistics, principal components were tested for normality and corrected using the Johnson transformation in SPSS v.27.

Degrees of intra- and inter-rater agreement are evaluated applying Cohen's Kappa statistics in SPSS v.27. Intra-rater reliability is calculated on the two evaluations of the author, while inter-rater reliability is analyzed on Cohen's Kappa statistics of each observer in comparison to the first author evaluation. Applying Kappa statistics, the level of agreement between two raters extracting the maxillary sinus morphologies was calculated. Results of the Cohen's Kappa statistics can range from -1 to +1 and interpretations of the values are proposed by McHugh (2012) (Table 8).

Table 8: Cohen's Kappa values and corresponding levels of agreement used in the intra- and inter-observer reliability study; (directly after McHugh, 2012)

Cohen's Kappa Values	**Level of Agreement**
0.01 - 0.20	None
0.21 - 0.39	Minimal
0.40 - 0.59	Weak
0.60 - 0.79	Moderate
0.80 - 0.90	Strong
Above 0.90	Almost perfect

2.6 Age Estimations

The development of maxillary sinuses is relatively well documented using volumetric approaches and measurements. However, only little research gives insights into morphological changes during development and growth. As with the uniqueness test, morphologies were extracted and separated into right and left-sided sinuses as only the same sided sinuses are set to compare. To ensure a blind study, all images were coded with a numerical number, and sinus morphologies were extracted randomly throughout all individuals age stages. The sample of this study includes 2.112 individuals from the three longitudinal growth studies of Bolton-Brush Growth, Oregon Growth and Burlington Growth (Table 3). Morphologies were categorised according to the age at the time the radiograph was taken. In total eight age clusters were developed for classification. A detailed distribution of the sample among the age clusters is available in section 6.1 (Age Cluster System).

2.6.1 Statistical Analysis

Measurement and correlation of Euclidean distances in SPSS v.27 demonstrate morphologic relationship between the sinuses of each individual. Euclidean distances between each individual's differently aged sinus morphologies are then used on the first principal component to understand age related changes (Table 9). Using the means per age cluster is beneficial as it delivers a more representative view of the typical values in the dataset. Using mean values minimises outlier and extreme value impacts, which increases the representativeness of the overall dataset (Zelditch et al., 2012). Therefore, mean value analyses are used in this study to allow a clearer and more scatter free representation of the data. Data availability for every individual varies significantly as for some individuals, there are seven differently aged x-ray images available, whereas, for others, only two images are present. As the ages of when the individuals were imaged differ, an age cluster system needs to be developed to sufficiently reflect the age distribution among the populations and understand the data set's composition, with age and sex being determinant factors (Table 9). Furthermore, examinations of the age clusters were undertaken to identify growth patterns.

The term 'growth rate', as used in this study, refers to the change of Euclidean distances throughout the individual's lifetime. Euclidean distance correlations propose a simple way to evaluate the distance between the morphologies as they map the distance between two items in a multidimensional space. The smaller the correlation factor, the more similar the objects. In order to calculate the distance, the results of the elliptical Fourier analyses are correlated by individual. As multiple x-ray images throughout each individual's lifetime and especially childhood exist, the correlated change of Euclidean distances can be mapped by individual. In this study's correlation, the youngest morphology of an individual acts as a baseline. Therefore, the values of the subsequently aged morphologies always account for the change dependent on the youngest morphology.

To understand the difference of Euclidean distances among age clusters, the mean of Euclidean distances within each age cluster was calculated. The development of averaged distances within populations and sexes with increasing age clusters is then made visible by applying a linear regression: $y = mx + b$, in which *y* describes the average Euclidean distances, *m* is the gradient, and *b* is defined as the y-intercept. Furthermore, the gradient in this formula is used to describe the growth rate in this study: $Growth\ Rate = \Delta ED : \Delta AC$, in which *ED* describes the Euclidean distances and *AC* the age cluster. Pearson's correlation coefficients are calculated to measure the linear association between the age clusters and the averaged Euclidean distances (Table 9).

Table 9: Statistical analyses used in the age estimation study

Statistical Analysis: Age-at-death Estimation
Development of age cluster system
Linear regression of Euclidean distance means per age cluster by population and sex
Calculation of Pearson's correlation coefficient per population and sex
Correlation of growth rates (gradients) per population and sex

Chapter 3 Results Part I: Uniqueness Testing

This chapter is concerned with the results of the statistical analyses carried out for the first part of this research: the uniqueness testing. Firstly, the independent morphological variation among the sinuses as well as the degrees of morphological difference within each analysed population is introduced in section 3.1. These evaluations build the foundation of all analyses. as similarities between morphologies prevent their use for human identification.

In section 3.2, testing the populations for their uniqueness is introduced by analysing morphological differences between all populations. Section 3.3 then unites the previous analyses and exhibits the results of the uniqueness test comparisons.

To maintain consistency throughout this research, the results in this chapter are presented in a standardised manner. Morphological evaluations are displayed as a whole dataset with no differentiation into male and female samples (with the exception of the Principal Component Clusterings). Furthermore, all results are described independently for each evaluation's right and left-sided maxillary sinus morphologies. Analyses were carried out using the output data from the Elliptic Fourier Analysis in the software Shape ver. 1.3. For a normal distribution, all data was corrected using the Johnson transformation.

3.1 Intra Population Analysis

3.1.1 Morphological Variation

Results of the intra populational analyses are displayed in text as well as in appendix 1. Morphological variation is presented by the first four effective principal components calculated from the chain code by the software SHAPE ver. 1.3. The main variation is illustrated by PC1 showing major differences in two dimensions. A minor variation is shown by PC2, PC3, and PC4. This distribution of variation shows that the first four principal components are the essential principal components for explaining the variation in sinus shapes and are therefore used for further statistical analyses.

Percentages among the four PCs of the populations used for this study show a reasonably even distributed morphological variation (Table 10 & 11). PC1 to PC4 cover over 81 % of the variation for both left and right-sided morphologies. Outlines of morphologies for each population reconstructed from the elliptic Fourier data can be found in Figure 13 to 32 in appendix 1.

Table 10: Distribution of left sided maxillary sinus morphology variation among 4 principal components in the uniqueness testing study (in percentages)

Population	**PC1 (%)**	**PC2 (%)**	**PC3 (%)**	**PC4 (%)**	**Cumulative (%)**
Poulton & Gloucester	42.94	27.86	15.15	6.48	92.44
Florence	36.83	21.89	15.23	7.61	81.58
Siracusa	42.41	25.08	12.44	7.01	86.95
Chelsea Old Church	41.97	25.19	14.21	5.62	87
St. Mary Spital	41.49	27.5	16.58	3.11	88.7
St. Bride's Lower Churchyard	42.05	25.26	19.01	2.88	89.2
Osteological Collection, University of Tübingen	42.22	21.3	16.33	5.96	85.82
Anatomical Collection, University of Leipzig	35.69	30.07	14.53	3.76	84.06
Bolton-Brush Growth	46.92	23.6	18.91	3.33	92.77
Oregon Growth	45.97	29.27	15.4	2.89	93.54

Table 11: Distribution of right sided maxillary sinus morphology variation among 4 principal components in the uniqueness testing study (in percentages)

Population	PC1 (%)	PC2 (%)	PC3 (%)	PC4 (%)	Cumulativ (%)
Poulton & Gloucester	51.81	24.21	11.45	7.02	94.51
Florence	37.90	23.54	14.91	5.59	81.96
Siracusa	51.18	22.31	12.24	4.97	90.72
Chelsea Old Church	40.87	21.43	17.99	7.52	87.82
St. Mary Spital	47.51	20.92	17.43	3.74	89.61
St. Bride's Lower Churchyard	44.1	24.1	15.7	3.67	87.59
Osteological Collection, University of Tübingen	39.2	22.6	17.02	5.67	84.51
Anatomical Collection, University of Leipzig	39.78	23.6	16.67	4.17	84.13
Bolton-Brush Growth	46.9	28.66	15.32	2.67	93.56
Oregon Growth	46.22	30.1	14.6	2.63	93.56

3.2 Inter Population Analysis

3.2.1 Principal Component Clustering

Figure 33 to 38 (appendix 1) illustrate distribution results for left and right-sided morphologies on two principal components. The scatter plots are documenting the dispersion of the 1,105 sinuses used for the uniqueness testing by individual, population, sex, and age.

Observed distributions by population indicate a loose association between all populations. For left-sided morphologies (Figure 33), populations of St. Mary Spital and St. Bride's Lower Churchyard hold the biggest fraction of analysed morphologies. However, there is no clear separation between those two populations among the two PCs and both exhibit morphologies located outside of the main cluster. Further isolated positions are inhabited by morphologies of Florence and Siracusa. Distributions of Bolton-Brush Growth and Oregon Growth do not necessarily reflect a geographic proximity. However, for right-sided morphologies (Figure 34), those two North American populations tend to be clustered together more closely. As with

the left sided morphologies, positions of the right-sided morphologies deriving from St. Mary Spital and St. Bride's Lower Churchyard display the highest amount of isolated morphologies outside of the main cluster. Populations of the Osteological Collection, University of Leipzig and the Anatomical Collection, University of Tübingen tend to be clustered closer together, while the sample size of morphologies from Poulton and Gloucester is too small to make an adequate statement.

Distributions clustered by sex present a loose association between the morphologies for both left and right sides. Both also indicate a meagre amount of indeterminate morphologies. For the left side (Figure 35), more males tend to hold isolated positions, while on the right side (Figure 36), this is distributed more evenly between females and males. Clustering by age presents an overall flowing distribution. As in the previous scatter plots, no immediate clusters are evident on both sides. However, indeterminate morphologies are evenly distributed.

For left-sided morphologies (Figure 37), isolated positions tend to be aged in the group of 20 to 30-year olds. On the right side, morphologies located outside of the main cluster include the age group 20 to 30 as well as 50 to 60 (Figure 38). Furthermore, the group of over 60-year olds is located centrally for both left and right-sided morphologies. Information on the distribution of the sample by age can be found in Figure 39.

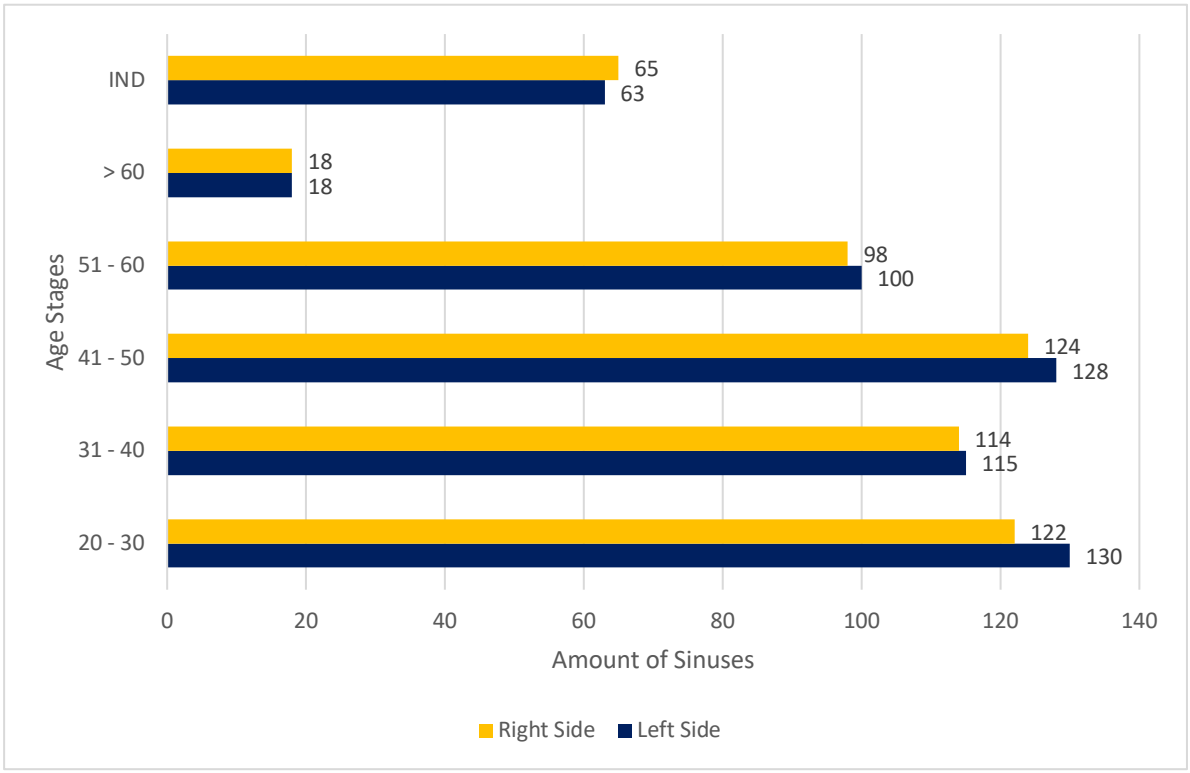

Figure 39: Bar chat illustrating the age distribution of the sample used in the uniqueness testing study

3.2.2 Morphological Differences

Inter population analyses are divided into three sections, all accessible in appendix 1 of this study. The first analysis is an ANOVA of all populations to continue understanding significant morphological differences between maxillary sinuses of all populations on the left and right-sided along the four principal components. Here, results show significant differences between with p-values below .05. Seen for example with the population analysis on the left side $[\mathrm{F}(9{,}546) = .400, \mathrm{p} = .009]$ (Table 12). Remaining significant analyses by populations on left and right side are accessible in appendix 1 in tables 13 to 19.

As a next step, morphological differences were analysed among age categories on all four principal components. Results of the ANOVA show significant morphological differences with p-values below .05. An example is the analysis among age categories on the left side with $[F(5{,}550) = .023, p = .022]$ (Table 20). Remaining analyses among age categories are accessible in appendix 1 in tables 21 to 27. The age distribution of the sample is accessible in Figure 39.

3.3 Uniqueness Test Comparison

Examinations of the data so far indicate a high reliability, which allows the uniqueness testing to commence. Due to the vast amount of morphologies evaluated and the subsequent size of the tables and graphs, only referencing pieces of the tables and graphs are included in this thesis. However, the entire data is permanently stored in a dropbox, accessible at: https://www.dropbox.com/sh/a8il32z7iqyjsei/AACKOzNS3vBuvAVLEWSwZ5Vda?dl=0.
A QR-code to access all data is accessible in Figure 40 in appendix 1.

Testing of morphological uniqueness is essential when evaluating the potential of the proposed method. As mentioned before, it is vital to detect whether morphological matches outside of each ante- and postmortem pairings exist, as this declares the method invalid. To test this, Euclidean distances between the antemortem- and postmortem datasets, resulting from the elliptic Fourier analyses, are correlated in a dissimilarity matrix. The dissimilarity ratio between the Euclidean distances is expressed in a numerical spectrum starting with 0.000 indicating morphological accordance of 100 %. The higher the numerical value, the less morphological accordance is indicated. All Euclidean distance results in this study are rounded to three decimals.

Excerpts of the correlations for left and right-sided sinus morphologies is available in Table 28 & 29. Entire tables are accessible through QR-codes in appendix 1 (Figure 41 & 42) or directly through this link: https://www.dropbox.com/scl/fo/cpqujonuympjhcgp45ale/h?dl=0&rlkey=1qzhq4rqenfdodm0ia6xl4jc8. Correlations of Euclidean distances between the ante- and postmortem datasets indicate that maxillary sinus morphologies are unique. Total matches are only achieved between left and right-sided morphologies for each ante- and postmortem pair. This is indicated by the distance value of 0.000. Degrees of difference vary among the other pairings, and distances as low as .008 for left-sided morphologies and .006 for right-sided morphologies can be recorded (see table online). However, total matches are only available between each antemortem morphology and their respective postmortem counterpart. Matches of 100%, marked with the value 0.000, are highlighted in the correlation tables in red.

Table 28: Excerpt of the correlation of Euclidean distances of left sided maxillary sinus morphologies used in the uniqueness testing study

Excerpt Proximity Matrix

Euclidean Distance

	555:PM1	556:PM2	557:PM3	558:PM4	559:PM5	560:PM6	561:PM7	562:PM8	563:PM9	564:PM10
1:AM1	0.000	0.332	1.051	0.093	0.552	1.857	0.226	0.926	1.559	1.631
2:AM2	0.760	0.000	1.287	0.328	0.788	2.093	0.010	1.162	1.795	1.866
3:AM3	1.015	1.871	0.000	1.447	0.987	0.318	1.765	0.613	0.020	0.091
4:AM4	0.474	1.330	0.053	0.000	0.446	0.859	1.224	0.072	0.561	0.632
5:AM5	0.302	1.158	0.224	0.734	0.000	1.031	1.052	0.100	0.733	0.804
6:AM6	1.270	0.414	1.797	0.838	1.298	0.000	0.520	1.672	2.305	2.376
7:AM7	0.281	0.575	0.808	0.151	0.309	1.614	0.000	0.683	1.316	1.387
8:AM8	1.324	2.181	0.798	1.757	1.297	1.658	2.075	0.000	0.290	0.218
9:AM9	0.788	0.068	1.315	0.356	0.816	2.121	0.038	1.190	0.000	1.894
10:AM10	1.311	0.454	1.837	0.879	1.339	2.643	0.560	1.712	2.345	0.000

*(Individuals = numbered; AM, PM = ante- and postmortem).

**(values in red indicate dissimilarity factors of 0.000 = accordance of 100 %).

Table 29: Excerpt of the correlation of Euclidean distances of right sided maxillary sinus morphologies used in the uniqueness testing study

Excerpt Proximity Matrix

Euclidean Distance

	542:PM1	543:PM2	544:PM3	545:PM4	546:PM5	547:PM6	548:PM7	549:PM8	550:PM9	551:PM10
1:AM1	0.000	0.682	1.878	0.887	0.521	0.649	1.476	1.006	0.805	0.705
2:AM2	2.064	0.000	0.841	1.833	2.199	2.071	1.243	1.713	3.525	2.015
3:AM3	1.570	1.543	0.000	1.338	1.705	1.576	0.749	1.219	3.030	1.520
4:AM4	0.059	0.085	1.281	0.000	0.076	0.052	0.879	0.410	1.402	0.108
5:AM5	0.723	0.750	1.946	0.954	0.000	0.716	1.544	1.074	0.738	0.772
6:AM6	0.844	0.870	2.066	1.075	0.709	0.000	1.664	1.194	0.617	0.893
7:AM7	1.023	1.050	2.246	1.254	0.888	1.016	0.000	1.374	0.438	1.072
8:AM8	0.082	0.055	1.141	0.150	0.217	0.089	0.739	0.000	1.542	0.032
9:AM9	0.711	0.684	0.512	0.479	0.846	0.717	0.110	0.360	0.000	0.661
10:AM10	0.205	0.179	1.017	0.026	0.340	0.212	0.615	0.146	1.666	0.000

*(Individuals = numbered; AM, PM = ante- and postmortem).

**(values in red indicate dissimilarity factors of 0.000 = accordance of 100 % between each individual's ante- and postmortem sinus morphology).

As a next step, to further confirm the uniqueness of the tested sample, a neighbour joining clustering has been applied. This offers the advantage to visualise degrees of similarity and dissimilarity between the morphologies and exploring them further. Neighbour joining clustering is a type of hierarchical clustering. However, with neighbour joining clustering, the data does not have to be ultrametric, and the dissimilarity of the morphologies is visualised in an unrooted dendrogram. Importantly, the clustering does not give any information about genetic relationships but maps the Mahalanobis distance between the morphologies. More similar morphologies are mapped closer together than morphologies with greater distances. Total matches are displayed on the same branch end.

As with the correlations, excerpts of the graphs are available in Figure 43 and 44. The whole dendrograms can be retrieved online through QR-codes in appendix 1 (Figure 45, 46) or directly through this link: https://www.dropbox.com/sh/ln63c8pl12fz6xo/AAAAMNt_-cRH8E-MsCF1cezsa?dl=0.

Due to the massive amount of morphologies analysed, branch ends are not as easily visible. However, even in the crowded areas of the dendrograms, the branch ends are evident and can be identified as blue vertical lines next to the mapped individuals and by each individuals ante- and postmortem sinus morphology being mapped next to each other. Varying amounts of left and right-sided maxillary sinus morphologies available for this study result in different quantities of morphologies displayed in the excerpts. Morphologies from the ante- and postmortem dataset are mapped together in the dendrograms for left and right-sided sinuses. Calculation of Mahalanobis distances results in one antemortem morphology mapped on each branch end only with their respective postmortem counterpart. This can be observed for the dendrograms for both left and right-sided morphologies. Therefore, as the correlations carried out before, these clusterings confirm the uniqueness of the morphologies. Spatial proximities between the clustered pairings indicate morphological similarity and dissimilarity. For example, in the dendrogram for right-sided morphologies, pairing 311 has more morphological resemblance with pairing 353 than pairing 56 (Figure 44).

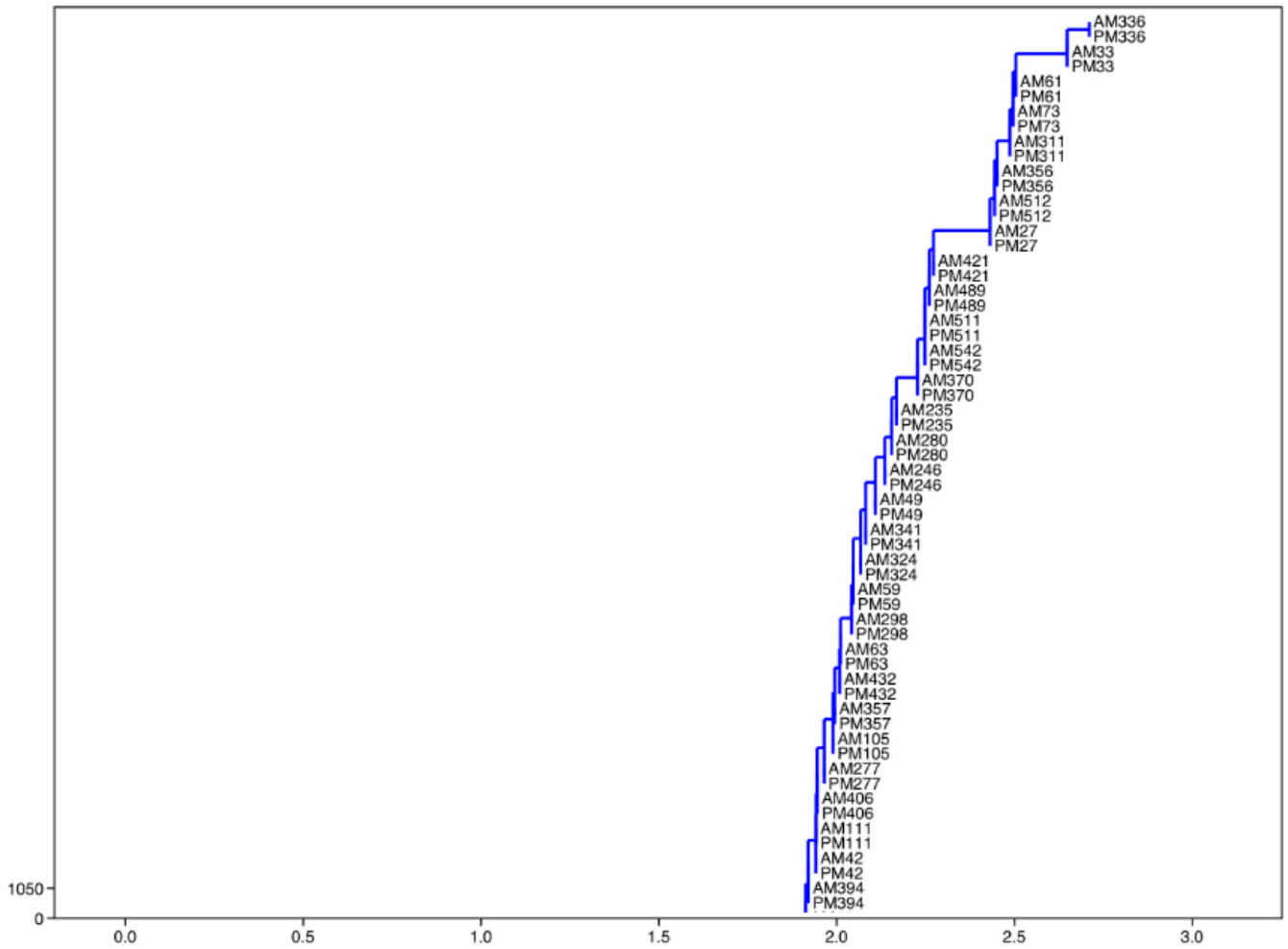

Figure 43: Excerpt of the neighbour joining clustering of Mahalanobis distances of left sided maxillary sinus morphologies used in the uniqueness testing study

**(Individuals = numbered; AM, PM = ante- and postmortem).*

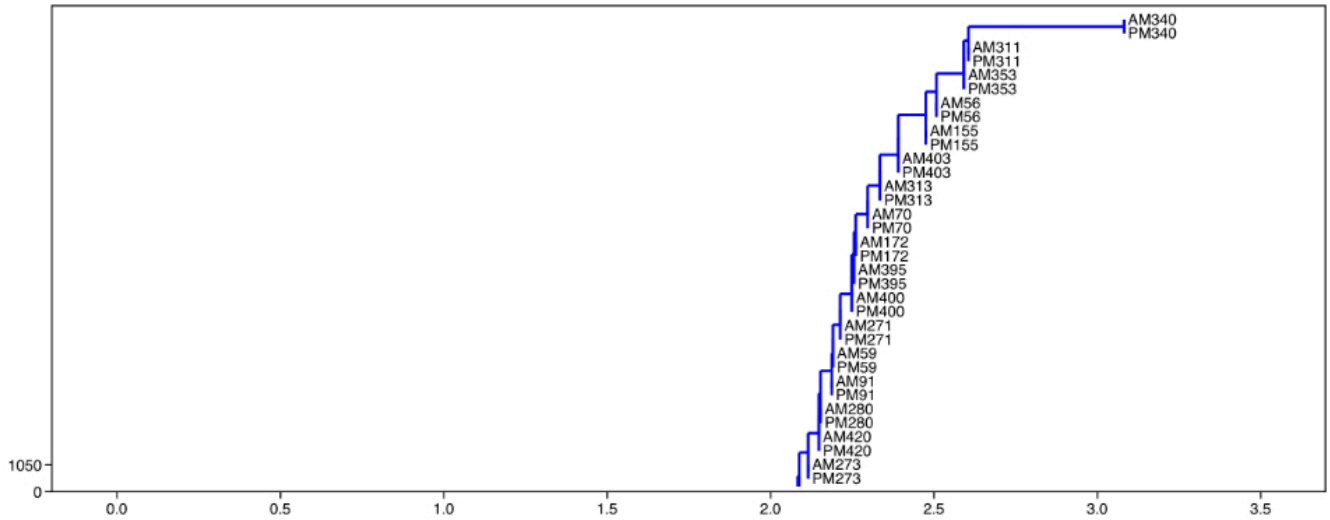

Figure 44: Excerpt of the neighbour joining clustering of Mahalanobis distances of right sided maxillary sinus morphologies used in the uniqueness testing study

**(Individuals = numbered; AM, PM = ante- and postmortem).*

Chapter 4 Results Part II: Case Study

When proposing a new method for identification, it is of utmost importance to assess its applicability. In the last chapter, the uniqueness of the morphological feature has been positively assessed. This section now marks the beginning of the application-oriented approach of this research.

While chapter 3 describes the uniqueness testing in a simulated environment, this case study has been developed to test how maxillary sinus uniqueness can be assessed in a more real-life application. Radiographs of the individuals used have been taken twice throughout the individuals' life (Table 6, section 2.4). Important to note, the individuals were alive when the second radiograph was taken. Nevertheless, the second image per individual is used as postmortem reference material. This marks a clear difference to the experimental design for the uniqueness testing in chapter 3, where the postmortem dataset was simulated by reassessing the same radiographs and CT images per individual.

4.1 Morphological Differences

The next step in the evaluation process is the calculation of Euclidean distances between the ante- and postmortem datasets of the left and right-sided morphologies. The dissimilarity matrices for right and left-sided morphologies (Table 30 & 31) indicate a similarity between the morphologies of 100 % (0.000) only for each antemortem morphology and its respective postmortem counterpart. Outliers are pair CS005 for both right and left-sided sinuses and pair CS008 for the left-sided sinuses. However, dissimilarity values are extremely low, with .002 for pair CS005 and ,001 for pairing CS008 on the left side and .001 for pair CS005 on the right side.

Table 30: Correlation of Euclidean distances of left sided maxillary sinus morphologies used in the case study

Proximity Matrix

	Euclidean Distance							
	9:PMCS001	10:PMCS002	11:PMCS003	12:PMCS004	13:PMCS005	14:PMCS006	15:PMCS007	16:PMCS008
1:AMCS001	0.000	2.280	0.380	2.067	1.488	2.948	0.960	2.274
2:AMCS002	0.287	0.000	1.094	0.593	0.014	1.473	0.514	0.800
3:AMCS003	0.661	0.431	0.000	0.218	0.360	1.099	0.889	0.425
4:AMCS004	0.776	0.316	1.584	0.000	0.476	0.984	1.004	0.310
5:AMCS005	0.376	1.469	0.431	1.256	0.002	2.136	0.149	1.463
6:AMCS006	2.346	1.253	3.153	1.466	2.045	0.000	2.574	1.259
7:AMCS007	0.459	1.552	0.348	1.339	0.760	2.220	0.000	1.546
8:AMCS008	1.451	0.358	2.258	0.571	1.150	0.309	1.679	0.001

This is a dissimilarity matrix

*(Individuals = numbered; AM, PM = ante- and postmortem).
**(values in red indicate dissimilarity factors of 0.000 = accordance of 100 %).

Table 31: Correlation of Euclidean distances of right sided maxillary sinus morphologies used in the case study

Proximity Matrix

	Euclidean Distance							
	9:PMCS001	10:PMCS002	11:PMCS003	12:PMCS004	13:PMCS005	14:PMCS006	15:PMCS007	16:PMCS008
1: AMCS001	0.000	1.794	4.171	3.142	2.392	2.349	3.732	1.518
2:AMCS002	3.463	0.000	1.359	2.387	3.138	3.180	1.797	4.011
3:AMCS003	1.488	1.761	0.000	0.412	1.163	1.205	0.178	2.036
4:AMCS004	0.671	0.943	1.434	0.000	0.345	0.388	0.995	1.219
5:AMCS005	1.090	1.363	1.015	0.014	0.001	0.807	0.576	1.638
6:AMCS006	0.218	0.490	1.887	0.858	0.108	0.000	1.449	0.766
7:AMCS007	2.421	2.693	0.316	1.344	2.095	2.137	0.000	2.968
8:AMCS008	0.546	0.818	1.559	0.531	0.220	0.262	1.121	0.000

This is a dissimilarity matrix

*(Individuals = numbered; AM, PM = ante- and postmortem).

**(values in red indicate dissimilarity factors of 0.000 = accordance of 100 %).

To conclude the evaluation, Mahalanobis distances between the morphologies were calculated. Clustering for both left (Figure 47) and right-sided morphologies (Figure 48) visualise similarities and dissimilarities of the morphologies. As with the correlation, matching morphologies are only evident with each antemortem morphology mapped solely with its postmortem counterpart on the branch ends. Interestingly, the outliers identified in the correlation analyses do not weigh into the clustering results. Moreover, the clustering still indicates a clear distinction between the morphology pairs. For left-sided morphologies, the pairs of CS005 and CS007 seem to have the closest Mahalanobis distance (Figure 47). For right-sided morphologies, this is the case for CS002 and CS007 (Figure 48).

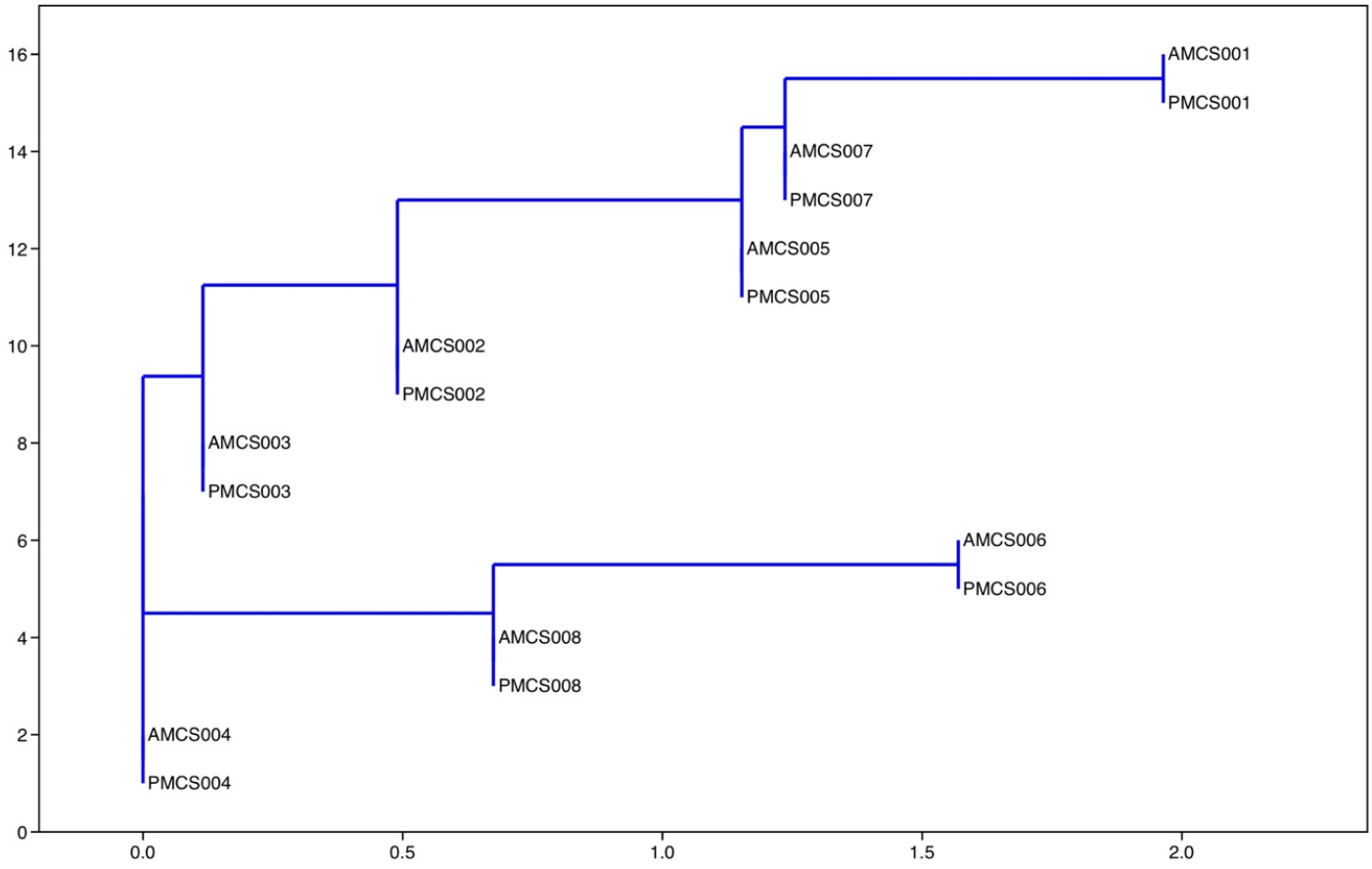

Figure 47: Neighbour joining clustering of Mahalanobis distances of left sided maxillary sinus morphologies used in the case study

**(Individuals = numbered; AM, PM = ante- and postmortem).*

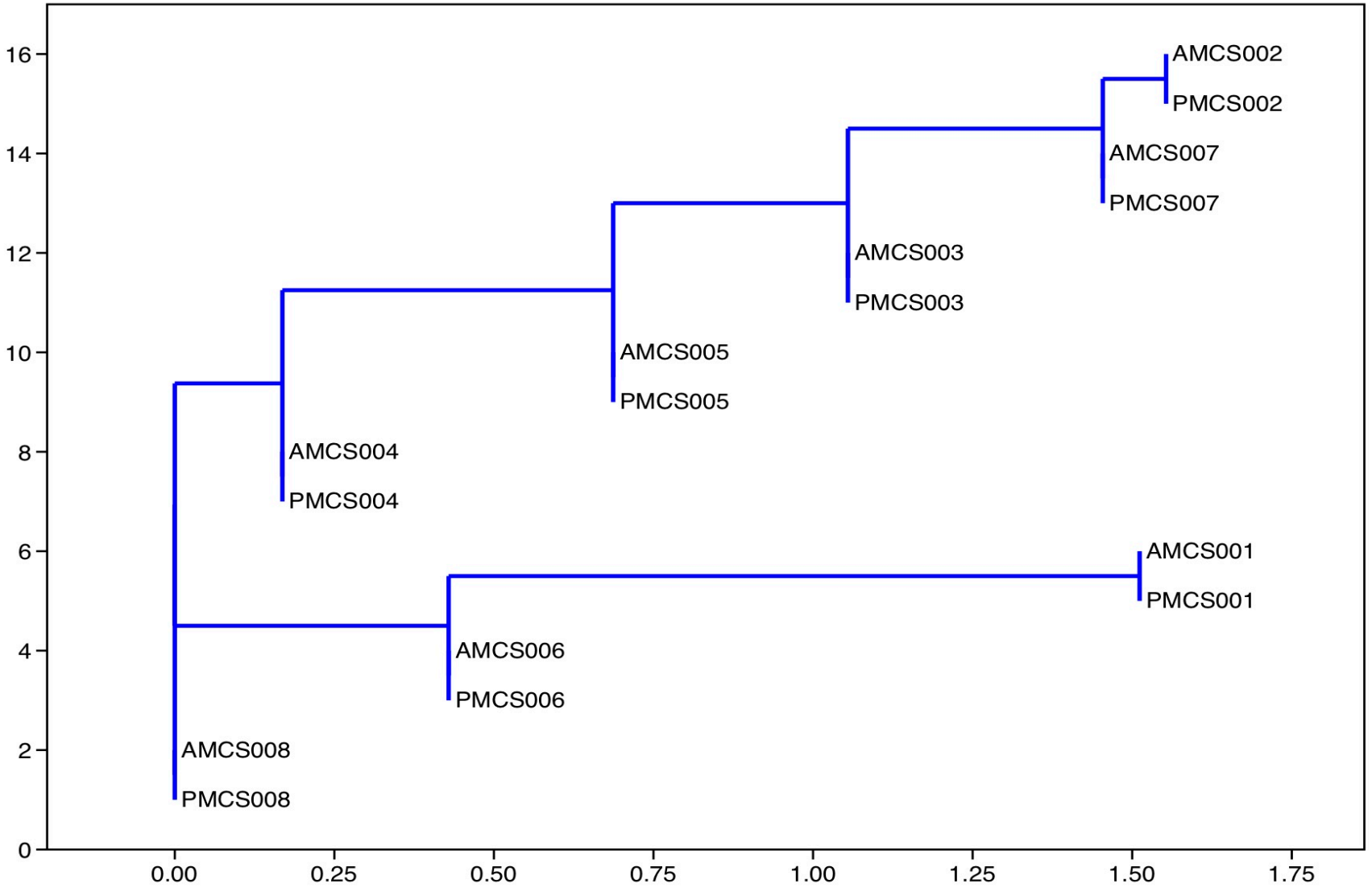

Figure 48: Neighbour joining clustering of Mahalanobis distances of right sided maxillary sinus morphologies used in the case study

**(Individuals = numbered; AM, PM = ante- and postmortem).*

4.2 Principal Component Clustering

Scatter plots on the first two PCs of the analysed morphologies for the case study allow a more holistic picture. Here, the individuals' population, age, and sex are included in the analyses. Focussing on the identified outlier from the correlation and clustering analyses for the left-sided morphologies, the scatter plots (appendix 2, Figure 49 to 56) help identify morphological relationships.

In correspondence with the preceding neighbour joining clustering, correlations between the morphology pairs of CS005 and CS007 as well as CS003 and CS004 are of interest for left-sided morphologies. Morphologies of CS005 and CS007 are located on the same Y-Axis plane (Figure 49); the individuals come from different populations (Figure 50) and have different sexes (Figure 51) but are in the same age group (Figure 52). Morphologies of CS003 and CS004 can be found on the same X-Axis level (Figure 49). They derive from the same population (Figure 50) and can be assigned to the same age group (Figure 52). However, CS003 is male, whereas CS004 is female (Figure 51).

For right-sided morphologies, the pairs of CS002 and CS007 and CS004 and CS008 are of interest following the neighbour joining clustering. CS002 and CS007 are positioned on the same X-Axis level (Figure 53). Although they derive from different populations (Figure 54), they have the same sex (Figure 55) and age group (Figure 56). CS004 and CS008 show very similar properties as they are both positioned on the same Y-Axis level (Figure 53). Furthermore, they belong to different populations (Figure 54), have the same sex (Figure 55) and age group (Figure 56).

Chapter 5 Results Part III: Intra- and Inter-Observer Reliability

The reproducibility of morphological extraction was tested by applying Cohen's Kappa statistics. As with the preceding analyses, morphologies have been evaluated separated into left and right-sided sinuses. In total, 20 % of the dataset used for the uniqueness testing of this study has been reassessed by the author as well as two independent observers (OB). Comparisons between Cohen's Kappa Values and the relating level of agreements can be found in Table 8 (section 2.5).

5.1 Intra-Observer Reliability

The intra-observer reliability testing was conducted six months after the primary data collection was concluded. Cohen's Kappa Values for left and right-sided sinus morphologies were above .90 (Table 32). Those scores translate to an almost perfect level of agreement between the intra-observer evaluation.

Table 32: Calculation of Cohen's kappa values in left and right sided maxillary sinus morphologies between two morphological evaluations of the author

Morphology	Cohen's Kappa Value	p-value	Level of Agreement
Left side	.908	< .001	Almost perfect
Right side	.901	< .001	Almost perfect

5.2 Inter-Observer Reliability

The inter-observer reliability testing was carried out a year after the initial data evaluation. Both observers evaluated the sinus morphologies very diligently on the x-ray images and overall achieved scorings of strong agreement (Table 33). Degrees of inter-rater reliability for

each observer are calculated in comparison to the author's evaluation. In comparison, inter-rater agreement between OB1 and the author reached higher Cohen's Kappa Values with all k-values >.850. Inter-rater agreement between OB2 and the author scored a strong level of agreement with left-sided sinus morphologies and a moderate agreement with right-sided morphologies. However, Cohen's Kappa Value for right-sided morphologies falls just below the strong agreement scores.

Table 33: Calculation of Cohen's kappa values in left and right sided maxillary sinus morphologies between the authors and each observer's morphological evaluation

Observer	**Morphology**	**Cohen's Kappa Value (Degree of Agreement with the author)**	**p-value**	**Level of Agreement**
OB1	Left side	.852	< .001	Strong
	Right side	.878	< .001	Strong
OB2	Left side	.837	< .001	Strong
	Right side	.799	< .001	Moderate

Chapter 6 Results Part IV: Age Estimation

In addition to the uniqueness testing, it is crucial to understand how biological factors like age and sex impact an identification method. This chapter evaluates the importance and influence of age on the maxillary sinus morphologies by incorporating sex as a determinant factor. In section 6.1, an age clustering system is applied to all three populations used for this part of the study. As image availability vastly varies among populations and individuals, it is essential to develop a system that introduces data stability and at the same time sufficiently reflects the age variability of the images. Following the clustering, section 6.2 applies Euclidean distance correlations to calculate growth rates per population and sex.

6.1 Age Cluster System

This study's sample includes individuals from three longitudinal growth studies and a total of 2.112 sinus morphologies (Table 3). Individuals from all three longitudinal growth studies have been imaged throughout their childhood, with some individuals possessing x-ray images during adult years as well. However, the timing of image recording varies among as well as within the three populations. Therefore, some individuals possess a cohesive imaging profile with x-ray images taken every five years, while others possess far fewer or more images. Those differences in image recording make comparability between the individuals difficult. For comparison and examination within this study, an age clustering system was applied that incorporates this variability in image recording (Table 34).

Table 34: Age clustering system used in the age estimation study with cluster numbers and responding age categories

Age Cluster	Related Age (in years)
1	0 - 2
2	3 - 5
3	6 - 10
4	11 - 15
5	16 - 20
6	21 - 25
7	26 - 30
8	31+

The system includes eight age clusters that contain different age ranges within each cluster. Age clusters one and two contain an age range of three years, while the remaining clusters include an age range of five years. Especially during the first few years of the individuals, imaging was executed regularly. Therefore, this difference in years within the age clusters was chosen to be able to integrate as many morphologies as possible into the analyses. In later years, a standard of five years was established for most individuals and is reflected in this study's age clusters. Although many studies suggest the maxillary sinuses to be fully grown at age twenty-one, in this study, individual age clusters are chosen up until age thirty-one. This extended age range was chosen firstly because the data allows for this individualised clustering and secondly because it is crucial to understand potential morphological changes even after the third molar eruption.

For some individuals, the adapted system with three or five years per cluster did not suffice, as they exhibited more than one image falling into the clustering stages. For those individuals, only one of the existing images was chosen per cluster, even if more images were available. Therefore, 294 morphologies had to be removed from this study due to duplication within the cluster. Figure 57 reflects the amounts of morphologies as classified into the age clustering system. Amounts for right and left-sided morphologies remain the same within this study. Age based clusters one, six, seven, and eight contain the least amount of morphologies. The body of images can be found in age clusters two to five. Within those clusters, Burlington Growth provides the most amount of morphologies within each cluster, with Oregon Growth following closely after.

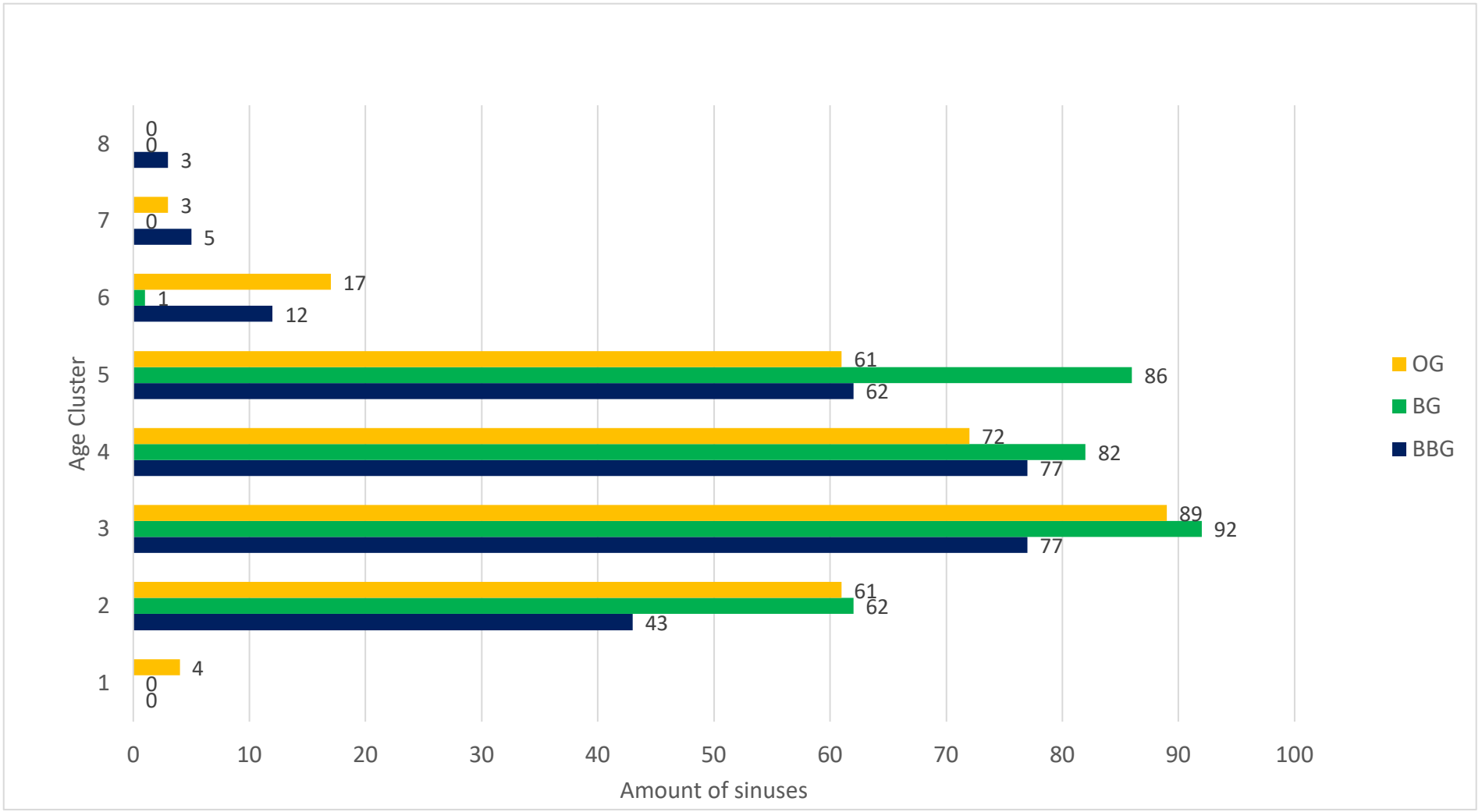

Figure 57: Bar chat illustrating the age distribution of the sample used in the age estimation study among populations

**(BBG: Bolton-Brush Growth; BG: Burlington Growth; OG: Oregon Growth).*

**(Responding ages per age cluster are accessible in *Table 34)*.

6.2 Growth Rate Estimation

6.2.1 Growth Rate Estimation by Population

The term ‘growth rate’, as used in this study, refers to the change of Euclidean distances throughout the individual’s lifetime. To understand the difference of Euclidean distances among age clusters, the mean of Euclidean distances within each population’s age cluster was calculated. Figure 58 shows the development of the averaged distances of left-sided morphologies with increasing age between all populations. All three populations show the same trend, with distances monotonously rising. Notably, Bolton-Brush Growth exhibits a high average Euclidean distance in cluster seven before a lower average in cluster eight. For both Bolton Brush Growth and Oregon Growth, low average distances are evident in cluster six (values for both are so similar that the data point for Oregon Growth overlays the data point for Bolton Brush Growth). Quasi-linear trend lines display a positively increasing tendency for all populations. With right-sided morphologies, the positively increasing trend is visible as well (Figure 59). However, while the quasi-linear trend lines showed a very similar progression for the left side, the trendline of Burlington Growth for right-sided morphologies appears to be more separated from the remaining populations.

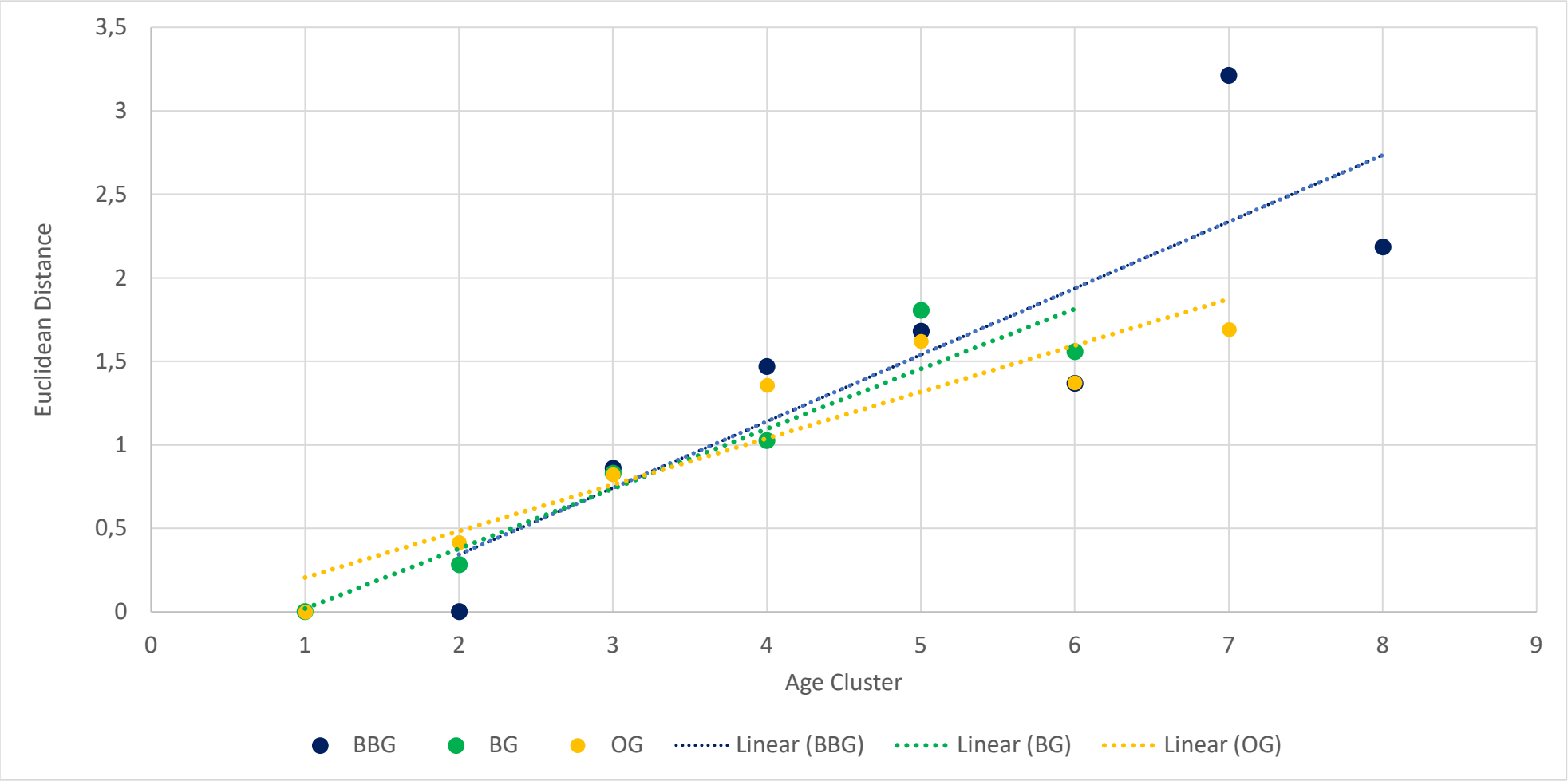

Figure 58: Comparison of each population's Euclidean distance means within each age cluster of left sided maxillary sinus morphologies used in the age estimation study among populations

**(BBG: Bolton-Brush Growth; BG: Burlington Growth; OG: Oregon Growth); **(Responding ages per age cluster are accessible in Table 34).*

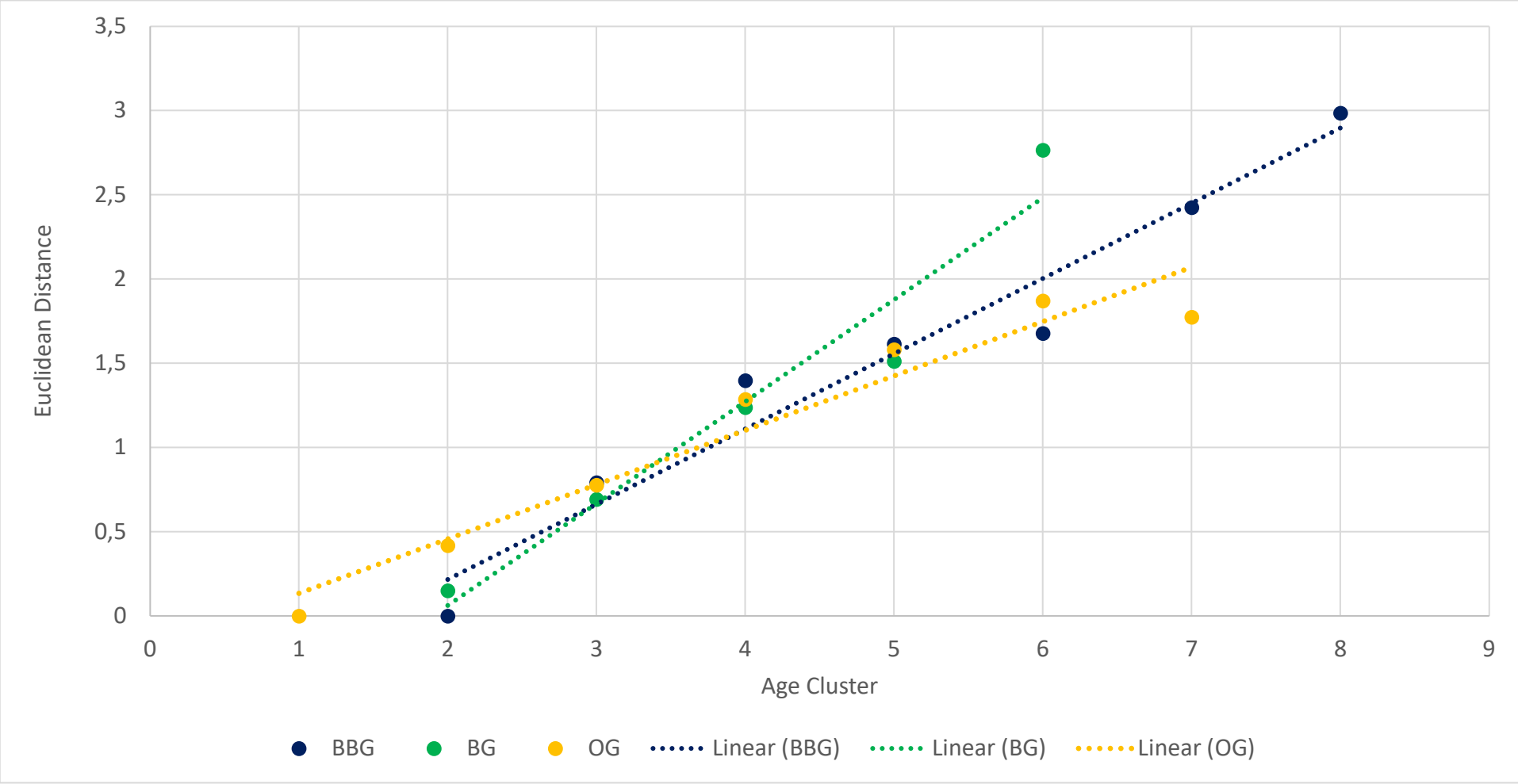

Figure 59: Comparison of each population's Euclidean distance means within each age cluster of right sided maxillary sinus morphologies used in the age estimation study among populations

**(BBG: Bolton-Brush Growth; BG: Burlington Growth; OG: Oregon Growth); **(Responding ages per age cluster are accessible in Table 34).*

Pearson's correlation coefficients were calculated to measure the linear association between the age clusters and the Euclidean distance means (Table 35). Overall, correlation coefficients exhibit a strong linear interrelation for both the left and the right side. With the exception of Bolton-Brush Growth's left-sided morphologies, values are above .94. However, the lower value of Bolton-Brush Growth still exhibits a strong positive linear correlation.

Table 35: Calculation of Pearson's correlation coefficient of the sample used in the age estimation study on left and right sided maxillary sinus morphologies

Population	**Side**	**Pearson's Correlations Coefficient**	**P-value**
Bolton-Brush Growth	Left	0.86	0.015
	Right	0.97	< 0.001
Burlington Growth	Left	0.95	0.003
	Right	0.99	0.006
Oregon Growth	Left	0.94	0.002
	Right	0.97	< 0.001

With the help of the quasi-linear trend lines, a gradient for each population is calculated. This gradient is considered the growth rate among the age clusters for every population (Table 36). Growth rates vary among left and right sides as well as between populations. The lowest growth rate is calculated for Burlington Growth, right side, while Oregon Growth exhibits the most considerable rate on the left side. Within populations, Burlington Growth displays the biggest gap between rates. Ranges of growth rates within Bolton-Brush Growth and Oregon Growth are substantially smaller between the left and right sides.

Table 36: Calculation of growth rates (gradients) per sample used in the age estimation study on left and right sided maxillary sinus morphologies

Population	Side	Growth Rate, Year^{-1}
Bolton-Brush Growth	Left	1.828
	Right	2.162
Burlington Growth	Left	2.549
	Right	1.509
Oregon Growth	Left	3.126
	Right	2.918

6.2.2 Growth Rate Estimation by Sex

In addition to the population analyses, growth rates were calculated by sex. For this part of the study, the sample is assembled by all females and males of all three populations (Figure 60). A mean Euclidean distance was calculated for every age cluster (Figure 61 & 62). As with the population analyses, averaged Euclidean distances continuously rise for both left and right side among both sexes. On the left side, low average distances are visible for the male sample in clusters five and eight. A monotonous increase of distances is recorded for both sexes on the right side. Quasi-linear trend lines display a positively increasing tendency for both sexes among the left and right side.

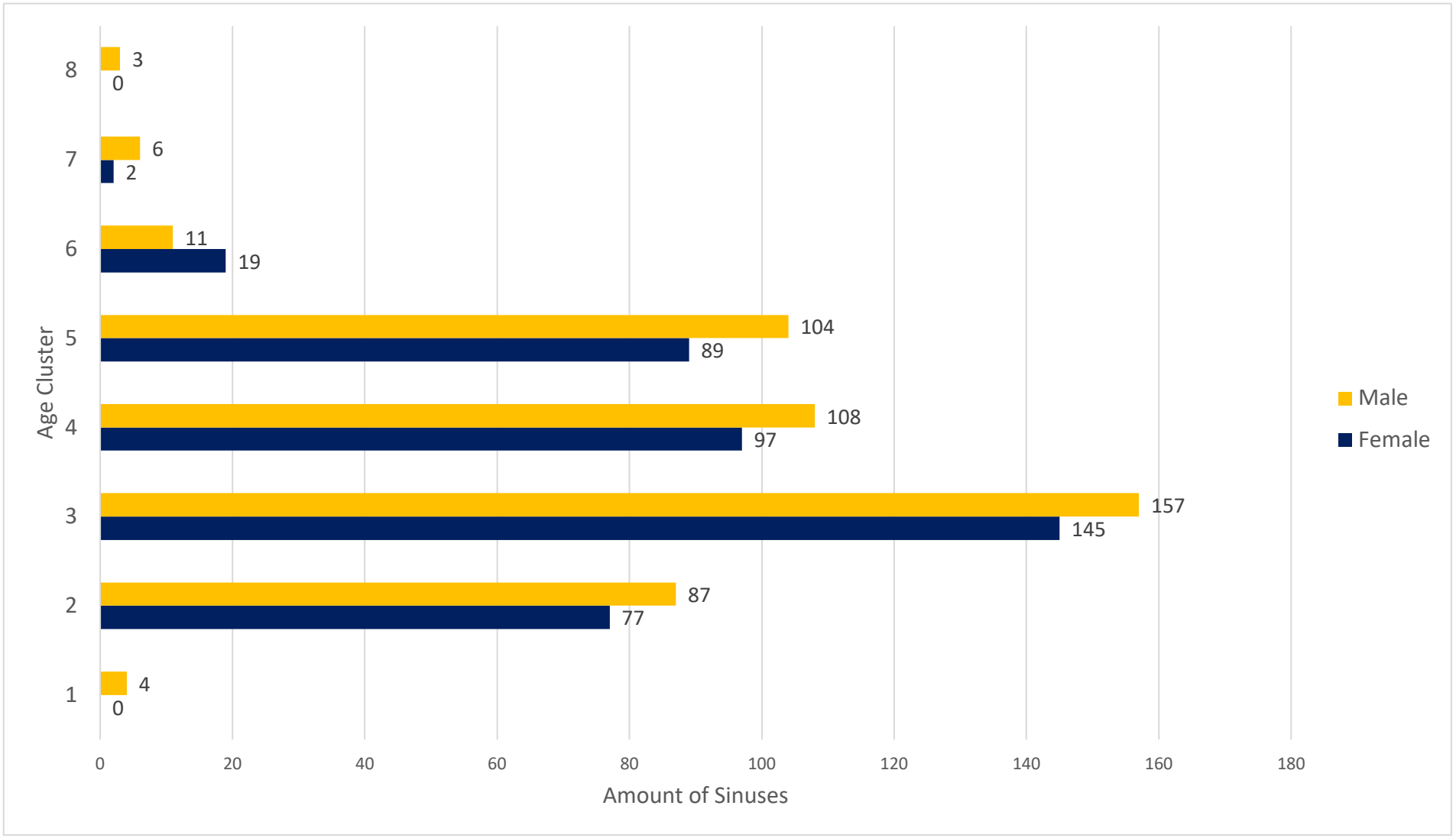

Figure 60: Bar chat illustrating the age distribution of the sample used in the age estimation study among sex

**(Responding ages per age cluster are accessible in Table 34*

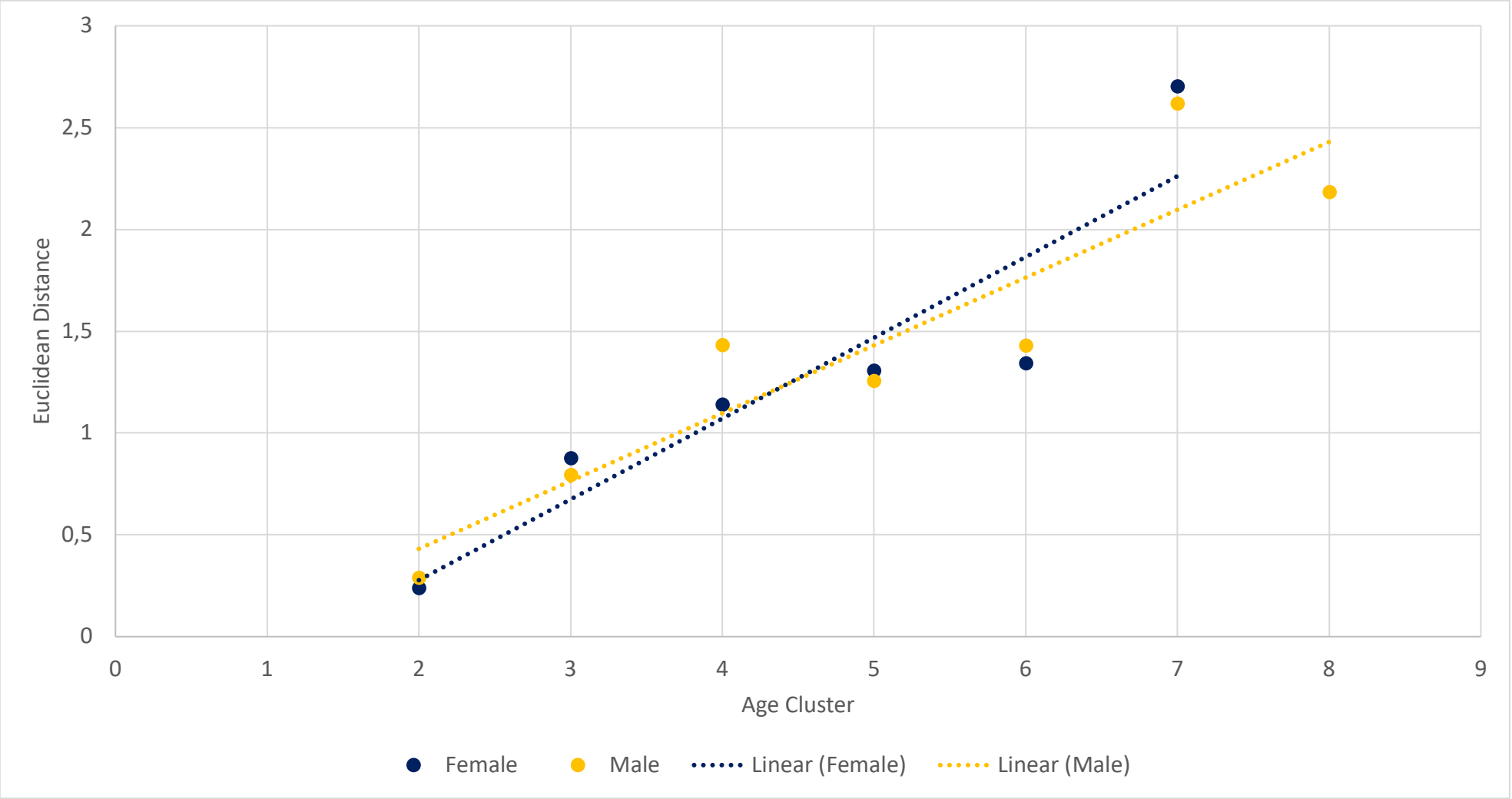

Figure 61: Comparison of each population's Euclidean distance means within each age cluster of left sided maxillary sinus morphologies used in the age estimation study among sex

**(Responding ages per age cluster are accessible in Table 34).*

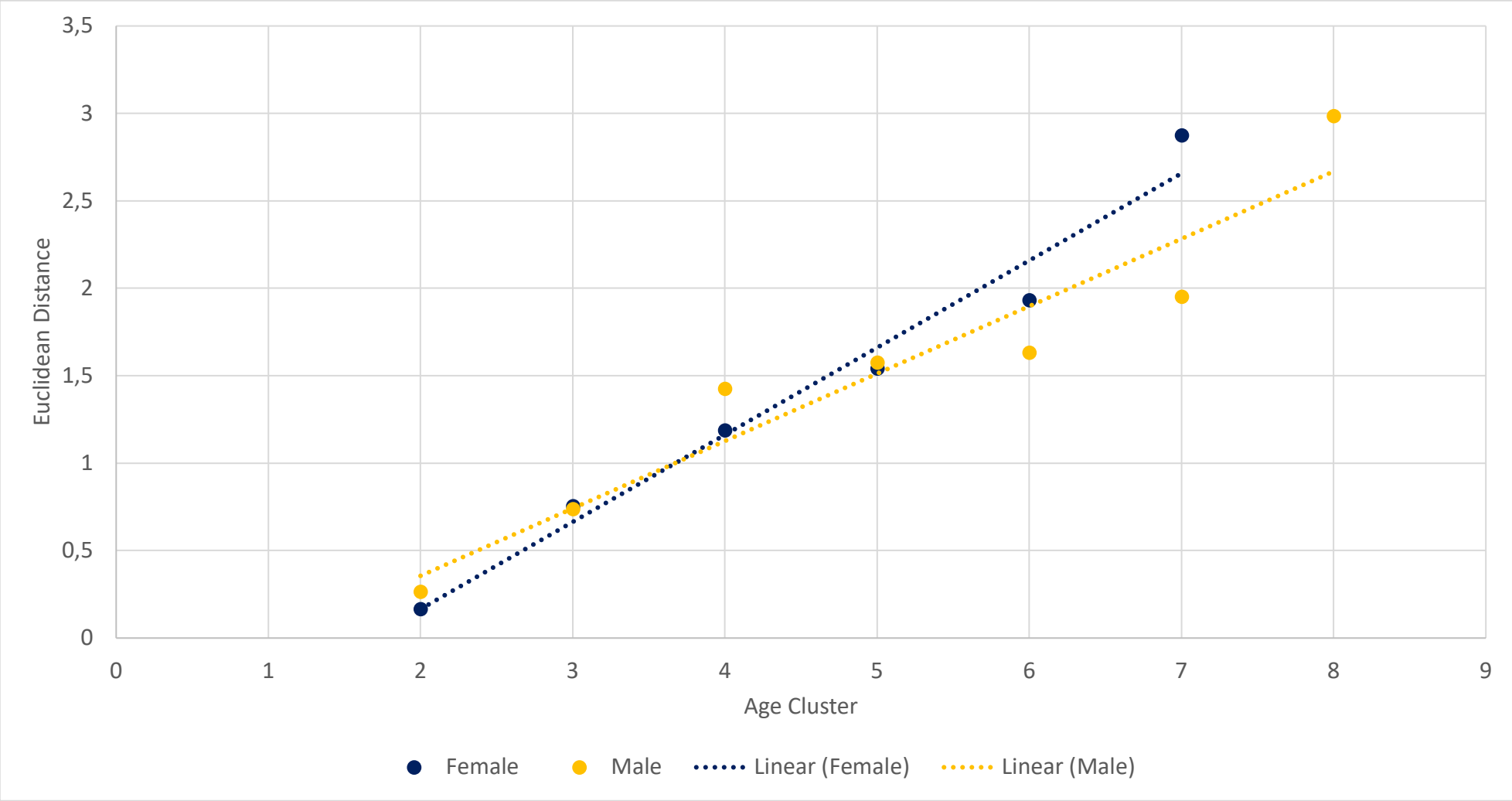

Figure 62: Comparison of each population's Euclidean distance means within each age cluster of right sided maxillary sinus morphologies used in the age estimation study among sex

**(Responding ages per age cluster are accessible in Table 34).*

Pearson's correlation coefficients exhibit a solid linear interrelation on the left and right sides for females and males. Calculated values all lie above .93 (Table 37). Most importantly, with the help of the quasi-linear trend lines, a gradient was calculated for left and right-sided morphologies of both sexes. As with the population analyses, this gradient functions as the growth rate for each sample. Growth rates vary among the sexes and sides (Table 38). Although values are different for both sexes, the left and right sides variation is very similar. Growth rates for males on both sides and females on the left side are above 2.299. However, the value for right-sided morphologies in the female sample is slightly lower.

Table 37: Calculation of Pearson's correlation coefficient in the age estimation study on left and right sided maxillary sinus morphologies among sexes

Sex	**Side**	**Pearson's Correlations Coefficient**	**P-value**
Female	Left	0.94	0.002
	Right	0.98	0.007
Male	Left	0.93	< 0.001
	Right	0.95	< 0.001

Table 38: Calculation of growth rates (gradients) in the age estimation study on left and right sided maxillary sinus morphologies among sexes

Sex	**Side**	**Growth Rate, Year^{-1}**
Female	Left	2.299
	Right	1.954
Male	Left	2.604
	Right	2.375

Chapter 7 Discussion

This research led to the assessment of 5,728[6] human maxillary sinuses from populations in Europe (Poulton Chapel, St. Owen's Church, Florence, Siracusa, Chelsea Old Church, St. Mary Spital, St. Bride's Lower Churchyard, Osteological Collection, University of Tübingen, Anatomical Collection, University of Leipzig) and North America (Bolton-Brush Growth, Oregon Growth, Burlington Growth). Within this research, each study and subsequently each chapter approaches one of the four objectives: First, Chapter 3 tests for morphological uniqueness, while chapter 4 examines the real-life applicability of the uniqueness testing method by developing a case study. Thereafter, chapter 5 assesses the reproducibility of the morphological extraction method. Finally, chapter 6 is concerned with age-related changes in sinus morphologies.

Each section of this research uses a different sample for analysis. The uniqueness testing in chapter 3 is conducted with 1,792 sinuses. Due to unsuitable age ranges, maxillofacial pathologies, and image overexposure, 687 sinuses had to be discarded during the extraction of sinus morphologies. Therefore, analyses were conducted with 1,105 sinuses (extracted twice to create an ante- and postmortem dataset) for this part of the study. The dataset for the case study in chapter 4 depends on eight individuals from the collections of Bolton-Brush Growth and Oregon Growth (Table 6, section 2.4). The assessment of reproducibility uses 20 % of the total dataset for the uniqueness testing. Lastly, age evaluations in chapter 6 use a sample of 2,112 maxillary sinus morphologies from all three longitudinal growth collections, which was reduced by 294 morphologies to fit the applied age clustering system (Table 3, chapter 2). All objectives described in chapter 1 are addressed, and interpretations of the main findings can be found below. Furthermore, the limitations of this research are addressed, and future approaches are recommended.

This research is concerned with maxillary sinus morphological evaluations for human identification. Human identification is conducted in a variety of methods including for example

[6] **3,584** (uniqueness testing = 988 individuals in total - 92 Burlington Growth individuals = 896 individuals = 1,792 left and right sinuses; 1,792 sinuses for antemortem dataset + 1,792 sinuses for postmortem dataset = 3,584 sinuses in total for the uniqueness testing) **+ 32** (case study = 8 individuals per ante- and postmortem dataset = 16 x 2 = 32 left and right sinuses) **+ 2,112** (age estimation study left and right side) **= 5,728 left and right sinuses**

fingerprinting, DNA analysis, dental comparison, and radiological assessments (Interpol, 2018; Wlodarczyk, 2012; de Boer et al., 2020; de Boer et al., 2018; Modesti et al., 2014). DNA analysis is a widely recognised method with a very high confidence level in court. However, it can be expensive and holds disadvantages, for example, when utilised in mass disasters (Tatlisumak et al., 2007). In contrast, radiographic analyses of skeletal elements have been used since 1921 (Schüller) in human identification and allow for a routinised approach due to their effectiveness and easy implementation (Bernstein, 1983). In the 20th century, up to 72 % of positive identifications were achieved through the comparison of both cranial and postcranial ante- and postmortem radiography (Kahana and Hiss, 1997). The evaluation of maxillary sinus morphologies as suggested in this research could add to the existing body of human identification methods (de Boer et al., 2019) for potential cross evidencing of identification methodologies in court (Interpol, 2018).

7.1 Uniqueness Testing

7.1.1 Morphological Variation

The main advantage of the elliptic Fourier analysis and the principal component analysis is the ability to identify even small morphological changes, which the human eye cannot detect. Furthermore, morphological evaluations not related to size are possible, making the analysis independent of visual judgements that often are influenced by such factors (Yoshioka et al., 2004). Evaluations of skeletal morphologies are routinely used in forensic anthropology (Caple et al., 2017). Assessments help to execute structured research that enhances reproducibility for court applications. Within the last thirty years the elliptic Fourier analysis, as used in this research, was applied increasingly for biological profiling (Chen et al., 2000; Sheridan et al., 1997; Thayer and Dobson, 2010; Rose et al., 2003) and analysis of force trauma (Lestrel and Kerr, 1993; Caple et al., 2017). In a forensic context, elliptic Fourier analyses were used to investigate cranial vault morphologies (Maxwell and Ross, 2014), craniofacial sexual dimorphisms (Lestrel et al., 2011), orbital morphologies (Nawrocki et al., 2018), paranasal sinus variability (Christensen, 2005; Butaric et al., 2022; Robles et al., 2020; de Barros et al., 2021), and mandibular sexual dimorphisms (Schmittbuhl et al., 2002). Further, forensic investigations applying elliptic Fourier analysis were conducted on the clavicle (Stephan et al.,

2014), the humerus (Tanaka et al., 2000; Dittrick and Suchey, 1986; Spradley and Jantz, 2011), the patella (Niespodziewanski et al., 2016), the os coxa (Velemínská et al., 2013; Walker, 2005; Patriquin et al., 2003), and the vertebra (Paolello and Cabo-Perez, 2008).

The foundation of using maxillary sinus morphologies in forensic anthropology lies in evaluating morphological uniqueness. Without confirmation of exclusiveness, application in human identification is not possible. In that regard, the sample of this research was initially screened to evaluate the morphological variation. After extracting the morphologies, they were assessed in the software SHAPE ver. 1.3 (Iwata and Ukai, 2002), applying elliptic Fourier analysis. The software applications in SHAPE ver. 1.3 automatically apply a normalisation in regards to the first harmonic which is corresponding to the first Fourier approximation of the contour information (Iwata and Ukai, 2002; Caple, 2017). Applied normalisations are affecting starting point and orientation of the contour as well as the size. The allometry, which describes the changes of size in relation to shape is highly discussed in geometric morphometrics (Rohlf and Marcus, 1993; Rosas and Bastir, 2002; Adams et al., 2004; Slice, 2007, Aranzamendi, 2010). As maxillary sinuses are highly morphologically diverse, it is important to apply normalisations in relations to size and shape. Normalisations regarding size were first suggested by Kuhl and Giradina (1982) who proposed a rescaling of the first harmonic's semi-major axis to a value of zero. Subsequently, the remaining coefficients are adjusted accordingly (Bookstein, 1997; Rohlf, 1990). In SHAPE ver. 1.3, normalisations based on the first harmonic are automatically applied and normalised elliptic Fourier coefficients are then used for the subsequent analyses.

The output of the elliptic Fourier analysis in SHAPE ver. 1.3 gives the first insight into the variation among the populations. The principal component scores obtained from the elliptic Fourier descriptors allow for mathematical distinction between the structures (Iwata and Ukai, 2002; Nawrocki et al., 2018) and therefore each population's morphologies. Both mathematically and visually, principal components number one and two amount for the most variation among the principal components. PC1 and PC2 show the most lateral variation within all populations with narrow, more crescent-like shapes. PC3 and PC4 display more broad types of morphologies with blunt bodies and no or minimal narrowing or curvature in lateral areas (Figure 13 to 32 in appendix 1). Evaluations of shape variation among left and

right maxillary sinuses show only minor differences (Table 10 & 11, section 3.1). This suggests that both sides are adequate to use for morphological analyses.

Characterisations of skeletal morphologies are necessary for objective and controlled research in forensic anthropology (Caple et al., 2017). Quantification of the morphologies in this research is achieved through the application and analyses of Euclidean distances. As mentioned before, reproducibility is a major factor of a forensic method (Morgan et al., 2019). Evaluations of Euclidean distances on the morphologies extracted via elliptic Fourier analyses impact forensic research by introducing reproducible standards (Caple et al., 2017). The use of Euclidean distance evaluations in forensic anthropology is well established and is used for example to understand morphological differences in skeletal growth (Niño-Sandoval et al., 2021). Furthermore, morphological studies include geographical and interpopulation variation of the human facial skeleton (Viðarsdóttir et al., 2002), examinations of mid facial cold adaption of northern Asian populations (Evteev et al., 2014), evaluations of cranial cold stress in rats and its adaptability on fossil hominins (Rae et al., 2006), as well as estimations of mandibular morphology (Omran et al., 2020). Additionally, measurements of Euclidean distances have been applied in virtual anthropology (Profico et al., 2019). With human paranasal sinuses, Euclidean distance evaluations are used frequently. Evteev (2019) examined links between climate and the morphology of the nasal cavity, while Souadih (2020) examined automatic morphological identifications on sphenoid sinuses. Furthermore, the method is used for morphological variations in frontal sinuses (Christensen, 2005) as well as to determine sinus capacities between different populations (Buck, 2014). In maxillary sinuses, Euclidean distances are used to understand ancestry-based distinctions (Kim et al., 2021). In this research, the uniqueness testing and case study evaluate Euclidean distances, as morphological variation based on principal component analyses can be calculated distinctly. Following Mahalanobis distances help to further visualise the results.

7.1.2 Population Analyses

More information about the connections within and between populations is highlighted when using principal component clustering among the first two principal components (Figure 33 & 34, appendix 1). Before assessing biological properties within the sample, the general distribution of morphologies shows a homogeneity between all populations. Clear separations that might be expected between the populations are absent, and a geographical affinity is not evident. This is, in part, unexpected, as a difference between the European and North American samples could have been assumed. Previous research on maxillary sinus volumes indicated a climactic influence (Butaric and Maddux, 2016; Butaric et al., 2010). Those studies investigated sub-Saharan and circumpolar populations (Butaric and Maddux, 2016) as well as populations from Germany, India, Egypt, Liberia, Peru, and Greenland (Butaric et al., 2010). The theory of climatic impact was supported by Evteev (2014), who compared mid-facial measurements and climatic variables and Marquez and Laitman (2008), who studied the nasal complex of macaques. Further studies implied a decrease of the maxillary sinus volumes in cold environments (Shea, 1977). Supporting this hypothesis, Rae (2006) found modifications of the craniofacial morphology in cold environments in rats and (2003) found reduced maxillary sinus volumes in cold environments in macaques. Further studies imply wider maxillary sinuses in cold than in hot environments (Butaric and Maddux, 2016). In contrast, Selcuk (2015) found no effect of climate and altitude on paranasal volume on Turkish populations. However, results of previous studies concentrated on measurements and volumes (Butaric et al., 2010; Evteev et al., 2014; Márquez and Laitman, 2008; Butaric and Maddux, 2016; Shea, 1977; Rae et al., 2006; Rae et al., 2003; Selcuk et al., 2015), while this research is concerned with paranasal morphology.

A variation among geographical markers is only evident when a bioclimatic influence makes a climatic adaption with anthropometric changes within the population necessary (Beals et al., 1984). The climate between the European and North American samples does vary as classifications after the Köppen-Geiger climate classification map show (Köppen and Geiger, 1928; Kottek et al., 2006). Rather than comparing the climate zones from every populations time zone dating back into medieval times, the updated Köppen-Geiger climate classification map using temperature and precipitation data from the year 1951 to 2000 is used (Rubel and Kottek, 2010; Peel et al., 2007). This ensures comparability between the different locations.

The populations of Florence (central Italy) and Siracusa (southeast Sicily) both are classified as Mediterranean climate, with an average temperature between 0 °C to 18 °C in the winter, less than less than 30 mm of precipitation in the summer, and a temperature above 22 °C for a minimum of one month in the summer (Csa = Warm temperate climate with dry, hot summers) (Köppen and Geiger, 1928; Rubel and Kottek, 2010; Peel et al., 2007). The populations located in the UK and Germany (Poulton Chapel, St. Owen's Church, Chelsea Old Church, St. Mary Spital, St. Bride's Lower Churchyard, Osteological Collection University of Tübingen, Anatomical Collection University of Leipzig), as well as the population of Burlington Growth are all classified into an oceanic climate. This climate classification includes an average temperature above -3 °C in the winter, the same average level of precipitation for each month, and an average temperature below 22 °C in the summer (Cfb = Warm temperate climate, fully humid with warm summers) (Köppen and Geiger, 1928; Rubel and Kottek, 2010; Peel et al., 2007). In contrast, the populations of Bolton-Brush Growth and Oregon Growth are classified as a humid continental climate. This classification involves averaged winter temperatures above -3 °C, temperatures below 22 °C in the summer, and the same average level of precipitation each month (Dfb = snow climate, fully humid with warm summers) (Köppen and Geiger, 1928; Rubel and Kottek, 2010; Peel et al., 2007). Except for the populations in Italy, climate classifications show only small changes. However, even differences in temperature and precipitation for the populations in Florence and Siracusa to the remaining populations can be described as moderate. Therefore, results of climate classification and morphological evaluation indicate that moderate climate and environmental variations do not significantly impact the morphology of human maxillary sinuses.

The results of homogeneity among the geographical regions might implicate challenges for geographical profiling on maxillary sinus morphologies. This could either indicate, that morphological evaluations hold less significance for geographical profiling in contrast to maxillary sinus volumes; or the climatic differences are too weak to adequately generate differences. Future studies should compare volumetric and morphological approaches within the same geographic populations to estimate and correlate the forensic impact of both methodologies. However, those considerations with the currently considered data are beyond the scope of this research. Additionally, as part of the population study analyses, future

research on maxillary sinuses should focus on effects of kinship on positive identification. Previous studies using frontal sinuses have measured identification accuracies within familial groups with very promising results (Cameriere et al., 2008; Cvrček et al., 2021). Similar research on maxillary sinus morphologies would further help to evaluate forensic implications of maxillary sinus identification.

Interestingly, no difference between the populations can be observed chronologically. The sample analysed is chronologically distant, as populations range from the Iron age to the 20th century (Table 3, chapter 2). However, most literature assumes the paranasal sinuses to be an early trait in mammals' evolutionary history that is somewhat influenced by diet and climate (Buck, 2014; Witmer, 1999; Rae and Koppe, 2014). A fundamental summary of the distribution of paranasal sinuses in catarrhine primates has been detailed before (Paulli, 1900c; Cave and Haines, 1940; Cave, 1967; Rae and Koppe, 2004), expressing the availability of maxillary sinuses in all hominoids. Furthermore, Rae and Koppe (2000) stipulated that hominoid allometric evaluations of maxillary sinus volumes compared to cranial size demonstrate no change of the maxillary sinus structure relative to skull size. Data available in the study currently under consideration only exhibits a small number of individuals dating in early periods, and a vast amount of data is available for the 12th to 19th centuries. Therefore, a sharp chronological difference in morphologies would have been unlikely. However, besides the availability of historic and modern samples, it was necessary to test whether those historic samples exhibited any evolutionary difference to the modern ones. No measurable difference between those chronologically distant samples, confirms the forensic suitability of the chosen samples and subsequently allows to establish forensic procedures from the overall sample. Results of these population analyses highlight the necessity to incorporate and consider findings from evolutionary and environmental effects for forensic identification as featured in other forensic disciplines (Tomberlin et al., 2011; Ross and Pilloud, 2021).

Analyses by sex and age do not indicate a significant classification of morphologies. Analyses by sex (Figure 35 & 36, appendix 1) exhibit a widely mixed data distribution. This result is in contrast to measurement and volumetric approaches, which indicate significant differences between females and males (Belgin et al., 2019; Gomes et al., 2019; Mathew and Jacob, 2020; Dhanak et al., 2019). However, the results of this study could implicate a difference between

volumetrics and measurements as well as morphological approaches and needs to be evaluated further. A similar mixed distribution is available with age (Figure 37 & 38, appendix 1). With increasing age, morphologies do not exhibit vast variations as seen with volumes (Belgin et al., 2019; Velasco-Torres et al., 2017) and measurements (Rani et al., 2017). As with the analyses of sex before, this result could indicate a difference between one structure's morphology and volume. This is incredibly fascinating as this suggests changes on three different levels. While measurements of specific bone markers (taken in 2D) increase with age and volumes (taken in 3D) tend to decrease, the morphology (taken in 2D) does not change significantly for adult individuals. A possible explanation could lie in the variability of the maxillary sinus. If the size of a specific bone marker increases, this does not automatically imply that the whole sinus grows. Even if the measurement increases in two different images, that does not mean that the volume has to increase equally. If simultaneously another segment decreases, the volume could potentially stay the same. The data in the scatterplots do not suffice to make an adequate statement on morphological changes in adult individuals. However, due to the equal age distribution in the sample, a skewing as a result of meagre data availability can be excluded. A necessary next step would be to further evaluate all three methods on the same sample to investigate the matter.

Next to variation assessments, ANOVA statistics give information about the samples' construction. Significant differences between populations deliver a solid framework for further uniqueness testing. As mentioned before, the sample used in this part of the research is chronologically highly diverse. Results of the scatterplots did not indicate differences in morphologies among the time periods. However, an ANOVA investigation of differences is necessary, as the data can be significantly different but still exhibit no clear tendencies within the scatterplots. All population analyses build a solid foundation for further uniqueness testing. The differences between morphologies make it possible to further test a methodological approach to match human maxillary sinus morphologies.

7.1.3 Uniqueness Test Comparison

Correlations of Euclidean distances and especially the clustering of Mahalanobis distances allow for a comfortable illustration of the uniqueness. Both methods complement each other and prove first the uniqueness of the sinus morphologies and second the usefulness in human identification. However, the experimental design shows disadvantages as the ante- and postmortem datasets used for matching originate from the same data source. Therefore, the experiment was transferred into a simulation realm. Using simulations to depict reality is common practice in the forensic community (Dean et al., 2005; De Angelis et al., 2012; Hona et al., 2021). Simulations can be necessary due to data deficiency, and are a great tool to help test hypotheses in a contained and monitored environment. Simulations in forensic anthropology can be used to increase sample sizes (Steadman, 2018) and are used in this study to produce an ante- and postmortem dataset for comparison analyses. This studies uniqueness testing uses an adapted simulation in comparison to Dean et al. (2005), De Angelis et al. (2012), and Hona et al. (2021). While these studies simulate ante- and postmortem situations by taking two images at different times, the uniqueness study evaluates each individuals image multiple times to build the different datasets (see section 2.3 for explanation). Especially at the beginning of a methodological approach, it can be helpful to use a simulated environment to control testing parameters and develop likelihood values for methodological court application (Steadman, 2018). Therefore, in this part of the research, a simulated approach as seen in section 2.3 and 2.4 was preferred.

Only a few studies so far focus on maxillary sinus uniqueness. Furthermore, these studies concentrate mainly on measurements and volumetric assessments (Musse et al., 2009; Musse et al., 2011; Pinto et al., 2012; Xavier et al., 2015). Morphological evaluations of maxillary sinuses for human identification purposes have not received as much interest as evaluations of frontal sinuses (Xavier et al., 2015). Moreover, the maxillary sinus has previously been accused of offering too slight variation to be used in identification (Bolzan and Tucunduva, 2012). However, correlations of Euclidean distances and clustering of Mahalanobis distances in this study indicate equal usefulness of maxillary sinus morphologies to volumetric and dimensional methods. However, a main factor favouring maxillary sinuses over frontal sinus is their frequent availability on dental overview images (Altug and Ozkan, 2011), allowing to

compare dental status and maxillary sinus morphologies from the same data basis for cross-validation.

Correlations of Euclidean distances between the ante- and postmortem datasets allow for mathematic differentiation between the morphologies. Euclidean distance calculations in this study are based on elliptic Fourier analyses. Those analyses record the morphology of a structure by determining both their x- and y- coordinates. Those coordinates are then projected as waves onto the frequency domain (Caple et al., 2017). The advantage of the elliptic Fourier analysis over other standard geometric morphometric methods is the approach without specific landmarks (Haines and Crampton, 2000; Caple et al., 2017). Morphological matching can then be measured by calculating a dissimilarity matrix of Euclidean distances based on the principal components of the elliptic Fourier analyses.

As evident in both analyses, each individual's antemortem morphology only matches its postmortem counterpart in this sample. It is evident as well, however, that the Euclidean distances between the morphologies can vary. Some hold great distances, while others hold minor dissimilarities. The size of the distances reveals to what extent the morphologies from the ante- and postmortem dataset concur. The smaller the dissimilarity factor, the more uniform or equal are the compared structures (PSU, 2022). Now, it is essential to investigate whether only a dissimilarity factor of 0.000 indicates a total match or if very low factors could also make a reference to a matching morphology pair. Therefore, the need for a cut off value (threshold) should be examined. This threshold could then be used as a guideline giving information about the matching of sinus morphologies. As the morphologies in this study have all been extracted by hand, it would be possible that differences in extraction technique could alter the Euclidean distance score. However, consistent results of 0.000 between matching morphologies in the uniqueness testing indicate no influence of minor alteration during extraction. Yet, when considering the results of both the uniqueness testing and the case study, the slightly different outcomes of both studies stand out. While in the uniqueness testing, all pairs were honoured by a dissimilarity factor of 0.000 (total similarity), the results for the case study vary. Here, three pairs exhibit slightly elevated dissimilarity factors with 0.001 and 0.002. The relevance of those different factors needs to be investigated.

When comparing the two studies, firstly, their extremely different sample sizes stand out. Sample sizes are an important consideration in scientific research. Samples should neither be too small nor too large to obtain valid results. While sample sizes too small may avert extrapolations of the results, too large sample sizes might highlight non relevant statistical differences (Faber and Fonseca, 2014). Comparisons of unequal sample sizes are not lacking meaning per se. Especially when talking about the power of a statistical analysis with unequal sample sizes it is important to consider that the significance of the results is dependent on the smallest sample size (Grace-Martin, 2020). Considering that, inequality in sample size should not significantly affect the interpretation of the results, as the study exhibiting irregular values includes a smaller sample size. Another critical difference is the initial positioning of both studies. Both are simulations of an ante- and postmortem dataset. As stated before, simulations are common practice in forensic research (Hona et al., 2021; Dean et al., 2005; De Angelis et al., 2012), and are very beneficial when testing hypotheses in a contained and monitored environment. However, in contrast to the previously portrayed simulated environment of the uniqueness testing, the two datasets in the case study are not deriving from the same data basis. At first, it seems plausible that the simulation of the datasets from the uniqueness testing could have an influence on the results. However, the simulated postmortem dataset in the uniqueness testing was created by re-evaluating the original data instead of simply copying the data. Consequently, a matching between sinus morphologies is not created because both datasets are the same but because the Euclidean distances between morphologies of the antemortem dataset and the re-evaluated postmortem dataset are close.

However, when examining the two experimental designs, another difference appears. The uniqueness testing's ante- and postmortem dataset derives from the same radiographic material; there is no age gap between the datasets. The lack of an age gap between the ante- and postmortem dataset is not depicting reality as both images usually are taken during different times of the individuals' life. Hypothetically, although the maxillary sinus is believed to remain its size after eruption of the third molar (Iwanaga et al., 2019; Amin and Hassan, 2012; Adibelli et al., 2011), it could be realistic that small changes would appear that are not related to normal bone growth and development. Whether those affect the maxillary sinus morphology is unclear, which is why the uniqueness testing must commence in the future utilizing real life ante- and postmortem images. Referring to the difference in experimental

design mentioned above, the varying results in the study in the simulation realm (uniqueness testing) and the study using ante- and postmortem data with varying ages (case study) could indicate possible changes of the maxillary sinus morphologies after the eruption of the third molar. However, due to the unequal sample sizes of the two studies an adequate statement on the matter is difficult at this point. Further evaluations using non-simulated data for the uniqueness testing should be performed to evaluate morphological changes of the maxillary sinus in adulthood.

In the case study, each individuals' postmortem material is slightly to considerably higher in age than the antemortem counterpart. The affected individuals CS005 and CS008 in the case study exhibit a two-year and four-year age gap between their radiographic images, respectively (Table 6, section 2.4). Under the premise that the morphologies not only change during childhood but could also exhibit slight changes during adulthood, this theory might possess a possible answer. However, when examining the rest of the individuals in the case study, another individual with a large age gap draws the attention (CS001). Here, a dissimilarity factor of 0.000 questions the previous hypothesis. The small sample size of the case study makes explanations difficult. However, an essential difference between the two small age gapped individuals and the individual with a large age gap is their sex. Both individuals with small age gaps are female, while the individual with a large age gap is male. Investigations need to clarify, whether these results, contrary to the findings of the uniqueness testing, indicate a difference between the sexes. Looking back on the findings of the uniqueness testing, the scatterplots did not show a particular prevalence for females or males. Similarly, the scatterplot for the case study (Figure 51 & 55, appendix 2) only shows a slight indication of sex-related differences within the sample. However, this research does not want to emphasise the scatterplot results of the case study due to the small sample size. In contrast, preference should be placed on the hypothesis of a difference between each individual, rather than on age or sex level. Further examinations with a bigger sample size need to establish possible connections between the elevated Euclidean distances and the sex of the individual.

Returning to cut off values, an examination of all Euclidean distance values in the uniqueness testing and the case study shows that aside from the ante- and postmortem pairs of CS005

and CS008 in the case study, no other correlation exhibits such low values (Figure 41 & 42, appendix 1; Table 30 & 31, chapter 4). This allows the conclusion that not only Euclidean distance values of 0.000 indicate total morphological matches but also values up to 0.002. However, more information is needed to definitively decide on the specific cut off value.

7.1.4 The Benefit of Radiographic Morphologies for Human Identification

When identifying unknown skeletal material, postmortem radiographic images are compared to existing antemortem records of known individuals for potential identifications (de Boer et al., 2019). This frequently happens in disaster incidents (Mundorff et al., 2016). Disaster events are classified into closed and open disasters. Closed events describe incidents in which the amounts and identities of the missing people are known (de Souza et al., 2022). For example, with a plane crash, the names and identities of the people involved are registered on passenger lists, and the skeletal material presented can be compared to reference material of a limited group of people (Utsuno, 2019). In an event of a plane crash, aside from traditional identification methods, information such as location of the body in the aircraft and sex and age often can be used to assist the identification process (Vullo et al., 2021). However, with plane crashes, difficulties of identification increase in contrast to other closed disasters as the human remains often are burned and scattered and impacted by explosions (Utsuno, 2019). Open disasters are distinguished by the lack of numbers and identities of the missing people (Vullo et al., 2021). Examples for those kinds of incidents are train accidents without passenger lists, terrorist bombings, and earthquakes (de Souza et al., 2022; de Boer et al., 2019; Utsuno, 2019). However, if human remains are discovered without reference to a possible identity, different approaches to identify the person are necessary. A possibility would be to estimate the sex and age of the individual utilizing paranasal sinus morphologies to develop a possible identification of the deceased person (de Boer et al., 2019). However, in order to enable the usage of maxillary sinus morphologies not only in closed disaster events when identities of the deceased are known, this research proposes the development of radiographic databases to be utilized in open and closed disaster events. The radiographic images retained in the database then act as antemortem reference material to which postmortem data can be compared. Development of a radiographic database for identification purposes depends on

proper data storage, data protection, and database management. At the moment data protection is a national matter as seen in Germany (KVNO, 2020) and can even be handled differently on county or state level as seen in the UK (BMA, 2021) and the US (NCSL, 2014). This research recognises the difficulty of developing an internationally used database and suggests initially collecting and joining together digital image material on a local level through dental practices, before merging the local data on county level and then national level.

Statistical evaluations in Germany showed 57 million dental radiographs (extraoral and intraoral) being taken in 2014 (Nekolla et al., 2017). This is related to a population of ca. 81 million people in Germany in 2014 (bpb, 2020). Medians of dental radiographic imaging between the years of 2007 and 2014 revealed 0.6 to 0.7 images taken per person per year. Within the total amount of dental radiography, extraoral overview imaging increased in the factor of 30 % within the observed time frame (Nekolla et al., 2017). In 2018, 40 % of all radiographic imaging were accounted for in dentistry (BfS, 2022). Public health records of the National Health Service (NHS) showed an increase from 1.4 to 1.8 million panoramic radiographs taken in England and Wales in the years from 1992 to 2005. Furthermore, in 2004/05 the percentage of panoramic images amounted to 13.3 % of the total dental radiographs taken in the same regions (Public Health England, 2010). This is related to a population of ca. 50 million people in England (VNW, 2022a) and ca. 2 million people in Wales (VNW, 2022b) in 2005. Estimates from healthcare market research show recordings of 1.4 billion dental radiographs within the US in 2018. This includes both intra- and extraoral radiographs as well as cone-beam computed tomography, while intraoral radiographs hold 90 % of the collected data (iData, 2019). This data is related to an US population of ca. 326 million in 2018 (Statista, 2022). The imaging data from Germany, the UK and the US and the rising trend of panoramic/extraoral imaging increases the probability of most people having to take at least one dental overview image throughout their lifetime.

Retaining the images centrally for identification purposes would require altering the procedure in which dental radiographic images are taken and restored at dental practices. However, this research does not suggest intentionally exposing the patients to radiation by deliberately taking x-ray images solely for identification. However, once an image has to be taken regardless, for medical purposes, an overview image that can be used both for

diagnostic and identification functions is preferred over single tooth imaging. Although radiation exposure is slightly elevated with extraoral or panoramic imaging (Almohiy et al., 2020), the discovery of dental lesions is not diminished in comparison to intraoral imaging (Terry et al., 2016). As the statistical evaluations of dental radiography in Germany (Nekolla et al., 2017), England and Wales (Public Health England, 2010), and the US (iData, 2019) show, the vast majority of dental radiographs taken still are intraoral images. In order to advance the identification methods on maxillary sinuses it should be tested whether the intraoral images might also be suitable for examinations. Of course, only partials taken from the maxillary dental arcade are useful in that regard. On intraoral images from the canine, premolar and molar region, the lowest aspects of the maxillary sinus can be depicted. With those radiographic images it would be vital to record necessary information on image acquisition and the location of the teeth recorded in order to replicate the exact location in the postmortem recording. The methodology as described in this thesis is focussed on extracting and comparing the maxillary sinus as a whole. Future examinations would need to determine, whether the recording of a partial maxillary sinus in an intraoral radiographic image would also be suitable for human identification.

Another advantage of an imaging database is the possibility of comparing sinus morphologies and simultaneously assessing the dental status for human identification. When needed, the dental and sinus records can be compared simultaneously, and the identification of the unknown human remains can be accelerated. Furthermore, identifications using multiple methods and techniques, like for example dental records and maxillary sinus structures, cross-validate a person's identity, making it harder to challenge in court (NIST, 2018).

Many methods are available to confirm or deny a deceased person's identity. Standard methods are forensic odontology methods, DNA analysis, friction ridge analyses, and assessments of medical findings (Interpol, 2018). Primary methods like analyses of friction ridges are internationally used in forensic examinations, as retrieval and digital comparisons allow for systematic investigates on fingerprinting databases (Interpol, 2018). Furthermore, examinations of dental structures as well as extremely positive identification rates utilizing ante- and postmortem teeth comparisons makes forensic dentistry one of the primary methods for identification (Modesti et al., 2014; Malik et al., 2012; Interpol, 2018). Within the

group of primary human identification methods, DNA testing often is perceived as the gold standard and DNA evidence from a deceased person can be used to match it to the persons reference DNA material (Kayser, 2015). Furthermore, DNA profiles can be applied to predict (with limitations) certain biometric features (Chaitanya et al., 2017; Dembinski and Picard, 2014) for example when the deceased person is not recognisable anymore. Those primary identification methods often are applied concurrently as a means of cross evidencing. Additionally, each method applied is dependent on the body structures available for examinations (Interpol, 2018). Next to those primary methods, a vast range of secondary methods is used for human identification. Those secondary methods for example consist of personal data evaluations and medical clothing evidence (Interpol, 2018). Further evaluations utilize radiological examinations, facial reconstruction through osteological evaluations and comparisons of bodily marks (Wlodarczyk, 2012; de Boer et al., 2020)

With this array of expertise, the question can be posed as to why additionally use the comparisons of maxillary sinus morphologies for identification. Furthermore, to date, visual assessments of sinuses are still used as an addition to form a correct identification of skeletal material (Sathawane et al., 2020; Ruder et al., 2012). In comparison to elliptic Fourier analyses of the sinus morphologies, visual assessments are executed quickly and without any software assistance. However, especially when thinking about court applications, the method of morphological comparison must be preferred. Studies show, that examinations of anthropological material based on visual assessments are exposed to decisions based on the contextual information rather than the structure itself (Nakhaeizadeh et al., 2014). Furthermore, the United States Department of Justice claimed that structures in visual forensic evaluations are rather compared than measured (2021). Although it has been criticised that the US Department of Justice is not a scientific body (Albright, 2021), this declaration needs to be considered when thinking about court application. Therefore, considering biased evaluations and the statement of the department of justice, the methodological approach of sinus morphology comparison highly outweighs simple visual assessments.

Morphologies of the maxillary sinus are highly suitable for human identification due to their high anatomic variability (Sidhu et al., 2014; Ata-Ali et al., 2017). Furthermore, their relative

size and volume stability during adulthood allow utilization in ante- and postmortem comparability methods (Demiralp et al., 2019). The proposed method of morphological comparison could potentially be used in various environments to identify human skeletal remains. Aside from stationary x-ray machines in the laboratory or morgue, hand-held x-ray machines could be used for image acquisition as they produce well-structured pictures of the paranasal sinuses for medical use (Purchasea et al., 2019). However, whether image quality is sufficient for morphological sinus evaluations in human identification still needs to be confirmed. Additionally, in safety endangering situations and security incidents, x-ray acquisition of maxillary sinuses and subsequently morphological evaluations of that structure could be applied to human remains as well as living individuals as routinely done with frontal sinuses (Christensen and Hatch, 2018). This application could especially be interesting in situations dealing with traumatised persons, when low impact methods are needed.

Most importantly, however, radiographs covering the maxillary sinuses are frequently available in dentistry health records (Cox et al., 2009; Tatlisumak et al., 2007). Commonly, with dental overview/extraoral images taken for dental or orthodontal procedures, x-ray images of the dental arcade additionally cover the maxillary sinus region (Altug and Ozkan, 2011). This allows the potential usage of the same radiograph for dental comparison and morphological analyses of the maxillary sinuses. This availability of both structures used for human identification highlights the importance of maxillary sinus comparisons compared to frontal sinus analyses. Frontal sinus images are not as easy to obtain unless the individual has been imaged for a previous illness in this cranial region. In contrast, the likelihood of maxillary sinus radiographs already existing on panoramic or extraoral radiographs is much higher.

7.2 Intra- and Inter-Observer Reliability

In order to use maxillary sinus morphologies for human identification, it must be tested if and to what extent multiple practitioners can reproducibly repeat the extraction of morphologies. This also implies that only the connection between the data base and the used methodology are important in court applications in contrast to expertise of the expert witness alone (Steyn et al., 2012). However, the variability among practitioners poses issues about the

consistency of the method and the agreement among the specialists. Both a study and a methodological approach have to produce consonance measures between extraction repetitions and between different extractors (Garfinkel et al., 2009). Confidence in a methodological approach increases exponentially with the amount of agreement between the observers. With the confirmation of uniqueness, the topic of reproducibility massively gains relevance. Furthermore, in the US, Rule 702 of the 1975 Federal Rules of Evidence (FRE) ensure that in a trial the judge holds the deciding power whether a methodological approach and therefore the expert witness testimony is reliable and relevant (Christensen and Crowder, 2009). As this depending on the situation and circumstances could be positive or negative, it is crucial to develop methods according to Daubert standards and incorporate measures of validity, error rates, and reproducibility (Christensen, 2005).

Variability among data collectors is a function of experience in the field and interpretation approach. Errors mainly occur due to insufficient training with the extraction tools and the medium of radiographic imaging. However, variability cannot only occur between different observers but also between two extractions of the same observer. With one observer, a homogeneity of evaluations is assumed especially when the experimental environment stays the same (McHugh, 2012). Cohen's kappa (κ) can be utilised both for intra- and interrater reliability testing. Interpretation of correlation coefficients by Cohen are: <0 (no agreement), .01-.20 (none to slight agreement), .21-.40 (fair agreement), .41-.60 (moderate agreement), .61-.80 (substantial agreement), and .81-1.0 (almost perfect agreement) (Marston, 2010). However, this study rather follows the adapted coefficient evaluation of McHugh (2012) (Table 8, section 2.5). This interpretation adds a category and shifts the positive agreement interpretations. When the moderate agreement was achieved before with coefficients of .41 to .60, McHugh's interpretation allows this level of the agreement only with coefficients of .60 to .79. This new recommendation in agreement levels allows for a firm interpretation. With the new interpretation guidelines, levels below .60 suggest insufficient agreement. A huge advantage of calculating the Cohen's kappa coefficients is their easy and straightforward interpretation (McHugh, 2012).

Intra-observer reliability in this research was tested six months after the primary data collection commenced to avoid a habituation effect for the observer. Although, with the

amount of data evaluated and the randomisation put in place, this would hardly have been an issue. However, in order to establish a well-rounded study design, effects of bias need to be avoided. Attention needs to be focussed on randomisation and replication (Sullivan et al., 2016). For intra-observer reliability testing and therefore replication, it is vital to understand whether the two parts of this study were carried out under similar conditions. Randomisation of the structures helps to avoid this kind of confirmation bias (Althubaiti, 2016). Furthermore, the hiatus of six months between initial and re-evaluation should counteract a habituation effect.

Re-evaluation and extraction of the morphologies were equally assessed via the elliptic Fourier analyses, and subsequently, Cohen's kappa values for left and right-sided morphologies were calculated. Levels of intra-observer agreement on both sides exhibit an 'almost perfect' score, with values above .90. Inter-observer scores laid above .83 with one outlier at .79. In comparison to the hereinafter discussed studies these scores tend to be above average. Extraction of frontal sinuses on cone-beam computed tomography and radiographs by Soares et al. (2016) showed Cohen' Kappa values of .80 to 1.00 for intra observer reliability and .70 to 1.00 for inter observer reliability. The study by Rabelo et al. (2016) which focussed on extracting frontal sinuses from radiographic images, produced Cohen's Kappa values of .76 to 1.00 for intra observer reliability and .40 to 1.00 for inter observer reliability. Both of the two previously cited studies examined frontal sinuses for identification purposes. The study by Pérez Sayáns et al. (2020) focussed on maxillary sinus morphologies and volumes on cone-beam computed tomography images for medical purposes. Their inter-observer reliability testing showed a Cohen's Kappa value of .93. The interpretation of those values varies, depending on which interpretation guidelines are followed. While Cohen (1960) marked values ranging from .61 to .80 as substantial and .81 to 1.00 as almost perfect, the interpretation by McHugh (2012) is slightly more poignant. In this interpretation values ranging between .80 and .90 are marked as strong and values above .90 exhibit an almost perfect level of agreement. According to those agreement levels, anything below .80 should be considered invalid (McHugh, 2012). From this point of view, the previously mentioned agreement levels have to be considered critically as intra- and inter observer reliability scores of studies by Rabelo et al. (2016) and Soares et al. (2016) fall below this threshold. Interestingly, scores within those two studies showed a varied distribution

between .76 and 1.00, while agreement levels in this study consistently scored above .90. For inter-observer agreement variability is even more diverse with the two reference studies scoring in a range from .40 to 1.00, while this study's scores are mostly above .80. This could possibly be explained by differences in image extraction and interpretation as the reference literature mainly uses volumetric approaches and measurements while this study uses a morphological approach.

Overall, levels of agreement in this part of the study are very encouraging, with strong and moderate agreement levels (see chapter 5). The training levels of the external observers (OB1 and OB2) indicate the feasibility of the proposed methodological approach. Although little insecurities at the beginning of the extraction training strained the two observers, continuous training encouraged their confidence in handling and interpreting radiographic images. This is also determined by Spies et al. (2021) who found "that even very brief radiological training and experience can result in a drastic increase in sensitivity" when handling human bones. As trends in forensic anthropology indicate increases in virtual assessments and approaches in the future, it is highly beneficial for forensic anthropological practitioners to undergo radiological training (Spies et al., 2021; Flach et al., 2014).

The intra- and inter-observer reliability results in this study show that high quality extractions and interpretations are possible even with previously untrained staff. Of course, results of the intra-observer reliability testing demonstrate that interpretation skills increase with experience, but extraction of morphologies is replicable even with little to moderate training. These levels of agreement are highly encouraging, especially when thinking about applying a methodological approach in court. In comparison to the methodological approach used by Soares et al. (2016) and Rabelo et al. (2016), confidence level for this study's methodological approach rise due to its constantly high Cohen's Kappa values. Establishing a solid reproducibility level or level of confidence that is recognised for paranasal identification methods in the judicial system is difficult. Therefore, strong reliability values, such as the Cohen's kappa coefficients in this study, strain challenges from opposing councils and rival experts in court.

The regulation of sinus identification methods through Cohen's Kappa values is a good first step however, it is necessary to frame and regulate the field of forensic anthropology in order to establish further methodological standardisations (Passalacqua and Pilloud, 2021). Within the anthropological community, multiple individual codes of practices exist, like for example from the Forensic Anthropology Subcommittee (OSAC, 2022) and the Royal Anthropological Institute in cooperation with the Forensic Science Regulator (RAI, 2018). Additionally, many Forensic Anthropological organisations (e.g. the American Academy of Forensic Sciences, the British Association for Forensic Anthropology, the British Association for Biological Anthropology and Osteoarchaeology) adhere to an individual ethical code. Scientific expertise certificates are currently awarded by the Royal Anthropological Institute, the American Board of Forensic Anthropology, the Asociación Latinoamericana de Antropología Forense, and the Forensic Anthropology Society of Europe (Passalacqua and Pilloud, 2021). Though this practice of individual codes in every organisation seems to be very isolating while common sense would urge all members of the anthropological science community to adhere to the same codes of practice. It is therefore not surprising that overarching approaches are demanded and proposed (Passalacqua and Pilloud, 2018).

One step further in court, each country has their own regulations and codes of practice to manage expert witness admissibility. In the US on federal and state courts, the expert witness is an individual that is "qualified as an expert by knowledge, skill, experience, training, or education" (Lubet and Boals, 2020). Under rule 702, it is the judges task to assess whether the expert possesses required specialised knowledge and training that is aiding the tried case (Capra, 2018). Following Lubet and Boals (2020), after this initial testing, three additional criteria are applied to the expert:

> "1. the testimony must be based upon sufficient facts and data
> 2. the testimony must be a product of reliable principles and methods
> 3. the witness must have applied the principles and methods reliably to the facts of the case".

In the UK, expert witnesses likewise require high knowledge, experience, as well as training and need to abide the Criminal Procedure Rules (SFO, 2022). Furthermore, admissibility in the field of forensic anthropology is dependent on a certification of the Royal Anthropological Institute of Great Britain and Ireland to insure professional standards in ethical approaches

and code of conduct (Hackman et al., 2018). In non-jury-based countries like Germany, the selection of medical expert witnesses is regulated through each county's medical association (AEKNO, 2022).

Even though the methodology of morphological extraction of radiographic images in this study proves high success rates even with little to moderate training, it is sensible to seek periodic training in the advances of forensic radiology and, in particular, the radiology of the maxillofacial area. As demonstrated in this study, training plays a fundamental part in the success of the interpretation and elevates the achieved identification (Koot, 2003; Hogge et al., 1993). As well as training it is essential to provide a proficient and independent methodology (Ballantyne and Wilson-Wilde, 2020). The methodology of extracting sinus morphologies, applying elliptic Fourier analyses, and measuring Euclidean and Mahalanobis distances to uncover matching morphologies, allows for an objective analysis of human maxillary sinus morphologies. However, for court applications, the human element should not be neglected. Unfortunately, in the eyes of the jurors and the judge, the credibility of an expert witness is not only reflected through their reproducible and accredited methodological approach. Persuasiveness of the expert witness can also be influenced by their choice of style and attire (Brodsky et al., 2010). Furthermore, their communication style can influence their perception to the judge and jurors. Aiding their intention of convincing the audience of their expertise is a clear communication style avoiding jargon (McCarthy Wilcox and NicDaeidb, 2018). Brodsky et al. (2010) additionally found that a personal likability of the expert is the major factor influencing judge and jurors. Consequently, this indicates that a personal dislike of the expert could potentially influence the juror towards doubting the expert's testimony. Closely following likability, the factors of intelligence, trustworthiness, and believability can influence the jurors perception (Brodsky et al., 2010). McCarthy Wilcox and NicDaeidb (2018) found that confidence and demeanour and explanation style highly influence the opinion of judge and jurors. Furthermore, Blaua (2019) showed that the style of presenting evidence also impacts how the evidence is comprehended by the jurors. This shows, that an expert witness not only needs to concentrate on presenting factual correct evidence but also needs to emphasis supposedly secondary factors like appearance and delivery of facts.

This research set out to understand whether maxillary sinus morphologies can, in fact, be used in an ante- and postmortem scenario for human identification. The expert witnesses' job is to explain why the depicted evidence suggests a total match between ante- and postmortem material. However, it is essential to remember that the expert witness can only provide identification probabilities in a clear communication style (Neal, 2009), while judge and/or jury hold the deciding power. Therefore, the reproducibility of a methodology forms a solid and robust foundation for any court application. Methodological approaches used in forensic cases need to generate reliable and robust results that include information about the accuracy levels (Ballantyne and Wilson-Wilde, 2020). In order to present a valid and reliable scientific method before the court, multiple factors need to be considered. The foundation of a reliable and reproducible method lay in the standardised methods used and the accreditation of the laboratory in which they are carried out. Furthermore, the competency of the method is measured on the accreditation of the practitioners (Ballantyne and Wilson-Wilde, 2020). The factors of repeatability (intra-rater reliability) and reproducibility (inter-rater reliability) need to be connected with the factor of accuracy that is acting as an error control (Chin et al., 2019). In general, a shift is noticeable in forensic sciences arguing for a more open and transparent interaction with research products. This recent shift will probably broaden within the whole forensic community and allows for unlimited access of information on forensic methodology for anyone involved with the legal system, independent of geographic location (Houck et al., 2019).

7.3 Age Estimation

In recent years, the use of maxillary sinuses for age determination increased. As with the uniqueness testing, however, volumetric approaches (Belgin et al., 2019; Demiralp et al., 2019; Rani et al., 2017; Velasco-Torres et al., 2017) and the use of measurements (Subasree and Dharman, 2019; Velasco-Torres et al., 2017) are the favored methodological approach. Furthermore, while most studies use adult individuals for their examinations, samples of growing individuals are scarce (Maspero et al., 2020). However, the development of the maxillary sinus in subadult samples is critical to understand how changes affect the ability to apply ante- and postmortem comparisons. With an adult sample, the assumption is that

overall dimensions and volumes stay either the same, or exhibit only minor changes (Demiralp et al., 2019; Subasree and Dharman, 2019). Following this understanding of consistent sinuses during adult years, the ante- and postmortem comparisons of the structure should be possible even with the reference material being taken long before the postmortem images. Whether that in fact is possible with adult and subadult individuals or whether maxillary sinuses are too variable during the growth years and beyond still needs to be investigated.

This research used three longitudinal growth studies (AAOF, 2020), which provide multiple imaging of the same individuals throughout their subadult and adult years. The available data for adult years is much scarcer then for subadult years. This approach allows for more accurate results regarding ante- and postmortem comparisons and stands in contrast to other studies which investigate maxillary sinus changes in samples of growing individuals (Maspero et al., 2020). Studies using only one image per individual limit their approach as they cannot account for individual changes. However, in order to investigate age-related changes for ante- and postmortem comparison methods, it is vital to understand changes on an individual level. To this effect, working with longitudinal studies offers numerous advantages as they incessantly track and quantify changes in particular individuals (Caruana et al., 2015). Studies estimating age on only one image per individual are not able to define and detect specific growth events. Furthermore, they cannot monitor variations over time in an individual level. Longitudinal studies on the other hand can identify unique development trends and exhibit a high accuracy rate (Caruana et al., 2015). The accuracy rate is heightened as changes happen and are recorded in real time. However, one of the biggest advantages of longitudinal studies is the ability to eliminate recall bias (Caruana et al., 2015). This bias is excluded as data is collected even before certain growth events of the maxillary sinuses appear. All those advantages of longitudinal studies contribute to a high level of validity and a superiority over cross-sectional studies.

As described in section 6.1, the sample size of this study makes applying an adequate age clustering system difficult. Finding an appropriate age clustering system with meaningful age intervals is mostly dependent on the available data. However, in aid of comparability, a clustering system must be chosen that allows to draw comparisons to other established systems. Other research investigating age-related changes of maxillary sinuses mostly

resolved their clustering problems depending on their data availability. Belgin et al. (2019) used for their evaluation of maxillary sinus volumes five age groups with irregular intervals between six and nine years. Others used regular intervals of two years (Maspero et al., 2020) or ten years per cluster (Jun et al., 2005; Subasree and Dharman, 2019). The most irregular age clustering is used by Velasco-Torres et al. (2017). Here, the intervals decrease up until age fifty before starting to increase again.

As imaging intervals varied for every individual in this research's study, a clustering system included as many images as possible but excluded duplications of the same person within each cluster. Furthermore, the cluster range needed to be small enough to exhibit even minor changes. The chosen system exhibits eight clusters and amounts for the image density during years one to five. Furthermore, image availability allows understanding morphological development beyond age twenty-one in clusters six to eight. Many studies suggest the end of the growing period of the maxillary sinus around the eruption of the third molar. Often this eruption is equated with the twenty-first year of age (Iwanaga et al., 2019; Amin and Hassan, 2012; Adibelli et al., 2011). However, it is important to investigate whether changes in morphology correlate with those studies' dimensional and volumetric findings. Therefore, this study closely investigates changes up to the age of thirty (cluster seven) and looks at an additional six morphologies over the age of thirty-one.

Measurements and volumes of a structure can exhibit changes while its morphology remains unchanged. This is better explained by applying a thought experiment: a rectangular three-dimensional body with a volume V_0 has a specific (in this case rectangular) morphology. Taking a three-dimensional image reveals its volume (V_0). With help of a two-dimensional image, the structure's morphology can be extracted. Next, an identical rectangular object is placed on top of the first structure. After taking two- and three-dimensional images, the following is evident: The image shows no morphological changes. However, the volume of the imaged structure now increased to $V_1 = 2 \times V_0$. This shows, that the comparison of results of two- and three-dimensional approaches remains difficult, as the third dimension plays an important part in the evaluation of maxillary sinuses.

Growth rates are a standard tool used in biological studies to examine the rate of increase of a specific feature within a population (Hall et al., 2013; Iscan, 2005). In this study, the growth rate cannot be equated to a common length growth but describes the change of Euclidean distances of maxillary sinus morphologies per year. Correlations of averaged Euclidean distances with the age clusters in this study show monotonously rising distances with increasing age clusters. Quasi-linear trend lines of averaged Euclidean distances display a positively increasing tendency for all populations (Figure 58 & 59, section 6.2). Until the age of twenty (cluster five), Euclidean distances for all populations and on both sides rise continuously. These results are in agreement with the volumetric study of Maspero et al. (2020). Here, the volumes of maxillary sinuses increased with rising age. Additionally, they report a growth spurt during the ages of twelve to fourteen. However, this particular growth spurt cannot be found within the data of this study. Starting with age cluster six, data starts to deviate for left and right. While distances decrease for the left side, they increase for right-sided sinus morphologies. The decrease could be comparable with the findings of Ariji et al. (1996), who found increasing sinus volumes up to the age of twenty. After this threshold, a decrease is reported. In contrast, Jun et al. (2005) reported an increase in maxillary sinus volumes between the years of twenty to thirty (corresponding with cluster six in this study) before declining again. However, data availability for clusters one, six, seven, and eight is scarce in comparison to the remaining clusters (Figure 57, section 6.1). Although distances are averaged among all morphologies within each cluster, this study suggests discarding the data in clusters one, six, seven and eight. This leaves a monotonously increase in the Euclidean distances (supported by strong Pearson correlation coefficients in Table 35, section 6.2) within each population, similar to the volumetric results (Maspero et al., 2020; Ariji et al., 1996).

Correlations of averaged Euclidean distances and age clusters by sex show a positive increasing tendency as well, with quasi-linear trend lines (Figure 61 & 62, section 6.2) (supported by the Pearson correlation coefficient in Table 37, section 6.2). In cluster four (eleven to fifteen years), both sides exhibit a steep elevation for the male sample, especially the left side. This could be due to a pubertal growth spurt. However, in contrast to many other studies, morphologies of the maxillary sinuses overall are not more prominent in males than in females. Both with dimensional (Jehan et al., 2014; Kanthem et al., 2015; Khaitan et al., 2017; Mathew and Jacob, 2020) as well as with volumetric approaches (Kanthem et al., 2015;

Belgin et al., 2019) the literature suggests maxillary sinuses of females to be smaller than of males. Furthermore, Belgin et al. (2019) reports a significantly higher volume in males in the age group of eighteen to twenty-four. This age range corresponds to cluster six in this study, but the results are not visible here. In this study, cluster six shows marginally larger morphologies for males on the left side and larger morphologies for females on the right side. As with the correlation by population before, this study additionally suggests discarding the information in clusters one, seven, and eight due to insufficient data availability.

Interestingly, the results of the correlations dependant on sex exhibit vastly different results than the studies applying dimensional and volumetric methods. As mentioned before, those studies indicate smaller maxillary sinuses for females. Furthermore, those results are homogenous for dimensional (Jehan et al., 2014; Kanthem et al., 2015; Khaitan et al., 2017; Mathew and Jacob, 2020) and volumetric methodologies (Kanthem et al., 2015; Belgin et al., 2019). Exceptions can be found in a recent study by de Barros et al. (2022) which found no difference between females and males both for dimensions and volumes. The results of this study indicate no substantial morphological difference between females and males. This is interesting as it stands in contrast to the main dimensional and volumetric models but has comparable results to the most recent publication by de Barros et al. (2022). Although the first instinct could be to strengthen this studies' findings with the results of de Barros et al, it needs to be considered that de Barros et al. simultaneously did not find correlations between females and males on a volumetric level. This is diametral to all previous volumetric studies. Furthermore, de Barros et al. uses square millimetres as a measurement of sinus area, while this research's study uses a geomorphometric approach. Therefore, it is questionable, whether the study of de Barros et al. holds any power to validate this research's study.

However, differences to the remaining dimensional and volumetric studies could potentially be explained through differences in two- dimensional and three-dimensional structures. As explained with the thought experiment above: even if the overall mathematical volume between two different sinuses remains the same, the two-dimensional morphology of the sinus can change and vice versa. This hypothesis is not to say that there are no differences between female and male morphologies however, to date the differences are not as poignant to observe as with volumetric approaches.

Similar approaches can be taken with differences between this study's findings and research applying measurements on the maxillary sinuses. Although, with measurements the comparison is slightly more debatable than with volumes. Studies using measurements showed significant differences between the sexes (Jehan et al., 2014; Kanthem et al., 2015; Khaitan et al., 2017; Mathew and Jacob, 2020), while this study did not exhibit significant differences between the sexes. Again, this is not to say that there are no differences between the analysed structures, however as with volumetric approaches they are not as poignant to observe. Once again this could be explained with the structure's natural differences. In contrast to the above-mentioned volumetric hypothesis both entities are taken on a two-dimensional plane. However, this study uses the whole morphology of the sinus, while most other studies utilize biological landmarks for measuring distances or simply measuring the maximal craniocaudal diameter (Kanthem et al., 2015). A hypothesis could be that differences in for example the maximal craniocaudal diameter between the sexes do not affect the overall morphology enough to enable differentiations. While other studies only use one measurement for sex differentiation, this study uses multiple data points to describe the sinuses morphology. Therefore, the one maximal craniocaudal diameter that is taken to describe the difference does not significantly matter when considering the morphology as a whole. However, both comparisons with measurements and volumes are working hypotheses that need to be evaluated further

Another explanation could be an unspecific connection between the sex of an individual and its maxillary sinus morphology. However, as the literature suggests specific connections between the sex of an individual and its sinus volumes and measurements, no connection between the sex of an individual and its sinuses' morphology is unlikely. Therefore, this research is inclined to assume different behaviour of a structure's volume as compared to its morphology. However, testing both hypotheses is beyond the scope of this research and needs to be examined further in a sequential research.

The growth rates themselves, both for each population and sex, are calculated from the gradient of the correlations (Table 36 & 38, section 6.2). Growth rates for left-sided morphologies appear to be slightly higher. However, the contiguity of the rates, divided into left and right sides, would make a classification of unknown sinus morphologies into the

gradients difficult. Therefore, this study suggests using averaged growth rates per population and sex to simplify the procedure (Table 39).

Table 39: Averaged growth rate per population and sex (age estimation study).
(BBG: Bolton Brush Growth, BG: Burlington Growth, OG Oregon Growth)

Population/Sex	**Averaged Growth Rate, Year^{-1}**
BBG	1.995
BG	2.029
OG	3.022
Female	2.126
Male	2.489

Those averaged growth rate values make the classification slightly easier. However, the lack of a standard deviation complicates the procedure. A standard deviation processes the data scattering in a dataset and measures its variability. Therefore, a standard deviation acts as an estimate of the population's variability (El Omda and Sergent, 2021). With every research, the results of a study need to be described meticulously, as its outcomes can only be generalized to people and populations which are similar to the investigated sample (Andrade, 2020b). This especially applies in forensic research. When extrapolating information of a sample on one individual for biological profiling it is vital to understand the limitation of the studied sample (Faber and Fonseca, 2014; Andrade, 2020a). Measures of dispersion help that matter, as the standard deviation offers insight into the difference between the average person and the population mean. As standard deviations also are not affected much by extreme values, they offer a more accurate representation of population construction (Andrade, 2020b; Altman and Bland, 2005). In this case, standard deviations would allow to define a margin in which the averaged growth rates fluctuate per population and per sex and facilitate the applicability in a methodological approach. When thinking about applicability, the growth rates in this study by sex overall seem more utilizable. As the growth rates of Bolton-Brush Growth and Burlington Growth show very close values, only a classification into Oregon Growths or Bolton-

Brush Growth/Burlington Growth is possible. Growth rates by sex seem more suitable for the application.

The growth of maxillary sinuses has been investigated before. However, most research focusses on metric changes in subadults instead of morphological changes. Adibelli et al. (2011) investigated the development of all paranasal sinuses via magnetic resonance imaging. Asaumi et al. (2010) examined the development of maxillary sinuses in fetuses and found a correlation between maxillary sinus development and the formation of the nasal cavity. Other studies found that the volume of maxillary sinuses increased until age twenty before decreasing again (Sarilita et al., 2021). In contrast, Jun et al. (2005) found an earlier onset of maxillary sinuses in the female sample than in the male one with the female maxillary sinuses remaining overall smaller in volume. Early studies evaluated the correspondence of sinus floor height and sinus volume and found no connection between sinus volume and dentition status (Ariji et al., 1996). Lorkiewicz-Muszyńska et al. (2015) suggested a pubertal growth phase of maxillary sinuses concluded maxillary sinus changes in antero-posterior as well as horizontal and vertical directions. Other studies found very prominent sexual dimorphisms during the ages of fifteen and sixteen (Przystańska et al., 2020) and indicated steady growth until age eighteen with increases in depth and width until age twelve (Bhushan et al., 2016). A huge sector advancing maxillary sinus research is maxillofacial surgery. Growth studies often are used to understand typical development trends for surgical intervention (Lee et al., 2020) as knowledge on growth peaks simplifies treatment planning (Maspero et al., 2020) (Bahadir et al., 2008). Both parts of this age study (by population and by sex) indicate a continuous positive increase in Euclidean distances. Furthermore, morphological growth agrees with dimensional and volumetric growth by constantly increasing from birth to age twenty. Additional research needs to further evaluate individual growth rates for each age cluster to enable the age classification of the maxillary sinus morphologies. Calculated growth rates could potentially be used as a first indicator of the individuals' sex.

Chapter 8 Conclusion

This research continues prior investigations of maxillary sinus morphologies and concentrates on morphological uniqueness and the effects of age-related changes on the structures. Summarised, the research questions as stated in chapter 1 test morphological uniqueness in a simulated and real-life environment, assess reproducibility of the uniqueness testing, and establish age-related changes in maxillary sinus morphologies.

Samples used for each study of the research were evaluated at intra-populational as well as inter-populational levels. A complete account of all populations used and the composition for uniqueness testing and the age estimation study can be found in Table 3 in chapter 2. This research has given a detailed description of the state of the art in sinus identifications and considered the unfortunate scarceness of morphological sinus evaluations. Furthermore, the rarity of using maxillary sinuses for positive identification, in comparison to frontal sinuses, has been discussed.

Due to general paranasal variability (Marino et al., 2020), the following objectives were selected for this research:

1. **To test for morphological uniqueness between the ante- and postmortem dataset of the sample;**
   1.1. To assess differences between the maxillary sinus morphologies of the sample;
   1.2. To determine the biological properties of the sample;

   This research empirically assesses morphological sinus variability and shows distinct and quantifiable differences in morphologies. Euclidean distances of 0.000 and corresponding Mahalanobis distances were only found for ante- and postmortem morphology pairs in a simulated environment.

   - Euclidean and Mahalanobis distances demonstrate that each individual's maxillary sinus morphology is unique.

Both right and left sided sinus morphologies show equal variations throughout the study's populations. Furthermore, population analyses gave insights into inter- and intra-populational differences.

- Evaluations proved that both left and right-sided maxillary sinuses morphologies could be applied in forensic casework to identify unknown and deceased human individuals.
- Population analyses suggest no impact of moderate climate variations on adult maxillary sinus morphologies.
- Evaluated variances between populations indicate no differences between the maxillary sinuses neither chronologically nor geographically.

Additionally, this research evaluated biological properties of the maxillary sinus morphologies. Analyses by sex and age do not indicate a significant classification of morphologies, which stands in contrast to previous measurement and volumetric approaches.

- Analyses by sex and age exhibit a widely mixed data distribution and suggest no impact on adult maxillary sinus morphologies.
- Fascinating effects and differences between maxillary sinuses indicate a possible variability between volume, measurements and morphology in adult individuals.

2. To determine uniqueness of maxillary sinus morphologies in a real-life application (case study);

Evaluations of the case study show a morphological sinus variability as previously seen in the uniqueness testing. Euclidean distances up to 0.002 and corresponding Mahalanobis distances were only found for ante- and postmortem morphology pairs in a real-life environment. Those values show that each individual's antemortem morphology only matches its postmortem counterpart.

- Euclidean and Mahalanobis distances demonstrate that each individual's maxillary sinus morphology is unique.

Furthermore, the uniqueness testing and case study found extremely low Euclidean distances (0,000 to 0,002) for matching ante- and postmortem morphology pairs in a simulated and real-life environment.

- Close Euclidean distances are suggested as preliminary cut off values (Euclidean distance values of 0.002) between matching and non-matching sinus pairs and make an application in forensic cases possible.

3. To assess the reproducibility of the approach;

Developing a human identification method and the application of the methodology for routine use is an incentive for evaluating the methods reproducibility. Furthermore, reproducibility is an essential condition for methodological court application. This research's promising results for inter- and intra-observer biases, especially considering the methodological deficiencies discussed in chapter 7, show a methodological approach that is standardised and objective.

- Intra-observer agreements with 'almost perfect' scores and 'moderate' and 'strong' intra-observer agreements (interpretation categories after McHugh, 2012) clarify the reproducibility of the methodological approach.

Additionally, steps need to be taken to standardise and refine the approach. However, the methodology is advancing to meet the Daubert standard in court applications. Elliptic Fourier analyses of maxillary sinus morphologies offer clear and quantifiable identifications that can be reproduced by referencing methods.

In order to enable sinus morphological comparisons as a routine tool in human identification, databases of maxillary sinus radiographs are a necessary prerequisite. However, this would require altering the procedure of taking routinised dental

radiographs and developing proper storage of the digital images. When needed, dental and sinus records could then be ordered simultaneously, and the identification of the unknown human remains could be accelerated. Furthermore, identifications using dental records and maxillary sinus structures cross-validate a person's identity, making it harder to challenge in court.

4. To establish age-related changes in maxillary sinus morphologies of the sample;

4.1. To develop an age clustering system for the sample;

4.2. To calculate growth rates for the sample.

Age estimations in subadults pose the question of variability between evaluation methods of volumes, measurements, and morphologies. This research identified age-related changes in maxillary sinus morphologies and introduces an age clustering system adapted to the sample.

- The age clustering system is divided into cluster 1 (0 to 2 years), cluster 2 (3 to 5 years), cluster 3 (6 to 10 years), cluster 4 (11 to 15 years), cluster 5 (16 to 20 years), cluster 6 (21 to 25 years), cluster 7 (26 to 30 years), and cluster 8 (ages above 31 years).

Age-related changes within the populations are investigated on an individual level in longitudinal studies before drawing conclusions on populational levels. Growth rates are calculated by correlating averaged Euclidean distances with the age clusters. Those calculations of growth rates from the gradient of the Euclidean distance correlations give a good overview of the morphological change during growth.

- Growth rates indicate a change of morphologies up until age twenty-one.

However, applying growth rates for unknown skeletal material is a problematic approach. A method could be the conversion of growth rates into algorithms that can be used for scaling morphologies. This way, a down-scaling of a maxillary sinus

morphology taken postmortem can be achieved to compare it to existing antemortem reference material.

Overall, this research advances the use of maxillary sinus morphologies for human identification and demonstrates its advantages over other paranasal identification methodologies. Assessing patterns empirically is vital in anthropology and especially in forensics to interpret structures and assess their value. Using the maxillary sinuses for identification fits in well with the existing range of identification tools. In cases with available teeth or fingerprint records, these procedures would be applied before considering the maxillary sinus morphology. However, due to its durability, morphological analyses of the maxillary sinuses can prove to be extremely valuable and informative, even when parts of the skull are destroyed and dental records cannot be applied. This method associates productively with other statistical and forensic identification methods as a reliable tool for human identification. Therefore, this research acts as an essential first step toward using the proposed methodological framework in future forensic casework.

8.1 Study Limitations

Sample sizes in each of the research studies are substantial. However, samples sizes had to be decreased in every study of this research due to unsuitable age ranges or image overexposure. Additionally, images of individuals with maxillofacial pathologies were excluded from the studies as well. Maxillofacial pathologies like for example cysts were exclusively found within the historic populations. Still, sample sizes are substantial even after removing the inappropriate images. Only sample sizes in the case study are smaller than in the other studies (table 3, chapter 2).

For the uniqueness and observer bias studies, one set of anthropological data deriving from the evaluation of the skeletal material sufficed. However, differently aged data was needed from the same individuals for the age and case study. Those kinds of data are difficult to obtain. Most universities and museums which provided the appropriate data for the uniqueness and observer bias studies did not store relevant data for the remaining two studies

of this research. Such ante- and postmortem data usually is only available in hospitals and morgues. However, the willingness of those facilities to participate in this research was very scarce. Most hospitals reserved their data for their own medical research and did not show any interest in aiding with outside research. Hence, it was necessary to work with the available data from the longitudinal growth studies. Here, a limiting factor was the age range of the individuals. While subadults were needed for the age study, adult individuals were necessary for the case study. Only eight individuals fit those criteria and were used for the case study. A further limitation in the uniqueness testing is the need for a simulated ante- and postmortem situation. Developing a simulation was needed due to the data availability and would have been avoided with ante- and postmortem data from hospitals or morgues.

Especially for the uniqueness testing, the sample is composed of multiple populations. Those subsamples differ geographically, periodically, as well as in size. Furthermore, except for the populations of Poulton Chapel and St. Owen's Church, none of the radiographic images were taken specifically for this research. This also implies that each populations' skull radiographs were taken by different practitioners. All images were taken standardised anteroposterior. However, a differentiation in distance and positioning cannot be excluded. Another uncertainty with the populations not explicitly imaged for this research is the biological profiling of the individuals. Additionally, this research uses the biological information provided by each collection curator. Another potential limitation is the timing of image retrieval itself. For the three longitudinal populations, individuals were still alive during imaging, while images for the remaining populations were completed after death.

Apart from the observer bias study, the same researcher executed all evaluation, interpretation, and extraction of the maxillary sinus morphologies. Potential inaccuracies could pertain to interpreting the three-dimensional superimposed sinus features in the radiograph. Consequently, this would lead to a misinterpretation of the maxillary sinus morphology. However, as much as the single researcher is a disadvantage, it also poses benefits. Extraction by one single person ensures homogeneity in method implementation and allows, if existent, for a coherent interpretation error. In addition, a possible limitation is the handling of the graphic tablet used for morphological extraction. The interaction of the

digitizer tablet with the design software, as well as the unfamiliar handling of the stylus, can provide a challenge and affect the precise extraction of the morphologies.

When assessing the applicability of the methodological approach, it is necessary to circle back to the availability of the radiographic reference images. In order to allow a comparison method to be functional in a real-life situation, it is vital that reference material even exists. This takes clinical radiologists and other medical professionals into responsibility. They should familiarise themselves with the kind of images needed for identification purposes, as the absence of antemortem reference material invalidates the methodological approach itself. However, even if awareness among medical personnel is created (Kahana and Hiss, 1997), there is still a part of the population that, in the absence of dental or otolaryngologic intervention, does not possess any antemortem reference material. On the other hand, it is unclear if and how maxillofacial pathologies influence sinus morphologies in human identification. Therefore, even if images are available due to otolaryngologic procedures, they might not be useful.

Additionally, production of CT imaging is on the rise, and some individuals potentially only possess CT images instead of radiographs. In contrast to the absence of reference material, this situation does not pose a massive limitation as CT images and radiographs are easily comparable, as seen in chapter 2 of this research. Further limitations of the methodology itself are untrained staff. Logically, more training equals high-quality radiographic images. Furthermore, as this research shows, even light to moderately skilled staff can extract the morphologies after some training. All limitations discussed in this section have been carefully considered, and the effect on the research quality can be minimized.

8.2 Future Research and Recommendations

The results of this research open up as many questions as they answer. The confirmation of morphological sinus uniqueness proves to be a significant first step towards method applicability in human identification. However, the approach needs to be verified further. For the study of uniqueness testing, this implicates the application of a different sample. Here,

both sample size and sample construction have to be considered. Although the approach's effectiveness was proven in an academic environment, it is crucial to repeat examinations on real-life ante- and postmortem data of the same individuals. This process has been started in the case study of this research. However, bigger sample sizes are needed to make a more meaningful statement on morphological maxillary sinus identification. Only when stepping out of the simulated environment and establishing the same results with real-life ante- and postmortem data this morphological approach can be considered valid and ready for identification practice. Furthermore, simultaneously with applying ante- and postmortem data from the same individuals for comparison, a step back needs to be taken from historic populations. Those proved to be highly beneficial for the initial examinations carried out in this research. However, the focus should lie on modern morphological material with future examinations. Furthermore, future samples should include a broad climatic range and significant geographical altitude variations. This allows further testing of the impact of geographical location and climate on maxillary sinus morphologies. Additionally, in order to further understand the forensic impact of this research, future studies should add on to those geographical variations in sinus samples and compare morphological and volumetric approaches within the same and different geographical populations. Furthermore, population analyses and therefore forensic impact measurements of the methodological approach would benefit from future testing concerning the effect of kinship on maxillary sinus uniqueness.

It is vital to increase the sample size for further case study work to get a broader understanding of the methodological approach. As previously mentioned, maxillary sinus sizes are believed to stay unchanged after eruption of the third molar (Iwanaga et al., 2019; Amin and Hassan, 2012; Adibelli et al., 2011). However, realistically normal bone growth and development could result in small morphological changes throughout the individual's lifetime. Therefore, the application of real-life data for uniqueness testing has to be preferred. Investigations need to closely monitor possible connections between the elevated Euclidean distances and the sex of an individual. Looking back on the case study results, the difference in dissimilarity values between the sinus pairs comes to mind. While the male individuals with a large age gap between their ante- and postmortem morphology data exhibited a dissimilarity factor of 0.000, the female individuals with small age gaps displayed slightly elevated dissimilarity factors. Unfortunately, this study cannot sufficiently explain elevated

dissimilarity factors to sexual dimorphism. Therefore, utilizing the results at hand and due to the small sample size, this research tends to explain differences in Euclidean values on an individual level rather than with age or sex differences. However, future investigations must examine the impact of sex on maxillary sinus morphologies more closely to understand possible connections.

Coinciding with investigations into the impact of sex on maxillary sinus morphologies, future studies should evaluate the need for cut off values for Euclidean distances. Uniqueness testing results in a simulated environment indicate total matches with Euclidean distance values of 0.000. Results of the case study show dissimilarity factors of 0.000 as well as a few slightly elevated values up to 0.002 per ante- and postmortem morphology match. Results for unrelated morphologies exhibit considerably higher dissimilarity results. These results allow the conclusion of Euclidean distance values up to 0.002 indicating total morphological matches. However, as with previous conclusions, outcomes of cut off values need to be examined further on larger sample sizes for conclusive confirmation.

Future suggestions for the age estimation study include the incorporation of a greater number of adult individuals over the age of twenty. As the sample (three longitudinal studies) used for this part of the research mostly focussed on the skull growth in subadults, not much data was available after the age of twenty. With radiographic images of the same individuals primarily taken throughout their childhood and teenage years, with less data in adult years, the data availability is very uncommon in anthropological research. However, to accurately retrace changes in adult individuals and subadults, the data availability does not suffice. Therefore, this research suggested removing clusters one (years 0 to 2), six (years 21 to 25), seven (years 26 to 30), and eight (age over 31) for correlations of averaged Euclidean distances and age clusters by population. This is followed by clusters one (years 0 to 2), seven (years 26 to 30), and eight (age over 32) for correlations of averaged Euclidean distances and age clusters by sex. This research mainly evaluated the morphological variability and age-related changes in subadults. For a well-rounded insight into age-related morphological changes, the development in adult individuals needs to be assessed more closely. This would be achieved by incorporating more radiographic images of the same adult individuals as seen in this research's age estimation study with juvenile individuals. Additionally, with a higher sample

size, future studies should narrow down the age clustering system more detailed, especially in higher age categories. In this study, the age clustering system was adapted based on sample availability. This is a standard approach in scientific studies (Maspero et al., 2020; Belgin et al., 2019; Soman et al., 2016). However, this causes the juvenile age stages to be smaller in scale, while clusters get broader with rising ages. Therefore, larger sample sizes in ages above thirty would create more conform age clustering ranges and simplify comparability studies.

All radiographs used for this research's studies are taken in a standardised anteroposterior positioning. Images of individuals from the populations of Poulton Chapel and St. Owen's Church were taken specifically for this study, in contrast to the remaining sample. While it was possible to oversee the process of taking the images of Poulton Chapel and St. Owen's Church, this was not possible for the other populations used in this study. Furthermore, as radiology practitioners varied for all populations, it is unclear whether slight differences in image acquisition might have occurred. However, it needs to be considered that ante- and postmortem radiographs are always taken from different practitioners in a real-life situation. The antemortem imaging often occurs at a dental practice or the hospital preceding surgical intervention, while the postmortem radiograph is taken at the morgue. As a next step, it is crucial to investigate the impact of angled skull positioning during image acquisition on the agreement between ante- and postmortem sinus morphologies. In order to investigate all possible angulation pitfalls, the skull should be tilted, and imaging should occur with different angles both in horizontal as well as vertical directions. When studying the methodological approach, the data availability has to be considered. The vast majority of dental radiographs taken in Germany (Nekolla et al., 2017), England and Wales (Public Health England, 2010), and the US (iData, 2019) are taken intraorally. Therefore, those images are not available for the morphological approach taken in this research. Naturally, only intraoral images taken from the canine, premolar and molar regions of the maxillary dental arcade, depicting the lowest aspects of the maxillary sinus would be useful for examinations. As those intraoral images only carry partials of the maxillary sinuses, it would be vital to understand whether those partials could also be suitable for human identification. The utilisation of those additional intraoral images would potentially vastly broaden the applicability of the approach. In order to broaden the applicability of the methodological approach, the use of hand-held x-ray machines should be examined. As image quality for medical use resulting from hand-held imaging machines has

been proven successfully (Purchasea et al., 2019), it is still unclear whether it would suffice for forensic purposes.

While this research solely focuses on morphological changes of the maxillary sinuses, most preceding research concentrates on dimensional and volumetric alterations of the structure (Benjaphalakron et al., 2021; Dandekeri et al., 2020; Przystańska et al., 2020; Akhlaghi et al., 2017; Patel et al., 2020). Results of the correlations of averaged Euclidean distances and age clusters by sex display diametrically opposed results to comparable studies focusing on measurements or volumes. This research suspects a possible explanation in the difference between a structure's volume or measurements and its morphology. An assumption would be that although the volume of a structure might change, its morphology could remain virtually unchanged. The same could apply to measurements and the morphology of an object. However, this assumption needs to be examined further. Therefore, it is advised to execute a comparison study between volumes, measurements, and morphologies of the same maxillary sinuses to understand the connection between those three evaluation types.

The methodological approach itself could benefit from improvements and fine-tuning for the sake of time efficiency. The part requiring streamlining is the extraction of the morphologies before feeding them into the elliptic Fourier software tool. With the help of capturing software, the hand tracing of the morphology could be replaced by a smart software that automatically takes the shape of the object and extracts it for further processing. A possible way could also be the transformation of the radiograph into a binary image to avoid the capturing software confusing different grey scales in the radiograph. Furthermore, the development of an elliptic Fourier analysis tool specifically for forensic or anthropological use could facilitate the adoption of the method. In this software, the whole process from image extraction to calculation of elliptic Fourier descriptors and the subsequent application of principal component analysis could be performed. This would lead to a considerable reduction in workload and generally make the method easier to use.

Lastly, the possibility of data storage and the development of a sinus database needs to be addressed. Decreasing costs of imaging procedures and possibilities of digital cloud storage, in contrast to previous on-premise storage, enables the development of sinus databases for

identification. However, before proposing data storage possibilities, an effort to increase awareness of the importance of preserving records needs to be put forth. Previously, the suggestion of deliberate radiography and the subsequent indefinite storage of radiographic films (Law, 1934) has not been received positively by medical professionals. As techniques improve, so does the acceptance. However, medical data storage is no international and unilateral approach but falls under each country's data protection and medical negligence laws. Germany, for example, provides different periods for the storage of radiographs (KVNO, 2020): single radiographs, as taken for example for medical check-ups, are retained for two years. Images for x-ray diagnostics must be retained for ten years, while radiographic images used for specific therapies must be stored for thirty years. Radiographs taken to aid diagnostics or therapies in subadults are retained at least until the age of twenty-eight (KVNO, 2020). In contrast, retention periods in the US depend on each state's malpractice statutes of limitation (NCSL, 2014). In the UK, minimum lengths of retention of records varies (BMA, 2021). In Scotland, data from general practitioners (GP) is retained up until three years after the individual's death, while hospital records are destroyed either six years after the treatment ends or three years after the individual's death. Retention periods for England, Wales, and Northern Ireland vary (BMA, 2021). Here, retention periods for GP data are ten years after the individual's death. Hospital records are destroyed either eight years after treatment ending or directly after the individual's death. However, it is advised to retain electronic patient records indefinitely (BMA, 2021). To establish country-specific databases, the justice system and lawmakers need to lay a foundation considering the individual data protection and medical negligence laws. Furthermore, the creation of such databases cannot be expected to be immediate but is a growing process similar to the formation of the European DNA databases (Reed and Syndercombe-Court, 2014; Amelung et al., 2021).

References

AAOF. 2020. *AAOF Craniofacial Growth Legacy Collection* [Online]. American Association of Orthodontists Foundation (AAOF). Available: https://www.aaoflegacycollection.org/aaof_home.html [Accessed 30.07.2021 2021].

AASTHA. 2020. *X-Ray* [Online]. Available: https://www.aasthakidneyhospital.com/service/x-ray/ [Accessed 07.01.2022].

ADAMS, B. J. 2002. *Personal identification based on patterns of missing, filled, and unrestored teeth.* Ph.D., The University of Tennessee.

ADAMS, D. C., ROHLF, F. J. & SLICE, D. E. 2004. Geometric morphometrics: Ten years of progress following the 'revolution'. Italian Journal of Zoology, 71, 5-16.

ADIBELLI, Z. H., SONGU, M. & ADIBELLI, H. 2011. Paranasal sinus development in children: A magnetic resonance imaging analysis. *American Journal of Rhinology & Allergy,* 25**,** 30-5.

ADOBE INC. 2019. *Adobe Photoshop* [Online]. Available: https://www.adobe.com/products/photoshop.html [Accessed 05.08.2021].

AEKNO. 2022. *Ärztliche Gutachter* [Online]. Ärztekammer Nordrhein, Körperschaft des öffentlichen Rechts; Medical Evaluators [Online]. Medical Association North Rhine, corporation under public law. Available: https://www.aekno.de/patienten/aerztliche-gutachter [Accessed 08.06.2022].

AKHLAGHI, M., BAKHTAVAR, K., KAMALI, A., MAAREFDOOST, J., SHEIKHAZADI, A., MOUSAVI, F., SABERI ANARY, S. H. & SHEIKHAZADI, E. 2017. The diagnostic value of anthropometric indices of maxillary sinuses for sex determination using CT-scan images in Iranian adults: A cross-sectional study. *Journal of Forensic and Legal Medicine,* 49**,** 94-100.

ALBRIGHT, T. D. 2021. The US Department of Justice stumbles on visual perception. *Proceedings of the National Academy of Sciences,* 118**,** e2102702118.

ALMOHIY, H. M., HUSSEIN, K. L., ALQAHTANI, M. S., SAEED, M. K., HASSAN, E. H., ASIRI, A. A. M., SAAD, M., MUKHTAR, E. M., ADAM, M., ALSHAHRANI, M., ALSLEEM, H. A., AJMAL, M., ALSHAHRANI, I. & ABUHADI, N. 2020. Radiation Dose Measurements in Intraoral and Panoramic Dental Radiography in the Southern Region of Saudi Arabia. *Journal of Health Sciences,* 5**,** 39-46.

ALTHUBAITI, A. 2016. Information bias in health research: definition, pitfalls, and adjustment methods. *Journal of Multidisciplinary Healthcare,* 9**,** 211-217.

ALTMAN, D. G. & BLAND, J. M. 2005. Standard deviations and standard errors. *BMJ,* 331**,** 1.

ALTUG, H. A. & OZKAN, A., P. 2011. Diagnostic Imaging in Oral and Maxillofacial Pathology. *In:* ERONDU, O. F. (ed.) *Medical Imaging.* Rijeka: InTech.

AMELUNG, N., GRANJA, R. & MACHADO, H. 2021. Germany. *In:* AMELUNG, N., GRANJA, R. & MACHADO, H. (eds.) *Modes of Bio-Bordering: The Hidden (Dis)integration of Europe.* Singapore: Springer Singapore.

AMIN, M. F. & HASSAN, E. I. 2012. Sex identification in Egyptian population using Multidetector Computed Tomography of the maxillary sinus. *Journal of Forensic and Legal Medicine,* 19**,** 65-69.

AMINE, K., SLAOUI, S., KANICE, F. Z. & KISSA, J. 2020. Evaluation of maxillary sinus anatomical variations and lesions: A retrospective analysis using cone beam computed tomography. *Journal of Stomatology, Oral and Maxillofacial Surgery,* 121**,** 484-489.

AMOROSA, L. & LATINI, G. 2016. Chapter 4 - Maxillary Sinus: The Role of the Otolaryngologist. *In:* RINALDI, M., GANZ, S. D. & MOTTOLA, A. (eds.) *Computer-Guided Applications for Dental Implants, Bone Grafting, and Reconstructive Surgery (Adapted Translation).* St. Louis: Elsevier.

ANDERBERG, M. R. 2014. *Cluster analysis for applications: probability and mathematical statistics: a series of monographs and textbooks*, Academic press.

ANDRADE, C. 2020a. Sample Size and its Importance in Research. *Indian Journal of Psychological Medicine,* 42**,** 102-103.

ANDRADE, C. 2020b. Understanding the difference between standard deviation and standard error of the mean, and knowing when to use which. *Indian Journal of Psychological Medicine,* 42**,** 409-410.

ARANZAMENDI, M. C., MARTINEZ, J. J. & SAHADE, R. 2010. Shape differentiation and characterization in the two morphotypes of the Antarctic limpet Nacella concinna using Elliptic Fourier analysis of shells. Polar Biology, 33, 1163–1170.

ARIJI, Y., ARIJI, E., YOSHIURA, K. & KANDA, S. 1996. Computed tomographic indices for maxillary sinus size in comparison with the sinus volume. *Dentomaxillofac Radiol,* 25**,** 19-24.

ARSUAGA, J. L., MARTINEZ, I., GRACIA, A. & LORENZO, C. 1997. The Sima de los Huesos crania (Sierra de Atapuerca, Spain). A comparative study. *J Hum Evol,* 33**,** 219 - 281.

ASAUMI, R., SATO, I., MIWA, Y., IMURA, K., SUNOHARA, M., KAWAI, T. & YOSUE, T. 2010. Understanding the formation of maxillary sinus in Japanese human foetuses using cone beam CT. *Surgical and radiologic anatomy : SRA,* 32**,** 745-751.

ATA-ALI, J., DIAGO-VILALTA, J. V., MELO, M., BAGÁN, L., SOLDINI, M. C., DI-NARDO, C., ATA-ALI, F. & MAÑES-FERRER, J. F. 2017. What is the frequency of anatomical variations and pathological findings in maxillary sinuses among patients subjected to maxillofacial cone beam computed tomography? A systematic review. *Medicina oral, patologia oral y cirugia bucal,* 22**,** e400-e409.

ATKIN, M. 1990. Excavation in Gloucester, 1998. *Glevensis,* 24**,** 2-13.

ATKIN, M. & GARROD, A. P. 1990. Archaeology in Gloucester 1989. *Transactions of the Bristol and Gloucestershire Archaeological Society,* 108**,** 185-192.

AUST, R., STIERNA, P. & DRETTNER, B. 1994. Basic experimental studies of ostial patency and local metabolic environment of the maxillary sinus. *Acta Otolaryngol* 114**,** 7 - 10.

BAHADIR, O., BAHADIR, A., KOSUCU, P. & LIVAOGLU, M. 2008. The effect of maxillary sinus surgery on its development. *Acta Oto-Laryngologica,* 128**,** 551-555.

BALLANTYNE, K. N. & WILSON-WILDE, L. 2020. Assessing the reliability and validity of forensic science – an industry perspective. *Australian Journal of Forensic Sciences,* 52**,** 275-281.

BASS, W. M. 1984. Is it Possible to Consume a Body Completely in a Fire? *In:* RATHBUN, T. A. & BUIKSTRA, J. E. (eds.) *Human Identification: Case Studies in Forensic Anthropology.* Springfield: Thomas, C. C.

BEAINI, T. L., DUAILIBI-NETO, E. F., CHILVARQUER, I. & MELANI, R. F. 2015. Human identification through frontal sinus 3D superimposition: Pilot study with Cone Beam Computer Tomography. *J Forensic Leg Med,* 36**,** 63-9.

BEALS, K. L., SMITH, C. L. & DODD, S. M. 1984. Brain Size, Cranial Morphology, Climate, and Time Machines. *Current Anthropology,* 25**,** 301 - 330.

BECK, J. J. W. 2011. What is the future of imaging in forensic practice? *Radiography,* 17**,** 212 - 217.

BEITLER, J. J., MCDONALD, M. W., WADSWORTH, J. T. & HUDGINS, P. A. 2016. Chapter 36 - Sinonasal Cancer. *In:* GUNDERSON, L. L. & TEPPER, J. E. (eds.) *Clinical Radiation Oncology (Fourth Edition).* Philadelphia: Elsevier.

BEKVALAC, J. 2018. *RE: personal communication.*

BEKVALAC, J. 2021. *RE: personal communication.*

BEKVALAC, J. & KAUSMALLY, T. 2009. *Chelsea Old Church (post-medieval) cemetery summary* [Online]. Museum of London Archaeology. Available: https://www.museumoflondon.org.uk/collections/other-collection-databases-and-libraries/centre-human-bioarchaeology/osteological-database/post-medieval-cemeteries/chelsea-old-church-post-medieval [Accessed 30.07.2021 2021].

BELGIN, C. A., COLAK, M., ADIGUZEL, O., AKKUS, Z. & ORHAN, K. 2019. Three-dimensional Evaluation of Maxillary Sinus Volume in Different Age and Sex groups using CBCT. *European Archives of Oto-Rhino-Laryngology,* 276**,** 1493-1499.

BELL, G. W., JOSHI, B. B. & MACLEOD, R. I. 2011. Maxillary sinus disease: diagnosis and treatment. *British Dental Journal,* 210**,** 113-118.

BENJAPHALAKRON, N., JANSISYANONT, P., CHUENCHOMPOONUT, V. & KIATTAVORNCHAROEN, S. 2021. Evaluation of the maxillary sinus anatomical variations related to maxillary sinus augmentation using cone beam computed tomography images. *Journal of Oral and Maxillofacial Surgery, Medicine, and Pathology,* 33**,** 18-25.

BFS. 2022. *Röntgendiagnostik: Häufigkeit und Strahlenexposition für die deutsche Bevölkerung* [Online]. Bundesamt für Strahlenschutz; X-ray diagnostics: Frequency and radiation exposure for the German population [Online]. Federal Office for Radiation Protection. Available: https://www.bfs.de/DE/themen/ion/anwendung-medizin/diagnostik/roentgen/haeufigkeit-exposition.html [Accessed 24.06.2022].

BHUSHAN, B., RYCHLIK, K. & SCHROEDER, J. W. 2016. Development of the maxillary sinus in infants and children. *International Journal of Pediatric Otorhinolaryngology,* 91**,** 146-151.

BIGNON, F. 1889. Contribution a l'étude de la pneumaticité chez les oiseaux. Les cellules aeriennes cervico-céphalique des oiseaux et leurs rapports avec les os de la tete. *Mémoires de la Société Zoolologique de France;* Contribution to the study of pneumaticity in birds. The cervico-cephalic aerial cells of birds and their relation to the bones of the head. *Memoirs of the Zoological Society of France,* 2**,** 260 - 320.

BLANEY, S. P. A. 1990. Why paranasal sinuses? *J Laryngol Otol,* 104**,** 690 - 693.

BLANTON, P. L. & BIGGS, N. L. 1969. Eighteen hundred years of controversy: The paranasal sinuses. *American Journal of Anatomy,* 124**,** 135-147.

BLAUA, S., PHILLIPSC, E., O'DONNELLA, C. & MARKOWSKYD, G. 2019. Evaluating the impact of different formats in the presentation of trauma evidence in court: a pilot study. *Australian Journal of Forensic Sciences,* 51**,** 695-704.

BMA. 2021. *Retention of health records* [Online]. British Medical Association. Available: https://www.bma.org.uk/advice-and-support/ethics/confidentiality-and-health-records/retention-of-health-records [Accessed 08.04.2022].

BOLZAN, J. & TUCUNDUVA, M. 2012. ESTUDO RADIOGRÁFICO DA CAVIDADE NASAL E DOS SEIOS PARANASAIS E SUAS VARIAÇÕES; Radiographic study of the nasal cavity and paranasal sinuses and their variations. *Science in Health,* 3**,** 23-31.

BOOKSTEIN, F. L. 1997. Morphometric Tools for Landmark Data, Cambridge, UK, Cambridge University Press.

BOSWORTH, F. H. 1888. The phsyiology of the nose. *Med News,* 53**,** 117 - 124.

BPB. 2020. *Bevölkerungsentwicklung* [Online]. Bundeszentrale für politische Bildung; Population Development [Online]. Federal Agency for Civic Education. Available: https://www.bpb.de/kurz-knapp/zahlen-und-fakten/soziale-situation-in-deutschland/61532/bevoelkerungsentwicklung/ [Accessed 24.06.2022].

BRADTMÖLLER, M., PASTOORE, A., SLIEZEWSKI, A. & EWNIGER, G. C. 2010. NESPOS - A Digital Archive and Platform for Pleistocene Archaeology. *In:* CURDT, C. & BARETH, G. (eds.) *Proceedeings of the Data Management Workshop, 29. - 30.10.2009.* Cologne: Neanderhal Museum.

BRAUNE, W. & CLASEN, F. E. 1877. Die Nebenhöhlen der menschlichen Nase in ihre Bedeutung für den Mechanismus des Rieches; The sinuses of the human nose and their importance for the olfactory mechanism. *Z f Ana,* 2**,** 1 - 28.

BREMER, J. L. 1940. The pneumatization of the head of the common fowl. *J Morphol,* 67**,** 143 - 157.

BRODSKY, S. L., GRIFFIN, M. P. & CRAMER, R. J. 2010. The Witness Credibility Scale: An Outcome Measure for Expert Witness Research. *Behavioral Sciences and the Law,* 28**,** 892-907.

BROGDON, B. G. 1998. The Scope of Forensic Radiology. *Clinics in Laboratory Medicine,* 18**,** 203-240.

BROGDON, B. G. 2011. Definitions in Forensic and Radiology. *In:* THALI, M. J., MARK, M. D. & VINER, D. (eds.) *Brogdon's Forensic Radiology.* 2nd ed. Boca Raton: Taylor and Francis Group.

BROGDON, B. G. & LICHTENSTEIN, J. E. 2011. Forensic Radiology in Historical Perspective. *Brogdon's Forensic Radiology.* Boca Raton: Taylor and Francis Group.

BROTHWELL, D. R., MOLLESON, T. & METREWELI, C. 1968. Radiological aspects of normal variation in earlier skeletons: an exploratory study. *In:* BROTHWELL, D. R. (ed.) *The Skeletal biology of earlier human populations.* New York: Pergamon Press.

BUCK, L. T. 2014. *Craniofacial morphology, adaptation, and paranasal pneumatisation in Pleistocene hominins.* University of Roehampton.

BUHLER, P. 1970. Schädelmorphologie und Kiefermechanik der Caprimulgidae (Aves); Skull morphology and jaw mechanics of the Caprimulgidae. *Z f Morph der Tiere,* 66.

BUTARIC, L. N. & MADDUX, S. D. 2016. Morphological Covariation between the Maxillary Sinus and Midfacial Skeleton among Sub-Saharan and Circumpolar Modern Humans. *American Journal of Physical Anthropology,* 160**,** 483-497.

BUTARIC, L. N., MCCARTHY, R. C. & BROADFIELD, D. C. 2010. A preliminary 3D computed tomography study of the human maxillary sinus and nasal cavity. *American Journal Of Physical Anthropology,* 143**,** 426-436.

BUTARIC, L. N., RICHMAN, A. & GARVIN, H. M. 2022. The Effects of Cranial Orientation on Forensic Frontal Sinus Identification as Assessed by Outline Analyses. *Biology,* 11**,** 2-22.

CAMERIERE, R., FERRANTE, L., DE ANGELIS, D., SCARPINO, F. & GALLI, F. 2008. The comparison between measurement of open apices of third molars and Demirjian stages to test chronological age of over 18 year olds in living subjects. *International Journal of Legal Medicine,* 122**,** 493 - 497.

CAMERIERE, R., SCENDONI, R., LIN, Z., MILANI, C., VELANDIA PALACIO, L. A., TURIELLO, M. & FERRANTE, L. 2019. Analysis of Frontal Sinuses for Personal Identification in a Chinese Sample Using a New Code Number. *Journal of Forensic Science***,** 1-6.

CAMPBELL, N. A., REECE, J. B., URRY, L. A., CAIN, M. L., WASSERMAN, S. A., MINORSKY, P. V. & JACKSON, R. B. 2015. *Pearson. Biology,* Boston, Pearson Education Limited.

CAN, S. 2021. *Poesie und Pandemie,* Göttingen, Wallstein Verlag.

CAPACCIOLI, L. & MANNUCCI, P. 2003. Indagine antropologica radiodiagnostica odontostomatologica su un campione di popolazione vissuta nel XIX secolo in area fiorentina; Anthropological radiodiagnostic odontostomatological investigation on a sample of population living in the Florentine area in the 19th century. *In:* MANTEGAZZA, P. (ed.) *Archivio per l'antropologia e la etnologia.* Firenze: Societa Italiana di Antropologia e Etnologia.

CAPLE, J., BYRD, J. E. & STEPHAN, C. N. 2017. Elliptical Fourier analysis: fundamentals, applications, and value for forensic anthropology. *International Journal of Legal Medicine,* 131**,** 1675 - 1690.

CAPRA, D. J. 2018. Symposium on Forensic Expert Testimony, Daubert, and Rule 702. *Fordham Law Review,* 86**,** 1463-1550.

CARUANA, E. J., ROMAN, M., HERNÁNDEZ-SÁNCHEZ, J. & SOLLI, P. 2015. Longitudinal studies. *Journal of Thoracic Disease,* 7**,** E537-E540.

CAVE, A. J. & HAINES, R. W. 1940. The paranasal sinuses of the anthropoid apes. *Journal of anatomy,* 74**,** 493-523.

CAVE, A. J. E. 1967. Observations on the Platyrrhine Nasal Fossa. *American Journal of Physical Anthropology,* 26**,** 277 - 288.

CHAITANYA, L., PAJNIČ, I. Z., WALSH, S., BALAŽIC, J., ZUPANC, T. & KAYSER, M. 2017. Bringing colour back after 70 years: Predicting eye and hair colour from skeletal remains of World War II victims using the HIrisPlex system. *Forensic Science International: Genetics,* 26**,** 48-57.

CHEN, S. Y. Y., LESTREL, P. E., KERR, J. S. & MCCOLL, J. H. 2000. Describing shape changes in the human mandible using elliptical Fourier functions. *European Journal of Orthodontics,* 22**,** 205-216.

CHIN, J. M., RIBEIRO, G. & RAIRDEN, A. 2019. Open forensic science. *Journal of Law and the Biosciences,* 6**,** 255-288.

CHRISTENSEN, A. M. 2003. *An empirical examination of frontal sinus outline variability using Elliptic Fourier Analysis: Implications for *identification, standardization, and legal admissibility.* Ph.D., The University of Tennessee.

CHRISTENSEN, A. M. 2005. Assessing the variation in individual frontal sinus outlines. *American Journal of Physical Anthropology,* 127**,** 291-295.

CHRISTENSEN, A. M. & CROWDER, C. M. 2009. Evidentiary Standards for Forensic Anthropology. *Journal of Forensic Sciences,* 54**,** 1211-1216.

CHRISTENSEN, A. M. & HATCH, G. M. 2018. Advances in the Use of Frontal Sinuses for Human Identification. *In:* LATHAM, K. E., BARTELINK, E. J. & FINNEGAN, M. (eds.) *New Perspectives in Forensic Human Skeletal Identification.* London: Elsevier.

COLLINS, V. P. 1964. Origins of medico-legal and forensic roentgenology. *In:* BRUWER, A. J. (ed.) *Classic Descriptions in Diagnostic Radiology.* Springfield: Thomas, C. C.

COWIE, R., BEKVALAC, J. & KAUSMALLY, T. 2008. Late 17th- to 19th-century Burial at All Saints, Chelsea Old Church, Royal Borough of Kensington and Chelsea. *Museum of London Studies Series 18.* London: Museum of London Archaeology Service.

COX, M., MALCOLM, M. & FAIRGRIEVE, S. I. 2009. A new digital method for the objective comparison of frontal sinuses for identification. *J Forensic Sci,* 54**,** 761-72.

CRAMPTON, J. S. 1995. Elliptic Fourier shape analysis of fossil bivalves: some practical considerations. Lethaia, 28, 179-186.

CVRČEK, J., VELEMÍNSKÝ, P. & BRUŽEK, J. 2021. Frontal sinus anatomy of the noble Swéerts-Sporck family and verification of their biological relationships using similarity analysis. *The Anatomical Record,* 304**,** 1717–1731.

CZARNETZKI, A. 2006. Objekte der osteologischen Sammlung. Stumme Zeugen; Objects of the osteological collection. silent witnesses. *In:* VON HARMS, V., KORFF, G. & MICHELS, A. (eds.) *Achtunddreissig Dinge. Schätze aus den Natur- und Kulturwissenschaftlichen Sammlungen der Universität Tübingen.* Tübingen.

DA CARPI, G. B. 1521. Commentaria cum amplissimis additionibus super anatomia Mundini una cum textu ejusdem in pristinum et verum nitorem redacto; Commentaries with the most extensive additions on the anatomy of Mundini, together with the text of the same reduced to its original and true gloss. *Bononiae, imp. per H. de Benedictis*.

DA VINCI, L. 1489. *Quaderni d'anatomia. I-VI. pubblicati da C. L. Vangensten, A. Fonahn, H. Hopstock; Anatomy notebooks. I-VI. published by C. L. Vangensten, A. Fonahn, H. Hopstock. 6 vols. Christiania, F. Dyb- wad, 1911–1916*.

DANDEKERI, S., HEGDE, C., KAVASSERY, P., SOWMYA, M. & SHETTY, B. 2020. CBCT study of morphologic variations of maxillary sinus septa in relevance to sinus augmentation procedures. *Annals of Maxillofacial Surgery,* 10**,** 51-56.

DAVIS, B. 1865. The Neanderthal skull: its formation considered anatomically. *J Anthropol Soc Lond,* 3**,** 15 - 19.

DE ANGELIS, D., RIBOLI, F., GIBELLI, D., CAPPELLA, A. & CATTANEO, C. 2012. Palatal rugae as an individualising marker: Reliability for forensic odontology and personal identification. *Science and Justice,* 52**,** 181-184.

DE BARROS, F., DA SILVA FERNANDES, C. M., KUHNEN, B., FILHO, J. S., GONÇALVES, M. & DA COSTA SERRA, M. 2021. Paranasal sinuses and human identification. *Research, Society and Development,* 10**,** 1-13.

DE BARROS, F., DA SILVA FERNANDES, C. M., KUHNEN, B., SCARSO FILHO, J., GONÇALVES, M., GONÇALVES, W. & DA COSTA SERRA, M. 2022. Three-dimensional analysis of the maxillary sinus according to sex, age, skin color, and nutritional status: A study with live Brazilian subjects using cone-beam computed tomography. *Archives of Oral Biology,* 139**,** 2-9.

DE BOER, H. H., BLAU, S., DELABARDE, T. & HACKMAN, L. 2019. The role of forensic anthropology in disaster victim identification (DVI): recent developments and future prospects. *Forensic Schiences Research,* 4**,** 303 - 315.

DE BOER, H. H., MAAT, G. J. R., KADARMO, D. A., WIDODO, P. T., KLOOSTERMAN, A. D. & KAL, A. J. 2018. DNA identification of human remains in Disaster Victim Identification (DVI): An efficient sampling method for muscle, bone, bone marrow and teeth. *Forensic Science International,* 289**,** 253-259.

DE BOER, H. H., OBERTOVÁ, Z., CUNHA, E., ADALIAN, P., BACCINO, E., FRACASSO, T., KRANIOTI, E., LEFÉVRE, P., LYNNERUP, N., PETAROS, A., ROSS, A., STEYN, M. & CATTANEO, C. 2020. Strengthening the role of forensic anthropology in personal identification: Position statement by the Board of the Forensic Anthropology Society of Europe (FASE). *Forensic Science International,* 315**,** 110456.

DE SOUZA, M. A., DE OLIVEIRA URTIAGA, G., GRANGEIRO FERREIRA, R. C., MARQUES DA SILVA, L., GONÇALVES UMBELINO, J. K., DE MELO, F. R. & DE JESUS, S. 2022. Friction ridge analysis in disaster victim identification (DVI): Brazilian case studies. *Forensic Sciences Research,* 7**,** 323 - 329.

DEAN, D. & DELSON, E. 1992. Paleoanthropology. Second gorilla or third chimp? *Nature,* 359**,** 676 - 677.

DEAN, D. E., TATAREK, N. E., RICH, J., BROGDON, B. G. & POWERS, R. H. 2005. Human identification from the ankle with pre- and postsurgical radiographs. *Journal of Clinical Forensic Medicine,* 12**,** 5-9.

DEĞERMENCI, M., ERTEKIN, T., ÜLGER, H., ACER, N. & COŞKUN, A. 2016. The Age-Related Development of Maxillary Sinus in Children. *J Craniofac Surg,* 27**,** e38-44.

DEHAVEN JR., H. A. 2014. Anatomy and Physiology of the Maxillary Sinus. *Clinical Maxillary Sinus Elevation Surgery.*

DEMBINSKI, G. M. & PICARD, C. J. 2014. Evaluation of the IrisPlex DNA-based eye color prediction assay in a United States population. *Forensic Science International: Genetics,* 9**,** 111-117.

DEMIRALP, K. O., KURSUN CAKMAK, S., AKSOY, S., BAYRAK, S., ORHAN, K. & DEMIR, P. 2019. Assessment of paranasal sinus parameters according to ancient skulls' gender and age by using cone-beam computed tomography. *Folia Morphologica,* 78**,** 344.

DEOG, K., YOUNG, L., SANG OUK, P., DAE SOON, K. & SEUNG HO, H. 2013. Identification Using Frontal Sinus by Three-Dimensional Reconstruction from Computed Tomography*. *Journal of Forensic Sciences,* 58**,** 5-12.

DHANAK, K., INGALE, S., KOCHAR, S. & PATHAK, A. 2019. CT Scan of Maxillary Sinus: A Useful Tool for Forensic Identification. *Indian Journal of Forensic Medicine & Toxicology,* 13**,** 13-18.

DHANAPAL, S. & DIVYANAND, J. M. J. 2016. Dental Tags. *International Journal of Forensic Odontology,* 1**,** 6 - 8.

DIEULAFE, L. & LOEB, H. W. 1906. I. Morphology and Embryology of the Nasal Fossae of Vertebrates. *Annals of Otology, Rhinology & Laryngology,* 15**,** 1-60.

DITTRICK, J. & SUCHEY, J. 1986. Sex determination of prehistoric central California skeletal remains using discriminant analysis of the femur and humerus. *American Journal of Physical Anthropology,* 70**,** 3-9.

DU BRUL, E. L. 1965. The skull of the lion marmoset leontideus rosalia linneaus: a study in biomechanical adaptation. *Am J Phys Anthropol,* 23**,** 261 - 276.

DWIGHT 1878. *The Identification of the Human Skeleton: A Medicolegal Study,* Boston, Massachusetts Medical Society.

ECKERT, W. G. & GARLANT, N. 1984. The history of the forensic applications in radiology. *The American Journal of Forensic Medicine and Pathology***,** 53 - 56.

ECKLEY, W. T. 1904. On the accessory sinuses. *Chicago Med Recorder,* 26**,** 243 - 253.

EDINGER, T. 1938. Über Steinkerne der irn- und Ohr-Höhlen der Mesosuchier Goniopholis und Pholidosaurus aus dem Bückeburger Wälden; About stone cores of the irn and ear cavities of the Mesosuchian Goniopholis and Pholidosaurus from the Bückeburger Wälden. *Acta Zool,* 19.

EGUCHI, M. & NINOMIYA, S. 2008. Evaluation of soybean seed shape by elliptic Fourier descriptors. *WORLD CONFERENCE ON AGRICULTURAL INFORMATION AND IT*.

EKIZOGLU, O., INCE, E., SAYIN, I. & KAYHAN, I. O. 2014. The use of maxillary sinus dimensions in gender determination: a thin-slice multidetector computed tomography assisted morphometric study. *J. Craniofac. Surg.,* 20**,** 87-95.

EL OMDA, S. & SERGENT, S. R. 2021. *Standard Deviation,* Treasure Island, FL, StatPearls Publishing.

EMERY, M. M. 2000. *The Poulton Chronicles: Tales from a Medieval Chapel,* Williamsburgh, Virginia, Poulton Archaeological Press.

EMIRZEOGLU, M., SAHIN, B., BILGIC, S., BILGIC, S., CELEBI, M. & UZUN, A. 2007. Volumetric evaluation of the paranasal sinuses in normal subjects using computer tomography images: A stereological study. *Auris Nasus Larynx,* 34**,** 191 - 195.

EVTEEV, A., CARDINI, A. L., MOROZOVA, I. & O'HIGGINS, P. 2014. Extreme Climate, Rather Than Population History, Explains Mid-Facial Morphology of Northern Asians. *AMERICAN JOURNAL OF PHYSICAL ANTHROPOLOGY,* 153**,** 449-462.

EVTEEV, A. & GROSHEVA, A. N. 2019. Nasal cavity and maxillary sinuses form variation among modern humans of Asian descent. *American Journal of Physical Anthropology,* 169**,** 513 - 525.

FABER, J. & FONSECA, L. M. 2014. How sample size influences research outcomes. *Dental Press Journal of Orthodontics,* 19**,** 27-29.

FATTEH, A. V. & MANN, G. T. 1969. The Role of Radiology in Forensic Pathology. *Medicine, Science and the Law,* 9**,** 27-30.

FLACH, P. M., THALI, M. J. & GERMEROTT, T. 2014. Times Have Changed! Forensic Radiology—A New Challenge for Radiology and Forensic Pathology. *American Journal of Roentgenology,* 202**,** 325-334.

FRANCKEN, M. 2016. Skelette: Osteologische Sammlung. *Museen + Sammlungen der Universität Tübingen;* Osteological Collection. Museums + collections of the University of Tübingen*.* Tübingen: Ernst Seidl.

FRANCKEN, M. 2019. personal communication.

FREEMAN, H. 1974. Computer Processing of Line-Drawing Images. *Computing Survey,* 6, 57-97.

FREEMAN, H. Application of the generalized chain coding scheme to map data processing. IEEE Computer Society Conference on Pattern Recognition and Image Processing, May 31-June 2 1987 Chicago, Illinois.

GANNON, P. J., DOYLE, W. J., GANJIAN, E., MÁRQUEZ, S., GNOY, A., GABRIELLE, H. S. & LAWSON, W. 1997. Maxillary sinus mucosal blood flow during nasal vs tracheal respiration. *Arch Otolaryngol Head Neck Surg,* 123**,** 1336 - 1340.

GARFINKEL, S., FARRELLA, P., ROUSSEVC, V. & DINOLTA, G. 2009. Bringing science to digital forensics with standardized forensic corpora. *Digital Investigation,* 6**,** 2-11.

GARN, S. M. 1959. Review: Radiographic Atlas of Skeletal Development of the Hand and Wrist. *American Journal of Human Genetics,* 11**,** 282-283.

GIBELLI, D., CELLINA, M., CAPPELLA, A., GIBELLI, S., PANZERI, M. M., OLIVA, A. G., TERMINE, G., DE ANGELIS, D., CATTANEO, C. & SFORZA, C. 2019. An innovative 3D-3D superimposition for assessing anatomical uniqueness of frontal sinuses through segmentation on CT scans. *International Journal of Legal Medicine,* 133**,** 1159-1165.

GLASSER, O. 1958. Chapter III. *Dr. W. C. Röntgen.* 2nd ed. Springfield: Thomas, C. C.

GOMES, A. F., THIAGO DE OLIVEIRA, G., YAMASAKI, M. C., GROPPO, F. C., NETO, F. H. & ROSANA DE FÁTIMA, P. 2019. Development and validation of a formula based on maxillary sinus measurements as a tool for sex estimation: a cone beam computed tomography study. *International Journal of Legal Medicine,* 133**,** 1241-1249.

GRACE-MARTIN, K. 2020. *When Unequal Sample Sizes Are and Are NOT a Problem in ANOVA* [Online]. The Analysis Factor. Available: https://www.theanalysisfactor.com/when-unequal-sample-sizes-are-and-are-not-a-problem-in-anova/ [Accessed 30.06.2022].

GRÜNWALD, L. 1925. Deskriptive und topograhische Anatomie der Nase und ihrer Nebenhöhlen. *In:* DENKER, A. & KAHLER, O. (eds.) *Die Krankheiten der Luftwege und der Mundhöhle.* Berlin - München: Springer.

HACKMAN, L., BLACK, S., NIC DAEID, N. & DAVIES, C. 2018. Certification of Forensic Anthropology Practice in the United Kingdom and the Development of a Discipline Code of Practice. *EAFS.* Poster session presented at Lyons, France.

HAINES, A. J. & CRAMPTON, J. S. 2000. Improvements to the method of Fourier shape analysis as applied in morphometric studies. *Palaeontology,* 43**,** 765 - 783.

HALL, B. G., ACAR, H., NANDIPATI, A. & BARLOW, M. 2013. Growth Rates Made Easy. *Molecular Biology and Evolution,* 31**,** 232 - 238.

HANS, M. 2021. *Bolton-Brush Growth Study Center* [Online]. Case Western Reserve University: Case Western Reserve University. Available: https://case.edu/dental/departments-programs/bolton-brush-growth-study-center [Accessed 30.07.2021 2021].

HARRIS, T. 2021. *How X-rays Work* [Online]. Howstuffworks. Available: https://science.howstuffworks.com/x-ray.htm [Accessed 23.05.2021].

HARTIGAN, J. 1975. Clustering algorithms, New York, Wiley.

HÂRUTA, O. 2011. Elliptic Fourier analysis of crown shapes in Quercus petraea trees. *Annals of Forest Research,* 54**,** 99 - 117.

HARWARD, C., HOLDER, N., PHILLPOTTS, C. & THOMAS, C. 2019. *The Medieval Priory and Hospital of St Mary Spital and the Bishopsgate Suburb: excavations at Spitalfields Market, London E1, 1991–2007,* London, Museum of London Archaeology.

HERSHKOVITZ, P. 1977. *Living New World monkeys (Platyrrhini) with an Introduction to Primates,* Chicago, Chicago University Press.

HETTIARACHCHI, P. V. K. S., GUNATHILAKE, P. M. P. C., JAYASINGHE, R. M., FONSEKA, M. C., BANDARA, R. M. W. R., NANAYAKKARA, C. D. & JAYASINGHE, R. D. 2021. Linear and Volumetric Analysis of Maxillary Sinus Pneumatization in a Sri Lankan Population Using Cone Beam Computer Tomography. *BioMed Research International***,** 1-6.

HIGGINS, D. & AUSTIN, J. J. 2013. Teeth as a source of DNA for forensic identification of human remains: A Review. *Science & Justice,* 53**,** 433-441.

HOGGE, J. P., MESSMER, J. M. & DOAN, Q. N. 1993. Radiographic Identification of Unknown Human Remains and Interpreter Experience Level. *Journal of Forensic Sciences,* 39**,** 373-377.

HOLOBINKO, A. 2012. Forensic human identification in the United States and Canada: A review of the law, admissible techniques, and the legal implications of their application in forensic cases. *Forensic Science International,* 222**,** 394-394.

HONA, T. W. P. T., OLDITCH, C., BYRD, J. E. & STEPHAN, C. N. 2021. Infra-cranial radiographic comparison for human identification: A study of analyst expertise. *Journal of Forensic Sciences,* 0**,** 1-12.

HOUCK, M. M., HORSMAN, G., SAUZIER, G. & BIDMOS, M. 2019. What is open-access publishing and what it means for the forensic enterprise. *Forensic Science International: Synergy,* 1**,** 290-293.

IDATA. 2019. *How Many Dental X-Rays are Performed in the United States?* [Online]. iData Research. Available: https://idataresearch.com/how-many-dental-x-rays-are-performed-in-the-united-states/ [Accessed 24.06.2022].

IKEDA, A. 1996. Volumetric Measurement of the Maxillary Sinus by Coronal CT Scan. *Nippon Jibiinkoka Gakkai Kaiho,* 99**,** 1136 - 1143.

INGERSOLL, J. M. 1906. The function of the accessory cavities of the nose. *Ann Otol Rhinol Laryngol.,* 15**,** 757 - 770.

INGERSOLL, J. M. 1922. Some points in the comparative anatomy of the nose and the accessory sinuses which account for the variations in these structures in man. *Trans Am Laryngol Rhinol Otol Soc,* 28**,** 162 - 167.

INTERPOL 2018. Disaster Victim Identification Guide: Annexure 12.

IPU & ICRC 2016. *International Humanitarian Law. Handbook for Parlamentarians No. 25,* Geneva, Inter-parliamentary Union (IPU) and International Committee of the Red Cross (ICRC).

ISCAN, M. Y. 2005. Forensic anthropology of sex and body size. *Forensic Science International,* 147**,** 107 - 112.

ISCAN, M. Y. & STEYN, M. 2013. *The Human Skeleton in Forensic Medicine,* Springfield, Thomas, C C.

IWANAGA, J., WILSON, C., LACHKAR, S., TOMASZEWSKI, K. A. & WALOCHA, J. A. 2019. Clinical anatomy of the maxillary sinus: application to sinus floor augmentation. *Anat Cell Biol,* 52**,** 17-24.

IWATA, H., EBANA, K., UGA, Y. & HAYASHI, T. 2015. Genomic Prediction of Biological Shape: Elliptic Fourier Analysis and Kernel Partial Least Squares (PLS) Regression Applied to Grain Shape Prediction in Rice (Oryza sativa L.). *PLOS ONE,* 10**.**

IWATA, H., NIIKURA, S., MATSUURA, S., TAKANO, Y. & UKAI, Y. 1998. Evaluation of variation of root shape of Japanese radish (Raphanus sativus L.) based on image analysis using elliptic Fourier descriptors. *Euphytica,* 102**,** 143-149.

IWATA, H. & UKAI, Y. 2002. SHAPE: A computer program package for quantitative evaluation of biological shapes based on elliptic Fourier descriptors. *Journal of Heredity,* 93.

JACOB, S. 2008. Chapter 7 - Head and neck. *In:* JACOB, S. (ed.) *Human Anatomy.* Churchill Livingstone.

JASIM, H. H. & AL-TAEI, J. A. 2013. Computed tomographic measurement of maxillary sinus volume and dimension in correlation to the age and gender (comparative study among individuals with dentate and edentulous maxilla). *J. Bagh. College Dentist.,* 25**,** 87-93.

JEHAN, M., BHADKARIA, V., TRIVEDI, A. & SHARMA, S. K. 2014. Sexual Dimorphism of Bizygomatic distance & Maxillary sinus using CT Scan. *Journal of Dental and Medical Sciences,* 13**,** 91-95.

JOBLING, M. A. & GILL, P. 2004. Encoded evidence: DNA in forensic analysis. *Nature Reviews Genetics,* 5**,** 739-751.

JOHNSON, N. L. 1949. Systems of frequency curves generated by methods of translation. *Biometrika,* 36**,** 149 - 176.

JOHNSON, P. & WILLIAMS, R. 2004. Post-conviction DNA testing: the UK's first 'exoneration' case? *Science & Justice,* 44**,** 77-82.

JUN, B. C., SONG, S. W., PARK, C. S., LEE, D. H., CHO, K. J. & CHO, J. H. 2005. The analysis of maxillary sinus aeration according to aging process; volume assessment by 3-dimensional reconstruction by high-resolutional CT scanning. *Otolaryngology - Head and Neck Surgery,* 132**,** 429 - 434.

KAHANA, T. & HISS, J. 1997. Identification of human remains: forensic radiology. *Journal of Clinical Forensic Medicine,* 4**,** 7-15.

KANTHEM, R. K., GUTTIKONDA, V. R., YELURI, S. & KUMARI, G. 2015. Sex determination using maxillary sinus. *Journal of Forensic Dental Sciences,* 7**,** 163-167.

KARAKAS, S. & KAVAKLI, A. 2005. Morphometric examination of the paranasal sinuses and mastoid air cells using computed tomography. *Annals of Saudi Medicine,* 25**,** 41 - 45.

KAREEM, A. J. A., HULUGALLE, S. N. C. W. M. P. S. K. & AL-HAMADANI, H. K. 2017. A Quality Control Test for General X-Ray Machine. *World Scientific News,* 90**,** 11 - 30.

KAUSMALLY, T. 2008. *St. Bride's lower churchyard cemetery summary* [Online]. Available: https://www.museumoflondon.org.uk/collections/other-collection-databases-and-libraries/centre-human-bioarchaeology/osteological-database/post-medieval-cemeteries/st-brides-lower-post-medieval [Accessed 30.07.2021].

KAYSER, M. 2015. Forensic DNA Phenotyping: Predicting human appearance from crime scene material for investigative purposes. *Forensic Science International: Genetics,* 18**,** 33-48.

KEITH, A. 1902. The relationship of the eruption of the permanent molar teeth to the expansion of the maxillary sinus. *Br J Dent Sci,* 45**,** 529–544.

KELLERMAN, R. M. & SCHMIDT, C. 2009. The paranasal sinuses as a protective crumple zone for the orbit. *Laryngoscope,* 119**,** 1682 - 1690.

KHAITAN, T., KABIRAJ, A., GINJUPALLY, U. & JAIN, R. 2017. Cephalometric Analysis for Gender Determination Using Maxillary Sinus Index: A Novel Dimension in Personal Identification. *International Journal of Dentistry,* 2017.

KHANDELWAL, P. & HAJIRA, N. 2017. Management of Oro-antral Communication and Fistula: Various Surgical Options. *World journal of plastic surgery,* 6**,** 3-8.

KILLIAN, G. 1900. Anatomie der Nase menschilcher Embryonen. II Die ursprüngliche Morphologie der Siebbeingegend; Anatomy of the nose of human embryos. II The original morphology of the ethmoid region. *Arch für Laryngologie und Rhinologie Wien***,** 1004 - 1096.

KIM, S., WARD, L. A., BUTARIC, L. N. & MADDUX, S. D. 2021. Ancestry-based variation in maxillary sinus anatomy: Implications for health disparities in sinonasal disease. *The Anatomical Record,* n/a.

KIMBEL, W. H., JOHANSON, D. C. & RAK, Y. 1997. Systematic assessment of a maxilla of Homo from Hadar, Ethiopia. *Am J Phys Anthropol,* 103**,** 235 - 262.

KIRAN KUMAR KRISHANAPPA, S., EACHEMPATI, P., KUMBARGERE NAGRAJ, S., SHETTY, N. Y., MOE, S., AGGARWAL, H. & MATHEW, R. J. 2018. Interventions for treating oro-antral communications and fistulae due to dental procedures. *The Cochrane database of systematic reviews,* 8**,** CD011784-CD011784.

KOOT, M. G. 2003. *Radiographic Human Identification Using the Bones of the Hand: A Validation Study,* Chicago, Proceedings of the 55th annual meeting of the American Academy of Forensic Sciences February 17-22.

KOPPE, T. & OHKAWA, Y. 1999. Pneumatization of the facial skeleton in catarrhine primates. *In:* KOPPE, T., NAGAI, H. & ALT, K. W. (eds.) *The paranasal sinuses of higher primates.* Chicago: Quintessence Publishing Co, Inc.

KOTTEK, M., GRIESER, J., BECK, C., RUDOLF, B. & RUBEL, F. 2006. World Map of the Köppen-Geiger climate classification updated. Meteorologische Zeitschrift, 15, 259-263.

KÖPPEN, W. & GEIGER, R. 1928. Klimate der Erde; Climate of the Earth, Gotha, Verlag Justus Perthes.

KUHL, F. P. & GIARDINA, C. R. 1982. Elliptic Fourier Features of a Closed Contour. *Computer Graphics And Image Processing,* 18.

KUMAR, V., KUMAR, P. & SHARMA, S. 2017. Study of Fingerprint Patterns as an Absolute Identification Tool for Human Identification. *Indian Journal of Forensic Medicine & Toxicology,* 11**,** 124-129.

KVNO. 2020. *Dokumentationspflicht und Aufbewahrungsfristen* [Online]. Kassenärztliche Vereinigung Nordrhein; Documentation requirements and retention periods [Online]. North Rhine Association of Statutory Health Insurance Physicians. Available: https://www.kvno.de/praxis/recht-vertraege/dokumentation/ aufbewah rungsfristen [Accessed 08.04.2022].

LAMPERTI, T. 2020. *Sinus Surgery* [Online]. Available: https://www.rhinoplastyinseattle.com/uploads/images/schematic-of-the-paranasal-sinuses-on-frontal-and-profile-view.jpg [Accessed 17.11.2021].

LAW, F. M. 1934. Roentgenograms as a means of identification. *The American Journal of Surgery,* 26**,** 195-198.

LAWSON, W., PATEL, Z. M. & LIN, F. Y. 2008. The Development and Pathologic Processes that Influence Maxillary Sinus Pneumatization. *The Anatomical Record,* 291**,** 1554-1563.

LEAKEY, M. & WALKER, A. 1997. Afropithecus – function and phylogeny. *In:* BEGUN, D. R., WARD, C. V. & ROSE, M. D. (eds.) *Function, phylogeny, and fossils.* New York: Plenum Press.

LEE, S., FERNANDEZ, J. W., MAHADEVAN, M., TARR, G. & MIRJALILI, A. 2020. Using 3D-reconstruction to analyse typical growth trends of the maxillary sinus in children. *International Journal of Pediatric Otorhinolaryngology,* 138**,** 1-8.

LEE, T. S., KELLERMAN, R. M. & DARLING, A. 2014. Crumple zone effect of nasal cavity and paranasal si- nuses on posterior cranial fossa. *Laryngoscope,* 124**,** 2241 - 2246.

LESCIOTTO, K. M. 2015. The Impact of Daubert on the Admissibility of Forensic Anthropology Expert Testimony. *Journal of Forensic Sciences,* 60**,** 549-555.

LESTREL, P., KANAZAWA, E. & WOLFE, C. 2011. Sexual dimorphism using elliptical Fourier analysis: shape differences in the craniofacial complex. *Anthropological Sciences,* 119**,** 213-229.

LESTREL, P. E. & KERR, J. S. 1993. Quantification of function regulator therapy using elliptical Fourier functions. *European Journal of Orthodontics* 15**,** 481-491.

LIBERSA, C. & FABER, M. 1958. Etude Anatomo-radiologique du Sinus Frontal Chez L'enfant; Anatomo-radiological study of the Frontal Sinus in children. *Lille Med,* 3.

LIBERTI, L., LAVOR, C., MACULAN, N. & MUCHERINO, A. 2014. Euclidean distance geometry and applications. *Siam Review,* 56**,** 3 - 69.

LORKIEWICZ-MUSZYŃSKA, D., KOCIEMBA, W., REWEKANT, A., SROKA, A., JOŃCZYK-POTOCZNA, K., PATELSKA-BANASZEWSKA, M. & PRZYSTAŃSKA, A. 2015. Development of the maxillary sinus from birth to age 18. Postnatal growth pattern. *International Journal of Pediatric Otorhinolaryngology,* 79**,** 1393-1400.

LUBET, S. & BOALS, E. I. 2020. *Expert Testimony: A Guide for Expert Witnesses and the Lawyers Who Examine Them,* Boulder, National Institute for Trial Advocacy.

LUNDBERG, J. O. N., RINDER, J., WEITZBERG, E., LUNDBERG, J. M. & ALVING, K. 1994. Nasally exhaled nitric oxide in humans originates mainly in the paranasal sinuses. *Acta Physiol Scand,* 152**,** 431 - 432.

MAIER, W. 1986. Functional principles of the growing skull of primates as shown by the posterior cupula of the nasal capsule. *In:* M., S. (ed.) *Définition et Origines de L'Homme.* Paris: CNRS.

MALIK, R., MISRA, D., SRIVASTAVA, P. C., PANJWANI, S. & MISRA, A. 2012. Use of Maxillofacial Radiology in Forensic Dentistry. *Medico-Legal Update,* 12**,** 42-44.

MARINO, M. J., RILEY, C. A., WU, E. L., WEINSTEIN, J. E., EMERSON, N. & MCCOUL, E. D. 2020. Variability of Paranasal Sinus Pneumatization in the Absence of Sinus Disease. *Ochsner Journal,* 20**,** 170-175.

MÁRQUEZ, S. 2008. The Paranasal Sinuses: The Last Frontier in Craniofacial Biology. *The Anatomical Record,* 291**,** 1350-1361.

MÁRQUEZ, S. & LAITMAN, J. T. 2008. Climatic Effects on the Nasal Complex: A CT Imaging, Comparative Anatomical, and Morphometric Investigation of Macaca mulatta and Macaca fascicularis. *The Anatomical Record,* 291**,** 1420-1445.

MÁRQUEZ, S., LAWSON, W., SCHAEFER, S. D., PAGANO, A. S., PAPAXANTHOS, M., DELMAN, B. N. & LAITMAN, J. T. 2014. Anatomy of the Nose and Paranasal Sinuses. *Diseases of the Sinuses. A Comprehensive Textbook of Diagnosis and Treatment.* 2nd ed. New York: Springer.

MÁRQUEZ, S., MOWBRAY, K., SAWYER, G. J., JACOB, T. & SILVERS, A. 2001. A new fossil hominin calvaria from Indonesia—Sambungmacan 3. *Anat Rec,* 262**,** 344 - 368.

MARSTON, L. 2010. *Introductory Statistics for Health and Nursing Using SPSS,* Thousand Oaks, California, Sage Publications.

MASPERO, C., FARRONATO, M., BELLINCIONI, F., ANNIBALE, A., MACHETTI, J., ABATE, ANDREA & CAVAGNETTO, D. 2020. Three-Dimensional Evaluation of Maxillary Sinus Changes in Growing Subjects: A Retrospective Cross-Sectional Study. *Materials,* 13**,** 2-16.

MASRI, A. A., YUSOF, A. & HASSAN, R. 2013. A three dimensional computed tomography (3D-CT): a study of maxillary sinus in malays. *Can. J. Basic Appl. Sci. ,* 1**,** 125-134.

MATHEW, A. & JACOB, L. 2020. 3D evaluation of maxillary sinus in gender determination: A cone beam computed tomography study. *Journal of Indian Academy of Oral Medicine and Radiology,* 32**,** 384-389.

MAXWELL, A. & ROSS, A. 2014. A radiographic study on the utility of cranial vault outlines for positive identifications. *Journal of Forensic Sciences,* 59**,** 314-318.

MCCARTHY WILCOX A. & NICDAEIDB, N. 2018. Jurors' perceptions of forensic science expert witnesses: Experience, qualifications, testimony style and credibility. *Forensic Science International,* 291**,** 100-108.

MCCORMICK, W. F., STEWART, J. H. & LANGFORD, L. A. 1985. Sex determination from chest plate roentgenograms. *American Journal of Physical Anthropology,* 68**,** 173-195.

MCHUGH, M. L. 2012. Interrater reliability: the kappa statistic. *Biochemia medica,* 22**,** 276-282.

MERBS, C. F. 1969. Review: The Skeletal Biology of Earlier Human Populations. *American Anthropologist,* 71**,** 168-170.

MESSMER, J. M. & FIERRO, M. F. 1986. Personal Identification by Radiographic Comparison of Vascular Groove Patterns of the Calvarium. *The American Journal of Forensic Medicine and Pathology,* 7**,** 159 - 162.

MIHALKOVICS, V. 1898. *Nasenhöhle und jacobsonsches organ: eine morphologische studie;* Nasal cavity and Jacobson's organ: a morphological study*,* Wiesbaden, Bergmann, J. F.

MODESTI, L. D. M., VIEIRA, G. M., GALVÃO, M. F. & AMORIM, R. F. B. 2014. Human Identification by Oral Prosthesis Analysis with Probability Rates Higher than DNA Analysis. *Journal of Forensic Sciences (Wiley-Blackwell),* 59**,** 825-829.

MOLLISON, T. 1932. Review: The Indians of Pecos Pueblos. A Study of their Skeletal Remains. *Anthropologischer Anzeiger,* 9**,** 199-202.

MORGAN, R. M., MEAKIN, G. E. F., J. C. & NAKHAEIZADEH, S. 2019. Crime reconstruction and the role of trace materials from crime scene to court. *WIREs Forensic Sciences,* 2**,** 2-18.

MORI, G., BELONGIE, S. & MALIK, J. 2005. Efficient shape matching using shape contexts. *IEEE Transactions on Pattern Analysis and Machine Intelligence,* 27**,** 1832-1837.

MOURET, J. 1898. Anatomie des cellules ethmöidales. *Revue hebd de Laryng d'Otol et de Rhinol,* 31**,** 913 - 924.

MUNDORFF, A. Z., BLACK, S. M., BLAU, S. & KOSALKA SHORE, R. C. 2016. Disaster Victim Management: Role of Anthropologist. *In:* PAYNE-JAMES, J. & BYARD, R. W. (eds.) *Encyclopedia of Forensic and Legal Medicine.* 2nd ed. Oxford: Elsevier.

MUSSE, J., MARQUES, J. A. & OLIVEIRA, J. 2009. Contribuição da análise do seio maxilar para a identificação humana; Contribution of the maxillary sinus analysis for human identification. *Saúde, Ética & Justiça,* 14**,** 65-76.

MUSSE, J., MARQUES, J. A., VILAS BOAS, C. & SOUSA, R. 2011. Importância pericial das radiografi as panorâmicas e da análise odontológica para identifi cação humana: relato de caso; Expert importance of panoramic radiographs and dental analysis for human identification: case report. *Rev Odontol,* 40**,** 108-111.

MUTALIK, V. S., MENON, A., JAYALAKSHMI, N., KAMATH, A. & RAGHU, A. R. 2013. Utility of cheiloscopy, rugoscopy, and dactyloscopy for human identification in a defined cohort. *Journal of Forensic Dental Sciences,* 5**,** 2-6.

NAKHAEIZADEH, S., DROR, I. E. & MORGAN, R. M. 2014. Cognitive bias in forensic anthropology: Visual assessment of skeletal remains is susceptible to confirmation bias. *Science & Justice,* 54**,** 208-214.

NARAGHI, M., DEROEE, A. F., EBRAHIMKHANI, M., KIANI, S. & DEHPOUR, A. 2007. Nitric oxide: a new concept in chronic sinusitis pathogenesis. *Am J Otolaryngol,* 28**,** 334 - 337.

NAWROCKI, S. P., LATHAM, K. E., GORE, T., HOFFMAN, R. M., BYRAM, J. N. & MAIERS, J. 2018. Using Elliptical Fourier Analysis to Interpret Complex Morphological Features in Global Populations. *In:* LATHAM, K. E., BARTELINK, E. J. & FINNEGAN, M. (eds.) *New Perspectives in Forensic Human Skeletal Identification.*

NCSL. 2014. *Medical Liability/Malpractice Statutes of Limitation* [Online]. National Conference of State Legislatures. Available: https://www.ncsl.org/research/financial-services-and-commerce/medical-liability-malpractice-statutes-of-limitation.aspx [Accessed 08.04.2022].

NEAL, T. M. S. 2009. Expert Witness Preparation: What Does the Literature Tell Us? *The Jury Expert,* 21**,** 44-52.

NEGUS, V. 1957. The function of the paransal sinuses. *AMA Arch Otolaryngol.,* 66**,** 430 - 442.

NEGUS, V. 1958. *The Comparative Anatomy and Physiology of the Nose and Paranasal Sinuses,* Edinburgh, E & S Livingstone.

NEKOLLA, E. A., SCHEGERER, A. A., GRIEBEL, J. & BRIX, G. 2017. Häufigkeit und Dosis diagnostischer und interventioneller Röntgenanwendungen. *Radiologe,* 57**,** 555 - 562.

NEMOURS, P. R. 1931. A comparison of the accessory nasal sinuses of man with those of lower vertebrates. *Trans Am Laryngol Rhinol Otol Soc***,** 195 - 199.

NIA 2022. *Computed Tomography (CT)* [Online]. National Institute of Biomedical Imaging and Bioengineering. Available: https://www.nibib.nih.gov/science-education/science-topics/computed-tomography-ct [Accessed 29.04. 2023].

NIESPODZIEWANSKI, E., STEPHAN, C. N., GUYOMARC'H, P. & FENTON, T. W. 2016. Human Identification via Lateral Patella Radiographs: A Validation Study. *Journal of Forensic Sciences (Wiley-Blackwell),* 61**,** 134-140.

NIÑO-SANDOVAL, T. C., FRAZÃO, M. & VASCONCELOS, B. C. E. 2021. Differences in skeletal growth patterns: an exploratory approach using elliptic Fourier analysis. *Clinical Oral Investigations,* 25**,** 2007-2015.

NIÑO-SANDOVAL, T. C., FRAZÃO, M. & VASCONCELOS, B. C. E. 2021. Shape differences among symmetrically shaped skeletal growth patterns in a panoramic view: a Fourier analysis. *Brazilian Oral Research,* 35**,** 1-13.

NIST. 2018. *Forensic Anthropology in Disaster Victim Identification: Best Practice Recommendations for the Medicolegal Authority* [Online]. National Institute of Standards and Technology. Available: https://www.nist.gov/system/files/documents/2018/02/13/forensic_anthropology_in_dvi-_best_practice_recommendations_for_the_medicolegal_authority.pdf [Accessed 30.06.2022].

NUÑEZ-CASTRUITA, A., LÓPEZ-SERNA, N. & GUZMÁN-LÓPEZ, S. 2012. Prenatal Development of the Maxillary Sinus:A Perspective for Paranasal Sinus Surgery. *Otolaryngology–Head and Neck Surgery,* 146**,** 997-1003.

ØLBERG, J.-V. & GOODWIN, M. 2016. Automated Dental Identification with Lowest Cost Path-Based Teeth and Jaw Separation. *Scandinavian Journal of Forensic Science,* 22**,** 44-56.

OMAR, A., ANDREO, P. & POLUDNIOWSKI, G. 2020. A model for the energy and angular distribution of x rays emitted from an x-ray tube. Part I. Bremsstrahlung production. *Medical Physics,* 47**,** 4763 - 4774.

OMRAN, A., WERTHEIM, D., SMITH, K., LIU, C. Y. J. & NAINI, F. B. 2020. Mandibular shape prediction using cephalometric analysis: applications in craniofacial analysis, forensic anthropology and archaeological reconstruction. *Maxillofacial Plastic and Reconstructive Surgery,* 42**,** 2-14.

ONCOLOGYMEDICALPHYSICS. 2021. *X-ray Spectrum* [Online]. Available: https://oncologymedicalphysics.com/kilovoltage-x-ray-generation/ [Accessed 07.01.2022 2022].

ONODI, A. 1903. Des rapports entre le nerf optique et le sinus sphénoidal. La cellule ethmoidale postérieure en particulier; Of the relations between the optic nerve and the sphenoidal sinus. The posterior ethmoidal cell in particular. *Revue hebd de Laryng d'Otol et de Rhino,* 25**,** 721 - 740.

OSAC. 2022. *Forensic Anthropology Subcommittee* [Online]. NIST. Available: https://www.nist.gov/organization-scientific-area-committees-forensic-science/forensic-anthropology-subcommittee [Accessed 23.06.2022].

PALMER, M., PONS, G. X. & LINDE, M. 2004. Discriminating between geographical groups of a Mediterranean commercial clam (Chamelea gallina (L.): Veneridae) by shape analysis. *Fisheries Research,* 67**,** 93-98.

PANKANTI, S., PRABHAKAR, S. & JAIN, A. K. 2002. On the individuality of fingerprints. *IEEE Transactions on Pattern Analysis and Machine Intelligence,* 24**,** 1010-1025.

PAOLELLO, J. & CABO-PEREZ, L. 2008. Elliptical Fourier analysis of vertebral outlines for victim identification. *In:* AAFS (ed.) *Proceedings of the American Academy of Forensic Sciences 60th annual scien- tific meeting.* Washington, DC.

PAPINI, A., GALLI, M., DI MARTINO, N., ZAVATTARO, M. & CECCHI, J. M. 2015. Studio delle simmetrie e asimmetrie ossee mascellari in collezioni italiane presenti nella cranioteca del Museo di Storia Naturale dell'Università di Firenze tramite CBCT; Study of maxillary bone symmetries and asymmetries in Italian collections present in the craniotheque of the Museum of Natural History of the University of Florence using CBCT. *Museologia Scientifica,* 14**,** 87 - 90.

PARENTI, R. 1952. Caratteristiche angolari del cranio umano nel piano sagittale; Angular features of the human skull in the sagittal plane. *In:* MANTEGAZZA, P. (ed.) *Archivio per l'antropologia e la etnologia.* Firenze: Societa Italiana di Antropologia e Etnologia.

PASSALACQUA, N. V. & PILLOUD, M. A. 2018. *Ethics and Professionalism in Forensic Anthropology,* London, Elsevier.

PASSALACQUA, N. V. & PILLOUD, M. A. 2021. The need to professionalize forensic anthropology. *European Journal of Anatomy,* 25**,** 35 - 47.

PASSALI, D. & BELLUSSI, L. 1995. La fisiologia dei seni paranasali; The physiology of the paranasal sinuses. In: I tumori maligni dei seni paranasali. *Relazione ufficiale dell'82° congresso SIO (a cura di Antonelli AR) Pacini***,** 31 - 56.

PASTOORS, A. 2016. *NESPOS. Pleistocene People and Places* [Online]. Available: https://www.nespos.org/x/fQnIAQ [Accessed 04.08.2021].

PATEL, U. P., MAKARDAR, U. K., LAYEEQEU, K. M. & BALKUND, K. 2020. Identification of Sex from Maxillary Sinus in Western Maharashtra Population. *Indian Journal of Forensic Medicine & Toxicology,* 14**,** 607-611.

PATIL, N., KARJODKAR, F. R., SONTAKKE, S., SANSARE, K. & SALVI, R. 2012. Uniqueness of radiographic patterns of the frontal sinus for personal identification. *Imaging Sci Dent,* 42**,** 213-7.

PATRIQUIN, M. L., LOTH, S. R. & STEYN, M. 2003. Sexually dimorphic pelvic morphology in south African whites and blacks. *Homo,* 53**,** 255-262.

PAULLI, S. 1900a. Über die Pneumaticität des Schädels bei den Säugethieren. Eine morphologische Studie I. Über den Bau des Siebbeins. Über die Morphologie des Siebbeins der Pneumaticität bei den Monotremen und den Marsupialiern; The pneumaticity of the skull in mammals. A morphological study I. The structure of the ethmoid. The morphology of the ethmoid of the pneumaticity in the Monotremes and the Marsupialians. *Gegenbaurs. Morph Jahrb,* 28**,** 147 - 178.

PAULLI, S. 1900b. Über die Pneumaticitaät des Schädels bei den Säugethieren. Eine morphologische Studie II. Über die Morphologie des Siebbeins der Pneumaticität bei den Ungulaten und Probosciden; The pneumaticity of the skull in mammals. A morphological study II. The morphology of the ethmoid of pneumaticity in the ungulates and proboscids. *Gegenbaurs. Morph Jahrb,* 28**,** 179 - 251.

PAULLI, S. 1900c. Über die pneumaticität des Schädels bei den Säugethieren. Eine morphologische Studie III. Über die Morphologie des Siebbeins und Pneumaticität bei den Insectivoren, Hyra- coideen, Chiropteren, Carnivoren, Pinnipedien, Edentates, Rodentiern, Prosimien und Primaten; The pneumaticity of the skull in mammals. A morphological study III. The morphology of the ethmoid and pneumaticity in insectivores, hyracoidea, chiroptera, carnivores, pinnipeds, edentates, rodents, prosimians and primates. *Gegenbaurs. Morph Jahrb,* 28**,** 483 - 564.

PEEL, M. C., FINLAYSON, B. L. & MCMAHON, T. A. 2007. Updated world map of the Köppen-Geiger climate classification. Hydrology and Earth System Sciences, 11, 1633-1644.

PELINSARI LANA, J., MOURA RODRIGUES CARNEIRO, P., DE CARVALHO MACHADO, V., EDUARDO ALENCAR DE SOUZA, P., RICARDO MANZI, F. & CAMPOLINA REBELLO HORTA, M. 2012. Anatomic variations and lesions of the maxillary sinus detected in cone beam computed tomography for dental implants. *Clinical Oral Implants Research,* 23**,** 1398-1403.

PÉREZ SAYÁNS, M., SUÁREZ QUINTANILLA, J. A., CHAMORRO PETRONACCI, C., M. , SUÁREZ PEÑARANDA, J. M., LÓPEZ JORNET, P., GÓMEZ GARCÍA, F. & GUERRERO SÁNCHEZ, Y. 2020. Volumetric study of the maxillary sinus in patients with sinus pathology. *PLoS One,* 15.

PETRIE, W. M. F. 1898. *Deshasheh,* London, Egyptian Exploration Fund.

PIETRUSEWSKY, M. 2007. Metric Analysis of Skeletal Remains: Methods and Applications. In: KATZENBERG, M. A. & SAUNDERS, S. R. (eds.) Biological Anthropology of the Human Skeleton. New Jersey: Wiley.

PINTO, R. M., MOURA, E. G., MEDEIROS, L. B. A. & OLIVEIRA, H. G. 2012. Análise de seios maxilaresem radiografias panorâmicas: um método auxiliar nos processos de estimativae identificação humana; Analysis of maxillary sinuses in panoramic radiographs: an auxiliary method in human estimation and identification processes. *Ext. Soc.,* 1**,** 130-136.

PONCE DE LEÓN, M. S. & ZOLLIKOFER, C. P. E. 2001. Neanderthal cranial ontogeny and its implications for late hominid diversity. *Nature,* 412**,** 534 - 538.

POULTON. 2014. *History of Poulton. Poulton Research Project* [Online]. Available: http://www.poultonresearchproject.co.uk/history-of-poulton/ [Accessed 04.08.2021].

PROETZ, A. W. 1953. *Essays on the applied physiology of the nose,* St. Louis, Annals Publishing.

PROFICO, A., BUZI, C., DAVIS, C., MELCHIONNA, M., VENEZIANO, A., RAIA, P. & MANZI, G. 2019. A New Tool for Digital Alignment in Virtual Anthropology. *The Anatomical Record,* 302**,** 1104-1115.

PRZYSTAŃSKA, A., REWEKANT, A., SROKA, A., GEDRANGE, T., EKKERT, M., JOŃCZYK-POTOCZNA, K. & CZAJKA-JAKUBOWSKA, A. 2020. Sexual dimorphism of maxillary sinuses in children and adolescents – A retrospective CT study. *Annals of Anatomy - Anatomischer Anzeiger,* 229**,** 151437.

PSU. 2022. *Measures of Similarity and Dissimilarity* [Online]. The Pennsylvania State University. Available: https://online.stat.psu.edu/stat508/lesson/1b/1b.2/1b.2.1 [Accessed 01.07.2022].

PUBLIC HEALTH ENGLAND. 2010. *Medical and dental x-rays: frequency and collective doses in the UK* [Online]. GOV.UK. Available: https://www.gov.uk/government/publications/medical-and-dental-x-rays-frequency-and-collective-doses-in-the-uk [Accessed 24.06.2021].

PURCHASEA, S. L., BAZALIISKIIB, V. I. & LIEVERSEC, A. R. 2019. An innovative method to visualise mastoiditis using a hand-held X-ray T system. *International Journal of Paleopathology,* 26**,** 22 - 26.

QUATREHOMME, G., FRONTY, P., SAPANET, M., GRÉVIN, G., BAILET, P. & OLLIER, A. 1996. Identification by frontal sinus pattern in forensic anthropology. *Forensic Science International,* 83**,** 147-153.

RABELO, K. A., DOS ANJOS PONTUAL, M. L., DE QUEIROZ JORDAO, N., DE PAIVA, K. M., DE MORAES RAMOS-PEREZ, F. M., DOS SANTOS, M. S. & DOS ANJOS PONTUAL, A. 2016. Human identification by FSS system adapted to cephalometric radiographs. *Forensic Sci Int,* 262**,** 227-32.

RADINOVIĆ, M. & KAJTEZ, I. 2021. Outlining the knapping techniques: Assessment of the shape and regularity of prismatic blades using elliptic Fourier analysis. Journal of Archaeological Science: Reports, 38, 1-11.

RAE, T. 1997. The early evolution of the hominoid face. *In:* BEGUN, D., WARD, C. & ROSE, M. (eds.) *Function, phylogeny, and fossils: mio- cene hominoid evolution and adaptations.* New York: Plenum Press.

RAE, T. C. 2008. Paranasal pneumatization in extant and fossil Cercopithecoidea. *Journal of Human Evolution,* 54**,** 279-286.

RAE, T. C., HILL, R. A., HAMADA, Y. & KOPPE, T. 2003. Clinal Variation of Maxillary Sinus Volume in Japanese Macaques (Macaca fuscata). *American Journal of Primatology,* 59**,** 153 - 158.

RAE, T. C. & KOPPE, T. 2000. Isometric scaling of maxillary sinus volume in hominoids. *Journal of Human Evolution,* 38**,** 411-423.

RAE, T. C. & KOPPE, T. 2004. Holes in the head: Evolutionary interpretations of the paranasal sinuses in catarrhines. *Evolutionary Anthropology: Issues, News, and Reviews,* 13**,** 211-223.

RAE, T. C. & KOPPE, T. 2014. Sinuses and flotation: Does the aquatic ape theory hold water? *Evolutionary Anthropology: Issues, News, and Reviews,* 23**,** 60-64.

RAE, T. C., VIDARSDOTTIR, U. S., JEFFERY, N. & STEEGMANN, A. T. 2006. Developmental response to cold stress in cranial morphology of Rattus: implications for the interpretation of climatic adaptation in fossil hominins. *Proc Biol Sci,* 273**,** 2605-10.

RAI. 2018. *Code of Practice for Forensic Anthropology* [Online]. Available: https://therai.org.uk/images/stories/Forensic/Code_of_Practice_for_Forensic_Anthropology.pdf [Accessed 23.06.2022].

RANI, S. U., RAO, G. V., KUMAR, D. R., SRAVYA, T., SIVARANJANI, Y. & KUMAR, M. P. 2017. Age and gender assessment through three-dimensional morphometric analysis of maxillary sinus using magnetic resonance imaging. *Journal of Forensic Dental Sciences,* 9**,** 81-85.

REED, K. & SYNDERCOMBE-COURT, D. 2014. A comparative audit of legislative frameworks within the European Union for the collection, retention and use of forensic DNA profiles. *In:* EUROFORGEN (ed.). London: EUROFORGEN-NoE.

RESNIK, R. R. & PREECE, J. W. 2017. Radiographic Complications and Evaluation. *In:* RESNIK, R. R. & MISCH, C. E. (eds.) *Misch's Avoiding Complications in Oral Implantology.* Elsevier Inc.

RHYS EVANS, P. H. 1992. The paranasal sinuses and other enigmas: an aquatic evolutionary theory. *J Laryngol Otol,* 106**,** 214 - 225.

RIBEIRO, F. D. A. 2000. Standardized measurements of radiographic films of the frontal sinuses: An aid to identifying unknown persons. *Ear, Nose & Throat Journal,* 79**,** 26-33.

RIEPERT, T., ULMCKE, D., SCHWEDEN, F. & NAFE, B. 2001. Identification of unknown dead bodies by X-ray image comparison of the skull using the X-ray simulation program FoXSIS. *Forensic Science International,* 117**,** 89-98.

ROBLES, M., RANDO, C. & MORGAN, R. M. 2020. The utility of three-dimensional models of paranasal sinuses to establish age, sex, and ancestry across three modern populations: A preliminary study. *Australian Journal of Forensic Sciences*.

ROHLF, F. J. 1990. Morphometrics. Annual Review of Ecology, Evolution, and Systematics, 21, 299-316.

ROHLF, F. J. & MARCUS, L. F. 1993. A Revolution in Morphometrics. Tree, 8, 129-132.

RÖNTGEN, W. C. 1895. *Über eine neue Art von Strahlen; About a new kind of ray,* Würzburg, Physikalisch-Medizinischen Gesellschaft.

ROSAS, A. & BASTIR, M. 2002. Thin-Plate Spline Analysis of Allometry and Sexual Dimorphism in the Human Craniofacial Complex. American Journal of Physical Anthropology, 117, 236-245.

ROSE, A., WOODS, M., CLEMENT, J. & THOMAS, C. 2003. Lateral facial soft- tissue prediction model: analysis using Fourier shape descriptors and traditional cephalometric methods. *American Journal of Physical Anthropology,* 121**,** 172-180.

ROSS, A. H. & PILLOUD, M. A. 2021. The need to incorporate human variation and evolutionary theory in forensic anthropology: A call for reform. *American Journal of Physical Anthropology,* 176**,** 672-638.

ROSSIE, J. B., SIMONS, E. L., GAULD, S. C. & RASMUSSEN, D. T. 2002. Paranasal sinus anatomy of Aegyptopithecus: implications for hominoid origins. *Proc Natl Acad Sci USA,* 99**,** 8454 - 8456.

RUBEL, F. & KOTTEK, M. 2010. Observed and projected climate shifts 1901-2100 depicted by world maps of the Köppen-Geiger climate classification. Meteorologische Zeitschrift, 19, 135-141.

RUDER, T. D., KRAEHENBUEHL, M., GOTSMY, W. F., MATHIER, S., EBERT, L. C., THALI, M. J. & HATCH, G. M. 2012. Radiologic identification of disaster victims: A simple and reliable method using CT of the paranasal sinuses. *European Journal of Radiology,* 81**,** 132-138.

RUNGE, H. G. 1928. Identification by comparison of roentgenograms of nasal accessory sinuses and mastoid processes. *Deutsche Zeitschrift für die gesamte gerichtliche Medizin,* 11**,** 86-86.

SANCHEZ FERNANDEZ, J. M., ANTA ESCUREDO, J. A., SANCHEZ DEL REY, A. & SANTAOLALLA MONTOYA, F. 2000. Morphometric Study of the Paranasal Sinuses in Normal and Pathological Conditions. *Acta Otolaryngol,* 120**,** 273-278.

SARILITA, E., LITA, Y. A., NUGRAHA, H. G., MURNIATI, N. & YUSUF, H. Y. 2021. Volumetric growth analysis of maxillary sinus using computed tomography scan segmentation: a pilot study of Indonesian population. *Anatomy & Cell Biology,* 54**,** 431-435.

SATHAWANE, R. S., SUKHADEVE, V. A., CHANDAK, R. M., LANJEKAR, A. B. & MOON, G. V. 2020. Sex determination by maxillary sinus dimensions using cone-beam computed tomography and discriminant function: An analytical study. *International Journal of Forensic Odontology,* 5**,** 19-22.

SAYINCI, B., KARA, M., ERCIŞLI, S., DUYAR, Ö. & ERTÜRK, Y. 2015. Elliptic Fourier analysis for shape distinction of Turkish hazelnut cultivars. *Erwerbs-Obstbau,* 57**,** 1-11.

SCHAEFFER, J. P. 1910. The sinus maxillaris and its relations in the embryo, child and adult man. *American Journal of Anatomy,* 10**,** 313 - 368.

SCHATZ, C. J. & BECKER, T. S. 1984. Normal CT anatomy of the paranasal sinuses. *Radiol Clin North Am,* 22**,** 107 - 118.

SCHMIDT, G. & KALLIERIS, D. 1982. Use of radiographs in the forensic autopsy. *Forensic Science International,* 19**,** 263-270.

SCHMITTBUHL, M., LE MINOR, J., SCHAAF, A. & MANGIN, P. 2002. The human mandible in lateral view: elliptical Fourier descriptors of the outline and their morphological analysis. *Annals of Anatomy - Anatomischer Anzeiger,* 184**,** 199-207.

SCHÜLLER, A. 1921. Das Röntgenogram der Stirnhöhle: ein Hilfsmittel für die Identitätsbestimmung von Schädeln; The roentgenogram of the frontal sinus: a tool for the identification of skulls. *Monatsschrift Ohrenheilkunde Laryngorhinol,* 5**,** 1617-1620.

SCHÜLLER, A. 1943. A note on the identification of skulls by X-ray pictures of the frontal sinuses. *Medical Journal of Australia,* 1**,** 554 - 557.

SCHUMMER, A., NICKEL, R. & SACK, W. O. 1979. *The viscera of the domestic mammals,* New York, Springer.

SCHWARTZ, J. H. 1987. *The red ape: orang-utans and human origins,* Boston, Houghton Mifflin.

SEIBERT, J. A. 2004. X-Ray Imaging Physics for Nuclear Medicine Technologists. Part 1: Basic Principles of X-Ray Production. *Journal of Nuclear Medicine Technology,* 32**,** 139 - 147.

SEIBERT, J. A. & BOONE, J. M. 2005. X-Ray Imaging Physics for Nuclear Medicine Technologists. Part 2: X-Ray Interactions and Image Formation*. *Journal of Nuclear Medicine Technology,* 33**,** 3 - 18.

SEIDLER, H., FALK, D., STRINGER, C., WILFING, H., MÜLLER, G., ZUR NEDDEN, D., WEBER, G., REICHEIS, W. & ARSUAGA, J. L. 1997. A comparative study of stereolithographically modelled skulls of Petralona Pand Broken Hill: implications for future studiesof middle Pleistocene hominid evolution. *J Hum Evol,* 33**,** 691 - 703.

SELCUK, O. T., EROL, B., RENDA, L., OSMA, U., EYIGOR, H., GUNSOY, B., YAGCI, B. & YILMAZ, D. 2015. Do altitude and climate affect paranasal sinus volume? *Journal of Cranio-Maxillofacial Surgery,* 43**,** 1059-1064.

SENSE ABOUT SCIENCE. 2017. *Making Sense of Forensic Genetics* [Online]. Available: http://senseaboutscience.org/activities/making-sense-of-forensic-genetics/ [Accessed 26.02.2017].

SFO. 2022. *Expert witness guidance* [Online]. Serious Fraud Office. Available: https://www.sfo.gov.uk/publications/information-victims-witnesses-whistleblowers/expert-witness-guidance/ [Accessed 08.06.2022].

SHAH, R. K., DHINGRA, J. K., CARTER, B. L. & REBEIZ, E. E. 2003. Paranasal Sinus Development: A Radiographic Study. *The Laryngoscope,* 113**,** 205-209.

SHEA, B. T. 1977. Eskimo craniofacial morphology, cold stress and the maxillary sinus. *American Journal of Physical Anthropology,* 47**,** 289-300.

SHERIDAN, C., THOMAS, C. & CLEMENT, J. 1997. Quantification of ethnic differences in facial profile. *Australian Orthodontic Journal,* 14**,** 218-224.

SIDHU, R., CHANDRA, S., DEVI, P., TANEJA, N., SAH, K. & KAUR, N. 2014. Forensic importance of maxillary sinus in gender determination: A morphometric analysis from Western Uttar Pradesh, India. *European Journal of General Dentistry,* 3**,** 53.

SIERON, H. L., SOMMER, F., HOFFMANN, T. K., GROSSI, A. S., SCHEITHAUER, M. O., STUPP, F. & LINDEMANN, J. 2020. Funktion und Physiologie der Kieferhöhle; Function and physiology of the maxillary sinus. *HNO,* 68**,** 566-572.

SIEUR, C. & JACOB, O. 1901. *Recherches anatomiques cliniques et ope´ra- toires sur les fosses nasales et leurs sinus; Clinical and operative anatomical research on the nasal fossae and their sinuses,* Paris, Rueff, J.

SILVA, R. F., PRADO, F. B., CAPUTO, I. G., DEVITO, K. L., BOTELHO TDE, L. & DARUGE JUNIOR, E. 2009. The forensic importance of frontal sinus radiographs. *J Forensic Leg Med,* 16**,** 18-23.

SKAUDICKAS, D., VEIKUTIS, V., VITKUS, A., PECIULYTĖ, G., MARCIULIONYTE, D., SAKALYTE, G., KRISCIUKAITIS, A. & VAITIEKAITIS, G. 2014. Evaluation of complexity of induced necrosis zone shape by means of principal component analysis. *Journal of Vibroengineering*, 16, 4115-4125.

SLICE, D. E. 2007. Geometric Morphometrics. Annual Review of Anthropology, 36, 261-281.

SMITH, V. A., CHRISTENSEN, A. M. & MYERS, S. W. 2010. The Reliability of Visually Comparing Small Frontal Sinuses. *Journal of Forensic Sciences,* 55**,** 1413-1415.

SOARES, C. B., ALMEIDA, M. S., LOPES PDE, M., BELTRAO, R. V., PONTUAL ADOS, A., RAMOS-PEREZ, F. M., FIGUEROA, J. N. & PONTUAL, M. L. 2016. Human identification study by means of frontal sinus imaginological aspects. *Forensic Sci Int,* 262**,** 183-9.

SOMAN, B. A., SUJATHA, G. P. & LINGAPPA, A. 2016. Morphometric evaluation of the frontal sinus in relation to age and gender in subjects rediding in Davangere, Karnataka. *Journal of Forensic Dental Science,* 8**,** 12-16.

SOUADIH, K., BELAID, A., BEN SALEM, D. & CONZE, P.-H. 2020. Automatic forensic identification using 3D sphenoid sinus segmentation and deep characterization. *Medical & Biological Engineering & Computing,* 58**,** 291-306.

SPIES, A. J., STEYN, M., PRINCE, D. N. & BRITS, D. 2021. Can forensic anthropologists accurately detect skeletal trauma using radiological imaging? *Forensic Imaging,* 24**,** 2-8.

SPOOR, F., JEFFERY, N. & ZONNEVELD, F. 2000. Imaging skeletal growth and evolution. *In:* O'HIGGINS, P. & COHN, M. (eds.) *Development, growth and evolution: implications for the study of the hominid skeleton.* London: Academic Press.

SPOOR, F., JEFFERY, N. & ZONNEVELD, F. 2001. Imaging Skeletal Growth and Evolution. *In:* O'HIGGINS, P. & COHN, M. (eds.) *Development, Growth and Evolution.* San Diego: Academic Press.

SPOOR, F., WOOD, B. & ZONNEVELD, F. 1994. Implications of early hominid labyrinthine morphology for the evolution of human bipedal loc- motion. *Nature,* 169**,** 645 - 648.

SPRADLEY, K. & JANTZ, R. 2011. Sex estimation in forensic anthropology: skull versus postcranial elements. *Journal of Forensic Sciences,* 56**,** 289-296.

STATISTA. 2022. *Total population in the United States by gender from 2010 to 2025* [Online]. Statista. Available: https://www.statista.com/statistics/737923/us-population-by-gender/ [Accessed 24.06.2022].

STEADMAN, D. W. 2018. Who Needs Data? I've Got Experience! *Human Biology,* 90**,** 77 - 82.

STEPHAN, C., AMIDAN, B., TREASE, H., GUYOMARC'H, P., PULSIPHER, T. & BYRD, J. 2014. Morphometric comparison of clavicle outlines from 3D bone scans and 2D chest radiographs: a shortlisting tool to assist radiographic identification of human skeletons. *Journal of Forensic Sciences,* 59**,** 306-313.

STEYN, M., BECKER, P. J., L'ABBÉ, E. N., SCHOLTZ, Y. & MYBURGH, J. 2012. An assessment of the repeatability of pubic and ischial measurements. *Forensic Science International,* 214**,** 1-4.

SUBASREE, S. & DHARMAN, S. 2019. Age and Gender Determination Using Maxillary Sinus and Sella Turcica in Forensics-A Lateral Cephalometric Study. *Indian Journal of Forensic Medicine & Toxicology,* 13**,** 151-157.

SULLIVAN, L. M., WEINBERG, J. & KEANEY, J. F. 2016. Common Statistical Pitfalls in Basic Science Research. *Journal of the American Heart Association,* 5**,** 1-9.

SWIFT, B. & RUTTY, G. N. 2006. Recent Advances in Postmortem Forensic Radiology. *In:* TSOKOS, M. (ed.) *Forensic Pathology Reviews.* Totowa, NJ: Humana Press.

TAKAHASHI, R. Y. O. 1983. The formation of the human paranasal sinuses. *Acta Otolaryngol Suppl.,* 408**,** 2 - 28.

TANAKA, H., LESTREL, P., UETAKE, T., SUSUMU, K. & OHTSUKI, F. 2000. Sex differences in proximal humeral outline shape: elliptical Fourier functions. *Journal of Forensic Sciences,* 45**,** 292-302.

TANG, J. P., HU, D. Y., JIANG, F. H. & YU, X. J. 2009. Assessing forensic applications of the frontal sinus in a Chinese Han population. *Forensic Sci Int,* 183**,** 104 1-3.

TATLISUMAK, E., YILMAZ OVALI, G., ASLAN, A., ASIRDIZER, M., ZEYFEOGLU, Y. & TARHAN, S. 2007. Identification of unknown bodies by using CT images of frontal sinus. *Forensic Sci Int,* 166**,** 42-8.

TERRY, G. L., NOUJEIM, M., LANGLAIS, R. P., MOORE, W. S. & PRIHODA, T. J. 2016. A clinical comparison of extraoral panoramic and intraoral radiographic modalities for detecting proximal caries and visualizing open posterior interproximal contacts. *Dentomaxillofacial Radiology,* 45**,** 1-7.

THAYER, Z. M. & DOBSON, S. D. 2010. Sexual dimorphism in chin shape: implications for adaptive hypotheses. *American Journal of Physical Anthropology,* 143**,** 417-425.

TILLIER, A. M. 1977. La pneumatization du massif cranio-facial chez les homes actuels et fossils (suite). *Bull Et Mem.de la Soc D'Anthrop de Paris,* 4**,** 287–316.

TOMBERLIN, J. K., BENBOW, M. E., TARONE, A. M. & MOHR, R. M. 2011. Basic research in evolution and ecology enhances forensics. *Trends in Ecology and Evolution,* 26**,** 53 - 55.

UNDERWOOD, A. S. 1910. An Inquiry into the Anatomy and Pathology of the Maxillary Sinus. *Journal of anatomy and physiology,* 44**,** 354-369.

UNITED NATIONS 1948. *217 A (III). Universal Declaration of Human Rights,* New York, United Nations General Assembly.

US DEPARTMENT OF JUSTICE. 2021. *United States Department of Justice Statement on the PCAST Report: Forensic Science in Criminal Courts: Ensuring Scientific Validity of Feature-Comparison Methods* [Online]. Available: https://www.justice.gov/olp/page/file/1352496/download. [Accessed 08.06.2022].

UTHMAN, A. T., AL-RAWI, N. H., AL-NAAIMI, A. S. & AL-TIMIMI, J. F. 2011. Evaluation of Maxillary Sinus Dimensions in Gender Determination Using Helical CT Scanning. *Journal of Forensic Sciences,* 56**,** 403-408.

UTSUNO, H. 2019. Victim identification in large-scale disasters using dental findings. *IATSS Research,* 43**,** 90 - 96.

VALORIANI, S. 2019. *Cranial remains from the graveyard to the laboratory: restoration, conservation and craniometric analysis of medieval British skeletal samples.* PhD, Liverpool John Moores University.

VELASCO-TORRES, M., PADIAL-MOLINA, M., AVILA-ORTIZ, G., GARCÍA-DELGADO, R., O'VALLE, F., CATENA, A. & GALINDO-MORENO, P. 2017. Maxillary Sinus Dimensions Decrease as Age and Tooth Loss Increase. *Implant Dentistry,* 26**,** 288-295.

VELEMÍNSKÁ, J., KRAJÍČEK, V., DUPEJ, J. & GOMÉZ-VALDÉS, J. 2013. Technical note: geometric morphometrics and sexual dimorphism of the greater sciatic notch in adults from two skeletal collections: the accuracy and reliability of sex classification. *American Journal of Physical Anthropology,* 152**,** 558-565.

VIÐARSDÓTTIR, U. S., O'HIGGINS, P. & STRINGER, C. 2002. A geometric morphometric study of regional differences in the ontogeny of the modern human facial skeleton†. *Journal of Anatomy,* 201**,** 211-229.

VIDYA, C. S., SHAMASUNDAR, N. M., B., M. & RAICHURKAR, K. 2013. Evaluation of size and volume of maxillary sinus to determine gender by 3D computerized tomography scan method using dry skulls of south indian origin. *International Journal of Current Research and Review* 5**,** 97-100.

VLCEK, E. 1965. Die Sinus frontales bei Europaischen Neanderthalern; The frontal sinus in European Neanderthals. *Anthropol Anz,* 28**,** 166 - 189.

VNW. 2022a. *Population of England* [Online]. Visit North West. Available: https://www.visitnorthwest.com/population/england/ [Accessed 24.06.2022].

VNW. 2022b. *Population of Wales* [Online]. Visit North West. Available: https://www.visitnorthwest.com/population/wales/ [Accessed 24.06.2022].

VULLO, C. M., CATELLI, L., IBARRA RODRIGUEZ, A. A., PAPAIOANNOU, A., ÀLVAREZ MERINOD, C., LOPEZ-PARRAE, A. M., GAVIRIAF, A., BAEZA-RICHERE, C., ROMANINI, C., GONZÁLEZ-MOYA, E., CASALS, F., CALAFELL, F., BERARDI, G., IANNACONE, G. C., VICUNA GIRALDO, G. C., ZORBA, G. K., BOSCHI, I., VALDIVIA OLARTE, J., RUIZ GOMEZ, J. E., ACIERNO, J. P., LÓPEZ SOTO, M., VELÁZQUEZ MIRANDA, M., GARCÍA KING, M. D., MARRUCCI, M. A., PORTO, M. J., HERRERA PIÑERO, M., ALER, M., STEPHENSON OJEA, M. M., COBOS NAVARRETE, S., TOSCANINI, U., SARAGONI, V. G., BOZZO, W., POSADA POSADA, Y. C., BAJUNOVIC, Z., PRIETO SOLLA, L. & PARSONS, T. 2021. Second GHEP-ISFG exercise for DVI: "DNA-led" victims' identification in a simulated air crash. *Forensic Science International,* 53**,** 2 - 14.

WALKER, P. 2005. Greater sciatic notch morphology: sex, age, and population differences. *American Journal of Physical Anthropology,* 127**,** 385-391.

WEGNER, R. N. 1958. Die Nebenhöhlen der Nase bei den Krokodilen; The sinuses of the nose in crocodiles. *Wissensch Z Ernst Moritz Arndt Univ Greifswald, Germany,* 7**,** 1 - 39.

WHYTE, A. & BOEDDINGHAUS, R. 2019. The maxillary sinus: physiology, development and imaging anatomy. *Dentomaxillofacial Radiology,* 48**,** 2 - 54.

WILDER, H. H. & WENTWORTH, B. 1932. *Personal Identification Methods for the Identification of Individuals,* Boston, Mass., Badger Richard G.

WITMER, L. 1999. The phylogenetic history of paranasal sinuses. *In:* KOPPE, T., NAGAI, H. & ALT, K. (eds.) *The Paranasal Sinuses of Higher Primates: Development, Function and Evolution.* Chicago: Quintessence.

WLODARCZYK, R. 2012. Biometric Features Used for Forensic Identification of Humans. *Internal Security,* 4**,** 125-140.

XAVIER, T. A., DIAS TERADA, A. S. S. & DA SILVA, R. H. A. 2015. Forensic application of the frontal and maxillary sinuses: A literature review. *Journal of Forensic Radiology and Imaging,* 3**,** 105-110.

YOSHIOKA, Y., IWATA, H., OHSAWA, R. Y. O. & NINOMIYA, S. 2004. Analysis of Petal Shape Variation of Primula sieboldii by Elliptic Fourier Descriptors and Principal Component Analysis. *Annals of Botany,* 94**,** 657-664.

ZHAN, Q. & WANG, X. 2012. Elliptic Fourier Analysis of the Wing Outline Shape of Five Species of Antlion (Neuroptera: Myrmeleontidae: Myrmeleontini). *Zoological Studies,* 51**,** 399 - 495.

ZIMMER, C. 2004. *Soul made flesh - The discovery of the brain - and how it changed the world,* New York, Free Press.

ZUCKERKANDL, E. 1892b. *Normale und pathologische Anatomie der Nasenhöhle und ihrere pneumatischen Anhänge. Anatomie der Nasenscheidewand; Normal and pathologic anatomy of the nasal cavity and its pneumatic appendages. Anatomy of the nasal septum. Bd. II,* Wien, Braumüller, W.

ZUCKERKANDL, E. 1893. *Normale und pathologische Anatomie der Nasenhöhle und ihrere pneumatischen Anhänge; Normal and pathologic anatomy of the nasal cavity and its pneumatic appendages,* Wien, Braumüller, W.

ZUCKERKANDL, E. W. 1882a. *Normale und Pathologische Anatomie der Nasenhöhle und ihrere Pneumatischen Anhänge; Normal and pathological anatomy of the nasal cavity and its pneumatic appendages,* Wien, Braumüller, W.

Appendix 1
Uniqueness Test Comparison

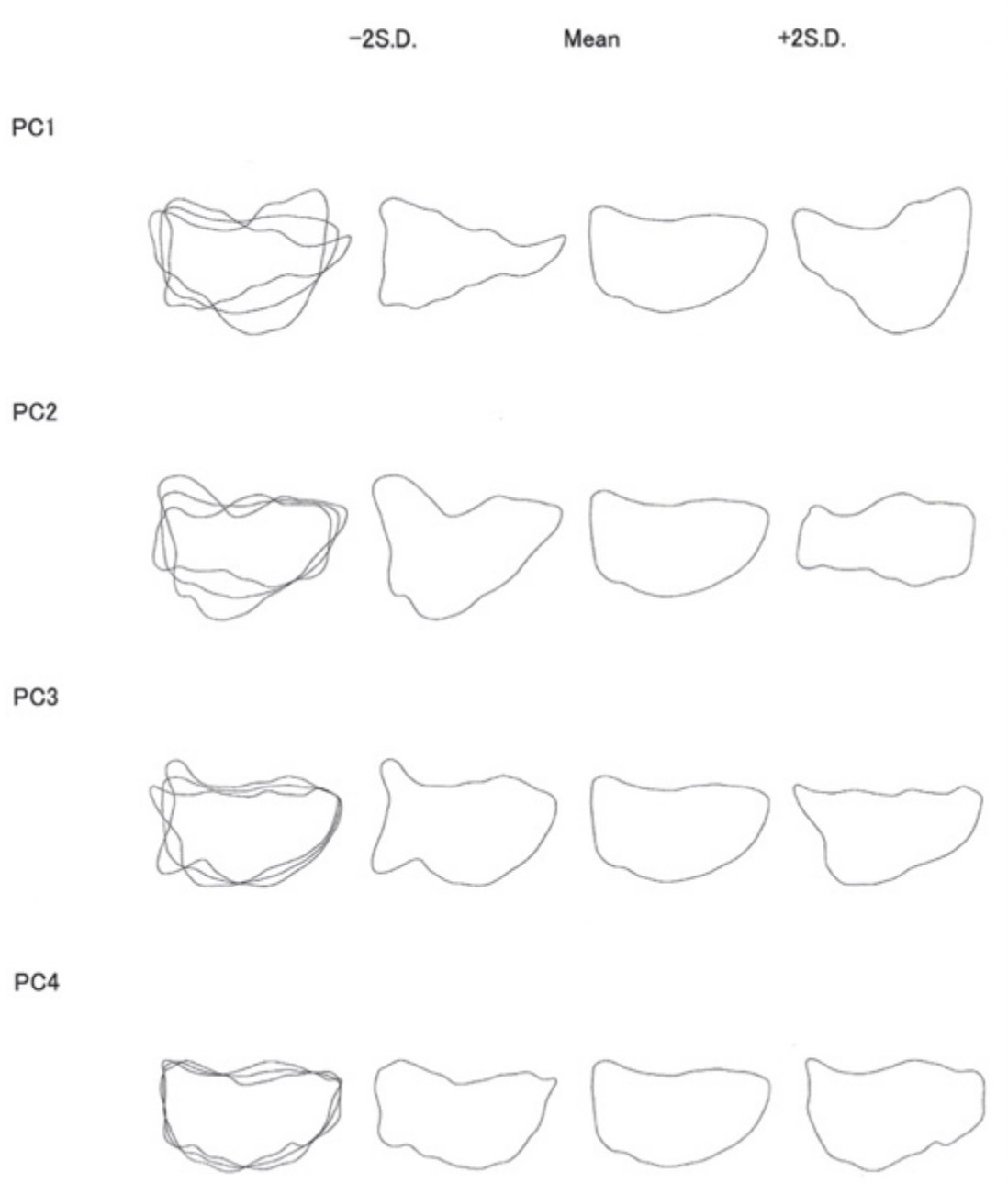

Figure 13: Reconstructed morphologies of left sided maxillary sinus shape variations among the populations of Poulton Chapel and St. Owen's Church (PC 1: 42.94 %; PC 2: 27.86 %; PC 3: 15.15 %; PC 4: 6.48 %). The PC scores pertaining to mean, -2SD and +2SD illustrate the whole shape variation in the uniqueness testing study

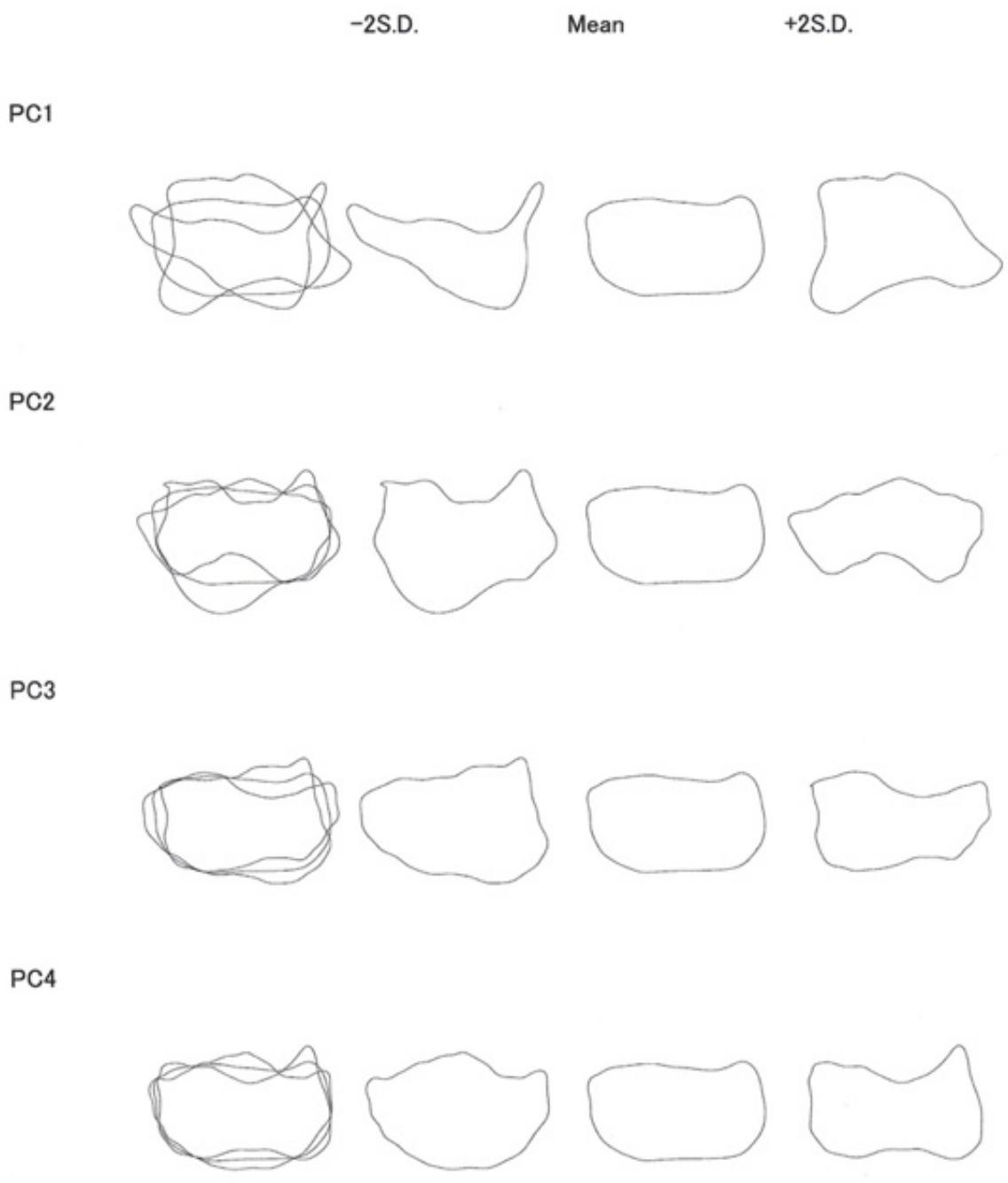

Figure 14: Reconstructed morphologies of right sided maxillary sinus shape variations among the populations of Poulton Chapel and St. Owen's Church (PC 1: 51.81 %; PC 2: 24.21 %; PC 3: 11.45 %; PC 4: 7.02 %). The PC scores pertaining to mean, -2SD and +2SD illustate the whole shape variation in the uniqueness testing study

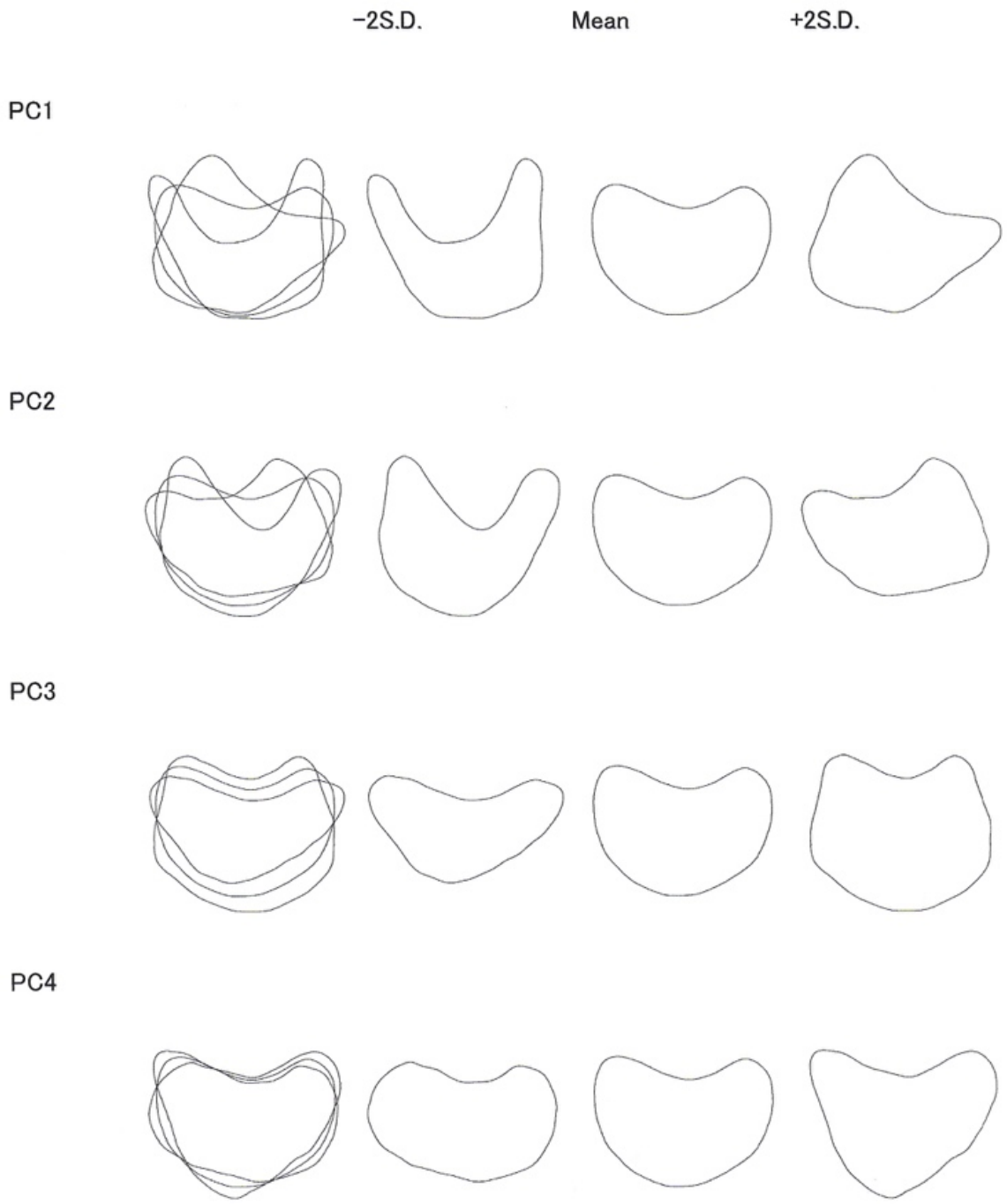

Figure 15: Reconstructed morphologies of left sided maxillary sinus shape variations among the population of Florence (PC 1: 36.83 %; PC 2: 21.89 %; PC 3: 15.23 %; PC 4: 7.61 %). The PC scores pertaining to mean, -2SD and +2SD illustate the whole shape variation in the uniqueness testing study

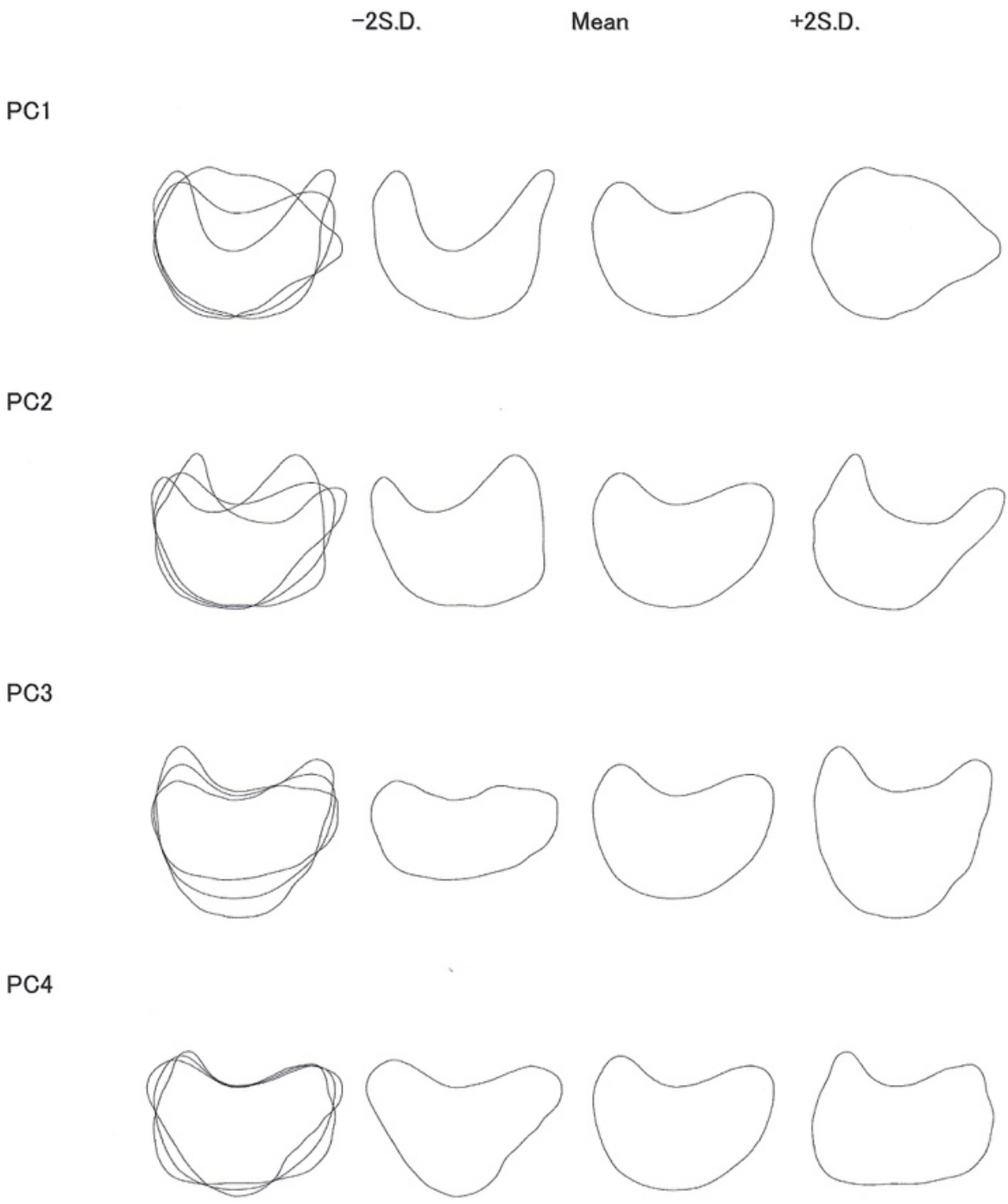

Figure 16: Reconstructed morphologies of right sided maxillary sinus shape variations among the population of Florence (PC 1: 37.90 %; PC 2: 23.54 %; PC 3: 14.91 %; PC 4: 5.59 %). The PC scores pertaining to mean, -2SD and +2SD illustate the whole shape variation in the uniqueness testing study

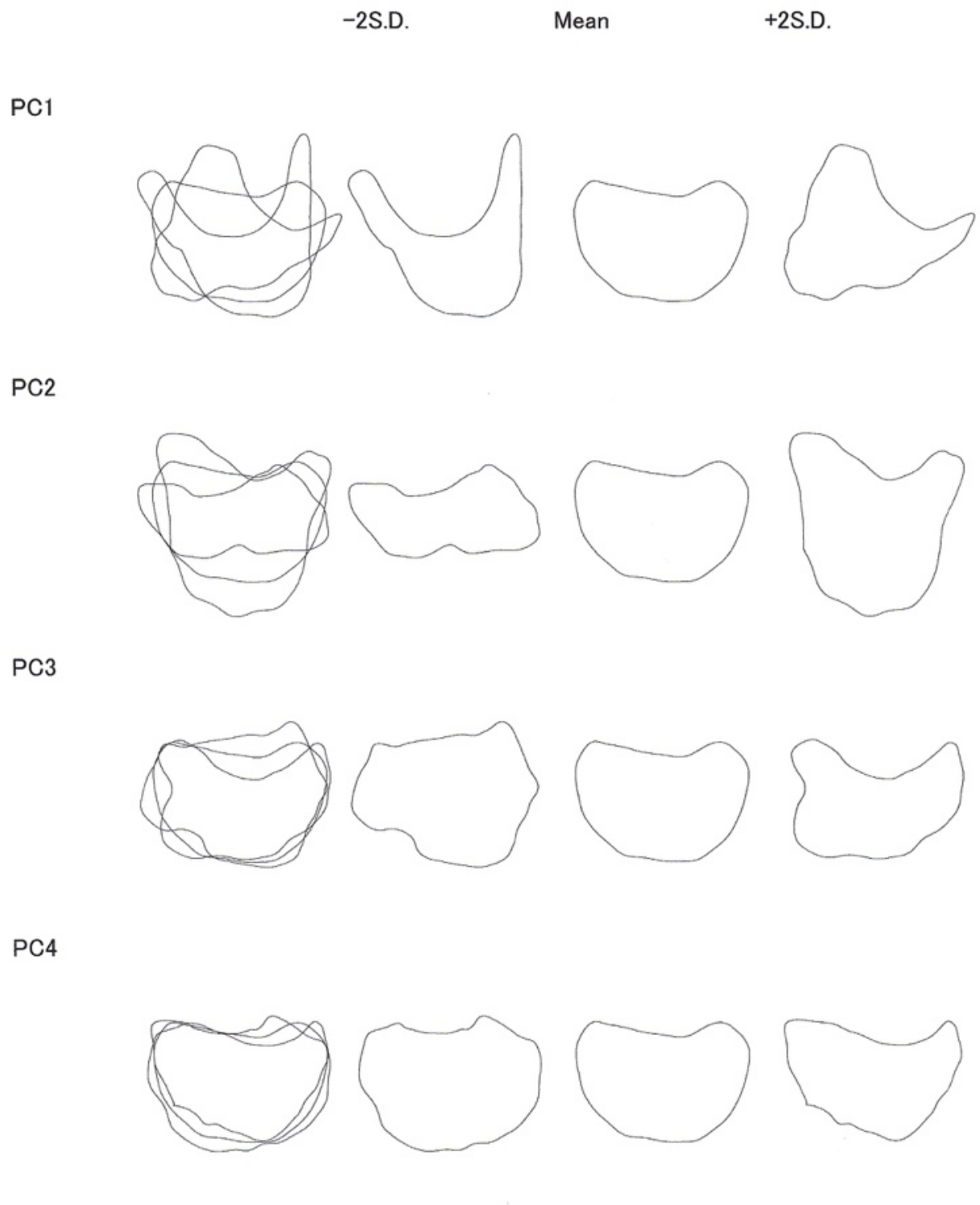

Figure 17: Reconstructed morphologies of left sided maxillary sinus shape variations among the population of Siracusa (PC 1: 42.41 %; PC 2: 25.08 %; PC 3: 12.44 %; PC 4: 7.01 %).The PC scores pertaining to mean, -2SD and +2SD illustate the whole shape variation in the uniqueness testing study

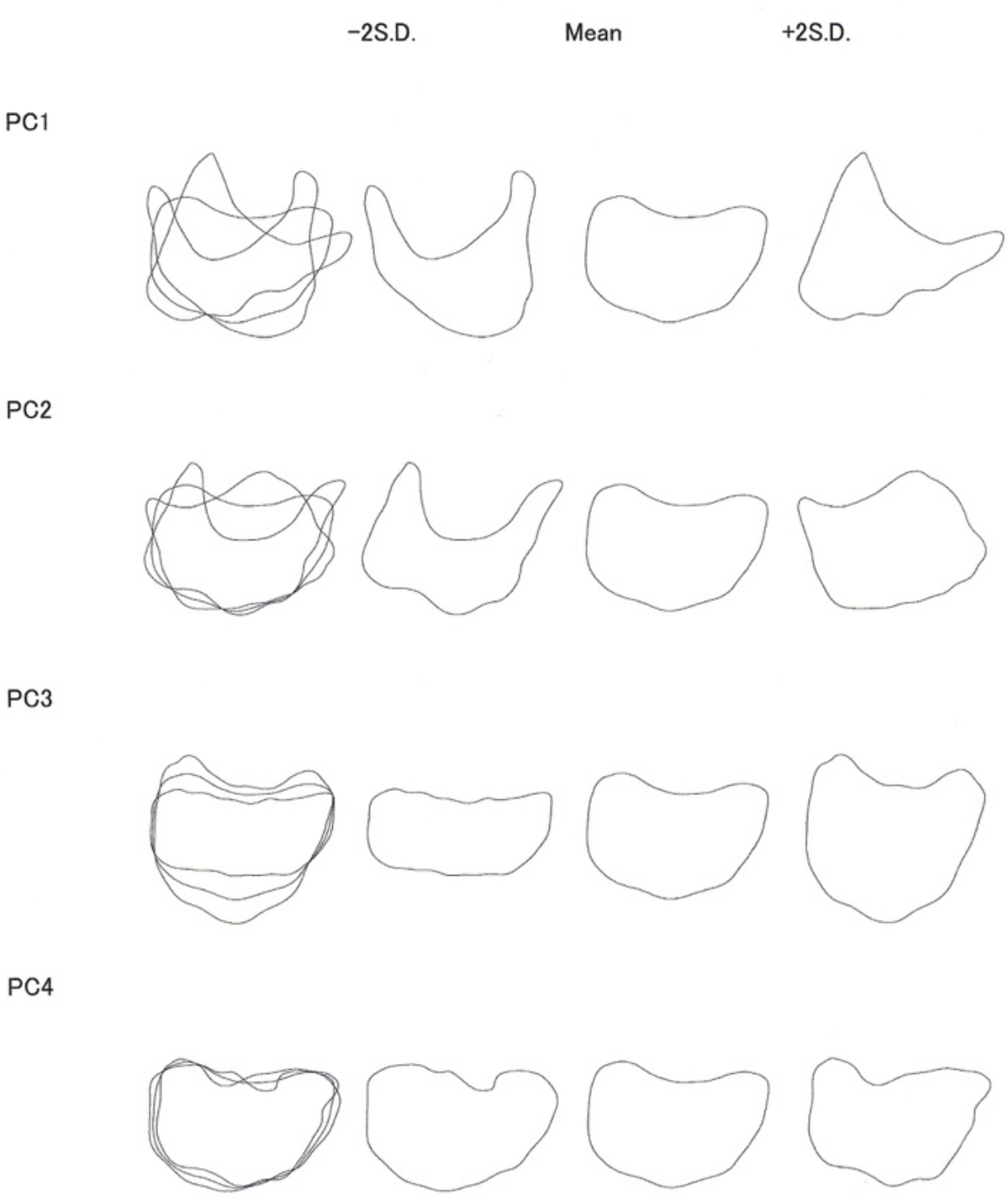

Figure 18: Reconstructed morphologies of right sided maxillary sinus shape variations among the population of Siracusa (PC 1: 51.18 %; PC 2: 22.31 %; PC 3: 12.24 %; PC 4: 4.97 %). The PC scores pertaining to mean, -2SD and +2SD illustate the whole shape variation in the uniqueness testing study

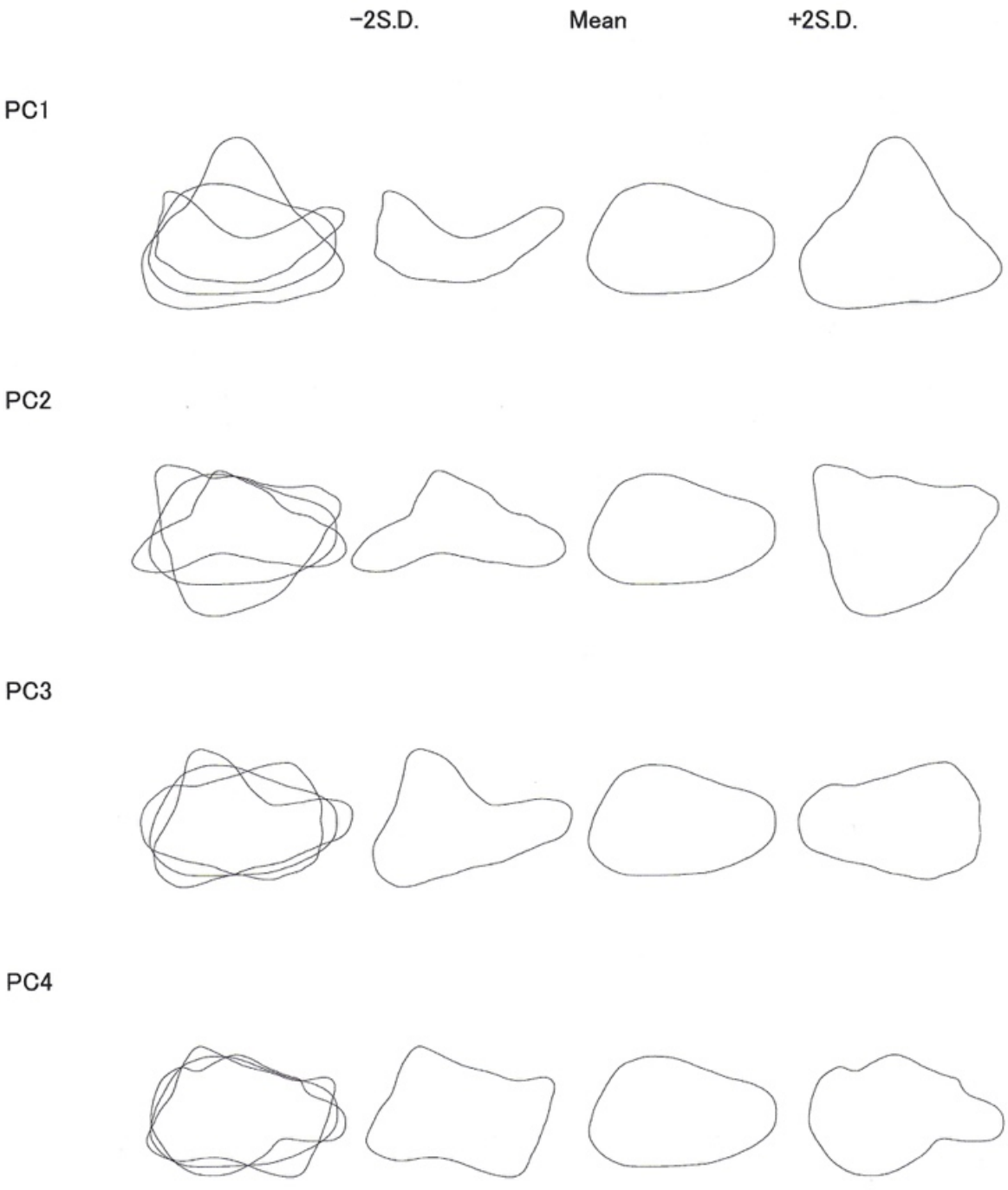

Figure 19: Reconstructed morphologies of left sided maxillary sinus shape variations among the population of Chelsea Old Church (PC 1: 41.97 %; PC 2: 25.19 %; PC 3: 14.21 %; PC 4: 5.62 %). The PC scores pertaining to mean, -2SD and +2SD illustate the whole shape variation in the uniqueness testing study

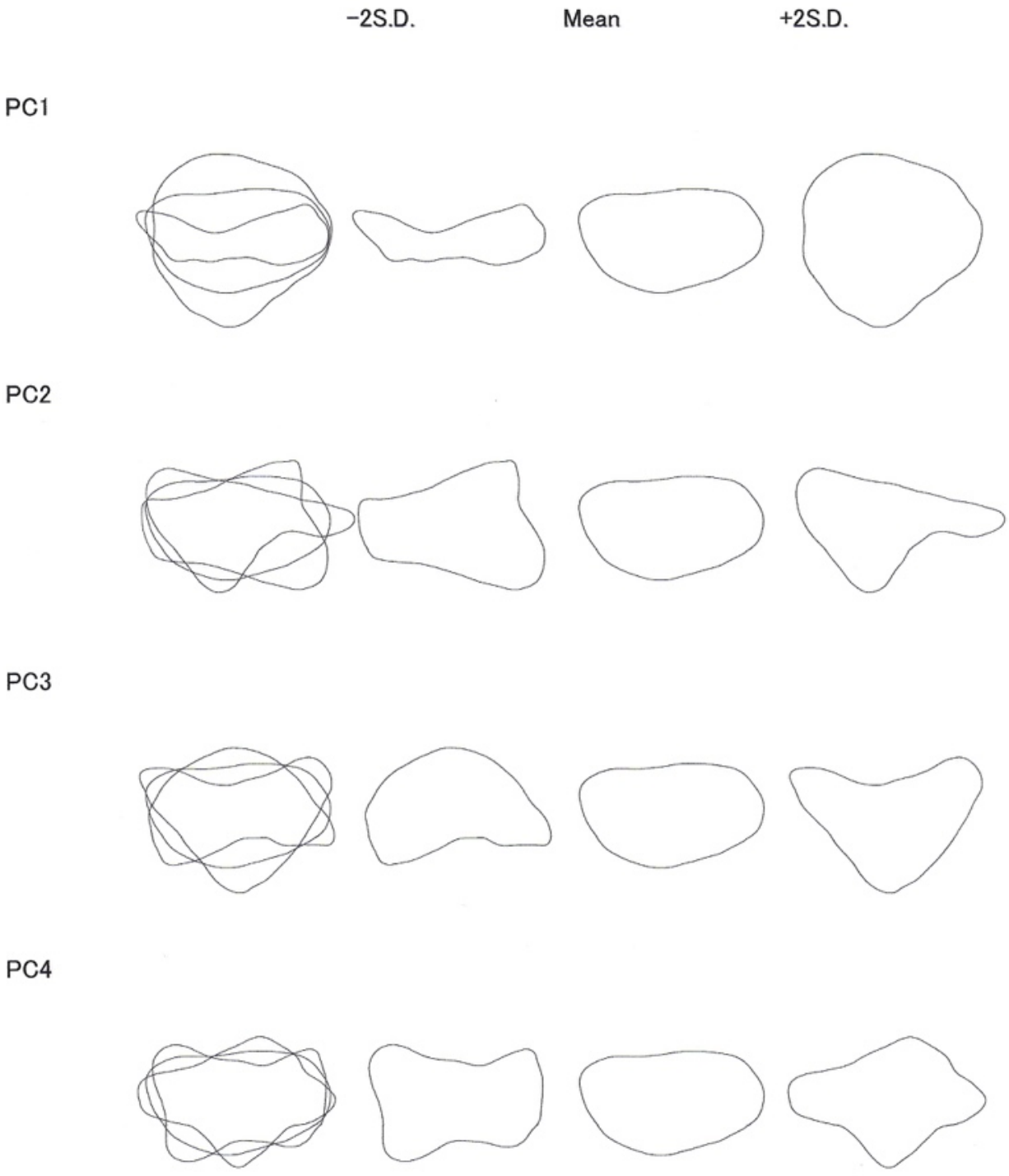

Figure 20: Reconstructed morphologies of right sided maxillary sinus shape variations among the population of Chelsea Old Church (PC 1: 40.87 %; PC 2: 21.43 %; PC 3: 17.99 %; PC 4: 7.52 %). The PC scores pertaining to mean, -2SD and +2SD illustate the whole shape variation in the uniqueness testing study

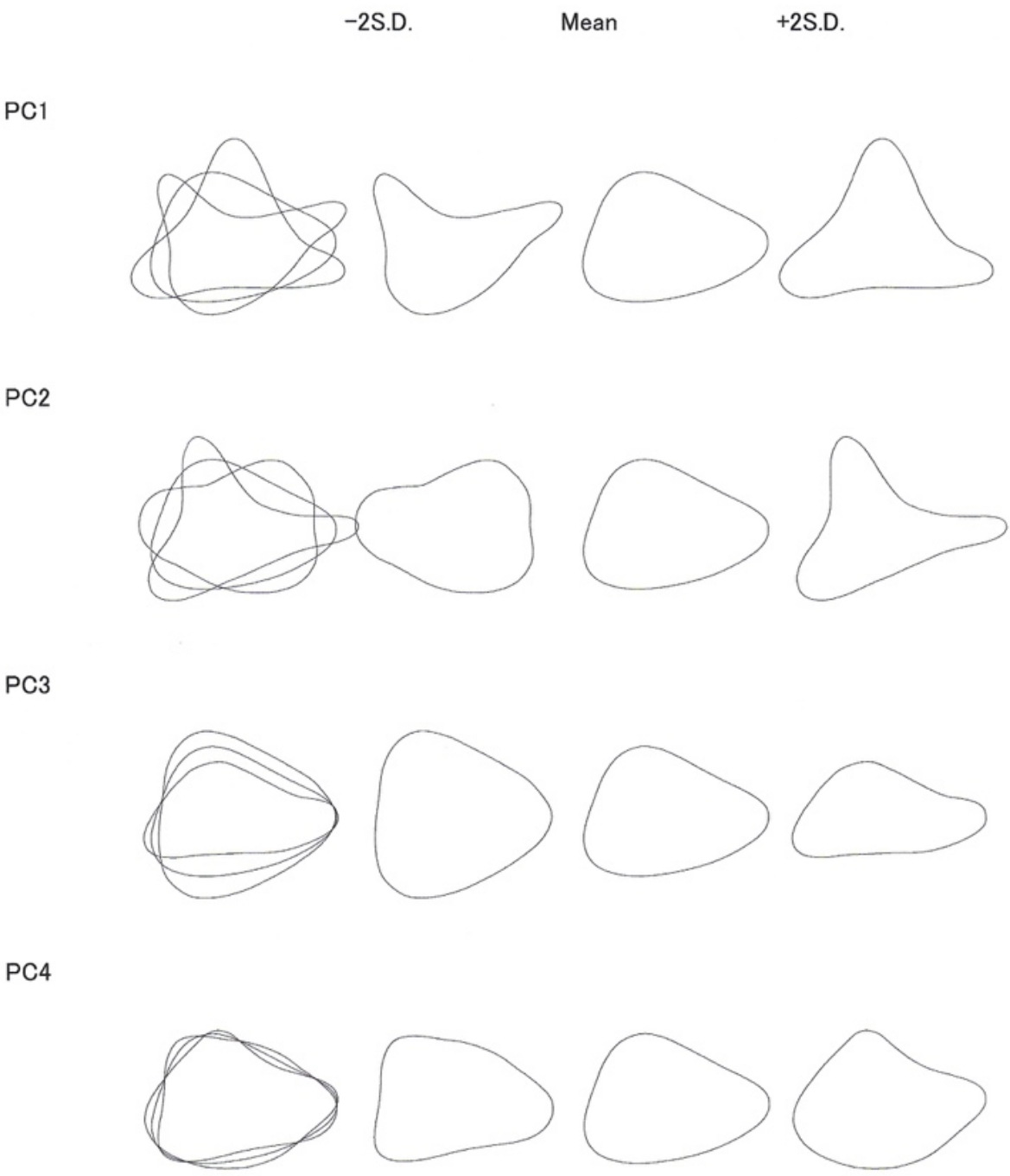

Figure 21: Reconstructed morphologies of left sided maxillary sinus shape variations among the population of St. Mary Spital (PC 1: 41.49 %; PC 2: 27.5 %; PC 3: 16.58 %; PC 4: 3.11 %). The PC scores pertaining to mean, -2SD and +2SD illustate the whole shape variation in the uniqueness testing study

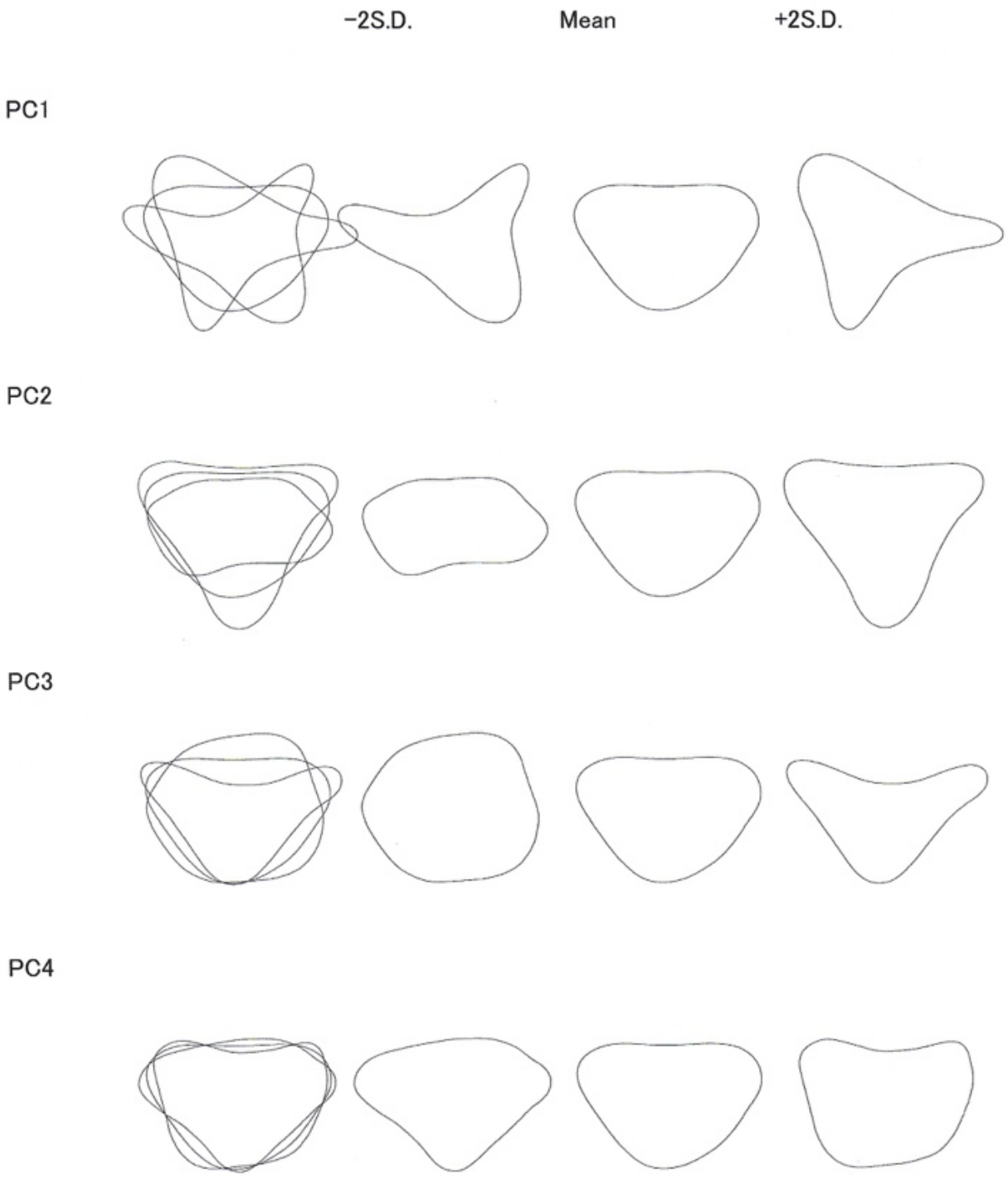

Figure 22: Reconstructed morphologies of right sided maxillary sinus shape variations among the population of St. Mary Spital (PC 1: 47.51 %; PC 2: 20.92 %; PC 3: 17.43 %; PC 4: 3.74 %). The PC scores pertaining to mean, -2SD and +2SD illustate the whole shape variation in the uniqueness testing study

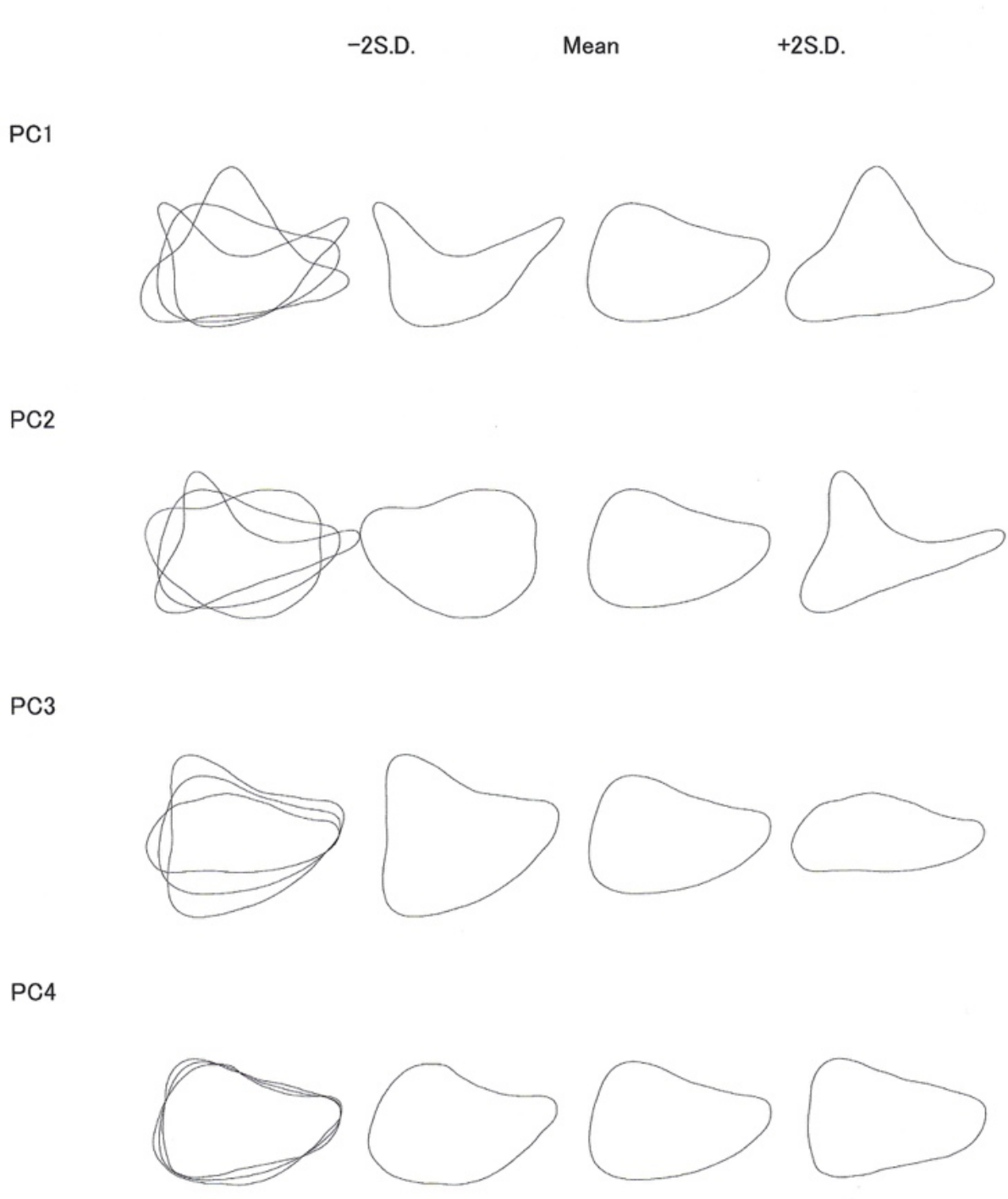

Figure 23: Reconstructed morphologies of left sided maxillary sinus shape variations among the population of St. Bride's Lower Churchyard (PC 1: 42.05 %; PC 2: 25.26 %; PC 3: 19.01 %; PC 4: 2.88 %). The PC scores pertaining to mean, -2SD and +2SD illustate the whole shape variation in the uniqueness testing study

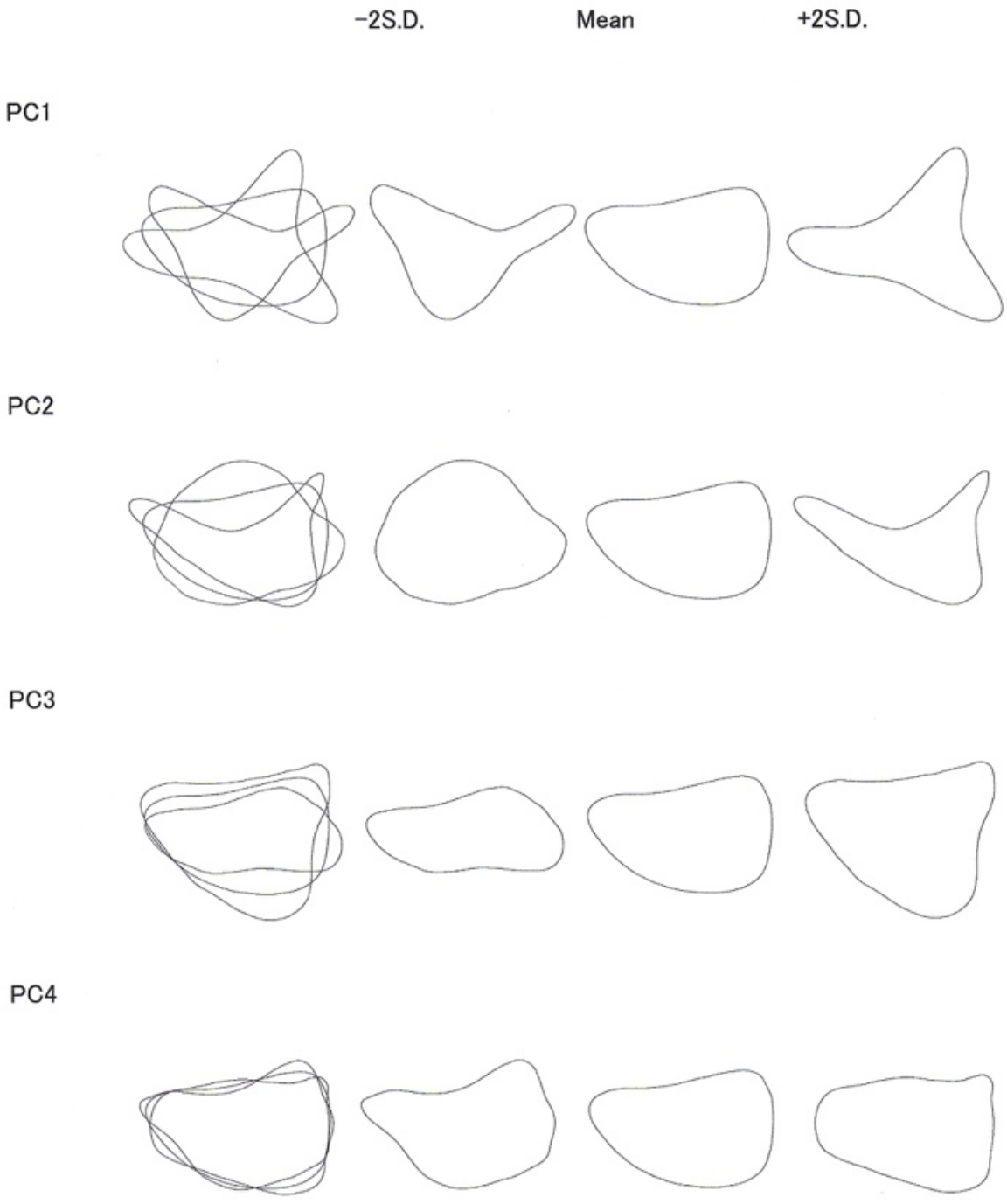

Figure 24: Reconstructed morphologies of right sided maxillary sinus shape variations among the population of St. Bride's Lower Churchyard (PC 1: 44.1 %; PC 2: 24.1 %; PC 3: 15.7 %; PC 4: 3.67 %). The PC scores pertaining to mean, -2SD and +2SD illustate the whole shape variation in the uniqueness testing study

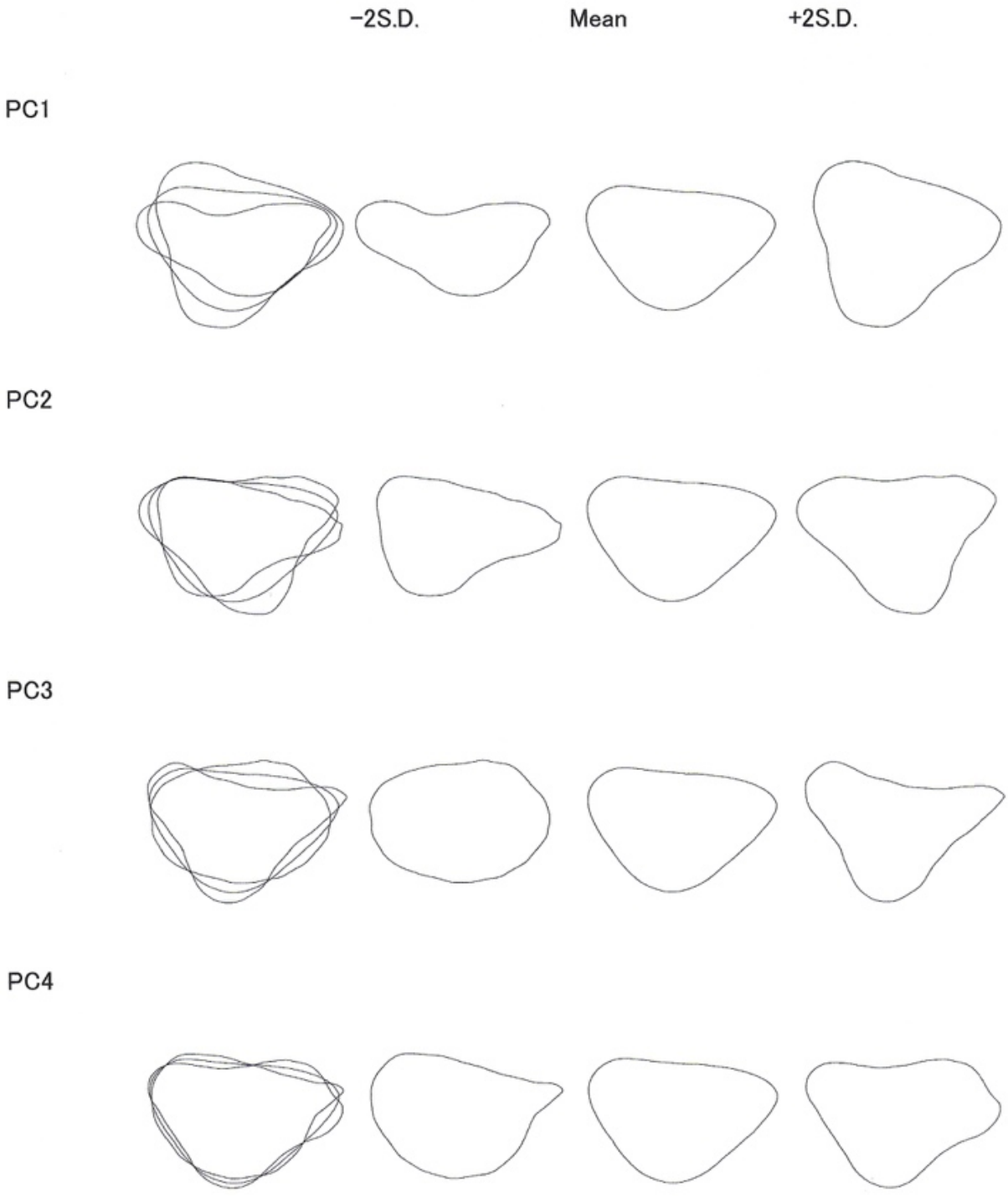

Figure 25: Reconstructed morphologies of left sided maxillary sinus shape variations among the population of Osteological Collection, University of Tübingen (PC 1: 42.22 %; PC 2: 21.3 %; PC 3: 16.33 %; PC 4: 5.96 %). The PC scores pertaining to mean, -2SD and +2SD illustate the whole shape variation in the uniqueness testing study

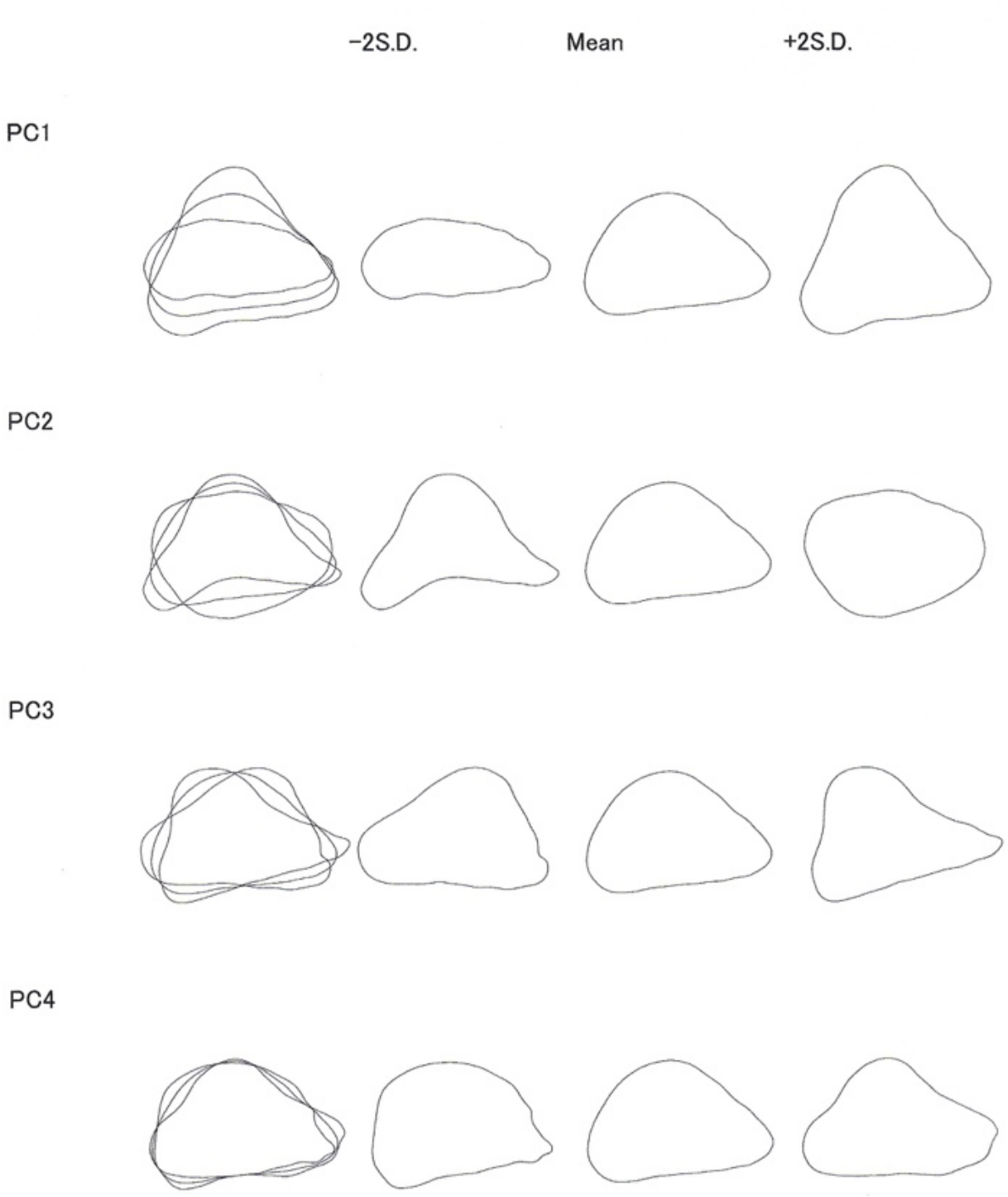

Figure 26: Reconstructed morphologies of right sided maxillary sinus shape variations among the population of Osteological Collection, University of Tübingen (PC 1: 39.2 %; PC 2: 22.6 %; PC 3: 17.02 %; PC 4: 5.67 %). The PC scores pertaining to mean, -2SD and +2SD illustate the whole shape variation in the uniqueness testing study

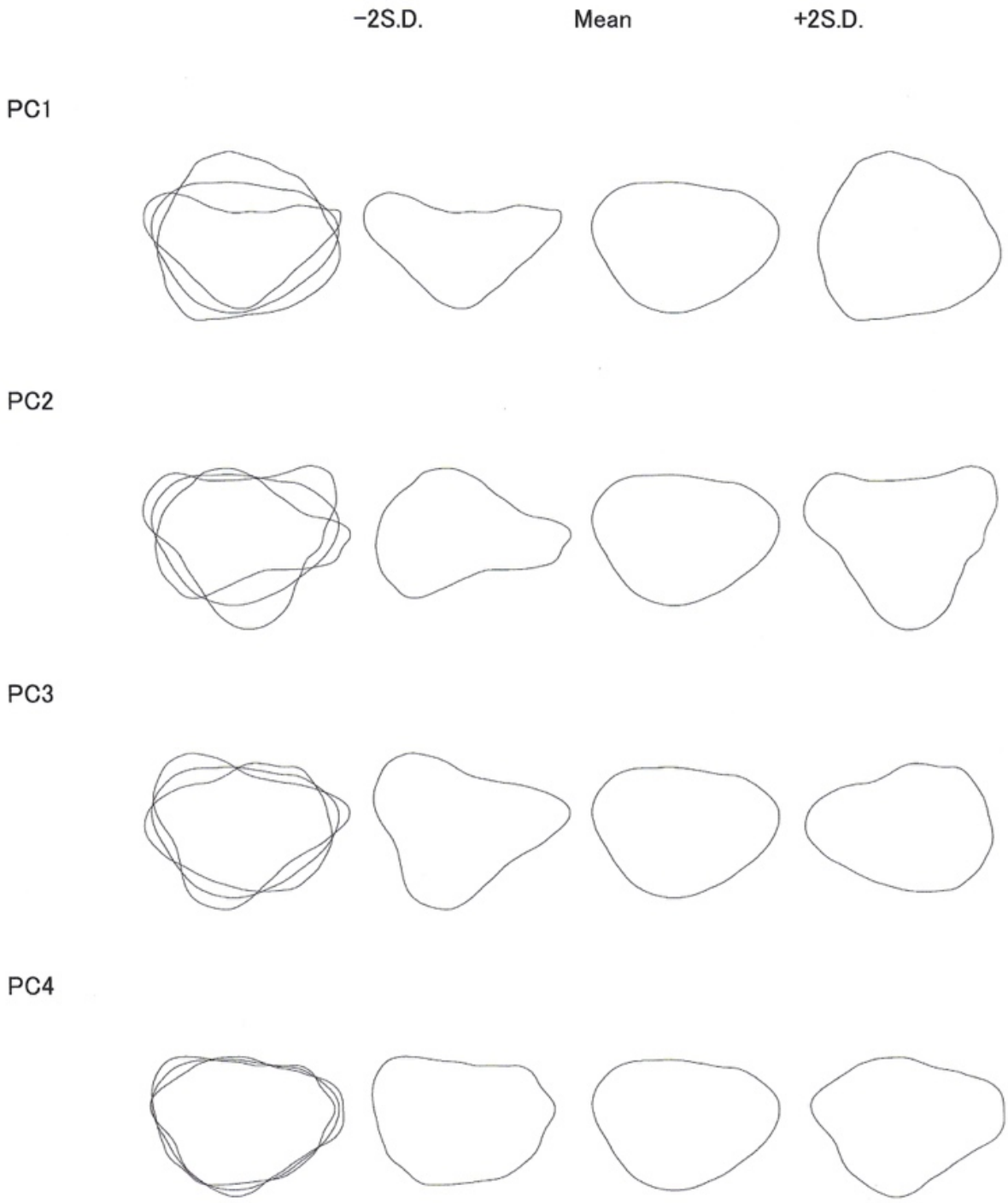

Figure 27: Reconstructed morphologies of left sided maxillary sinus shape variations among the population of the Anatomical Collection, University of Leipzig (PC 1: 35.69 %; PC 2: 30.07 %; PC 3: 14.53 %; PC 4: 3.76 %). The PC scores pertaining to mean, -2SD and +2SD illustate the whole shape variation in the uniqueness testing study

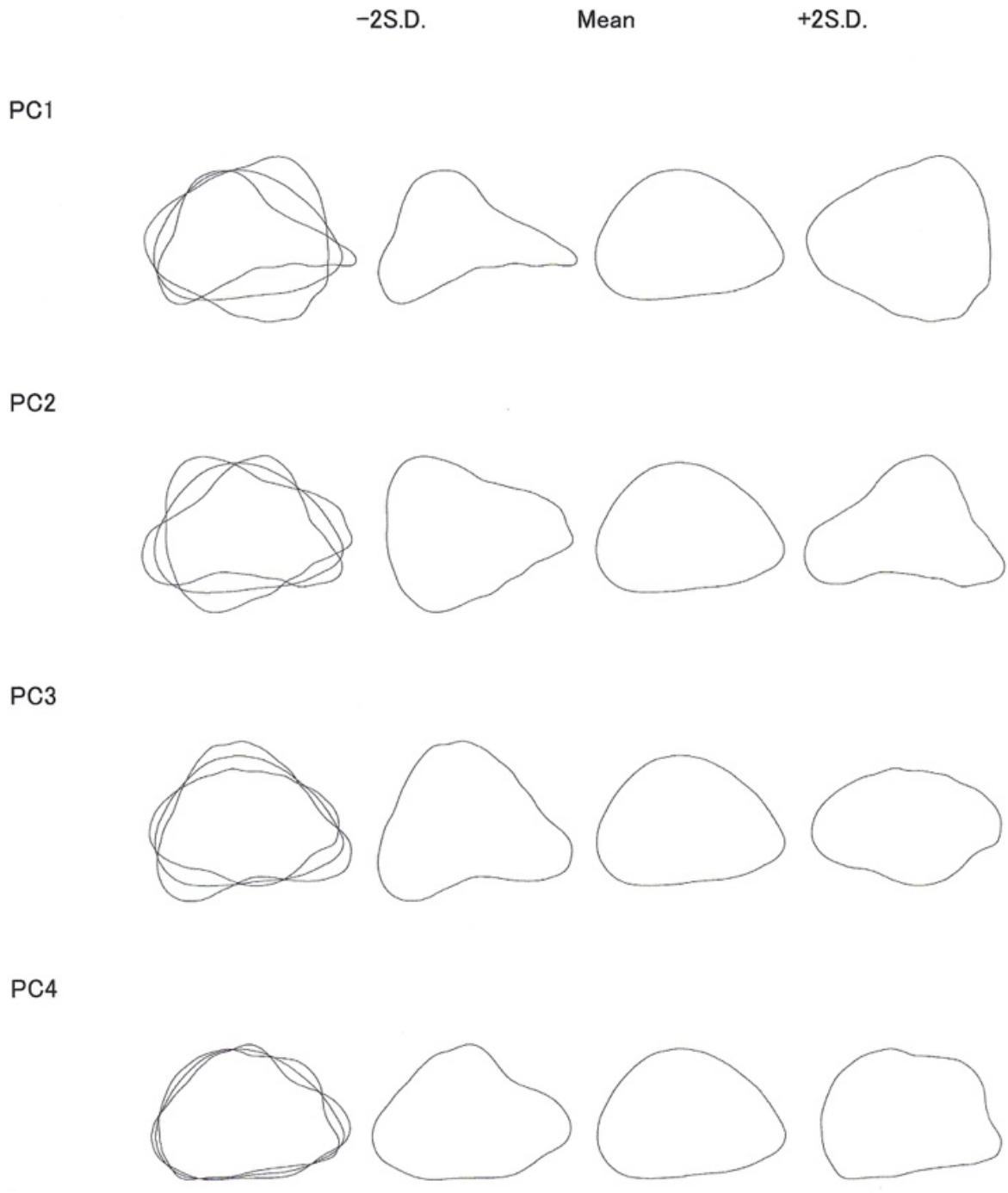

Figure 28: Reconstructed morphologies of right sided maxillary sinus shape variations among the population of the Anatomical Collection, University of Leipzig (PC 1: 39.78 %; PC 2: 23.6 %; PC 3: 16.67 %; PC 4: 4.17 %). The PC scores pertaining to mean, -2SD and +2SD illustate the whole shape variation in the uniqueness testing study

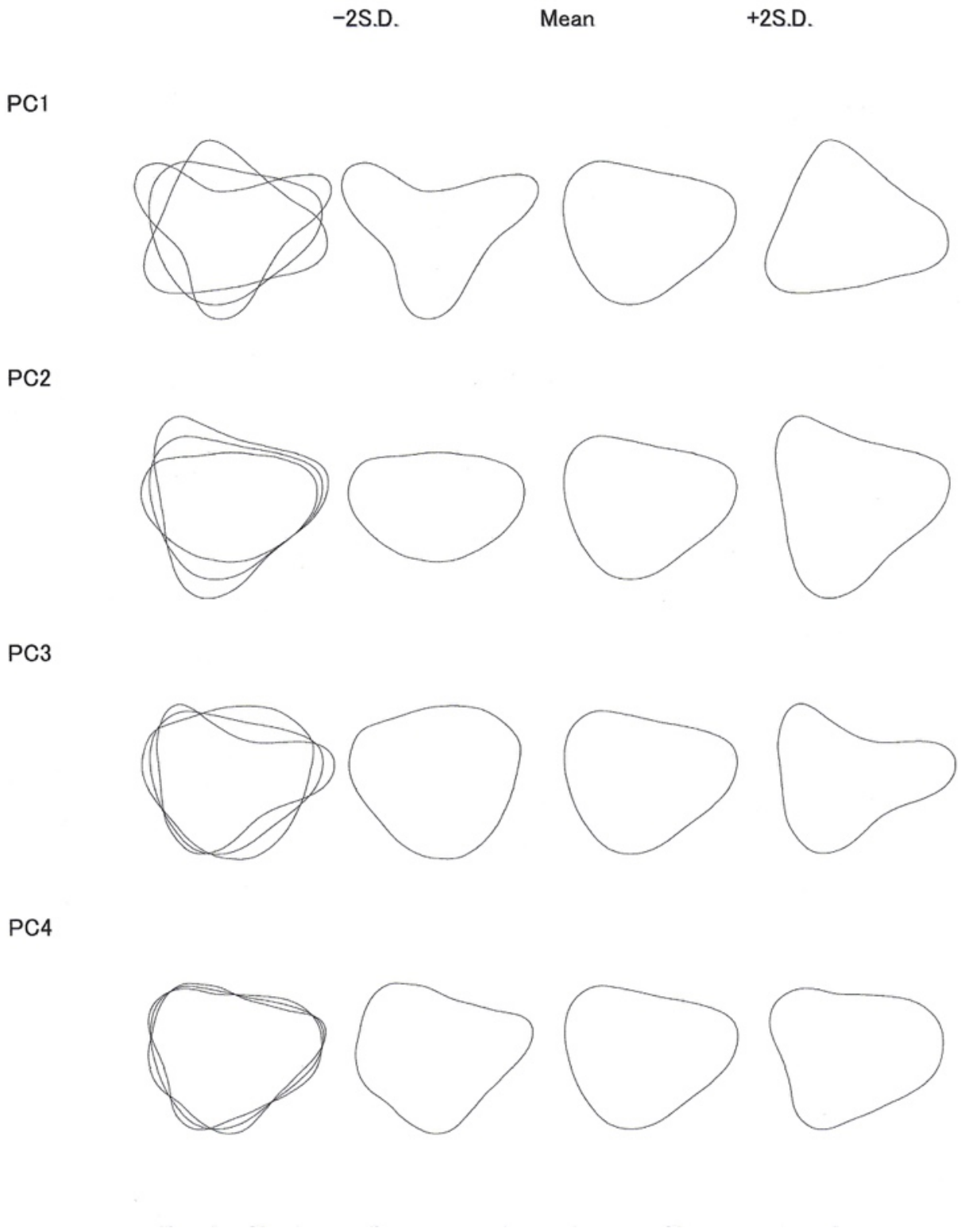

Figure 29: Reconstructed morphologies of left sided maxillary sinus shape variations among the population of Bolton-Brush Growth (PC 1: 46.92 %; PC 2: 23.6 %; PC 3: 18.91 %; PC 4: 3.33 %). The PC scores pertaining to mean, -2SD and +2SD illustate the whole shape variation in the uniqueness testing study

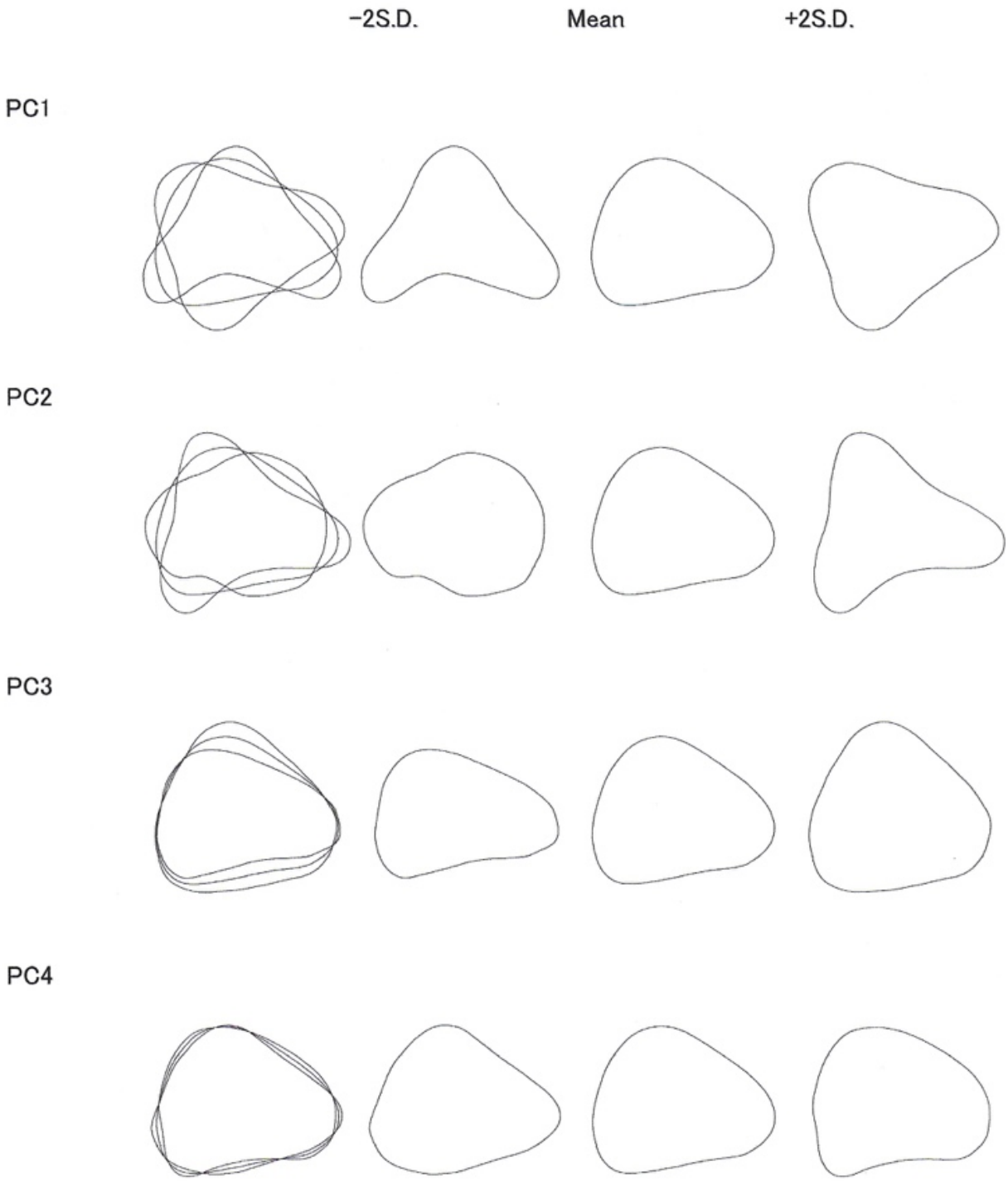

Figure 30: Reconstructed morphologies of right sided maxillary sinus shape variations among the population of Bolton-Brush Growth (PC 1: 46.9 %; PC 2: 28.66 %; PC 3: 15.32 %; PC 4: 2.67 %). The PC scores pertaining to mean, -2SD and +2SD illustate the whole shape variation in the uniqueness testing study

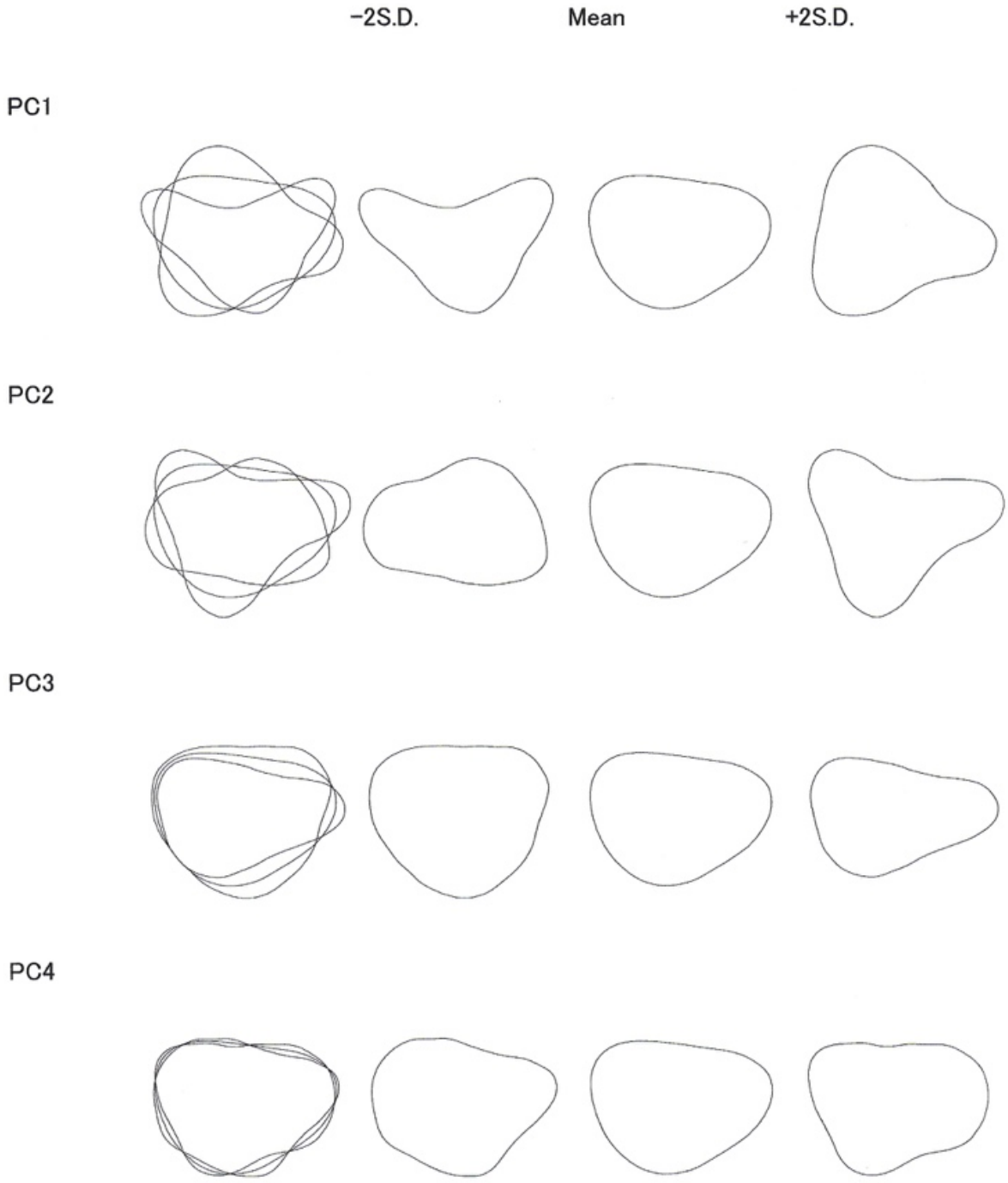

Figure 31: Reconstructed morphologies of left sided maxillary sinus shape variations among the population of Oregon Growth (PC 1: 45.97 %; PC 2: 29.27 %; PC 3: 15.4 %; PC 4: 2.89 %). The PC scores pertaining to mean, -2SD and +2SD illustate the whole shape variation in the uniqueness testing study

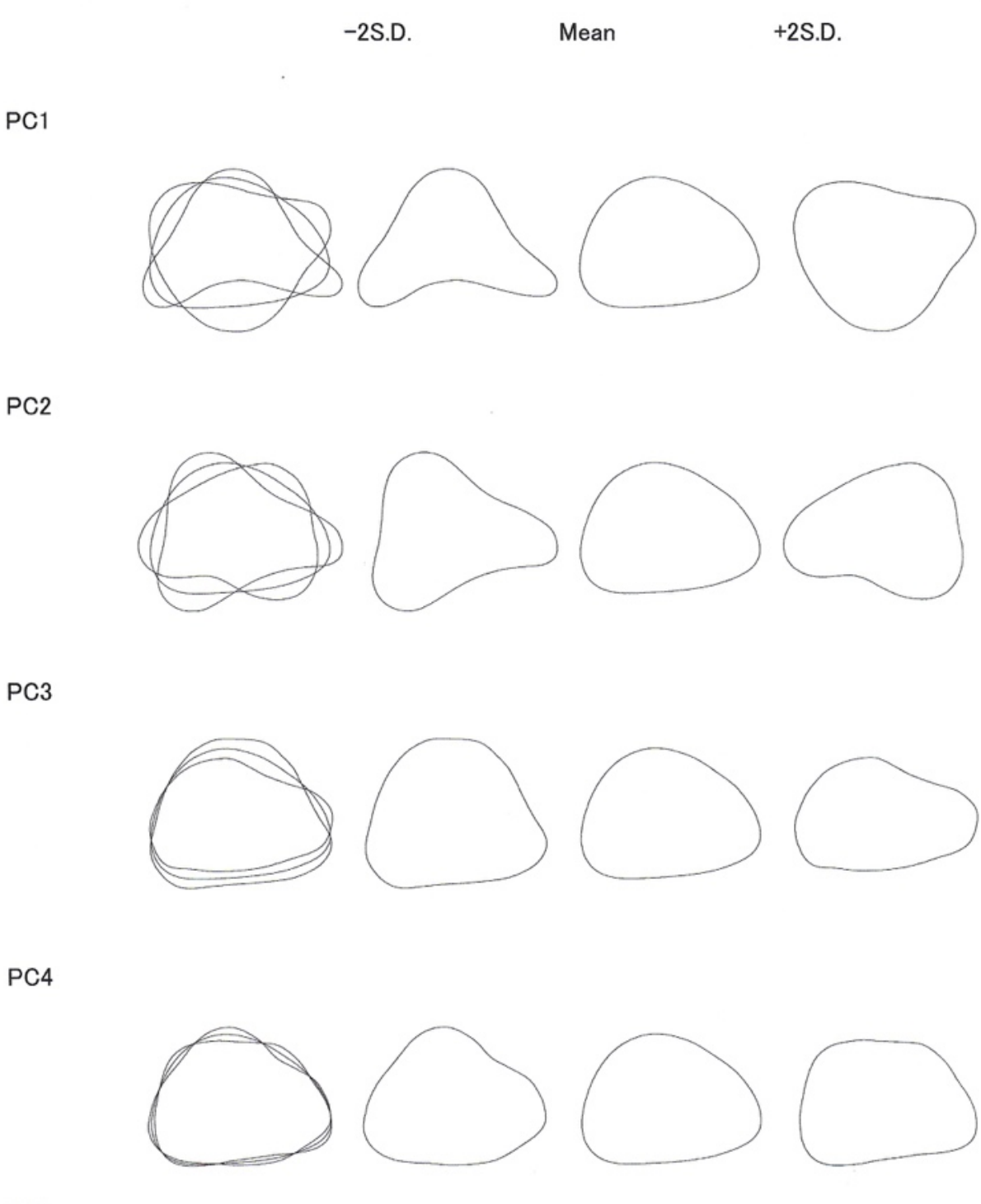

Figure 32: Reconstructed morphologies of right sided maxillary sinus shape variations among the population of Oregon Growth (PC 1: 46.22 %; PC 2: 30.1 %; PC 3: 14.6 %; PC 4: 2.63 %). The PC scores pertaining to mean, -2SD and +2SD illustate the whole shape variation in the uniqueness testing study

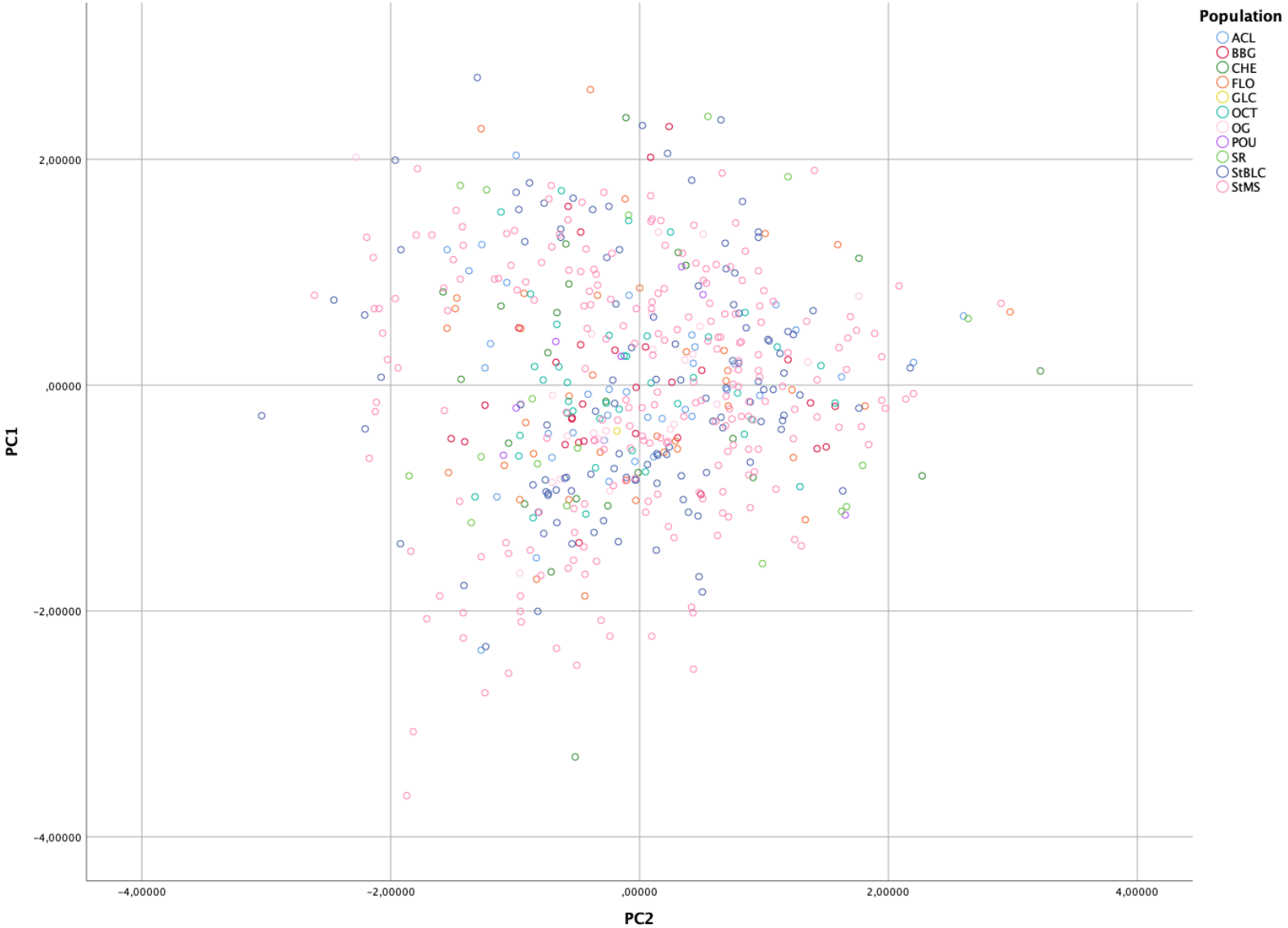

Figure 33: Two-dimensional scatterplot showing PC1 and PC2 of left sided maxillary sinus morphologies used for the uniqueness testing study by population

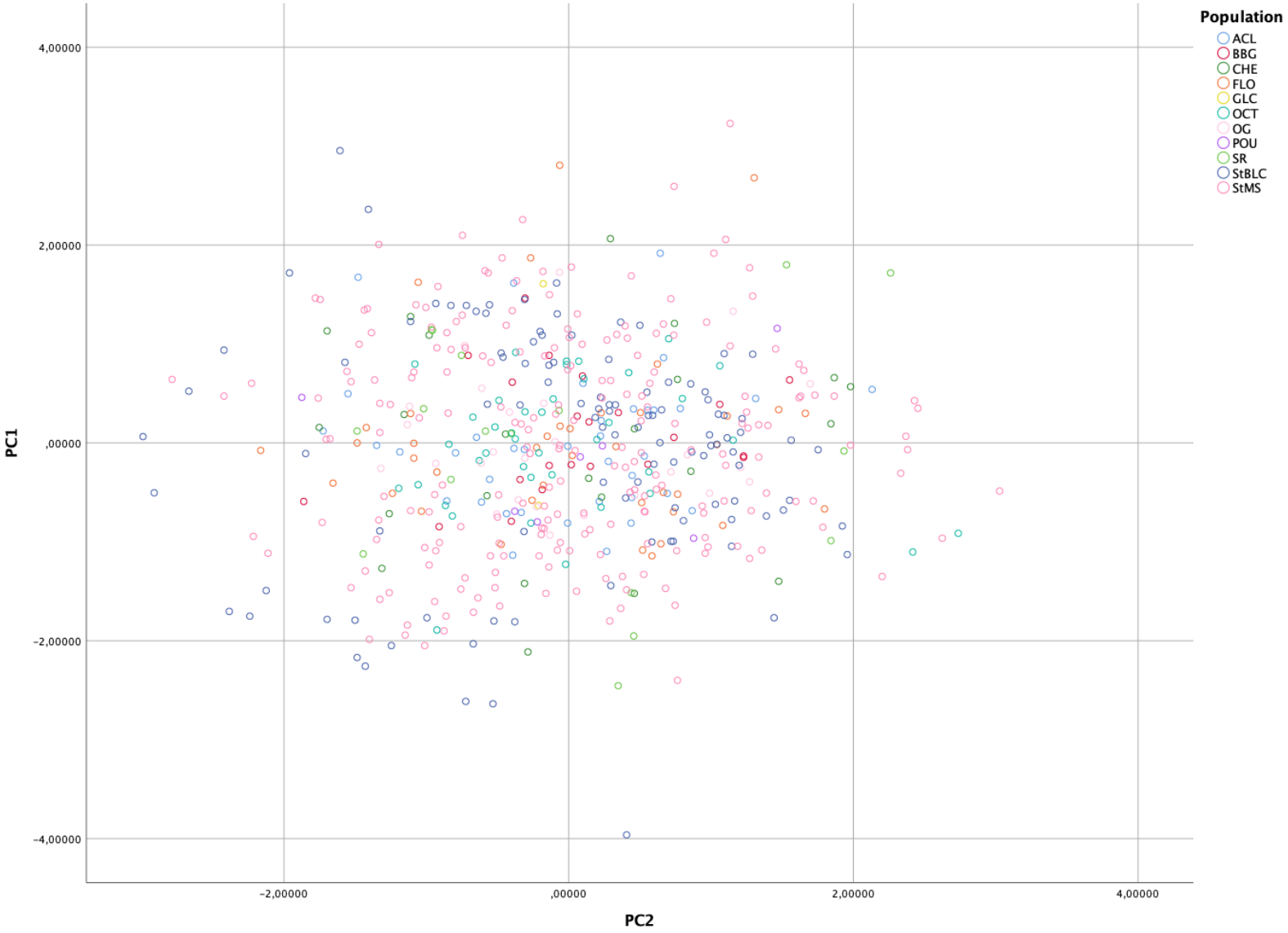

Figure 34: Two-dimensional scatterplot showing PC1 and PC2 for right sided maxillary sinus morphologies used for the uniqueness testing study by population

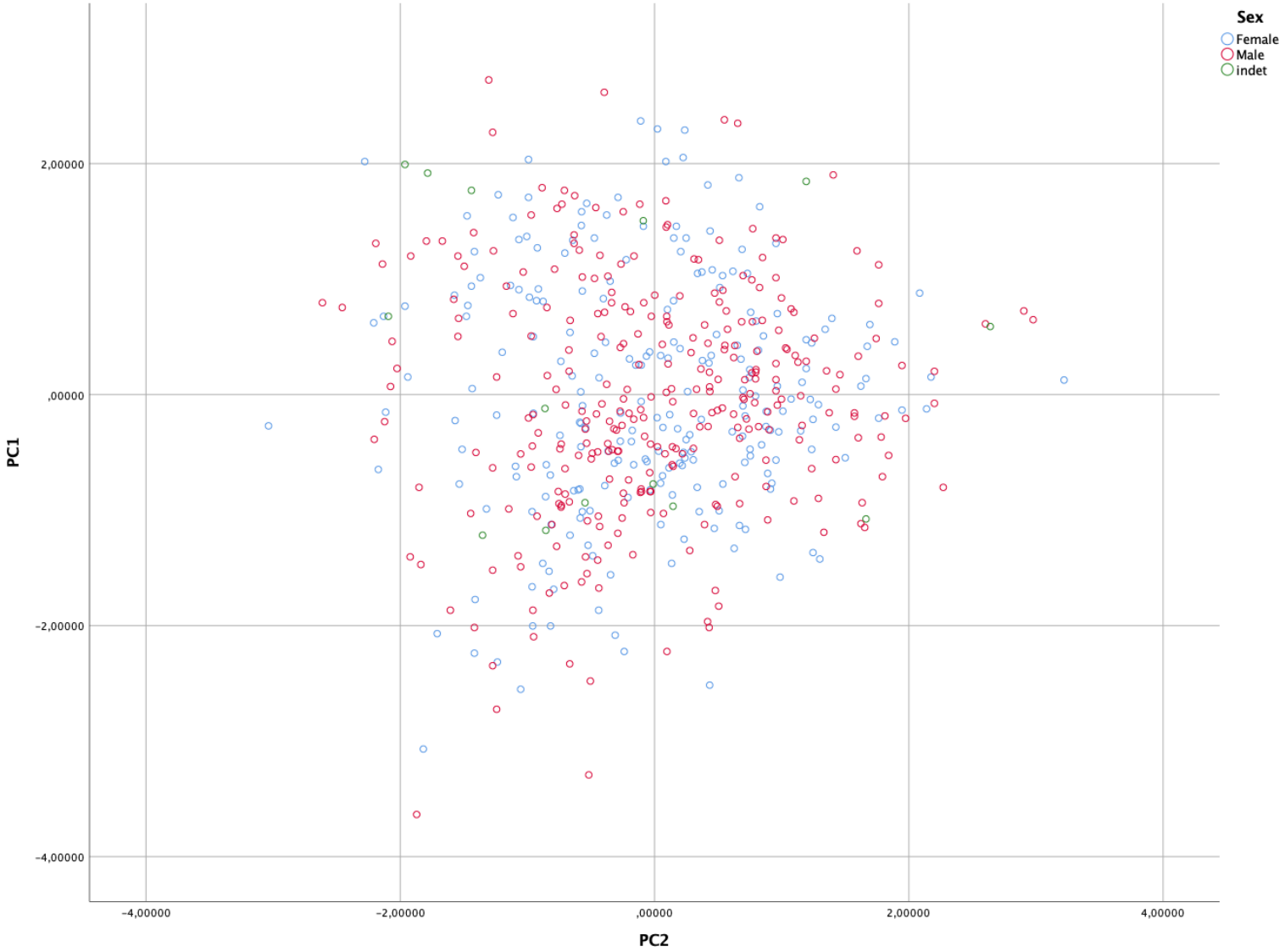

Figure 35: Two-dimensional scatterplot showing PC1 and PC2 for left sided maxillary sinus morphologies used for the uniqueness testing study by sex

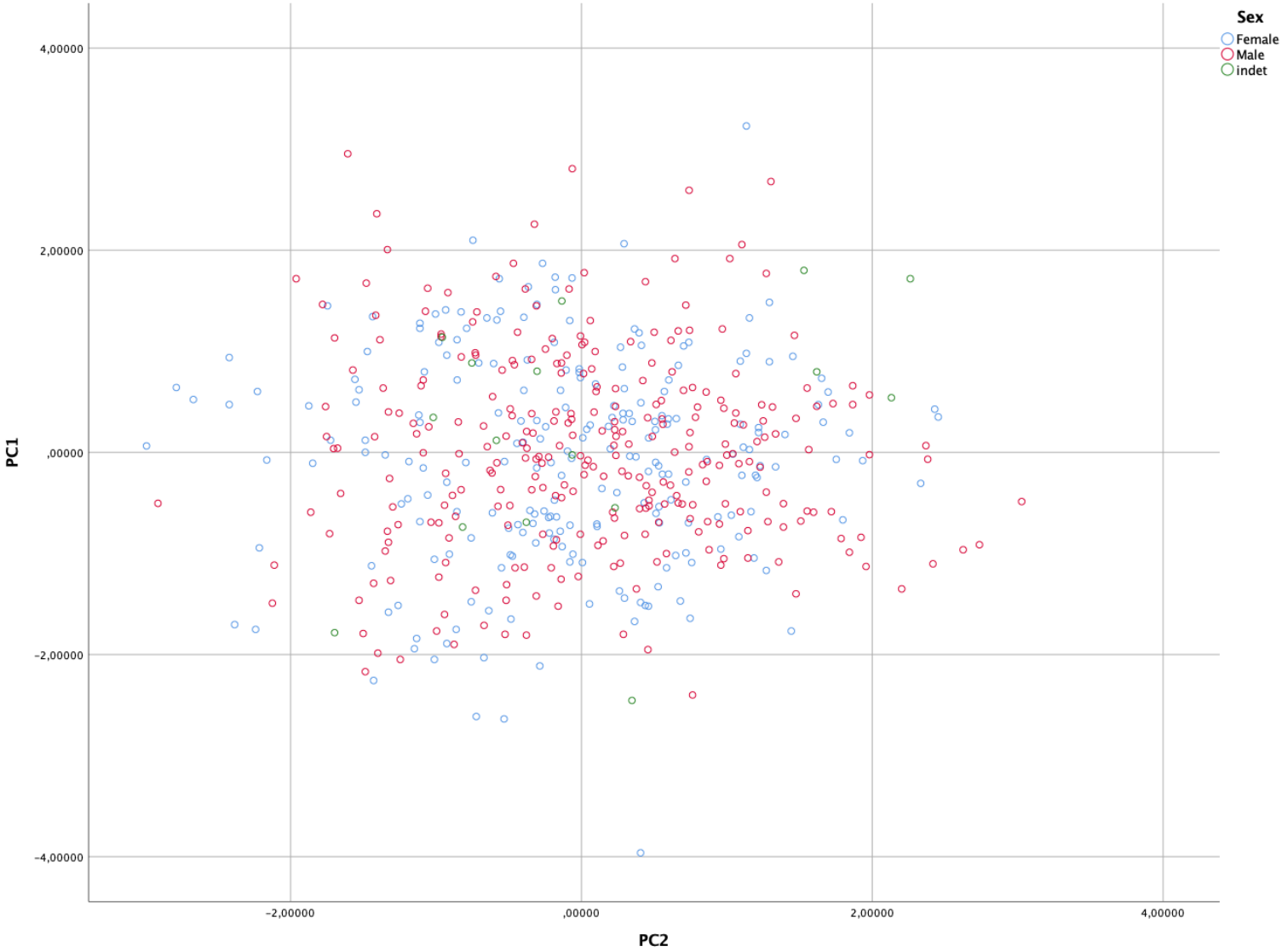

Figure 36: Two-dimensional scatterplot showing PC1 and PC2 for right sided maxillary sinus morphologies used for the uniqueness testing study by sex

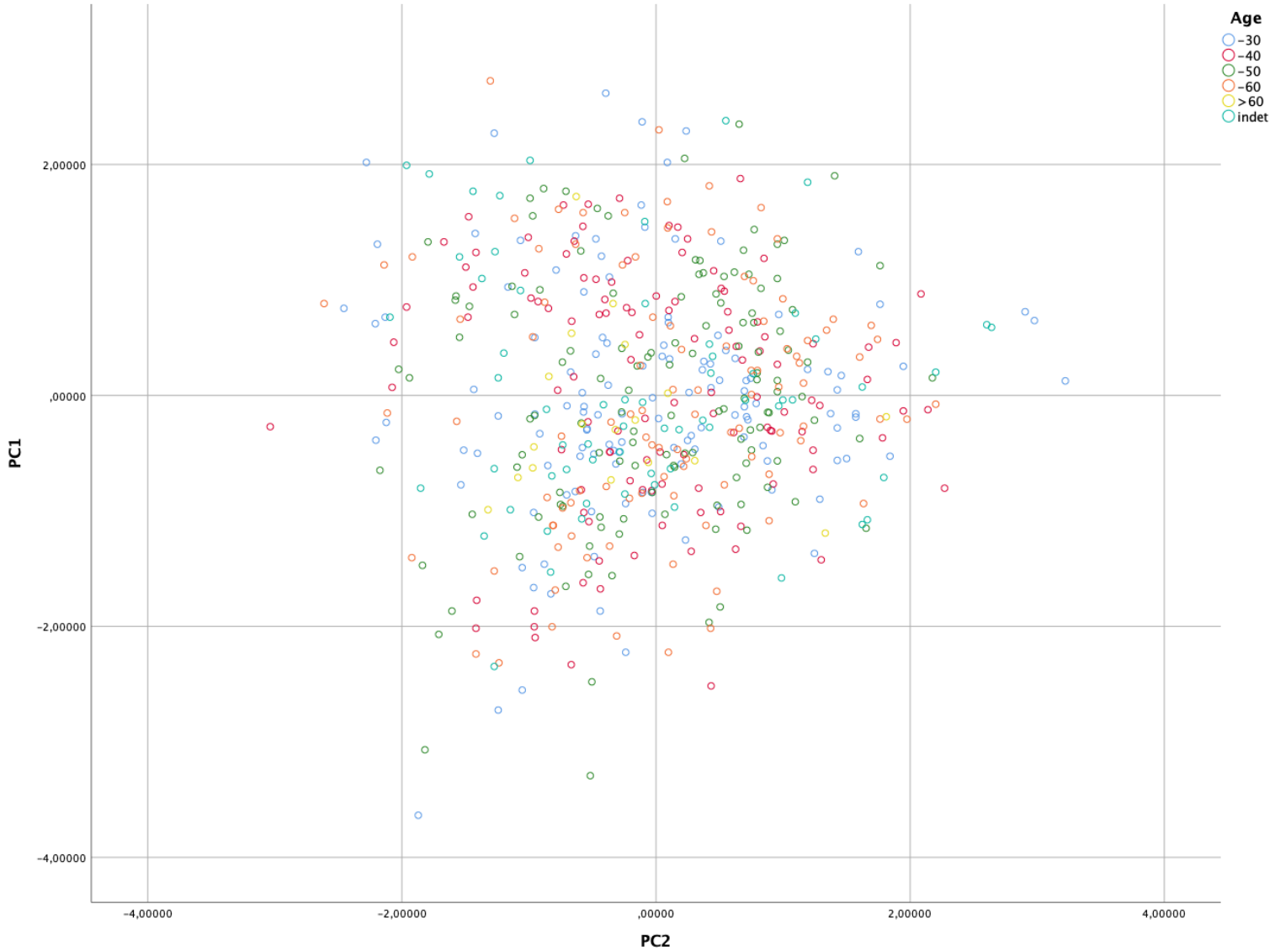

Figure 37: Two-dimensional scatterplot showing PC1 and PC2 for left sided maxillary sinus morphologies used for the uniqueness testing study by age

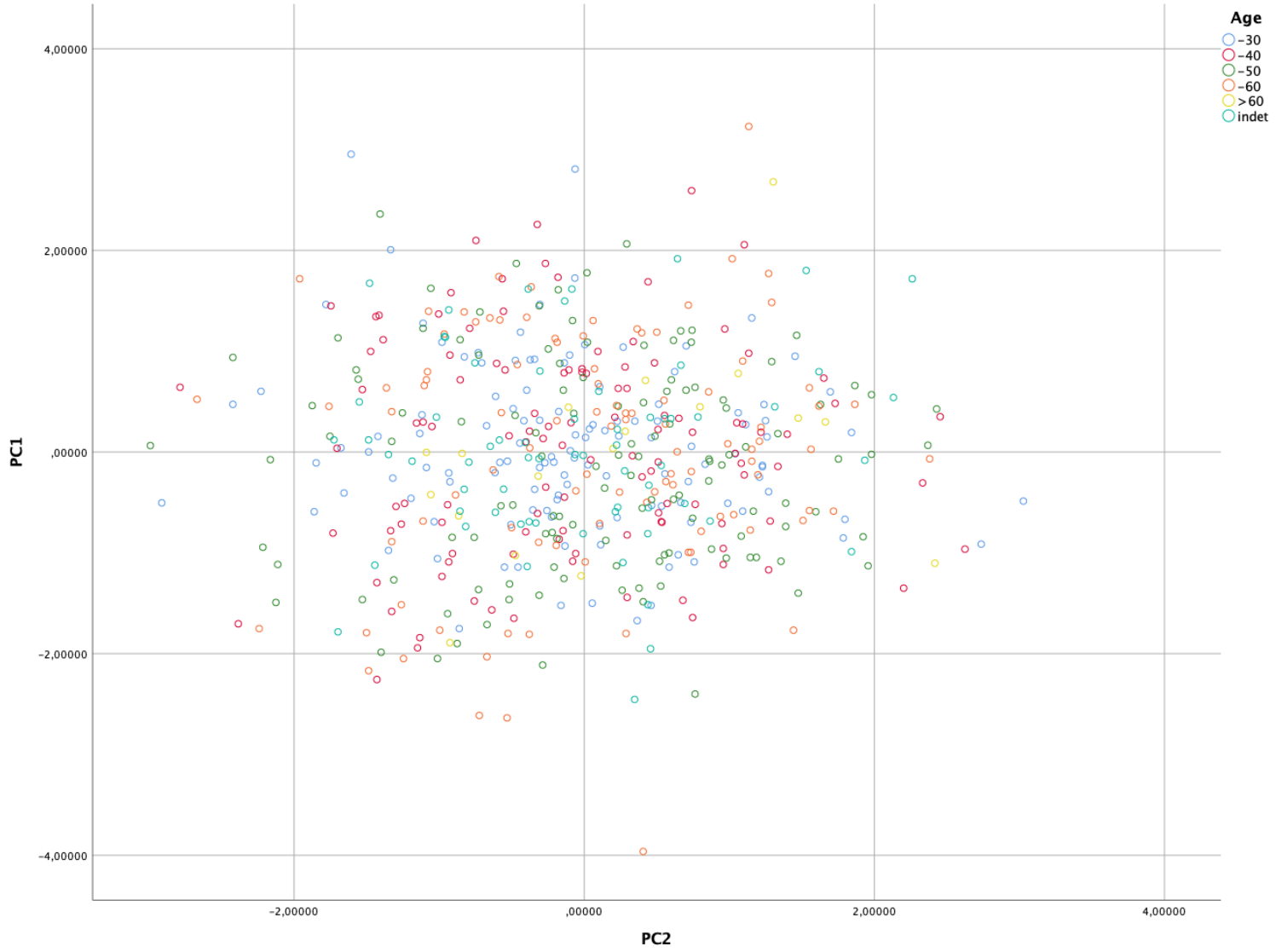

Figure 38: Two-dimensional scatterplot showing PC1 and PC2 for right sided maxillary sinus morphologies used for the uniqueness testing study by age

Table 12: ANOVA statistics showing significant differences of left sided maxillary sinus morphologies of all populations used for the uniqueness testing study on the first principal component

ANOVA

PC1

	Sum of Squares	df	Mean Square	F	Sig.
Between Groups	107.324	9	11,925	.400	.009
Within Groups	16231.858	546	29,729		
Total	16339.182	555			

Table 13: ANOVA statistics showing significant differences of left sided maxillary sinus morphologies of all populations used for the uniqueness testing study on the second principal component

ANOVA

PC2

	Sum of Squares	df	Mean Square	F	Sig.
Between Groups	44.371	9	4.930	.682	.028
Within Groups	3939.714	546	7.199		
Total	3975.085	555			

Table 14: ANOVA statistics showing significant differences of left sided maxillary sinus morphologies of all populations used for the uniqueness testing study on the third principal component

ANOVA

PC3

	Sum of Squares	df	Mean Square	F	Sig.
Between Groups	44.494	9	4.944	.435	.039
Within Groups	6180.484	546	11.320		
Total	6224.978	555			

Table 15: ANOVA statistics showing significant differences of left sided maxillary sinus morphologies of all populations used for the uniqueness testing study on the fourth principal component

ANOVA

PC4

	Sum of Squares	df	Mean Square	F	Sig.
Between Groups	152.397	9	16.933	.274	.016
Within Groups	33659.851	546	61.648		
Total	33812.248	555			

Table 16: ANOVA statistics showing significant differences of right sided maxillary sinus morphologies between all populations used for the uniqueness testing study on the first principal component

ANOVA

PC1

	Sum of Squares	df	Mean Square	F	Sig.
Between Groups	87.198	9	9.689	.584	.018
Within Groups	8807.832	539	16.341		
Total	8895.029	548			

Table 17: ANOVA statistics showing significant differences of right sided maxillary sinus morphologies between all populations used for the uniqueness testing study on the second principal component

ANOVA

PC2

	Sum of Squares	df	Mean Square	F	Sig.
Between Groups	81.941	9	9.105	.579	.028
Within Groups	8476.618	539	15.727		
Total	8558.559	548			

Table 18: ANOVA statistics showing significant differences of right sided maxillary sinus morphologies between all populations used for the uniqueness testing study on the third principal component

ANOVA

PC3

	Sum of Squares	df	Mean Square	F	Sig.
Between Groups	92.103	9	10.234	.679	.037
Within Groups	8121.002	539	15.067		
Total	8213.106	548			

Table 19: ANOVA statistics showing significant differences of right sided maxillary sinus morphologies between all populations used for the uniqueness testing study on the fourth principal component

ANOVA

PC4

	Sum of Squares	df	Mean Square	F	Sig.
Between Groups	10.242	9	1.138	.311	.007
Within Groups	1969.209	539	3.653		
Total	1979.451	548			

Table 20: ANOVA statistics showing significant differences of left sided maxillary sinus morphologies between all age categories used for the uniqueness testing study on the first principal component

ANOVA

PC1

	Sum of Squares	df	Mean Square	F	Sig.
Between Groups	3.405	5	.681	.023	.022
Within Groups	16311.986	550	29.658		
Total	16315.391	555			

Table 21: ANOVA statistics showing significant differences of left sided maxillary sinus morphologies between all age categories used for the uniqueness testing study on the second principal component

ANOVA

PC2

	Sum of Squares	df	Mean Square	F	Sig.
Between Groups	57.784	5	11.557	1.623	.015
Within Groups	3917.301	550	7.121		
Total	3975.085	555			

Table 22: ANOVA statistics showing significant differences of left sided maxillary sinus morphologies between all age categories used for the uniqueness testing study on the third principal component

ANOVA

PC3

	Sum of Squares	df	Mean Square	F	Sig.
Between Groups	47.140	5	9.428	.838	.024
Within Groups	6177.838	550	11.232		
Total	6224.978	555			

Table 23: ANOVA statistics showing significant differences of left sided maxillary sinus morphologies between all age categories used for the uniqueness testing study on the fourth principal component

ANOVA

PC4

	Sum of Squares	df	Mean Square	F	Sig.
Between Groups	387.743	5	77.549	1.275	.027
Within Groups	33424.505	550	60.772		
Total	33812.248	555			

Table 24: ANOVA statistics showing significant differences of right sided maxillary sinus morphologies between all age categories used for the uniqueness testing study on the first principal component

ANOVA

PC1

	Sum of Squares	df	Mean Square	F	Sig.
Between Groups	50.741	5	10.147	.623	.032
Within Groups	8844.288	543	16.288		
Total	8895.029	548			

Table 25: ANOVA statistics showing significant differences of right sided maxillary sinus morphologies between all age categories used for the uniqueness testing study on the second principal component

ANOVA

PC2

	Sum of Squares	df	Mean Square	F	Sig.
Between Groups	79.653	5	15.931	1.020	.014
Within Groups	8478.906	543	15.615		
Total	8558.559	548			

Table 26: ANOVA statistics showing significant differences of right sided maxillary sinus morphologies between all age categories used for the uniqueness testing study on the third principal component

ANOVA

PC3

	Sum of Squares	df	Mean Square	F	Sig.
Between Groups	46.012	5	9.202	.612	.021
Within Groups	8167.094	543	15.041		
Total	8213.106	548			

Table 27: ANOVA statistics showing significant differences of right sided maxillary sinus morphologies between all age categories used for the uniqueness testing study on the fourth principal component

ANOVA

PC4

	Sum of Squares	df	Mean Square	F	Sig.
Between Groups	9.674	5	1.935	.546	.020
Within Groups	1924.894	543	3.545		
Total	1934.568	548			

Figure 40: QR-code to access the complete and permanently stored Euclidean and Mahalanobis distance analyses used for the uniqueness testing study

Figure 41: QR-code to access the complete and permanently stored correlation of Euclidean distances of left sided maxillary sinus morphologies used for the uniqueness testing study

Figure 42: QR-code to access the complete and permanently stored correlation of Euclidean distances of right sided maxillary sinus morphologies used for the uniqueness testing study

Figure 45: QR-code to access the complete and permanently stored neighbour joining clustering of Mahalanobis distances of left sided maxillary sinus morphologies used for the uniqueness testing study

Figure 46: QR-code to access the complete and permanently stored neighbour joining clustering of Mahalanobis distances of right sided maxillary sinus morphologies used for the uniqueness testing study

Appendix 2
Case Study

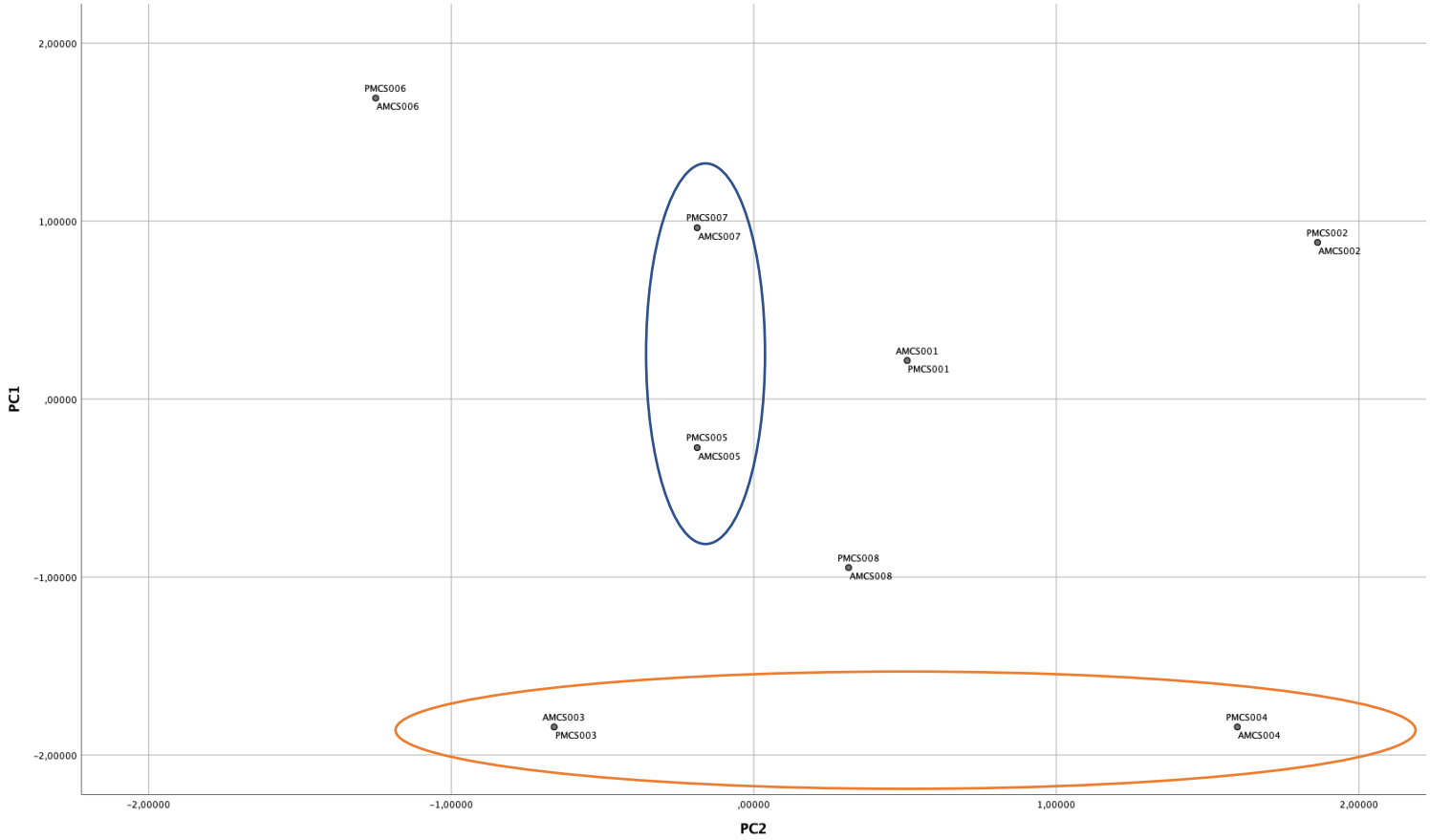

Figure 49: Two-dimensional scatterplot showing PC1 and PC2 for left sided maxillary sinus morphologies used for the case study by individual

**(Individuals = numbered; AM, PM stands = ante- and postmortem; blue oval = CS005 & CS007; orange oval = CS003 & CS004).*

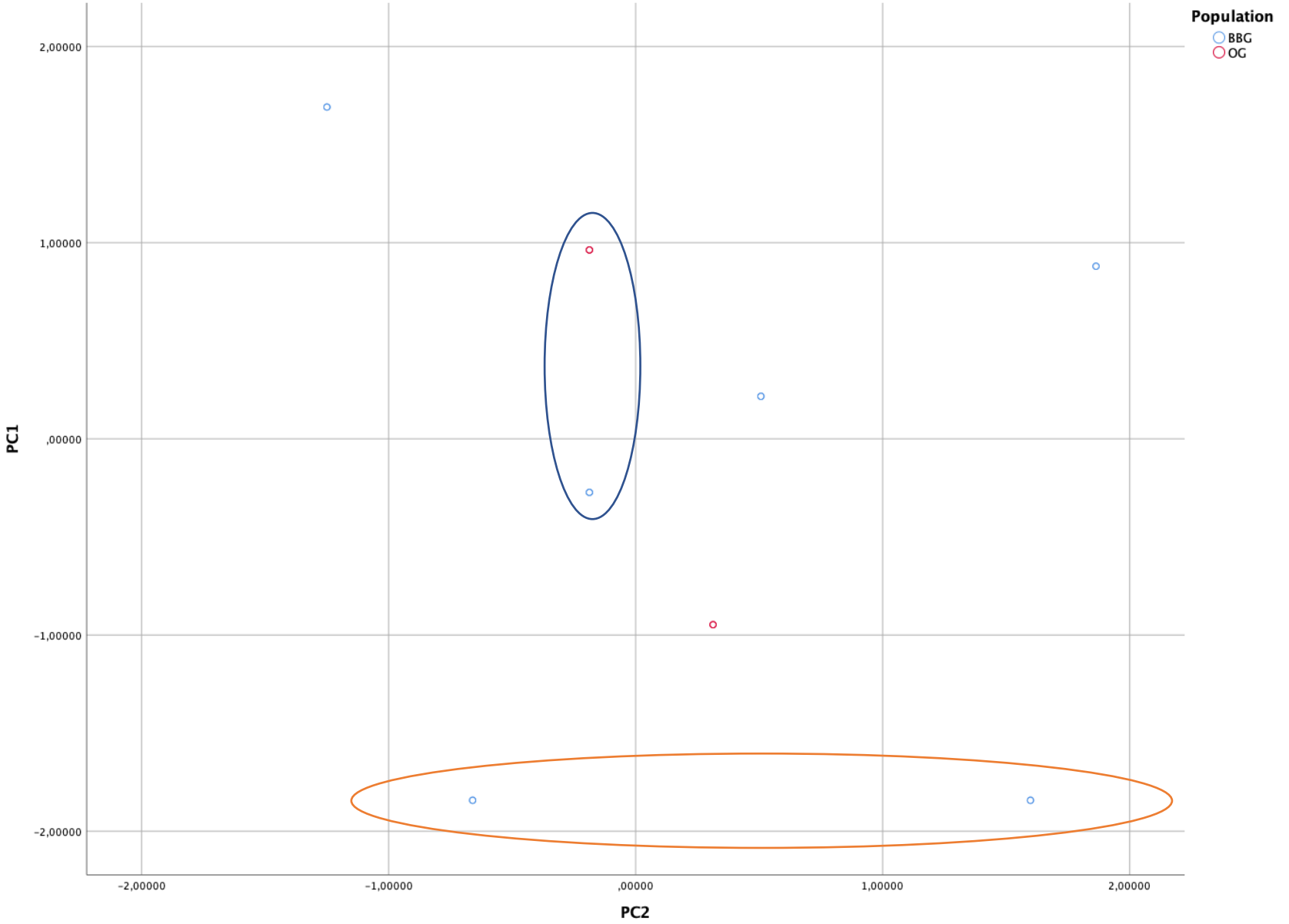

Figure 50: Two-dimensional scatterplot showing PC1 and PC2 for left sided maxillary sinus morphologies used for the case study by population

**(Individuals = numbered; AM, PM stands = ante- and postmortem; blue oval = CS005 & CS007; orange oval = CS003 & CS004).*

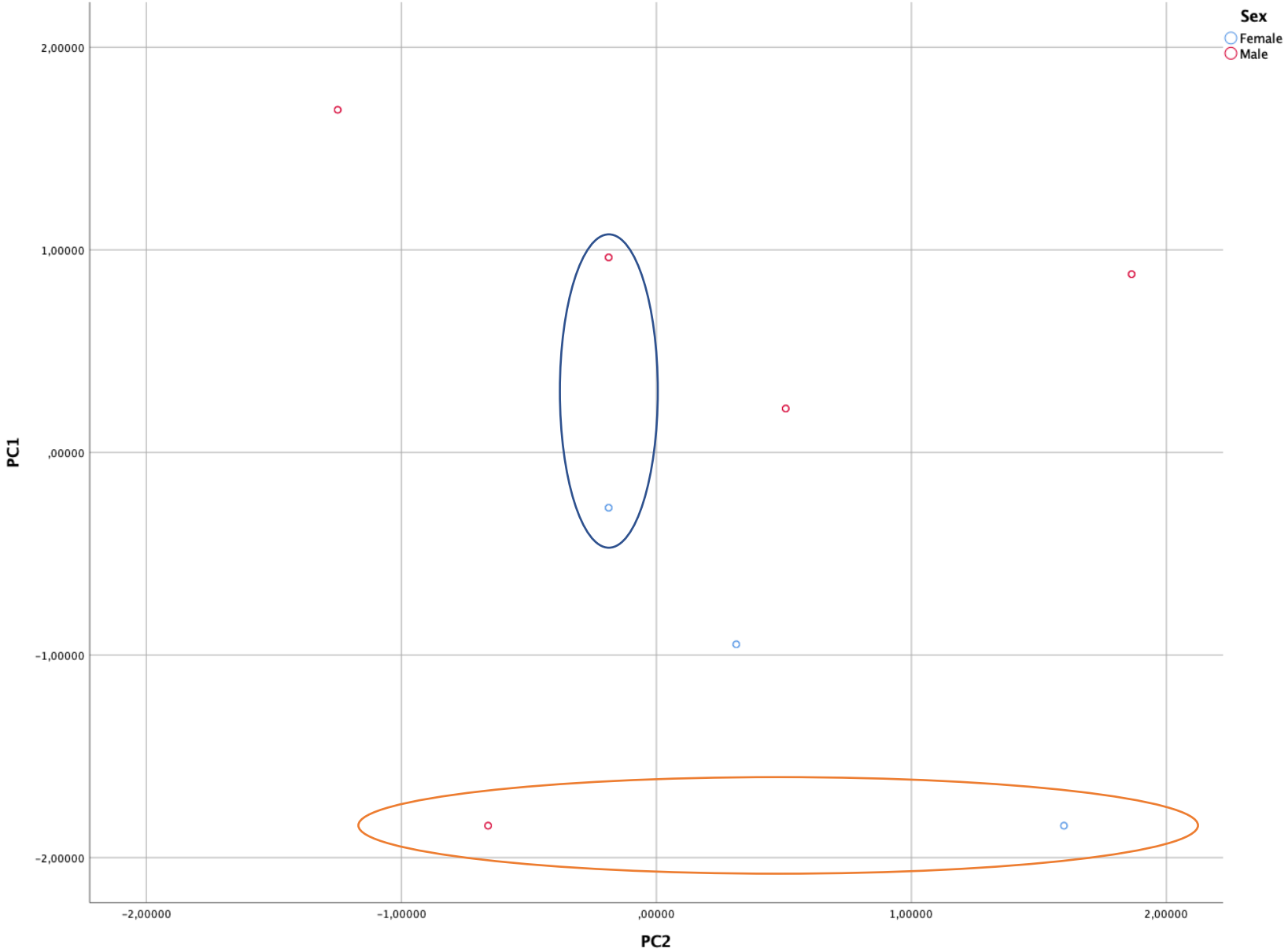

Figure 51: Two-dimensional scatterplot showing PC1 and PC2 for left sided maxillary sinus morphologies used for the case study by sex

**(Individuals = numbered; AM, PM stands = ante- and postmortem; blue oval = CS005 & CS007; orange oval = CS003 & CS004).*

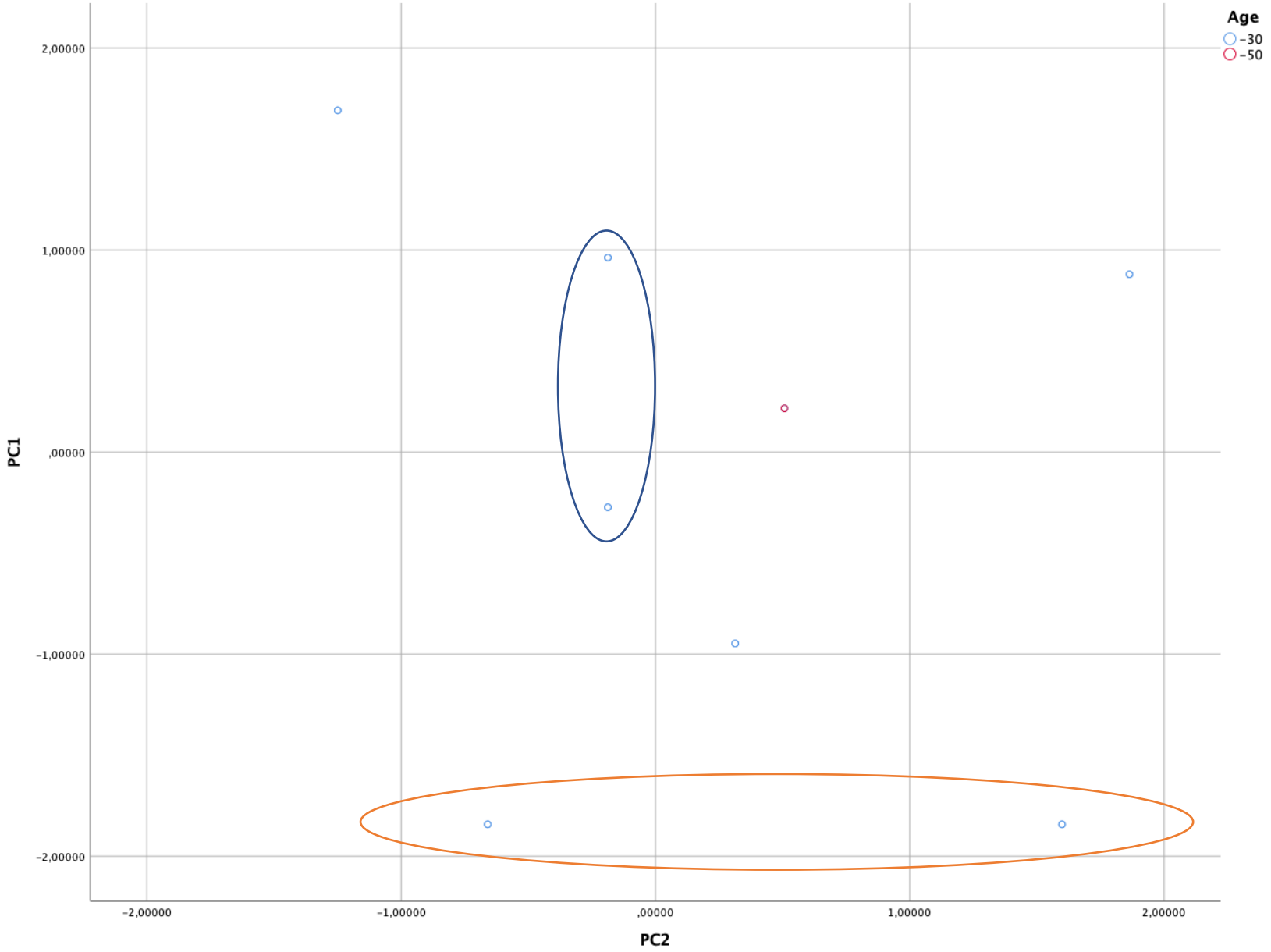

Figure 52: Two-dimensional scatterplot showing PC1 and PC2 for left sided maxillary sinus morphologies used for the case study by age

**(Individuals = numbered; AM, PM stands = ante- and postmortem; blue oval = CS005 & CS007; orange oval = CS003 & CS004).*

Figure 53: Two-dimensional scatterplot showing PC1 and PC2 for right sided maxillary sinus morphologies used for the case study by individual

**(Individuals = numbered; AM, PM stands = ante- and postmortem; green oval = CS004 & CS008; yellow oval = CS002 & CS007).*

Figure 54: Two-dimensional scatterplot showing PC1 and PC2 for right sided maxillary sinus morphologies used for the case study by population

**(Individuals = numbered; AM, PM stands = ante- and postmortem; green oval = CS004 & CS008; yellow oval = CS002 & CS007).*

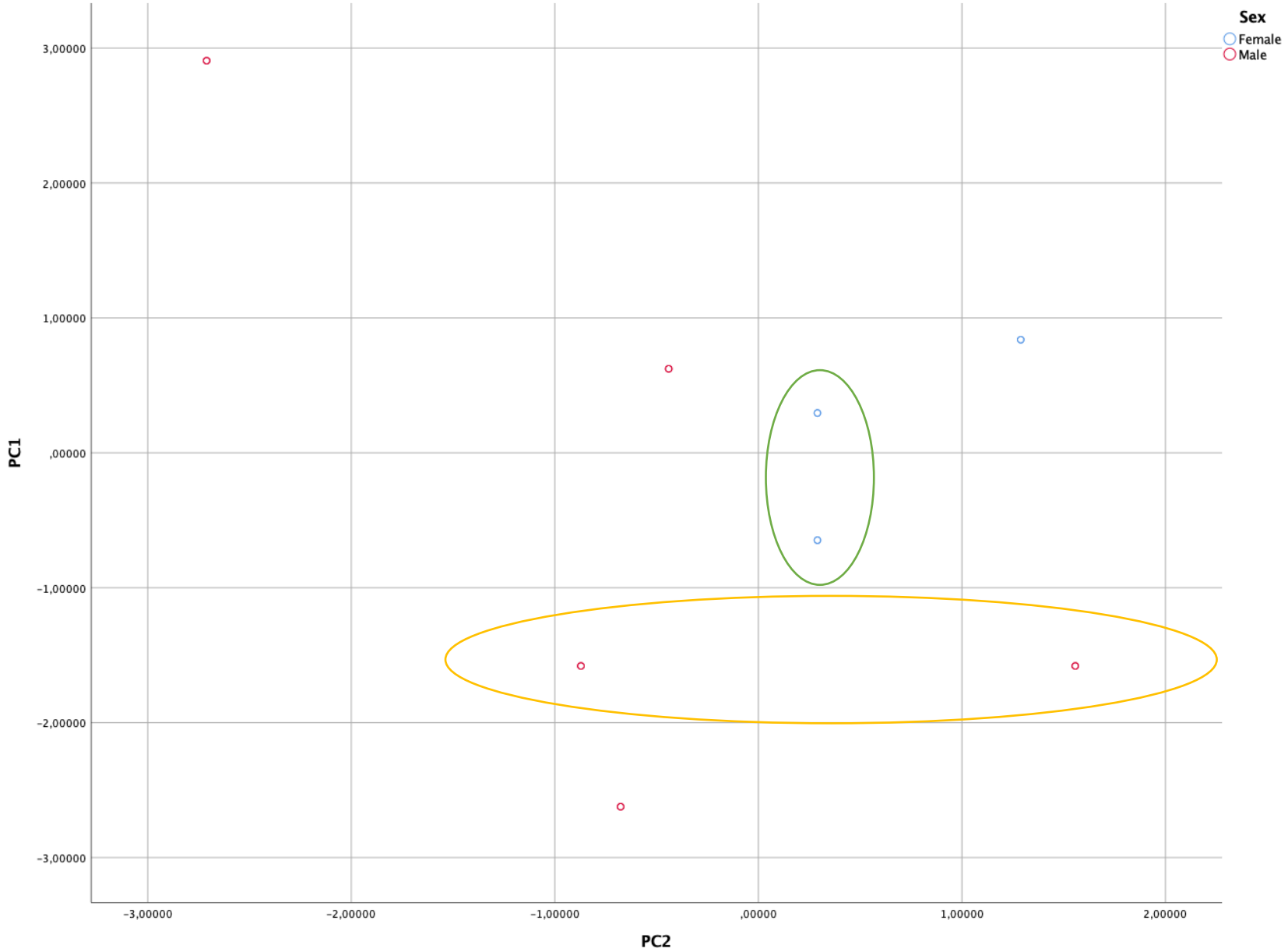

Figure 55: Two-dimensional scatterplot showing PC1 and PC2 for right sided maxillary sinus morphologies used for the case study by sex

*(Individuals = numbered; AM, PM stands = ante- and postmortem; green oval = CS004 & CS008; yellow oval = CS002 & CS007).

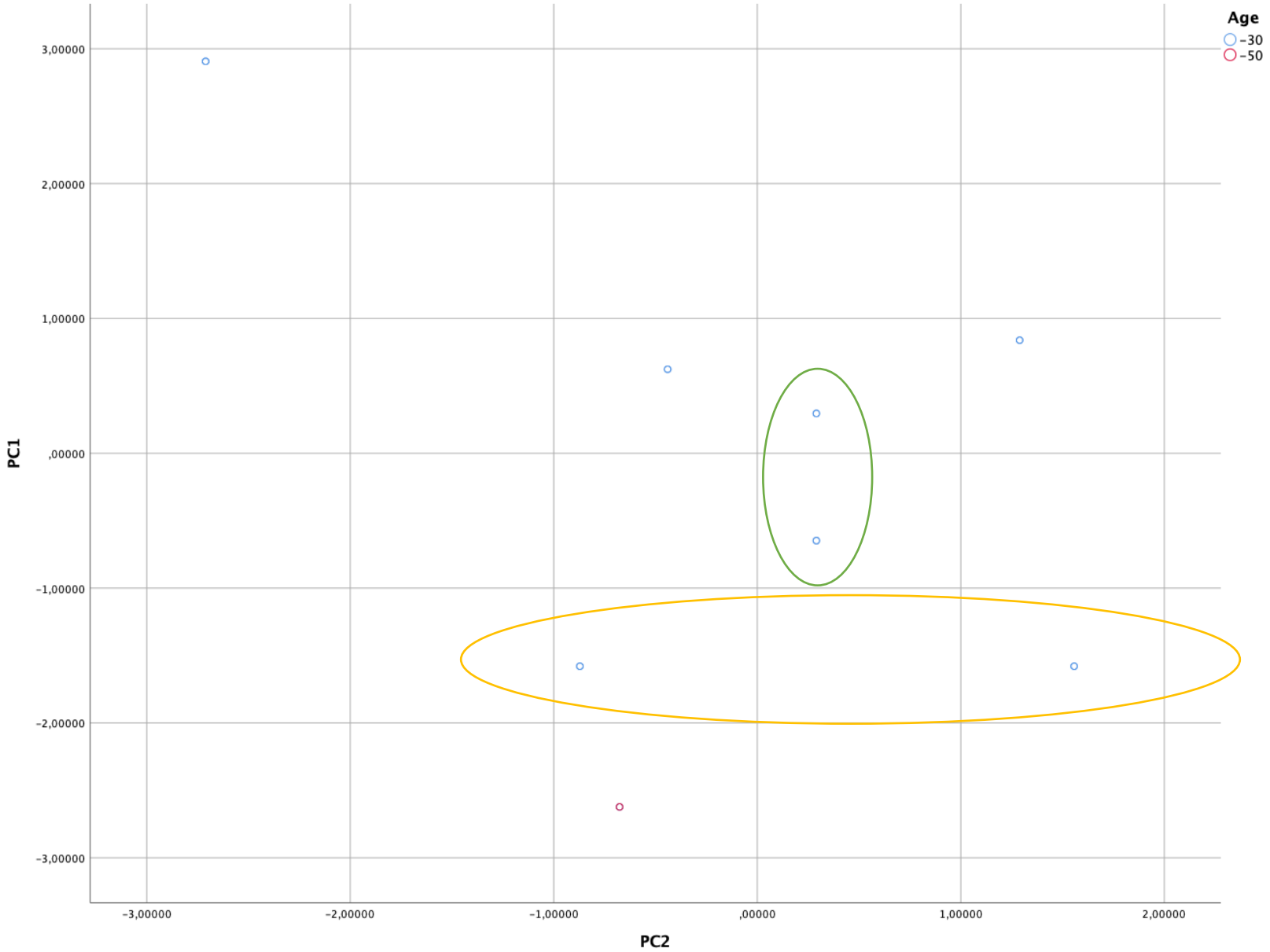

Figure 56: Two-dimensional scatterplot showing PC1 and PC2 for right sided maxillary sinus morphologies used for the case study by age

**(Individuals = numbered; AM, PM stands = ante- and postmortem; green oval = CS004 & CS008; yellow oval = CS002 & CS007).*